



<https://theses.gla.ac.uk/>

Theses Digitisation:

<https://www.gla.ac.uk/myglasgow/research/enlighten/theses/digitisation/>

This is a digitised version of the original print thesis.

Copyright and moral rights for this work are retained by the author

A copy can be downloaded for personal non-commercial research or study,  
without prior permission or charge

This work cannot be reproduced or quoted extensively from without first  
obtaining permission in writing from the author

The content must not be changed in any way or sold commercially in any  
format or medium without the formal permission of the author

When referring to this work, full bibliographic details including the author,  
title, awarding institution and date of the thesis must be given

Enlighten: Theses

<https://theses.gla.ac.uk/>  
[research-enlighten@glasgow.ac.uk](mailto:research-enlighten@glasgow.ac.uk)

CREEP OF THICK-WALLED CYLINDERS  
SUBJECTED TO INTERNAL PRESSURE

by

J.Fairbairn

Submitted for the Degree of Ph.D.,

The University of Glasgow.

May, 1968.

ProQuest Number: 10647089

All rights reserved

INFORMATION TO ALL USERS

The quality of this reproduction is dependent upon the quality of the copy submitted.

In the unlikely event that the author did not send a complete manuscript and there are missing pages, these will be noted. Also, if material had to be removed, a note will indicate the deletion.



ProQuest 10647089

Published by ProQuest LLC (2017). Copyright of the Dissertation is held by the Author.

All rights reserved.

This work is protected against unauthorized copying under Title 17, United States Code  
Microform Edition © ProQuest LLC.

ProQuest LLC.  
789 East Eisenhower Parkway  
P.O. Box 1346  
Ann Arbor, MI 48106 – 1346

CONTENTS

	<u>Page No.</u>
PREFACE	(iii)
ACKNOWLEDGEMENTS	(v)
CHAPTER 1	1
Review of literature on behaviour of metals under complex stress.	
1.1 Brief review of theory of plasticity.	1
1.2 Creep under constant complex stress systems.	6
1.3 Creep under changing complex stress systems.	13
CHAPTER 2	19
Creep of thick-walled cylinders under internal pressure - review of literature.	
2.1 Analytical approaches.	19
2.2 Secondary creep analyses.	21
2.3 Primary creep analyses.	24
2.4 Review of experimental work.	32
2.4.1 Investigations using lead and lead alloys.	33
2.4.2 Investigations at elevated temperatures.	36
2.4.3 Discussion of experimental techniques.	42
CHAPTER 3	48
Experimental investigation.	
3.1 Introduction.	48
3.2 Tensile creep tests.	51
3.2.1 Tensile specimen.	53
3.2.2 Temperature control system.	54
3.2.3 Temperature measurement.	55
3.2.4 Strain measurement.	56
3.2.5 Initial application of the load.	57
3.3 Internal pressure tests.	57
3.3.1 Test specimen.	57
3.3.2 Arrangement of the specimen in the test rig.	58
3.3.3 Pressure system.	59
3.3.4 Temperature measurement and control.	60
3.3.5 Diametral strain measurement.	60
3.3.6 Axial strain measurement.	64
3.4 Summary of experimental work.	66
3.4.1 Tensile creep tests.	66
3.4.2 Internal pressure creep tests.	69
CHAPTER 4	72
Analysis of tensile creep data.	
4.1 Introduction.	72
4.2 Constant-stress data.	74
4.3 Constant-load data.	80
CHAPTER 5	84
Analysis of thick-walled cylinder creep data.	
5.1 Introduction.	84
5.2 Application of general relationships to thick cylinder creep data.	91

CHAPTER 6	Discussion of the results of the investigation.	111
	6.1 Choice of strain system.	111
	6.2 Tensile creep tests.	112
	6.3 Internal pressure creep tests.	114
	6.3.1 Possible extension of skeletal point analysis to finite strain range.	119
CONCLUSIONS		124
APPENDIX I	The test material.	126
APPENDIX II	Design of constant-stress mechanism.	128
APPENDIX III	Investigation of creep occurring in fillet radii of tensile specimens.	134
APPENDIX IV	Tensile specimen loading jack.	138
APPENDIX V	Thermal compensation of transducer framework.	140
APPENDIX VI	"Comparison of constant-load and constant- stress tensile creep data for an aluminium - 0.07 per cent titanium alloy at 250°C"	142
APPENDIX VII	Short time tensile properties of the material.	147
APPENDIX VIII	Derivation of wall-thinning equation.	148
APPENDIX IX	"A simple method of obtaining creep rates of a thick-walled cylinder under internal pressure.	150
BIBLIOGRAPHY		156
FIGURES		169

PREFACE

This thesis describes an experimental investigation into the creep of thick-walled cylinders under internal pressure. The object of the investigation was the accurate prediction of thick-walled cylinder creep data from associated uniaxial tension creep data. The problem is of considerable industrial significance and is also of academic interest since the stress system acting in the wall of a thick cylinder under internal pressure at elevated temperature is triaxial and changes with time due to stress redistribution and wall-thinning. Although an extensive literature exists on the theoretical aspects of the problem, relatively little relevant experimental data has been published.

The test material was an aluminium - 0.06 per cent titanium alloy obtained in the form of a continuously cast billet. This simple material was selected because of its expected isotropy and low creep resistance permitting large creep strains at stresses low enough to prevent appreciable initial loading strains.

Three series of creep tests were carried out,

- (i) internal pressure tests on ten thick-walled cylinders.
- (ii) constant-stress uniaxial tension tests at eight stress levels.
- (iii) constant-load uniaxial tension tests at six stress levels.

The constant-stress tension data was correlated to provide a mathematical description of the material creep behaviour for use in the prediction of the internal pressure test data. The constant-load tests provided data for a simply varying stress system and served as an intermediate step between the constant-stress data and the thick cylinder data. Good agreement with the thick cylinder experimental data was obtained by means of an analysis

based on the uniaxial tension data.

By means of the "skeletal point" concept of Marriott and Leckie, a method was developed for predicting the creep rates of a thick cylinder under internal pressure from the results of a single creep test in uniaxial tension, based on the method of Soderberg for thin cylinders. This analysis is applicable only at small strains and a means of extending the strain range was suggested.

ACKNOWLEDGEMENTS

The research described here was initially supported by the Central Electricity Generating Board and later by the Science Research Council and Imperial Chemical Industries Ltd. The writer is indebted to these supporting bodies.

The writer is also indebted to :-

The late Professor James Small, and Professor R.S.Silver, James Watt Professor of Mechanical Engineering in whose department he has been privileged to carry out his research.

Mr. W.W.Mackie, under whose guidance the research was carried out, for many stimulating discussions and practical assistance.

The staff of the University Workshops, under Mr. J.Baird, for the care with which the necessary apparatus was manufactured, and in particular Mr. J.Holmes for many months spent manufacturing test specimens from an unsympathetic material.

His colleagues in the department for their assistance.

Mr. M.R.Gibson for his assistance with the computer programming.

Mrs. P.Smith who typed the thesis, and Mr. W.Reynolds and Mr. A.McNair for assistance in the production of the figures.

CHAPTER 1

REVIEW OF LITERATURE ON BEHAVIOUR OF METALS

UNDER COMPLEX STRESS

1.1 Brief review of theory of plasticity

The phenomenological theory of creep of metals under the action of complex stress systems is based to a great extent on the theory of plasticity since the stress dependence of both mechanisms is generally similar. The foundations of the theory of plasticity of metals were laid about a century ago and many laws have been proposed since to define the stress state producing yielding of an isotropic material. It was established by Bridgeman (1) that the state of stress causing yielding was independent of the hydrostatic component of stress and confirmed by the results of Ros and Eichinger (2) and Crossland (3). This led to the rejection of all but two of the yield criteria in common use. These two criteria are:-

1. The criterion of Tresca (1864), based on the results of experiments in extrusion of metals, which states that yielding occurs when the maximum shear stress attains a critical value. This may be expressed as:-

$$\bar{\sigma} = \sigma_1 - \sigma_3 \quad \text{for } \sigma_1 \geq \sigma_2 \geq \sigma_3$$

where  $\sigma_1$ ,  $\sigma_2$  and  $\sigma_3$  are the principal stresses and  $\bar{\sigma}$  is the yield stress in uniaxial tension.

2. The criterion generally attributed to von Mises (1913) which states that yielding occurs when the sum of the squares of the principal stress differences attains a critical value. This may be expressed as:-

$$\sigma^* = \frac{1}{\sqrt{2}} [(\sigma_1 - \sigma_2)^2 + (\sigma_2 - \sigma_3)^2 + (\sigma_3 - \sigma_1)^2]^{\frac{1}{2}}$$

where  $\sigma^*$  is the yield stress in uniaxial tension.

The von Mises criterion was proposed on mathematical grounds, but was interpreted by Hencky (1924) as the condition of maximum elastic strain energy and Nadai (4) has shown that it is proportional to the maximum shear stress on the octahedral planes. It was shown by Sachs (1928) that, statistically, the von Mises criterion for a polycrystalline material was the natural corollary of the maximum shear stress criterion for a single crystal. This point was made independently by Cox and Sopwith (5) and again by Beeching (6) who suggested that the correspondence of the von Mises criterion with maximum shear strain energy or octahedral shear stress was fortuitous. The von Mises function is perhaps best considered simply as an effective stress, proportional to  $J_2$ , the second invariant of the stress tensor.

$$J_2 = \frac{1}{6} [(\sigma_1 - \sigma_2)^2 + (\sigma_2 - \sigma_3)^2 + (\sigma_3 - \sigma_1)^2]$$

$$\therefore J_2 = \frac{1}{3} \sigma^{*2}$$

Yield criteria can be represented as surfaces in stress space with the orthogonal axes representing values of the principal stresses. Since hydrostatic pressure does not cause yielding, the yield surface is a cylinder with generator parallel to the (1,1,1) direction. A two dimensional representation is obtained by projecting the surface on a plane perpendicular to the hydrostatic stress axis. This representation of the Tresca and von Mises criteria is shown in fig.(1) where the reduced plane

is the plane of the paper.

A great deal of experimental work has been carried out to determine the validity of these criteria for the onset of yielding and although many of the early experiments may be open to criticism on the grounds of inadequate material isotropy, the superiority of the von Mises criterion has been demonstrated for ductile metals by several series of carefully controlled tests (7,8,9). Morrison (10), however, has found that the upper yield point of some steels follows the Tresca criterion while the lower yield point follows the von Mises criterion.

The relationship between stress and plastic strain was first investigated by St. Venant (1870) who proposed that the principal axes of stress and strain-increment were coincident. Lévy (1871) and von Mises (1913) proposed the same set of equations relating the strain-increments to the principal stresses. These equations may be written:-

$$\frac{d\epsilon_1 - d\epsilon_2}{\sigma_1 - \sigma_2} = \frac{d\epsilon_2 - d\epsilon_3}{\sigma_2 - \sigma_3} = \frac{d\epsilon_3 - d\epsilon_1}{\sigma_3 - \sigma_1}$$

where  $d\epsilon_1$ ,  $d\epsilon_2$  and  $d\epsilon_3$  are the increments of plastic strain in the principal directions.

The first experimental investigation of these equations was made by Lode (e.g. 11), whose results on tubes under combined tension and internal pressure indicated a deviation from the simple relationship. This deviation was confirmed by the classical experimental work of Taylor and Quinney (7) in which a much greater emphasis was placed on material isotropy. These tests were performed on thin-walled tubes under combined tension and torsion

and the stress ratios were varied during the tests so that rotation of the principal axes of stress took place. The value of Lode's results, however, is greatly reduced by the probability of anisotropy being present in the test specimens and it is quite possible that anisotropy was still present in the experiments of Taylor and Quinney. Fraenkel (12) has demonstrated the effect of anisotropy and shown that deviation from the Lévy Mises equations is small for an annealed material and much larger for a material which is definitely anisotropic and that the deviation increases with increasing strain. Hill (11) has suggested that, in the light of the experimental evidence, the Lévy Mises equations are a good approximation to the behaviour of real materials and improvement may only be achieved in a complicated manner.

The condition that plastic deformation occurs at constant volume, which follows from the ineffectiveness of hydrostatic stress in causing plastic deformation, may be expressed as:-

$$d\epsilon_1 + d\epsilon_2 + d\epsilon_3 = 0$$

Combining this condition with the Lévy Mises equations gives:-

$$d\epsilon_1 = d\lambda \left[ \sigma_1 - \frac{1}{2}(\sigma_2 + \sigma_3) \right]$$

$$d\epsilon_2 = d\lambda \left[ \sigma_2 - \frac{1}{2}(\sigma_3 + \sigma_1) \right]$$

$$d\epsilon_3 = d\lambda \left[ \sigma_3 - \frac{1}{2}(\sigma_1 + \sigma_2) \right]$$

where  $d\lambda$  is a scalar factor of proportionality and is a function of the yield criterion.

In 1930 Reuss generalised these equations to include the elastic component of strain. These equations may be expressed as:-

$$d\epsilon_1 = d\lambda \left[ \sigma_1 - \frac{1}{2}(\sigma_2 + \sigma_3) \right] + \frac{1}{E} [d\sigma_1 - \mu(d\sigma_2 + d\sigma_3)]$$

$$d\epsilon_2 = d\lambda \left[ \sigma_2 - \frac{1}{2}(\sigma_3 + \sigma_1) \right] + \frac{1}{E} [d\sigma_2 - \mu(d\sigma_3 + d\sigma_1)]$$

$$d\epsilon_3 = d\lambda \left[ \sigma_3 - \frac{1}{2}(\sigma_1 + \sigma_2) \right] + \frac{1}{E} [d\sigma_3 - \mu(d\sigma_1 + d\sigma_2)]$$

$d\epsilon_1$  ,  $d\epsilon_2$  and  $d\epsilon_3$  are now increments of total strain.

In 1924, Hencky proposed that the total strain, rather than the strain increment was related to the stress distribution. This implies that the strain at any stage of plastic deformation depends only on the current stresses and is independent of prior strain history. This theory has received a great deal of attention although it leads to inaccuracy for many loading paths (11,13,14). For loading paths in which the ratios of the principal stress components remain constant, use of the Hencky, or deformation theory, and the incremental, or flow theory, provides identical results but different results are obtained when the directions of the principal stresses change during loading. Because of its mathematical simplicity, application of the deformation theory has been examined and it has been postulated (15) that the theory may be suitable for loading paths other than simple, proportional loading. Manson (16) has suggested that deformation theory may be useful in preliminary design calculations although the increasing availability of high speed computers has greatly reduced the difficulty of obtaining a more accurate incremental solution. The theories of plasticity thus developed have been applied on many occasions to plastic deformation of a thick-walled cylinder under internal pressure with particular regard to the problem of autofrettage. Hill, Lee and Tupper (17,18) have produced incremental solutions for an elasto-plastic thick cylinder, considering the case of zero axial strain and also of a

cylinder with closed ends carrying its own pressure end load, and shown that the simpler deformation theory leads to little error in these applications. Of the many thick-cylinder deformation theory solutions available, that of Allen and Sopwith (19) probably contains the fewest assumptions and provides results in good agreement with the incremental solutions. This analysis was used in the present investigation to estimate the initial stress distribution in the wall of the tubular creep test specimens on application of the internal pressure. The autofrettage problem is still of interest and a novel approach has been suggested recently by Berman and Pai (20).

## 1.2 Creep under constant complex stress systems

Bailey (21), in his classical 1935 paper, proposed relationships for the secondary creep rates of metals under steady complex stress systems which were of the form:-

$$\left. \begin{aligned} \dot{\epsilon}_1 &= A\sigma^{*m} [(\sigma_1 - \sigma_2)^{n-m} - (\sigma_3 - \sigma_1)^{n-m}] \\ \dot{\epsilon}_2 &= A\sigma^{*m} [(\sigma_2 - \sigma_3)^{n-m} - (\sigma_1 - \sigma_2)^{n-m}] \\ \dot{\epsilon}_3 &= A\sigma^{*m} [(\sigma_3 - \sigma_1)^{n-m} - (\sigma_2 - \sigma_3)^{n-m}] \end{aligned} \right\} \quad (1)$$

These equations were based on the von Mises criterion and assumed a power law relationship between effective strain-rate and effective stress.

$$\text{i.e. } \dot{\epsilon}^* = A\sigma^{*n}$$

where  $\dot{\epsilon}^*$  is the effective strain-rate associated with the von Mises criterion and has the form:-

$$\dot{\epsilon}^* = \frac{\sqrt{2}}{3} [(\epsilon_1 - \epsilon_2)^2 + (\epsilon_2 - \epsilon_3)^2 + (\epsilon_3 - \epsilon_1)^2]^{\frac{1}{2}}$$

Such a power law relationship was found to exist fairly generally from the results of uniaxial tension creep tests.

The form of the Bailey equations does not correspond to agreement with the Lévy Mises equations (often referred to as the von Mises flow rule) which requires equations of the form:-

$$\left. \begin{aligned} \dot{\epsilon}_1 &= A\sigma^{*n} [(\sigma_1 - \sigma_2) - (\sigma_3 - \sigma_1)] \\ \dot{\epsilon}_2 &= A\sigma^{*n} [(\sigma_2 - \sigma_3) - (\sigma_1 - \sigma_2)] \\ \dot{\epsilon}_3 &= A\sigma^{*n} [(\sigma_3 - \sigma_1) - (\sigma_2 - \sigma_3)] \end{aligned} \right\} (2)$$

In contribution to the Bailey paper Cook observed that if the von Mises criterion was valid and the material was isotropic, then  $(n - m)$  has the value 1 or 3. The Bailey equations then are of the same form as equations (2). Relationships, similar in form to these equations were proposed by Odqvist, also in contribution to the Bailey paper, and have also been proposed by Soderberg (22), Marin (23) and Nadai (24). The main assumptions inherent in the development of these theories are the validity of the von Mises criterion and flow rule and that creep occurs at constant volume and is uninfluenced by hydrostatic stress. Equations of this form are obviously closely related to incremental plastic strain relationships.

The basis for the formulation of Bailey's equations was a series of creep tests on thin-walled cylinders, of carbon steel under combined tension and torsion at 450 °C, and lead under internal pressure and axial

load at room temperature (5). Johnson (26) has suggested that the form of relationship required by Bailey to represent his experimental results was almost certainly due to anisotropy of the specimens, and has used a similar relationship to describe a simple form of anisotropy occurring in some creep tests on a carbon steel at 450 °C (27). Bailey concluded that a hydrostatic component of stress was ineffective in causing creep, from the similarity of creep behaviour of thin cylinders under tension and torsion and thin cylinders under internal pressure where the stress systems differed only by a hydrostatic component.

Probably the greatest individual contribution to the field of behaviour of metals at elevated temperatures under complex stress systems has been made by A.E. Johnson, who, in association with others, carried out investigations in this field from 1932 until his death in 1966. His work on elevated temperature, complex stress behaviour, has included investigations of time independent stress - plastic strain relations, creep, relaxation, and fracture of metallic alloys. A review of most of this work has been published by Johnson, Henderson and Khan (28). A great number of creep tests were carried out by Johnson et al under constant complex stress systems on a group of six metallic materials at temperatures and stresses within their normal working range. The materials were chosen to be representative of basic groups of materials used in practice in machinery operating at elevated temperatures. The greatest possible care was taken to ensure that the materials used were isotropic and careful tests were carried out to check the degree of isotropy. The creep tests were carried out under combined tension and torsion and also under pure tension and

pure torsion as the simplifications of the combined stress tests. Tests under combined tension and torsion provide a valid representation of general complex stress systems only if creep is unaffected by hydrostatic stress. If this is the case, any triaxial system of stresses may be reduced to a biaxial system, which is equivalent for creep, by the addition or subtraction of a hydrostatic stress component. Thus creep tests on thin-walled tubes under combined tension and torsion are sufficient to represent creep behaviour under many, more general, stress systems. The validity of this assumption was verified experimentally by Johnson and Frost (27) by means of creep tests on a magnesium alloy in the form of thin-walled tubes under combined tension and torsion, and flat plates under biaxial tension, in which the stress systems were made to differ by a hydrostatic component only. In the main testing programme on the six materials, creep tests were limited to times of about 150 hours and the results relate almost entirely to the primary stage of creep. For a given material and test temperature, geometric similarity of creep curves of strain against time for different stress levels was almost invariably a feature of the results. It was concluded therefore that creep strain could be expressed as functions of stress and time,

$$\text{i.e. } \epsilon = f_1(\sigma)f_2(t)$$

where  $f_1$  and  $f_2$  are separable functions.

The stress dependence, for a given material and temperature, was therefore determined by comparing creep rates produced by different stress systems at a constant reference time. The time chosen was 150 hours. It was generally concluded that for most of the materials at moderate stresses

and temperatures the creep behaviour could be represented adequately by relations of the form of equations (2). In addition it was found that in all cases the creep curves could be closely represented by a simple power function of time.

Stowell and Gregory (29) have pointed out that the uncertainties introduced into the investigations of Johnson et al by making use of the functional independence of stress and time to compare strain-rates which were changing at the reference time of 150 hours could be avoided by confining attention to the secondary stage of creep where the strain-rate is constant. Constant stress creep tests were carried out by these authors on thin-walled aluminium alloy tubes under combined tension and torsion. All the tests were carried on into the tertiary stage of creep allowing secondary creep rates to be established. Biaxial stress equations given by Nadai (30), based on the von Mises criterion and flow rule were used to analyse the results, and a hyperbolic sine function of stress was employed instead of a power function. Good agreement was found with the experimental secondary creep rates. In addition it was found that this agreement applied during the primary regions, within the limits of the experimental data, largely substantiating the Johnson hypothesis.

Soderberg (31) made use of relationships of the form of equations (2) to analyse the results obtained by Norton (32), from creep tests on thin steel cylinders under internal pressure, and obtained reasonable correlation of secondary creep rates. This analysis will be discussed more fully in a later chapter. General agreement with this analysis was obtained by Rowe, Stewart and Burgess (33), who carried out internal pressure, creep-rupture tests on thin-walled cylinders of type 316 stainless steel, although the

secondary creep rates obtained for the cylinder tests were not reliable. These creep rates were estimated from cylinder dimensions before and after each test, by assuming that the primary and tertiary stages of creep were negligible.

The stress dependence of secondary creep has also been investigated by Kennedy, Harms and Douglas (34) who carried out constant-stress creep tests on thin-walled tubes of inconel at 1500 °F under internal pressure and axial load. It was intended to investigate sections of the biaxial stress plane not previously covered by tests under combined tension and torsion or pure internal pressure. Only axial strains were measured, tangential and radial strains being estimated from measurements made at the conclusion of the tests. Correlation of the test results using the measured axial secondary creep rates was carried out. Relations of the form of equation (2) were used and also similar equations based on the Tresca criterion but still embodying the von Mises flow rule. These latter equations may be written as:-

$$\dot{\epsilon}_1 = A\bar{\sigma}^{-n} [(\sigma_1 - \sigma_2) - (\sigma_3 - \sigma_1)]$$

$$\dot{\epsilon}_2 = A\bar{\sigma}^{-n} [(\sigma_2 - \sigma_3) - (\sigma_1 - \sigma_2)]$$

$$\dot{\epsilon}_3 = A\bar{\sigma}^{-n} [(\sigma_3 - \sigma_1) - (\sigma_2 - \sigma_3)]$$

where  $\bar{\sigma}$  is the Tresca criterion

$$\text{i.e. } \bar{\sigma} = \sigma_1 - \sigma_3 \quad \text{for } \sigma_1 \geq \sigma_2 \geq \sigma_3$$

A reasonable correlation of the data was achieved, with the von Mises criterion being slightly superior to the Tresca criterion.

A further relationship is possible by applying the Tresca criterion and its associated flow rule. This leads to equations of the form:-

$$\dot{\epsilon}_1 = B\bar{\sigma}^{-(n+1)},$$

$$\dot{\epsilon}_1 = -\dot{\epsilon}_3 ; \quad \epsilon_2 = 0 \quad \text{for } \sigma_1 \geq \sigma_2 \geq \sigma_3$$

Equations of this form have been applied by Wahl (35) to the creep of a rotating disc. It was found by Wahl (36) that the use of equations based on the Tresca criterion provided a better correlation of rotating disc creep data than equations based on the von Mises criterion and Finnie (37) carried out an experimental investigation to further examine these theories. Creep tests were carried out on thin-walled tubes of aluminium at 250 °C and lead at 60 °C, under pure torsion, internal pressure, and uniaxial tension and compression. It was found that the results could not be correlated satisfactorily by either of the theories and it was concluded that the poor correlation might be due to the effect of hydrostatic stress at temperatures above half the melting point. This suggestion has yet to be investigated experimentally since the tests by Johnson and Frost on the magnesium alloy were carried out at a temperature of only 0.31 of the melting point. There is also the possibility that at least part of the lack of correlation was due to anisotropy. The isotropy was checked by comparing creep rates of compression specimens from three directions in the billet. Creep curves for uniaxial tension and compression at the same stress level were compared for a time of 15 hours and Hancock pointed out in contribution to the paper that the test time of 15 hours was very short and there were already signs of divergence of

the compression and tension test results.

### 1.3 Creep under changing complex stress systems

All phenomenological theories of creep assume the existence of a mechanical equation of state for the material, i.e. a mathematical relationship connecting the appropriate physical variables e.g. stress, strain, time, temperature, etc. This concept was introduced by Ludwick in 1909 who proposed an equation of the form:-

$$\dot{\epsilon} = f(\sigma, \epsilon, T)$$

where  $\dot{\epsilon}$  is the strain-rate,  $\epsilon$  is the strain,  $\sigma$  is the stress and  $T$  is the temperature.

Such an equation implies that the strain-rate at any instant is a function only of the current stress, strain and temperature, and is independent of the previous history of the material. A great deal of attention has been paid to the determination of the validity of the concept of an equation of state. It has been shown (e.g. 38, 39) that such a concept cannot in general be valid since the instantaneous behaviour of a material is dependent on the conditions under which previous deformation took place. Many attempts have been made to derive functions for a material which include prior history effects and towards this end Dorn et al have carried out extensive tensile creep testing and have obtained a parameter describing the structure of the material (e.g.40, 41). The work of Dorn et al has emphasised the importance of creep data, for correlation purposes, being obtained from tests on specimens having the same initial structure. The Dorn approach to creep has been reviewed

by Kennedy (42). The investigation of structural parameters has, as yet, been restricted to uniaxial stress conditions and the equation of state concept is almost universally applied in stress analysis under creep conditions. The concept has been defended by Graham (43) on the grounds that very often relations based on an equation of state fit experimental results very well. Lubahn and Felgar (44) have suggested, with due regard for the evidence against the existence of an equation of state, that the concept is still of considerable value, since it can be applied to conditions where metallurgical changes do not occur and the temperature remains constant and it may be possible by modification to the equation of state to allow for temperature changes or metallurgical instability. It may also be the only method of obtaining an approximate solution to an urgent problem.

For isothermal conditions a general equation of state may be formulated as:-

$$\epsilon = f_1(\sigma)f_2(t) \quad \text{e.g. Johnson.}$$

If the stress and time dependence are described by simple power functions, this equation may be written for uniaxial stress as:-

$$\epsilon = A\sigma^n t^p \quad \dots\dots(3)$$

This equation applies to conditions of constant stress and is analogous to the deformation theory of plasticity. It will not be valid generally in cases where the stress is changing. An equation of state may be applied to conditions of changing stress, but only if strain-rate, rather than strain at any instant is considered. This form of equation is analogous to the incremental or flow theory of plastic deformation. Relationships of this form can be obtained from equation (3), considering stress as a constant,

(e.g. 45).

1. Differentiating equation (3) with respect to time

$$\frac{d\varepsilon}{dt} = pA\sigma^n t^{p-1}$$

time or age hardening form of equation.

2. Taking the  $p^{\text{th}}$  root of both sides of equation (3) and differentiating with respect to time,

$$\frac{d\varepsilon}{dt} = pA^{\frac{1}{p}} \sigma^{\frac{n}{p}} \varepsilon^{\frac{p-1}{p}}$$

strain hardening type of equation.

3. Squaring both sides of equation (3) and differentiating with respect to time,

$$\frac{d\varepsilon}{dt} = \frac{pA^2 \sigma^{2n} t^{2p-1}}{\varepsilon}$$

this is a combined strain and time hardening relationship since both strain and time are contained on the right hand side of the equation. Obviously an infinite number of relationships of this form can be obtained.

Under conditions of constant stress these relationships all yield identical results, since, if the stress is kept constant and integration with respect to time is carried out, each relationship reduces to equation (3). In general they will provide different results in varying stress situations. The complex stress forms of these equations may be obtained by application of the appropriate stress criterion and flow rule. Equations of this form are often referred to as mechanical theories of creep.

Creep tests under conditions of non-steady complex stress have been

carried out by Johnson, Henderson and Mathur (46) on some isotropic materials selected from the group used for the steady complex stress creep testing programme. These tests were again carried out on thin-walled tubes under combined tension and torsion. A pure tensile stress was initially applied to the specimens and at selected stages in the tests an increment of torsion was added. Thus the direction, together with the magnitude of the principal stresses, was varied during the tests. From the results of these tests, Johnson et al investigated the mechanical theories of creep and also a generalised version of the Boltzmann superposition theory in which it was considered that each element of loading, or corresponding element of creep strain, continued uninterrupted to the conclusion of all stages, the total creep being the sum of all such elements. The relationships were based on the von Mises criterion and flow rule and for the mechanical theories took the general form:-

$$1. \quad C_{ij} = AF(J_2) S_{ij} \phi(t)$$

time-hardening,

where  $C_{ij}$  is the creep rate and  $S_{ij}$  is the stress deviation term,

$$\text{i.e. } S_1 = \frac{2}{3} [\sigma_1 - \frac{1}{2}(\sigma_2 + \sigma_3)]$$

$$2. \quad C_{ij} = \frac{F_1 [AF(J_2)S_{ij}]}{f_1(\epsilon_{ij})}$$

strain-hardening,

$$3. \quad C_{ij} = \frac{F_2 [AF(J_2)S_{ij}] \phi(t)}{f_2(\epsilon_{ij})}$$

combined strain and time-hardening.

It was found that none of these theories provided a good representation

of the experimental results. In general, low values of total creep strain were predicted by the time-hardening and super-position theories, while high values were predicted by the strain-hardening and best form of combined theories, and it was necessary to make use of a more general relationship of the form:-

$$C_{ij} = [F(J_2) - f(I_2)] S_{ij} \phi(t)$$

where  $f(I_2)$  is the integrated invariant creep strain before the current stage of the test.

Later work by Johnson and Khan (47) showed that the simple time-hardening form of equation was able to represent the results of similar tests on copper at 250 °C.

Further creep tests under changing complex stress have been reported by Namestnikov (48). These tests were carried out on thin-walled tubes of aluminium alloy, copper and austenitic steel under combined tension and torsion. The applied loading was varied during these tests in such a manner that the ratios of tension to torsion remained constant during the tests. It was concluded from these tests that the Lévy Mises relationships were applicable to changing complex stress systems in creep for the case of proportional loading and suggested that as in time independent plasticity, they should apply in cases somewhat removed from proportional loading.

In general it has been established that the creep behaviour of metals under complex stress systems, within a limited range of stress and temperature can very often be predicted satisfactorily by means of equations derived from theories of time independent plastic flow. Equations of this

form have been applied to provide solutions to many practical problems involving complex stress creep and their application to the creep of a thick-walled cylinder under internal pressure will be discussed in the following chapter.

CHAPTER 2

CREEP OF THICK-WALLED CYLINDERS UNDER  
INTERNAL PRESSURE - REVIEW OF LITERATURE

2.1 Analytical approaches

Many different methods of analysis are possible, depending upon the particular feature of cylinder creep behaviour of interest. On initial application of internal pressure to a metallic thick-walled cylinder at elevated temperature non-uniform stresses are set up in the wall of the cylinder instantaneously. If the applied pressure does not cause yielding of the cylinder material, the initial distributions of the principal stresses in the tangential, radial and axial directions, in the cylinder wall due to the pressure loading may be obtained from the Lamé equations, which apply to elastic behaviour of the cylinder material. If the internal pressure is high enough to cause plastic yielding of the cylinder material, the initial distribution of the principal stresses will not be the elastic distribution and may be estimated by methods based on the theory of plasticity (e.g. 1).

It is generally agreed that the initial stress distribution due to pressure loading is modified by creep and changes with time. Each element of material in the cylinder wall, therefore, is subjected to a system of changing complex stress. Creep, like plastic flow, occurs very substantially at constant volume and redistribution of the principal stresses continues until a stress distribution is attained which allows creep to proceed at constant volume while the strain compatibility requirements of the cylinder

are fulfilled without the contribution of changes in elastic strain which can only be obtained from changes in stress. This stress distribution is known as the steady-state stress distribution and Bailey (2) has derived equations providing the principal stress distributions in the cylinder wall under steady-state conditions. The time necessary for steady-state conditions to be set up in the cylinder wall depends upon the initial stress distribution and the nature of the material. Very long times may be required for creep resistant materials while very short times, of the order of seconds only, may be sufficient for materials with little creep resistance. As creep deformation takes place, the cylinder diameter increases and the wall thickness decreases causing a continuous increase in stress level if the internal pressure remains constant. The effect of this stress increase is probably negligible during stress redistribution when the total strains are small since the creep strains are of the same order of magnitude as the elastic strains.

Experimental creep data obtained from thick-walled cylinders under internal pressure yield creep curves similar in form to creep curves obtained from uniaxial tension tests and may be divided into stages of primary, secondary and tertiary creep leading to rupture of the cylinder. All of these features have received attention in the literature but the main concern here will be with primary and secondary creep analyses.

The simplest form of creep test is the uniaxial tension test, and almost all of the analytical work has been centered on the prediction of cylinder creep behaviour from uniaxial tension creep data. It was pointed out recently, however, that torsion creep data may be more rewarding than tension creep data for this purpose (3). If the prediction of cylinder

creep strains of the order of 1 per cent or more is the objective there is little error in neglecting elastic strains and stress redistribution and assuming that the steady-state stress distribution is set up in the cylinder wall immediately upon application of the internal pressure. This approach has been adopted by many investigators and has been applied to both primary and secondary creep. Other investigators, considering primary creep, have taken account of elastic effects and stress redistribution in their analyses.

A knowledge of the redistribution of stress which occurs with creep in the wall of a thick-cylinder under internal pressure is of importance in considerations of rupture life, as the criterion of failure may vary greatly among metallic materials. In high strength, low ductility materials used in the construction of high pressure plant the criterion of failure may be the maximum principal stress rather than a function of the shear stresses (e.g. 4) and in the wall of a thick cylinder during stress redistribution the maximum principal stress may change not only in magnitude but also in position in the wall.

## 2.2 Secondary creep analyses

Many analyses have been carried out in an attempt to describe the secondary creep of a thick cylinder under internal pressure where the creep rates are independent of time. Complex-stress creep relationships have been employed of the form discussed in section 1.2, considering steady state stress conditions. In these analyses, two main assumptions have been made in addition to the assumptions of isotropic material and constant volume creep deformation inherent in the creep-rate/stress relationships.

The first is that initially plane cross sections of the cylinder remain plane during creep, which is a very reasonable assumption for the central portion of a long cylinder from considerations of equilibrium and symmetry. The second is that the creep-rate in the axial direction of the cylinder is zero. Bailey (5), considering that the hydrostatic stress was ineffective in causing creep, compared the creep of a thin-walled cylinder under internal pressure with the creep of a thin cylinder in torsion. He postulated that constancy of wall thickness in a cylinder under torsion corresponded to a condition of constant axial length in a cylinder under internal pressure, and demonstrated the validity of his hypothesis from the results of an internal pressure creep test on a thick-walled lead cylinder. In his 1935 paper, (2), Bailey applied his generalised complex-stress creep relations to the case of a thick cylinder under internal pressure and obtained a closed solution for the secondary creep rates. He derived equations for the principal steady-state stresses, at any point in the cylinder wall, which were;

$$\sigma_{\theta} = \frac{P \left[ \left(\frac{a}{b}\right)^{\frac{2}{n}} - \frac{n-2}{n} \left(\frac{a}{r}\right)^{\frac{2}{n}} \right]}{1 - \left(\frac{a}{b}\right)^{\frac{2}{n}}}$$

$$\sigma_r = \frac{-P \left[ \left(\frac{a}{r}\right)^{\frac{2}{n}} - \left(\frac{a}{b}\right)^{\frac{2}{n}} \right]}{1 - \left(\frac{a}{b}\right)^{\frac{2}{n}}}$$

$$\sigma_z = \frac{P \left[ \left(\frac{a}{b}\right)^{\frac{2}{n}} - \frac{n-1}{n} \left(\frac{a}{r}\right)^{\frac{2}{n}} \right]}{1 - \left(\frac{a}{b}\right)^{\frac{2}{n}}}$$

where  $\sigma_{\theta}$ ,  $\sigma_r$  and  $\sigma_z$  are the principal stresses in the tangential, radial and axial directions respectively, P is the internal pressure, a, b and r are inside, outside and reference radii respectively, and n is the stress exponent obtained from uniaxial tension data.

Although Bailey's generalised creep-rate equations were of an anisotropic form which did not agree with the Lévy Mises equations, similar steady-state stress equations have been obtained from isotropic relationships based on the Lévy Mises equations and employing both von Mises and Tresca criteria (6, 7). Bailey showed also that the assumption of zero axial creep satisfies the axial equilibrium condition.

Similar analyses have been presented by Johnson (6), Traexlar (8) and Weir (9) and the case of heat transmission through the cylinder wall has been treated in (8) and (9). Finnie (10) has considered the case of a thick-walled cylinder under internal pressure with an end load applied in addition to the pressure end load. When the ratio of applied end load to pressure end load was very small or very large it was shown the stresses could be obtained accurately by direct superposition of the effects of pressure loading and the additional axial end load. However, in the intermediate region a numerical method had to be used to obtain the stress values. When the axial end load was zero, the analyses predicted zero axial creep. Although no assumptions concerning axial creep were made by Finnie in the analysis, the steady-state stress equations assumed for the case of no additional end load were similar to Bailey's and zero axial creep is inherent in these equations.

In these analyses, no account has been taken of the increase in stress level due to the change in cylinder dimensions as creep progresses. This problem was tackled by Rimrott (11) who presented a method of analysis

which in other respects was very similar to previous analyses. By means of the concept of true stress and true strain a solution was obtained for creep rates in terms of instantaneous cylinder dimensions. It was shown that for a material in the secondary stage of creep, cylinder creep rates are not constant but steadily increase because of the stress increase due to wall thinning. This demonstrates the limitation imposed upon steady state secondary creep analyses by virtue of the creep deformation itself.

### 2.3 Primary creep analyses.

In 1951, Bailey (12) presented a modified version of his general complex-stress creep relationships designed to cover steady-state creep in primary, secondary and tertiary stages. These equations were again based on the von Mises criterion but were now simplified to agree with the von Mises flow rule. The form of the equations was:-

$$\dot{\epsilon}_1 = A\sigma^{*n} \left[ \sigma_1 - \frac{1}{2}(\sigma_2 + \sigma_3) \right] t^p$$

$$\dot{\epsilon}_2 = A\sigma^{*n} \left[ \sigma_2 - \frac{1}{2}(\sigma_3 + \sigma_1) \right] t^p$$

$$\dot{\epsilon}_3 = A\sigma^{*n} \left[ \sigma_3 - \frac{1}{2}(\sigma_1 + \sigma_2) \right] t^p$$

i.e. time-hardening in form.

The stages of creep could be represented by adjusting the value of the time exponent. Thus for primary creep  $p$  is negative, for secondary creep  $p$  is zero and for tertiary creep  $p$  is positive. Bailey recognised that to break the creep curve into distinct stages characterised by specific values of  $p$  was an approximation and expected that  $p$  would gradually change from one stage to the next. These equations were applied

to the creep of a thick-walled cylinder under internal pressure and results were obtained for typical distributions of steady-state stresses in the wall of the thick cylinder during primary, secondary and tertiary creep. The stress distributions for each stage of creep were different and it was suggested by Bailey that stress redistribution was a function of the changing time exponent. This result is obtained purely because of the nature of the Bailey creep-rate equations. The equations used by Bailey to determine steady-state stress distributions had the same form as those presented in section 2.2 and the stresses, therefore, depend only upon internal pressure, cylinder dimensions and the value of stress exponent used in the creep relationships. The starting point for the derivation of these creep relationships was a uniaxial stress relationship of the strain-hardening form:-

$$\dot{\epsilon} = B\sigma^m \epsilon^{-q}$$

which was integrated with respect to time at constant stress:-

$$\epsilon = [B(q + 1)]^{\frac{1}{q+1}} \frac{\sigma^{\frac{m}{q+1}}}{t^{\frac{1}{q+1}}}$$

In this equation it can be seen that the stress exponent is now a function of the time exponent. This feature was retained during the analysis and is contained in the general creep-rate/stress relationships presented by Bailey in the paper. This means that if the time exponent changes during creep, the stress exponent must change also causing a corresponding change in the stress distribution obtained from the Bailey equations. It also implies that stress and time are not functionally separable variables. A great deal of evidence has been accumulated by

Johnson et al which demonstrates that these variables are, in fact, separable. No attempt has been made to apply the Bailey relationships to describe all stages of creep of a thick cylinder and their use has been restricted to the primary stage with the assumption that the time exponent is constant and that the functions of stress and time are separate.

The first solution for primary creep of a thick cylinder under internal pressure to take into account stress redistribution was presented by Coffin, Shepler and Cherniak (7). As in all the solutions described here the assumptions were made that the material was isotropic and that initially plane cross sections of the cylinder remained plane during creep deformation, and uniaxial tension creep data was used to describe material creep properties. Standard uniaxial tension creep curves of strain/time with stress as parameter were converted to isochronous curves of stress/strain. The curves were then converted to isochronous curves of effective stress/effective strain by considering that the Tresca criterion was the basis of equivalence of complex stress systems. These curves were used in conjunction with the equations of stress equilibrium and strain compatibility to obtain a solution for the stress and strain distributions in the cylinder wall at any selected time. A numerical, iterative procedure was adopted, starting from an assumed distribution of  $E\bar{\epsilon}$  against  $r/R_0$  in the cylinder wall (where E is Young's modulus,  $\bar{\epsilon}$  is the effective strain and r and  $R_0$  are the reference radius and the outside radius of the cylinder respectively). The iteration was continued until the distribution of  $E\bar{\epsilon}$  at the end of a trial had converged to the  $E\bar{\epsilon}$  distribution at the beginning of the trial. Generally convergence was achieved after only two or three such trials. The analysis was applied

to a 12 per cent chromium steel cylinder of diameter ratio 2 under an internal pressure of  $12,000 \text{ lbf/in}^2$  at  $850^\circ \text{F}$ , using tension creep data obtained by McVetty and presented by Soderberg (12). Sufficient times were selected to provide a description of the variation of stress and strain distributions in the cylinder wall with time. The solution was shown to be applicable to a cylinder with a steady radial temperature gradient in the wall, requiring only additional isochronous curves for the material at different temperatures. Although the analysis was designed for manual computation and convergence is rapid, the calculation is time consuming and the method can be easily adapted for calculation by digital computer. Recently the Coffin analysis was applied by Skelton and Crossland (13) and found to provide a poor representation of their thick-walled cylinder creep data. Probably the main criticism of the Coffin analysis is the use of deformation theory which eliminates the necessity of following the strain history of the material by means of small time increments. The solution is also independent of initial loading stress distribution.

Incremental methods of analysis were first applied to creep under changing complex stress by Poritsky and Fend (14) and Mendelson et al (15). The method consists essentially of obtaining some form of equation of state for the material, generally from uniaxial tension creep data. Starting then from the initial loading stress and strain distributions in the structure being investigated (e.g. thick-walled cylinder, rotating disc, beam etc.) stress and strain distributions are calculated at the end of very short intervals of time in such a way that the equations of force equilibrium and strain compatibility, in conjunction with any necessary

assumptions, are satisfied at the end of each interval. The use of a digital computer is essential in a solution of this nature.

Such a method has been applied to the creep of a thick-walled cylinder under internal pressure by Wilson and Davis (16). The equation of state for creep adopted was of the strain-hardening variety based on the von Mises criterion and flow rule and took the form:-

$$\frac{d\epsilon''_{EFF}}{dt} = \frac{K \sinh \frac{\sigma_{EFF}}{\sigma_1}}{(\epsilon''_{EFF})^m}$$

where  $\sigma_{EFF}$  and  $\epsilon''_{EFF}$  are the effective stress and effective creep strain respectively corresponding to the von Mises criterion.  $K$ ,  $\sigma_1$  and  $m$  are constants, evaluated from uniaxial tension creep tests. Total strain at any time was considered to be the sum of the elastic and creep components, and using the additional information obtained from the equations of equilibrium and compatibility a method of solution was described using an incremental approach similar to that suggested by Mendelson and Manson (17). Short time intervals were taken during which it was assumed that the stresses did not change. The total strains at the end of a time interval were determined together with the creep strains produced during the time interval. These creep strains were added to the accumulated creep strains at the beginning of the time interval to provide total accumulated creep strains at the end of the time interval. Accumulated creep strains were subtracted from total strains to obtain the elastic components of strain and hence the stresses to provide the starting point for the next time interval. The solution was applied to a copper cylinder of diameter ratio 4 under an internal pressure of 7,300 lbf/in<sup>2</sup> at 165 °C utilising uniaxial tension

creep data obtained by Davis (18). The computations were carried out at sixteen points in the cylinder wall by means of a digital computer and the results presented graphically. A systematic error was found to appear because of the method of stress calculation. The elastic strains and hence the stresses depended upon the difference between total strains and creep strains which became increasingly inaccurate with increasing strain.

Another incremental method of solution was presented by Smith (19). The only assumption necessary in this analysis was the existence of an equation of state for the material and any form of such equation could be accommodated. The analysis was also capable of dealing with transient temperature and pressure conditions. Again short time intervals were taken during which loading conditions were substantially constant. The equations necessary for a solution were obtained from considerations of equilibrium and compatibility and the relationship between total strain and creep, elastic and thermal strains. The creep strains occurring during a time interval were obtained from the specific creep relationship adopted. Using these values, the equations were solved simultaneously, by digital computer, using a numerical finite difference procedure and the complete stress/strain distribution in the cylinder wall determined at the end of the time interval. This provided the starting point for the next time interval. Results were presented for a cylinder of diameter ratio 2 of 0.2 per cent carbon steel under internal pressure of  $10 \text{ tons/in}^2$  at  $450^\circ \text{C}$ , the data being obtained from (20). This form of solution required a great deal of computer time.

A different form of incremental approach was adopted by Voorhees, Slipevich and Freeman (21) in an analysis designed to obtain information

concerning stress redistribution due to creep in the wall of a thick cylinder under internal pressure, with a view to prediction of creep rupture life. The cylinder was considered to be made up of thin, concentric shells in which the stresses and strain-rates were assumed constant during small time intervals. The elastic stress distribution was taken as the starting point and mean values of effective stress calculated at the radius of gyration of each shell. The effective strain in each shell was calculated at the end of a short time interval of steady creep. The shells were then made to fit together again by superimposing a compressive load on the inner face of each shell and a tensile load on the outer face. A new stress was then estimated for each shell from the algebraic sum of the original stress and the two increments of stress to provide the starting point for the next time interval. In this way an estimation of the redistribution of stress with time in the wall of the cylinder was obtained. Smith (22) has presented an analysis based on this concept which avoids the assumptions of the Voorhees analysis that strains may be equated at different radii in the cylinder wall and that a change in strain in one part of the wall does not immediately affect all other parts of the wall.

A method of analysis designed for manual computation has been presented by Johnson, Henderson and Khan (20) which provides a solution for stress and total strain-rate distributions in the wall of a thick cylinder during creep under internal and external pressures in the region where elastic and creep strains are of comparable magnitude. A von Mises criterion and flow rule was assumed and equations of the time-hardening variety were formulated for the total strain-rates in the cylinder wall,

$$\dot{\epsilon}_r = \frac{2}{3}A(J_2)^{\frac{n}{2}}[\sigma_R - \frac{1}{2}(\sigma_\theta + \sigma_z)]\phi(t) + \frac{1}{E} \frac{d[\sigma_R - \mu(\sigma_\theta + \sigma_z)]}{dt}$$

$$\dot{\epsilon}_\theta = \frac{2}{3}A(J_2)^{\frac{n}{2}}[\sigma_\theta - \frac{1}{2}(\sigma_r + \sigma_z)]\phi(t) + \frac{1}{E} \frac{d[\sigma_\theta - \mu(\sigma_r + \sigma_z)]}{dt}$$

$$\dot{\epsilon}_z = \frac{2}{3}A(J_2)^{\frac{n}{2}}[\sigma_z - \frac{1}{2}(\sigma_\theta + \sigma_r)]\phi(t) + \frac{1}{E} \frac{d[\sigma_z - \mu(\sigma_\theta + \sigma_r)]}{dt}$$

where  $\sigma_r$ ,  $\sigma_\theta$  and  $\sigma_z$  are the radial, tangential and axial stresses respectively,  $\dot{\epsilon}_r$ ,  $\dot{\epsilon}_\theta$  and  $\dot{\epsilon}_z$  are the total strain-rates in the radial, tangential and axial directions respectively,  $\mu$  is Poisson's ratio, and A and n are creep constants obtained from uniaxial tension creep data. It was assumed that, in the axial direction, the creep strain was zero and the elastic strain was constant with respect to time and radius. This assumption allowed the elimination of the axial stress from the analysis since now,

$$\sigma_z = \frac{\sigma_\theta + \sigma_r}{2}$$

and also  $\dot{\epsilon}_z$  is zero. These equations were combined with the conditions of radial equilibrium and total strain compatibility, and a procedure was described, involving graphical integrations, to determine the stress and total strain-rate distributions in the cylinder wall at any time. The boundary conditions imposed on the stress distributions were the initial elastic or Lamé stresses on loading at time zero and the steady-state or Bailey distribution at infinite time. The analysis was applied to thick cylinders of diameter ratio 2 of various materials at temperatures and pressures in their normal working range, by use of data accumulated by Johnson et al in experimental investigations using these materials. It

was suggested by Larke and Parker some years later (24) that the predictions of circumferential strain at the bore and outside surfaces of the cylinder inherent in the Johnson analysis are identical to the predictions of the simple Bailey analysis (12) which assumes a steady-state stress distribution and neglects elastic strains. This is not the case and will be considered in a later chapter. The Johnson analysis has also been applied by Skelton and Crossland (13) to their experimental cylinder creep data and found to provide a fair representation of the data, although it was felt that an even better correlation could be achieved if uniaxial tension creep data pertaining to times of greater duration than the 150 hours recommended by Johnson et al were used.

A novel method of primary creep analysis in the presence of stress redistribution has been presented by Marriott and Leckie (25). It was observed that during stress redistribution due to creep in the wall of a thick cylinder under internal pressure, there is a point in the wall at which the effective stress remains almost constant. This leads to a very simple method of primary creep strain prediction and will be discussed in more detail in a later chapter.

#### 2.4 Review of experimental work

Although the creep of thick-walled cylinders under internal pressure has been a problem of major significance, especially in the power industry, for many years and has led to a vast amount of analytical work, relatively few relevant experimental investigations have been undertaken. Moreover much of the data accumulated in these investigations has little application

to the general understanding of the subject since the object of the investigators was to obtain a timely answer to a specific pressing problem. The simplest, and most commonly used, form of creep test is the uniaxial tension creep test, and the accurate prediction of thick-walled cylinder creep data from uniaxial tension creep data is the main objective of the research described in the body of this thesis. This has also been the objective of some of the investigations discussed here. The major simplifying assumption inherent in most cylinder creep analyses is that of zero axial creep and this assumption has been investigated experimentally several times. Lead and lead alloys have been used extensively as a test material since low pressures and fairly conventional strain measuring techniques can be employed, generally at room temperature. The use of other, more creep resistant, materials entails the design and construction of more elaborate equipment to achieve elevated conditions of pressure and temperature, and strain measuring techniques to operate for long times under these conditions.

#### 2.4.1 Investigations using lead and lead alloys

Bailey (5) presented the results of a creep test on a lead cylinder of diameter ratio 3 carried out at room temperature with an internal pressure of  $1,200 \text{ lbf/in}^2$ . A microscope was used to measure changes in circumference and length during the test which had a duration of just over two hours and was designed to check the validity of the zero axial creep assumption. The test was continued until the mean circumferential strain was over 5 per cent and no appreciable change in length was detected up to the point where local bulging of the tube began.

Moore et al (26, 27) have described creep tests on tubes in the form of commercially produced lead alloy sheathing. The tests were carried out over long periods of time at room temperature with an internal pressure of  $25 \text{ lbf/in}^2$  produced by oil, pressurised by a mercury column. Diametral extension was measured during the tests by means of a dial gauge micrometer with anvils locating on steel studs soldered to the outside surface of the specimens. Although, in this way, no damage to the outside surface of the soft specimens was caused by the micrometer anvils, satisfactory diametral strain measurements could not be obtained since the steel studs constrained the specimens at their position of contact. Tensile creep tests were carried out on longitudinal and traverse specimens machined from a flattened sheet of the sheathing and the results showed that the material had no marked directional characteristics. It was shown, however, that these isotropy tests were invalid since the creep properties of the sheathing were severely affected by the flattening operation (28).

Creep tests on lead tubes at room temperature, in which the pressure was increased in steps and held constant at each step until a steady creep rate was recorded were reported by Nakahara (29). A tensile creep test was carried out in a similar manner with step increases in the applied load, to obtain constants for use in the Bailey analysis (2) to predict the tube strain-rates. This testing programme is clearly unsatisfactory because of the progressive difference in strain history between the tensile and tubular specimens. Long time creep tests on lead tubes at pressures up to  $150 \text{ lbf/in}^2$  have been reported by Latin (30). In these tests, low pressures were produced by nitrogen gas while the higher pressures in the

range were supplied by water, pressurised by nitrogen. Diametral strain measurements to an accuracy of  $2 \times 10^{-3}$  were made by means of a tape.

More recently Smith (31) carried out internal pressure tests on thick-walled tubes of a lead-tin alloy at  $30^{\circ}\text{C}$  in this laboratory. The main object was an investigation of axial creep in the tubes. Axial and diametral strains were measured by means of an intricate system of Martens extensometers attached directly to the gauge length of the specimen. While the sensitivity of this extensometry was much greater than in the previous experimental work on lead, the deformation of the specimens was to some extent constrained by the extensometry and inaccuracy due to "digging in" was encountered. An attempt was made to measure the internal diametral strain also. Two tubular specimens, differing in length by two inches, but identical in other respects were tested simultaneously. The additional pressurising oil supplied to provide for the increase in internal volume of the specimens during the tests was measured by providing a mercury/oil interface, the rise in level of the mercury in a glass capillary tube being measured by means of a cathetometer. The internal diametral strain was deduced from the difference between the quantities of oil supplied to the long and short tubes. To provide a constant internal pressure in the tubes a hydraulic accumulator was used, designed on the principle of the dead-weight balance and incorporating a Morrison seal. This system, designed to produce pressures up to  $4,000 \text{ lbf/in}^2$  was extremely sensitive and has been used in the present series of tests. The isotropy of the material was investigated by means of tensile creep tests and found to be poor. Smith concluded that the advantages of lead as a test material

were outweighed by the difficulties of obtaining isotropic material, and machining, handling and storing of the specimens which deformed under their own weight at room temperature, and continued his investigations using a magnesium alloy. The work of Smith was extended by King (23) who tested thick-walled cylinders of super-pure aluminium and an aluminium alloy under internal pressure at 250 °C. Uniaxial tension creep data were obtained for these materials and used to predict cylinder creep behaviour. Some of this work has also been reported in (32).

#### 2.4.2 Investigations at elevated temperatures

The first creep tests on tubes under internal pressure seem to have been carried out by White and Clark (33, 34) who tested tubes of carbon steel and chromium-carbon steel at temperatures up to 1500 °F and pressures up to 1,400 lbf/in<sup>2</sup>, to times of the order of 2,000 hours. The tubes were pressurised by nitrogen supplied from the high pressure side of an intensifier with oil on the low pressure side, pressurised by a dead-weight accumulator. The test temperature was maintained by a horizontal electric furnace mounted on wheels to facilitate its removal at regular intervals when the specimen diameter was measured by means of callipers. This method of measuring diametral expansion is not altogether satisfactory in view of the temperature cycling of the specimen introduced by the removal of the furnace.

The tests described by Norton (35, 36) and Norton and Soderberg (37) are quite outstanding for experimental technique, even by present day standards. The tests were carried out on cylinders of carbon-molybdenum

steel and chrome-molybdenum steel of 4 inches outside diameter and parallel length of about 24 inches. The diameter ratios were 1.07 and 1.23. Long time internal pressure creep tests were carried out at temperatures up to 1200 °F and pressures up to 9,240 lbf/in<sup>2</sup>. The test temperature was provided by a vertical electric furnace and temperature control was achieved by thermal expansion and contraction of the furnace tube, magnified by a lever system which operated contacts in the heating circuit. By this means the temperature level was controlled to  $\pm 1$  F° with a distribution over the specimen gauge length within  $\pm 3$  F°. This degree of temperature control is not easily achieved at the present time. Nitrogen from an accumulator was used to pressurise the cylinders. The accumulator, which contained oil at the bottom, was charged with bottled nitrogen up to a pressure of 2,000 lbf/in<sup>2</sup>. Thereafter higher pressures were attained by increasing the volume of oil in the accumulator by a hand pump. The volume of nitrogen inside the specimen was kept to a minimum by means of a filler which allowed only 1/16 inch free space inside the specimens. Cylinder creep rates were small and the pressure was maintained within  $\pm 1$  per cent by pumping up every morning and night. These tests are unique in that they are the only tests in which continuous and accurate diametral and axial creep strain measurements have been made at high temperatures. Diametral expansion was measured in two mutually perpendicular directions at the middle of the gauge length. Four small fused quartz tubes passed through the furnace wall in the required directions and each quartz tube was spring loaded against a platinum fixture welded to the outside surface of the specimen. A pair of telescopes were used

to measure the distance between the outer ends of the quartz tubes. The accuracy of the strain measurement was estimated at  $6 \times 10^{-6}$ . Axial strains were measured on diametrically opposite sides using the same telescopes to sight through windows in the furnace wall on Vee marks made in platinum wires spot welded to the specimen surface, providing a 10 inches gauge length. The accuracy of the axial strain measurements was estimated at  $2.5 \times 10^{-6}$ . In conjunction with these tests tensile creep tests were carried out on specimens with a 10 inch gauge length cut from the walls of the same batches of tubing. All specimens were carefully annealed before testing and it was assumed that the degree of anisotropy would be small.

Davis (38) reported creep tests under internal pressure and combined internal pressure and axial tension on thick-walled cylinders of type 316 stainless steel with diameter ratios of 2 and 3. The test temperature was 1200 °F and pressures up to 24,000 lbf/in<sup>2</sup> were applied. The specimens were enclosed in an electric furnace which was reinforced since rupture times were of major interest. Water was used as the pressurising medium and pressures were attained by an air operated pump. Constancy of pressure was maintained by a dead-weight pressure balance, continuous motion of the piston being assured by a small calibrated leak. In the pure internal pressure tests, diametral expansion was measured by some form of lateral extensometer with a magnification of 10 and the occurrence of creep in the axial direction checked by comparing specimen lengths before and after tests. In the tests under combined tension and internal pressure, axial strain was measured by an extensometer attached to the shoulders of the specimen, and diametral strain estimated at various times by stopping the test and

removing and measuring the specimen. Tensile creep tests were carried out on specimens from the same piece of material but no real consideration was given to isotropy. Tests similar to these combined tension and internal pressure tests have been reported by Ohnami and Awaya (39) who measured diametral and axial strain on tubes of 0.12 per cent carbon steel at 550 °C without interrupting the tests, by means of an arrangement of rods and levers, attached to the specimen and extending outside the electric furnace.

Other tests carried out in Japan have been described by Taira, Koterazawa and Ohtani (40) who tested cylinders of 0.19 per cent carbon steel of diameter ratio 2 at 450 °C and internal pressures up to 20,000 lbf/in<sup>2</sup>. The specimens were enclosed in an electric furnace and the temperature over the specimen gauge length maintained within  $\pm 1$  °C during the tests. Water from high pressure reservoirs was used as the pressurising medium, the pressure being attained by means of a hand operated pump. The pressure was maintained constant within  $\pm 1$  per cent by heaters, installed in the high pressure reservoirs and controlled by a pressure switch. Diametral expansion of the tubes was measured by diametrically opposed probes, passing through the furnace wall and contacting the specimen at three positions along its length. Movement of the probes was measured by means of dial gauges. Associated uniaxial tension creep data was obtained from the material and isotropy was investigated by means of uniaxial tension creep tests on specimens from the axial and tangential directions of the cylinder material. An attempt was also made to measure residual stresses in the wall of the cylindrical specimens after the tests.

Parker (40) has described equipment for creep testing thick-walled metal cylinders under internal pressures up to 10,000 lbf/in<sup>2</sup> at temperatures up to 400 °C. Very low creep-rate tests were envisaged of durations of the order of 10,000 hours and argon was employed as the pressurising medium to minimise the effects of chemical attack at the bore of the cylinders where the strains are highest. The test assembly was located in a blast-proof room separate from the main laboratory which contained the control gear. A geared motor drove a four piston oil pump which fed oil to one cylinder of a two cylinder mercury compressor. The second cylinder contained argon gas which was brought to the required pressure by the oil pump. Pressure control was by means of an electric contact pressure gauge which operated the motor and allowed automatic maintenance of the pressure. A warning light indicated a dangerously low level of argon in the mercury compressor which could be recharged. The 10 inch long specimen was arranged horizontally in an electric furnace which was also 10 inches long. It was found that even with so short a furnace the temperature variation over the central 4 inch length of the specimen did not exceed about 3 C° and the difference between bore and outside surface temperatures was never greater than 2 C°. Temperature conditions were maintained within  $\pm 1$  C° over long periods by means of a saturable reactor type of controller. Both diametral and axial strains could be measured, diametral extensions by a method similar to that of Norton (35) measuring probe movement by means of transducers with a nominal sensitivity of 10<sup>-6</sup> ins, and axial strains by means of a conventional design of extensometer employing two similar transducers and having a 2 inch gauge length.

Recently some results of a very comprehensive experimental investigation

of creep behaviour of thick-walled cylinders under internal pressure were published by Skelton and Crossland (42). The object of the investigation was the prediction of thick cylinder creep behaviour from associated uniaxial tension creep data. The material used in the investigation was a 0.19 per cent carbon steel and great care was taken to ensure that the material was as isotropic as possible. The internal pressure creep test equipment was designed for pressures up to 45,000 lbf/in<sup>2</sup> and temperatures up to 750 °C. The creep tests reported were carried out at 450 °C and pressures up to 20,000 lbf/in<sup>2</sup>. The specimen was enclosed in a five-zone horizontal electric furnace allowing the gauge length temperature gradient to be trimmed to less than 2 C° and temperature stability within  $\pm 1.5$  C° was achieved over 3000 hours by means of a saturable reactor type of temperature controller. Water was used as the pressurising fluid, a hand operated intensifier being used to induce the initial operating pressure. The test pressure was measured by means of an electric contact pressure gauge and maintained constant by a small pressure compensator in the form of a thick-walled cylinder water reservoir carrying a small electric heater. This heater was operated by the pressure gauge contacts when the test pressure fell and the pressure was restored by expansion of the water in the compensator. Provision was made for recharging the compensator without interruption of the pressure. In this way the test pressure was maintained within  $\pm 0.5$  per cent during the tests. To enable diametral strains to be measured during the tests small spherical indentations were machined at diametrically opposed points on the outer surface of the specimen at the middle of the gauge length. The extensometer consisted essentially of a rod, sliding freely in a tube. The specimen

was secured horizontally and the tube suspended from the upper spherical seat, while the rod was spring loaded into the lower spherical seat. The tube carried the body of a linear displacement transducer and the rod made contact with the core. Differential movement of the rod and tube due to changes in the specimen diameter were sensed by the transducer which was connected to a multi-channel read out meter. Creep strains of the order of  $5 \times 10^{-6}$  could be measured. The creep test rigs were located in separate, thermostatically controlled cubicles outside the main laboratory which contained the control and measuring equipment, to limit damage in the event of specimen rupture. Uniaxial tension creep tests were carried out, mainly on specimens taken from the material in the axial tube direction, but two specimens were taken from the transverse direction allowing an estimate of isotropy to be made.

#### 2.4.3 Discussion of experimental techniques

In an experimental investigation undertaken to examine the accuracy of description of thick-walled cylinder creep behaviour obtained by the use of data from creep tests in uniaxial tension, the question of isotropy of the test material is of great relevance. Ideally, the method of production of the test material should ensure isotropy as far as possible and this should then be checked by a series of creep tests under simple loading conditions. Most of the experimental work reviewed concerned tests on commercially produced tubing and it is likely that different creep properties would exist in the transverse and longitudinal directions of the cylinders even when the test specimens were carefully annealed prior

to testing (35). The lead alloy tube used by Smith (31) was extruded at a temperature which assured continuous recrystallisation of the material during extrusion and even then marked anisotropy was present in the specimens. Only comparatively rarely has isotropy been considered adequately in experimental work on creep of thick cylinders. In the investigation by King (23) all the specimens were machined from a continuously cast billet of material and the isotropy of the billet was checked by uniaxial tension creep tests at two stress levels on specimens from three mutually perpendicular directions in the billet. A similar approach was adopted by Skelton and Crossland (42) who obtained their material in the form of a core trepanned from a large ingot, in a similar manner to Johnson (43). Isotropy was investigated by an extensive metallographic examination and comparison of the uniaxial tension creep behaviour of specimens from the longitudinal direction of the billet with two specimens from the transverse direction. In experimental investigations of creep rupture properties of thick-walled cylinders under internal pressure, isotropy has been considered by Voorhees et al (21) and Chitty and Duval (44). A more detailed description of the procedure of Voorhees et al is contained in (45). Some of the material used was in the form of 2 ins. diameter rolled bar and tensile creep specimens with an overall length of about 1 in. were obtained from the radial, longitudinal and tangential directions with the gauge portions from about the same radial location with respect to the axis of the bar. By the use of these small specimens it was possible to carry out uniaxial tension creep tests in each of the tube principal stress directions and it was found that reasonably isotropic behaviour could be expected with respect to rupture

times. Chitty and Duval carried out similar tests on specimens obtained from the longitudinal and tangential directions of the wall of sections of steam piping. Larger specimens were used for these tests since the radial direction was not included. They also found little directional effect on creep rupture times but stressed that comparison of creep behaviour of a material in different forms of tests must be carried out on the same cast of the material since large differences in creep rupture behaviour were to be expected between different casts of material having the same nominal composition and heat treatment. Berman and Pai (46) have indicated that isotropy tests of this kind are insufficient since no indication is afforded of possible differences in uniaxial tensile and compressive creep behaviour which can have a pronounced effect on creep behaviour under complex stress. Working on the principle that all materials are seriously anisotropic they suggest a complex stress secondary creep relationship based on an anisotropic stress surface represented by a Berman and Hodge type linear piecewise model. Pai (47) has demonstrated that the relevant points on this stress surface for the case of a thick-walled cylinder under internal pressure may be obtained from data provided by uniaxial tension creep tests on specimens from the tangential direction of the cylinder and uniaxial compression creep tests on specimens from the radial direction. The ratio of tensile and compressive stresses required to produce the same secondary creep rate is calculated and forms part of the proposed creep relationships. Although the concept of an anisotropic stress surface which does not change with increasing strain seems somewhat untenable, uniaxial creep behaviour in compression is certainly worthy of inclusion in a detailed study of material isotropy.

Control of test temperature and pressure are also important considerations since creep behaviour is generally fairly sensitive to both temperature and stress. Most of the tests on lead were carried out at room temperature and required no heating system but were probably subject to fairly large temperature fluctuations (e.g. 26, 27). Smith carried out his tests at  $30^{\circ}\text{C}$  in an air space surrounded by a water jacket. Immersion heaters controlled by a toluene regulator heated the water which was circulated in the jacket. Temperature was maintained within  $\pm 0.1^{\circ}\text{C}$  on the specimen gauge length by this means. The system operated satisfactorily at  $130^{\circ}\text{C}$  when the water was replaced with Shell Voluta Oil 27. Finnie (48) described equipment for creep rupture testing of tubes under complex stress in which a temperature of  $250^{\circ}\text{C} \pm 0.1^{\circ}\text{C}$  was achieved for periods in excess of 1000 hours on specimens immersed in a bath of silicone fluid with temperature control by means of a proportional controller operated by a resistance thermometer. At temperatures above this the electric furnace is almost always used and an extensive literature is available on the design, construction and operation of such furnaces, and although the ingenious control system of Norton provided excellent stability, similar testing conditions can be achieved by means of the relatively inexpensive proportional controllers commercially available at the present day. The manually operated pressure control system of Norton was satisfactory because of the very low tube creep rates, but later investigators employed devices with a greater degree of automatic compensation. In investigations of creep rupture in tubes (49, 50) the pressurising medium, water, was supplied from a large, thermostatically controlled high pressure reservoir which ensured that small changes in specimen volume had little effect on the pressure. Here again the occasional necessary adjustments were made

manually. Essentially similar fully automatic pressure control systems have been used for creep and creep rupture testing (42,44). At lower pressures, dead-weight pressure balance systems can provide excellent pressure stability over long periods. The device used by Smith was shown to be sensitive to better than  $\pm 0.1$  per cent.

Accurate continuous measurement of creep strains occurring in a thick cylinder under internal pressure presents many difficulties. To provide a fairly complete strain record it is necessary to measure the axial strain together with the diametral creep strain at the bore or outside surface. The largest strain is the diametral creep strain at the bore but measurement of this is extremely difficult and has been attempted rarely (31, 23). For maximum accuracy the extensometry should be attached directly to the specimen gauge length. Testing at elevated temperatures requires the specimen to be enclosed in a furnace and gauge length deformation has, therefore, to be transmitted outside the furnace before it can be measured. This generally entails some system of rods or probes and the overall accuracy is limited by variations in length of extensometer limbs due to thermal fluctuations. In room temperature tests on lead this problem does not arise, but extensometry which comes in contact with the surface of the soft specimens can interfere with the natural course of the deformation and provide inaccurate readings due to "digging in" or denting of the specimen surface. The problem of accurate strain measurement of specimens enclosed in furnaces at high temperatures is being solved by advances in high temperature electrical strain measuring techniques. Of these, inductive and capacitive probe systems have probably a better future in the field of high temperature materials research than resistance strain gauges. The

latter are generally limited to measurement of small strains and can set up local discontinuities in the stress system at points of contact with specimens of less creep resistant materials. One advantage of resistance strain gauges is their application to the measurement of local strain on very small gauge lengths, but this form of measurement can also be carried out by means of transducer devices in small gauge length extensometers.

Attempts have been made to measure, continuously, axial creep of cylinders under internal pressure by Bailey (5), Norton (35), Smith (31) and King (23). Bailey found negligible axial creep until local bulging of the tube began. The axial creep measured by Norton was very small indeed, and both positive and negative values were observed. This effect was attributed to directional properties in the material. Smith observed negative axial creep in his anisotropic lead tubes and positive axial creep in magnesium alloy tubes (51) and King found positive axial creep in thick aluminium tubes. In the latter investigations, however, the magnitude of the axial creep was also very small compared with creep in the tangential direction. It appears from the results of these investigations that the analytical assumption of zero axial creep which has often been made is reasonable and should lead to little inaccuracy in a determination of cylinder creep rates.

CHAPTER 3

EXPERIMENTAL INVESTIGATION

3.1 Introduction

The investigation is aimed at the accurate prediction of creep behaviour of thick-walled cylinders under internal pressure from associated uniaxial tension creep data and is largely an extension of work carried out previously in this laboratory by Smith (1, 2) and King (3, 4). It was proposed to carry out a large number of internal pressure creep tests on thick-walled cylinders over a wide range of pressure, and fairly large external diametral strains were envisaged as the effect of wall-thinning was of interest. A material was required with which such creep strains could be obtained at moderate temperature and stress levels in test times up to about 1000 hours. If any degree of success is to be achieved in such an investigation it is important that the test material is isotropic and metallurgically stable at the test temperature and also that the grain size is small enough to provide a large number of grains in the cross section of the test specimens. Ideal materials are difficult to obtain and several materials were examined in the previous work.

Smith, in his investigations of axial creep of thick tubes, used a lead alloy and a magnesium alloy. The lead alloy was found to be unsuitable as discussed in Chapter 2 and the magnesium alloy, although isotropic, was excessively creep resistant at the test temperature, requiring reduction of the diameter ratio to 1.5 to provide measurable creep strains in short times. Initially the investigation of King was concerned with the prediction of

thick cylinder secondary creep-rates from associated tension data and super-pure aluminium was chosen as the test material. This material proved unsuitable since appreciable grain growth occurred at the test temperature and the investigation was continued using an aluminium - 0.07 per cent titanium alloy. The small titanium addition refined the grain size of the material which was found to be isotropic and metallurgically stable at a test temperature of 250 °C. Unfortunately the material was unsuitable for an investigation of secondary creep behaviour since it exhibited primary creep to quite large strain levels in the tensile creep tests. The secondary stage of creep obtained in these tests was characterised more by a point of inflection on the creep curves between the primary and tertiary stages than by a period of constant creep-rate.

These tensile creep tests were of the conventional constant load type and it was thought that the minimum creep-rate and tertiary stage was caused mainly by the increase of tensile stress due to thinning of the specimens. The investigation was directed towards the primary stage of creep and difficulty was experienced in analysing the tensile creep data because of the appreciable increase of stress at high strain.

King measured diametral and axial creep strains on the thick-walled cylinders. Diametral strains were measured by means of a system based on that of Norton (5), probe movement being detected by means of dial gauges fixed to a frame surrounding the furnace. The dial gauges were found to provide sufficient sensitivity as the measurements were influenced slightly by expansion and contraction of the frame due to ambient temperature fluctuations. To measure axial strains, two specimens, differing in length

by 2 ins. were tested simultaneously. Changes in the lengths of the specimens were measured by means of extensometry secured to the end closures. It was assumed that end effects were identical in both specimens and that the difference between the change in length of the long and short specimens provided the axial strain on the 2 in. gauge length. This system requires the provision of a uniform temperature distribution over a long section of the furnace and is not entirely satisfactory due to non-uniform creep of the specimen material in the end closures since non-uniform "bolting-up" stresses cannot be avoided.

The aluminium-titanium alloy appeared to be very suitable for an investigation of complex stress creep behaviour involving large strains and accordingly material of the same nominal composition was selected for the present investigation. A continuously cast billet was obtained from the British Aluminium Company. The billet was 24 ins. long and  $9\frac{5}{8}$  ins. diameter allowing the manufacture of all the specimens necessary for the investigation and also tensile creep specimens from three mutually perpendicular directions of the billet for isotropy tests at various stress levels. The composition of the billet, "cutting up" procedure for production of the specimens, and results of metallurgical examination are contained in Appendix I. A test temperature of  $250^{\circ}\text{C}$  was again selected to provide material creep behaviour in the high temperature region above half the melting point.

It was decided to carry out uniaxial tension creep tests under conditions of constant stress to simplify analysis of the material creep behaviour in simple tension and also to carry out constant load creep tests to investigate the material creep behaviour under a simple varying

stress system. Accurate prediction of the constant load data by means of the constant stress data would provide a useful intermediate step towards prediction of the thick-walled cylinder creep data. The form of specimen used in both types of test should be identical and if possible the same testing machine should be employed to keep the number of experimental variables between the tests to a minimum. A testing machine was built which enabled the fulfilment of both these requirements.

In the internal pressure tests it was desired to measure external diametral strains and axial strains. A diametral extensometer was designed with increased sensitivity with which it was hoped strains of the order of the initial elastic strains could be measured. An axial extensometer was designed to measure strains on a single tubular specimen by direct attachment to the parallel gauge length.

### 3.2 Tensile creep tests

A tensile creep test machine was built to carry out both constant-load and constant-stress tests. Many systems have been devised to maintain constant stress in a tensile creep specimen (e.g. 6, 7, 8, 9, 10, 11, 12). For the present investigation a cam system of the Andrade-Chalmers type (7) was adopted for constant-stress tests, in conjunction with a constant radius wheel for constant-load tests (12). A description of the cam profile design is contained in Appendix II.

The profile was designed for one length of specimen, assuming that all the creep deformation in the system occurs in the specimen, the cross section of which is completely uniform between the grips. In fact the specimen has a fillet radius at each end of the gauge length to

reduce the effect of stress concentration, and creep in these fillets differs in magnitude from creep in a similar length of the parallel portion of the specimen. It is necessary, therefore, to take the effect of creep in the fillet radii into account in the determination of the effective length of specimen to be used in the cam design. Creep in the fillets of a tensile specimen has been considered by Kinsey (13) in an attempt to estimate the effective gauge length of a tensile creep specimen when the extensometry is secured to the grips. Appendix III describes the simple form of analysis employed in the present investigation and an attempt to check the validity of the analysis from experimental data. The tensile specimen was designed as shown in fig (2) and the effective length was taken as 6 ins. The framework of the machine, which supported the cam assembly and the furnace, was manufactured from mild steel channel, 5 ins. x  $2\frac{1}{2}$  ins. in section, to ensure rigidity.

Care was taken to limit inaccuracy due to non-axiality of loading. The usual method of securing the specimen to the pull-rods by means of screwed ends can lead to non-axiality and in the present tests the specimen ends were secured in double cone grips since this type of grip had proved successful in the previous creep tests (3). This type of grip has the additional advantages that the conical ends are easy to machine on specimens of soft material and the specimen is easily removed after the tests. In addition universal couplings were included in the pull-rod system above and below the specimen. To prevent bending of the specimen during assembly of the grips a simple jig was designed as shown in fig (3). The jig end pieces were bored to provide 0.002 in. clearance on the outside

diameter of the grips. The specimen was located in the grips, the loose assembly set in the jig, and the jig end pieces tightened together. Because of the small clearance the specimen and grip assembly was able to rotate freely in the jig. The grips were gradually tightened, care being taken to ensure that the assembly still rotated freely at each stage in the process. When the specimen was firmly secured in the grips, the complete assembly was connected to the pull-rods in the machine before the jig was removed. A diagrammatic layout of the loading system is shown in fig (4). For constant stress tests the applied load is connected to the cam and for constant load tests to the constant radius wheel. The load is transmitted over the curved surfaces by means of thin steel strip, 0.5 in. x 0.020 in. in section, and the strip is secured to the cam and constant radius wheel by small clamping plates with strips of thin rubber sheet inserted between the metal faces to reduce the possibility of slip. A weight was suspended from the wheel on the opposite side from the specimen assembly to balance the weight of the specimen and pull-rod assembly and ensure that the system was in equilibrium before application of the load. The bottom pull-rod was secured to a rigid cross-member in the framework.

### 3.2.1 Tensile specimen

The form of the tensile specimen, shown in fig (2), was devised from considerations discussed in Appendix III. The specimens were machined from blanks of square cross section cut from the billet of material. Maximum dimensional consistency was ensured by producing the specimens on a copying lathe requiring only diametral settings to be made by the technician. Difficulty was experienced with the

machining operations as the material was extremely ductile and cuttings did not form chips which could be easily washed away. The removed material formed a continuous strip which had to be guided away from the tool point to prevent an excessive lateral load on the specimen causing buckling. A liberal supply of cutting fluid was used and light cuts were taken at all stages to prevent possible changes in the structure of the material during manufacture of the specimens. The finished gauge length diameters of all the specimens were within  $\pm 0.0002$  in. of nominal size, and contained approximately twenty grains.

### 3.2.2 Temperature control system

A vertical electric resistance furnace was built, 2 ft. long and 10 ins. outside diameter. Use was made of the design principles described in references (14) and (15). The windings were arranged in five zones with separate shunts on the top four, and an additional guard heater was provided at the bottom of the furnace to control the axial temperature distribution. The resistance wire was wound on a silica furnace tube, and a copper liner,  $\frac{1}{8}$  in. thick, was set inside the furnace tube to reduce the effects of radiation on the specimen and assist in damping out temperature fluctuations. The copper liner had a bore of  $3\frac{1}{4}$  ins., providing adequate space for the specimen and grip assembly. Alumina powder was used as insulation. The temperature level was controlled by means of a proportional controller of the saturable reactor type. The sensing element was a ventilated platinum resistance thermometer set in a slot in the copper liner with the element about 9 ins. from the top of the

furnace. The circuit diagram is shown in fig (5). By means of the shunts and guard heater, the temperature gradient on the 5 in. gauge length of the specimen could be reduced to less than  $0.5\text{ }^{\circ}\text{C}$  fairly easily and the controller maintained the temperature level within  $\pm 0.5\text{ }^{\circ}\text{C}$ , enabling the specimen gauge length temperature to be maintained at  $250\text{ }^{\circ}\text{C} \pm 1\text{ }^{\circ}\text{C}$  for periods up to 1400 hours, The furnace was set in vertical guides and could be raised to allow assembly of the specimen in the pull-rods. Counter balancing was employed to facilitate the lifting operation.

### 3.2.3 Temperature Measurement

The specimen gauge length temperature distribution was measured during the tests by means of platinum/10 per cent platinum-rhodium thermocouples. Thin-walled P.T.F.E. sleeving was used as insulation to provide flexibility of the thermocouples. Calibration of these thermocouples within the temperature range  $245\text{ }^{\circ}\text{C}$  to  $255\text{ }^{\circ}\text{C}$  was carried out against a standard platinum resistance thermometer, using the creep furnace to provide the temperature levels. Occasional re-calibration of the thermocouples during the testing programme indicated that the temperature-e.m.f. characteristics remained almost constant. Thermocouples were secured to the test specimen, at the top, middle and bottom of the gauge length by means of quartz string. In the first test the hot junctions were held against the specimen surface by means of glass insulating tape which had a thermosetting adhesive. It was found, however, that the tape and adhesive set rigidly at the test temperature and severely hindered creep deformation of the specimen at the thermocouple locations. In subsequent tests it was found satisfactory

to shield the hot junctions by means of tape, wound with the adhesive to the outside so that the tape stuck to itself and not the specimen. The thermocouple e.m.f's were measured by means of a precision potentiometer and a high sensitivity galvanometer.

#### 3.2.4 Strain Measurement

Because of the ductility of the specimen material, especially at the test temperature, it was considered inadvisable to make use of extensometry which was fixed directly to the thin specimen gauge length. Extensometry secured to the specimen grips was also rejected because of the difficulty in determining the effective gauge length of the specimen (13), and a method similar to that of King (3) was adopted. Creep strains were measured by direct observation of the specimen through slits in the furnace wall. Two light grooves, approximately 0.002 in. deep and 0.080 in. apart were made around the specimen diameter at each end of the 5 in. gauge length. During the tests, the relative displacement of these marks was measured at regular intervals of time by means of telemicroscopes carried by a small precision cathetometer. The telemicroscopes had a magnification of approximately 15X and the cathetometer had a fine adjustment micrometer with subdivisions of  $8 \times 10^{-5}$  in. The micrometer travel was about 1 in. allowing strains of approximately 15 per cent to be measured without resetting the instrument. Two gauge marks were required at each end of the gauge length since the furnace winding was continuous and occasionally obscured one of the marks. The slits in the furnace wall were sealed with plate quartz windows allowing continuous observation of the specimen without loss of temperature distribution due to excessive convection. The initial gauge length of each

specimen was measured before the tests by means of a projection microscope. The accuracy and reproducibility of the system was investigated before the tests. A steel specimen was made and light grooves were machined at various positions along its length in a manner similar to the specimen gauge marks. The positions of these marks were measured first on the projection microscope, and then with the specimen assembled in the furnace, by means of the tele-microscopes. In this way it was estimated that the accuracy of strain measurement was within  $\pm 1 \times 10^{-4}$ .

### 3.2.5 Initial application of the load

To provide smooth application of the load at a constant rate for all the specimens a simple screw jack system operated by an electric motor was used. The design of this system is described in Appendix IV.

## 3.3 Internal pressure tests

### 3.3.1 Test specimen

The form of the test specimen is shown in fig (6). The parallel length was made relatively long to provide a long axial gauge length while ensuring that end effects would be small, and the diameter ratio was made as large as possible. The maximum specimen outside diameter was limited effectively by the number of specimens required from the billet cross section while the minimum bore size was limited by the difficulty of machining a long straight hole of small diameter. The specimens were machined from blanks of square cross section cut from the billet. The blanks were first set in a large radial drilling machine and the

bores produced by means of a series of long drills and boring bits. Very slow cutting speeds were employed and the cutting edge was flushed continuously with a strong flow of paraffin. The bores were finished with a specially designed reamer, taking a cut of approximately 0.001 in. This method was found to produce straight bores with a good surface finish. The bored out blanks were secured to a close fitting mandrel and the outside diameter produced on a copying lathe. At this stage the mandrel was mounted in a dividing head and conical dimples for locating the axial extensometry were machined in a vertical mill. Finally the specimens were fitted in a jig, which clamped the conical ends, and the end faces and sealing ring grooves produced.

Measurement of the dimensions of the finished specimens showed that the outside diameters were uniform to within  $\pm 0.0002$  in. and bores uniform to within  $\pm 0.0005$  in.

### 3.3.2 Arrangement of the specimen in the test rig

The arrangement has been described before (3). Double cone end closures were employed with the sealing arrangement modified by the addition of a Viton rubber 'O' ring 1 in. inside diameter x  $\frac{1}{8}$  in. section. The sealing arrangement proved satisfactory to times of over 1000 hours although at times of this order the 'O' ring material had deteriorated to such an extent that the seal was entirely provided by metal to metal contact of the specimen bore and end closure spigots. The specimen was suspended vertically from a spherical collar inside the furnace and fine adjustment was possible to ensure coincidence of the specimen and furnace

axes. The load applied to the centre of the specimen gauge length by the combined weights of the bottom end closure, filler bar, and one half of the specimen was carefully counterbalanced to ensure that the stress system acting at the centre of the gauge length during the tests was that of a cylinder under internal pressure, carrying its own pressure end load.

### 3.3.3 Pressure system

A diagrammatic layout of the system is shown in fig (7). Silicone fluid, M.S.550, was used as the pressurising medium. Liquid paraffin was pressurised by a dead-weight accumulator which incorporated a Morrison seal (1), and the pressure was transmitted to the silicone fluid via a mercury interface. The piston of the dead-weight accumulator was continuously rotated at about 3 r.p.m. by a small geared electric motor, to reduce friction between the piston and cylinder. A simple high pressure level indicator was included in the system to allow observation of the position of the mercury-silicone fluid interface during the tests and a trap was included to prevent mercury spreading through the system in the event of sudden leakage at the specimen end closures. The test pressure was measured by means of a standard test gauge which was checked before and after the test programme. The accumulator provided about 60 hours test time before resetting of the piston, by means of the hand pump, was required. This operation could be carried out in about a minute and on no occasion was a change of pressure at the specimen indicated on the pressure gauge during this operation. A pressure transducer connected to a chart recorder was included in the system to record the initial pressure time loading curve for each test. A small intensifier was connected to the silicone fluid

side of the system to reset the mercury level for each test. Although the test temperature of 250 °C is towards the top end of the useful temperature range of silicone fluid no apparent deterioration of the fluid occurred even after test times of over 1000 hours. Other fluids, suitable for use at temperatures considerably in excess of the test temperature, are available, but all have a corrosive effect on aluminium.

#### 3.3.4 Temperature measurement and control

The test temperature was provided by means of a vertical electric furnace, 3 ft. 6 ins. long and 12 ins. diameter, of similar construction to the tensile test furnace. The windings were arranged in five zones and the currents proportioned by rheostats as shown in fig (8). Temperature control was provided by means of a proportional controller of the silicon controlled rectifier type. The sensing element was a ventilated platinum resistance thermometer with the element close to the copper furnace liner about 12 ins. from the top of the furnace. During the tests the temperature gradient along the parallel length of the specimen was never greater than 1 C° and the controller maintained temperature fluctuations within  $\pm 0.3$  C°.

Specimen temperature was measured by means of thermocouples similar to those used in the tensile tests, positioned at the top, middle and bottom of the specimen parallel length.

#### 3.3.5 Diametral strain measurement

A method similar in principle to that of Norton (5) was used. Two pairs of diametrically opposed rods pass through the furnace wall and make

contact with the outside surface of the specimen at the middle of the gauge length. Any change in the outside diameter of the specimen causes displacement of the rods and diametral strains can therefore be determined by measuring the movement of the ends of the rods outside the furnace.

Quartz was selected as the rod material because of its very low coefficient of thermal expansion (approximately  $5 \times 10^{-7}$  in/in  $^{\circ}\text{C}$ ). The rods were produced from lengths of quartz of 4 mm. nominal diameter, specially selected for uniformity and straightness. Guides for the rods were made in the form of thin-walled stainless steel tubes with the rods a good sliding fit in the bores of the tubes. The furnace tube which carried the windings was in the form of halves, separated by a sindanyo disc in which the guides were fitted. A dividing table was clamped to the table of a horizontal mill and the sindanyo disc secured to the dividing table in a horizontal plane with the disc and table centres coincident. Four radial holes were bored in the disc at right angles to each other. The squareness of the axes of the holes was within  $\pm 10^{\circ}$  of arc. The stainless steel guides were a push fit in these holes. During assembly of the furnace, care was taken to set the sindanyo disc in a plane at right angles to the furnace axis. A diamond impregnated grinding wheel was used to produce flat ends on the quartz probes, at right angles to the probe axes. When in position, the lines of action of the probes intersected at the centre of the furnace. During assembly in the test rig, the specimen could be set with its axis vertical and within  $\pm 0.1$  in. of the furnace axis. To ensure that each pair of rods made contact with the specimen surface on a diameter, caps of fired pyrophyllite were cemented on the ends of the

rods inside the furnace. These caps provided the rods with flat ends, 0.350 in. diameter, and ensured that opposite rods were always located on a specimen diameter.

Movement of the ends of the rods outside the furnace was measured by means of C.N.S. linear displacement transducers of the differential transformer type. The transducers were held in position during the tests by a frame surrounding the furnace. It was essential that the line of action of the core of each transducer coincided with that of its associated quartz probe and the supporting frame arrangement was designed to ensure this. The frame was made from 'Permant' low thermal expansion alloy, in four sections, joined by means of combined lap and butt joints to form a square. Care was taken on assembly of the sections to ensure squareness, and dowel pins were inserted in the joints to enable the sections to be dismantled and reassembled in the same position. The assembled frame was clamped to a dividing table on a vertical mill with the centre of the frame coincident with the centre of the table. The longitudinal travel of the mill table was used to cut slots on opposite sides of the frame so that the axes of the slots were coincident. The frame was then rotated through  $90^{\circ}$  on the dividing table and two more slots cut in the same way.

Four mild steel base plates were made, with longitudinal spigots, which were a good fit in the slots of the frame. Each base plate had a hole to carry an adjusting micrometer and two longitudinal Vee grooves on the top face. Care was taken to ensure that the axes of the spigot, micrometer hole and Vee grooves were parallel. Four transducer slides were made from Permant. On the bottom face of each slide, a Vee groove

and a groove of rectangular cross section was machined and a Tufnol block was mounted on the top face to clamp the transducer. Again care was taken to ensure that the axes of both grooves and the transducer hole were parallel. Steel balls,  $\frac{1}{4}$  in. diameter, separated by a thin brass shim cage were placed in the Vee grooves of the base plates and the transducer slides set on these. The balls located between the Vee groove in the slide and the corresponding Vee groove in the base plate ensured that the axes of these grooves were parallel and, therefore, that the lines of action of opposite transducers were parallel and those of adjacent transducers at right angles. The transducer slides were kept in contact with the anvils of the adjusting micrometers by means of coil springs. A framework was built around the furnace from sections of mild steel angle to support the transducer frame assembly. Three adjusting screws were provided to enable the ends of the transducer cores to be lined up with the ends of the quartz rods. To avoid point contact between the frame and the screws three steel plates were made with a conical recess in each. The ends of the adjusting screws were balled and the frame was laid on the steel plates with the ball end of each adjusting screw in a conical hole. This provided a large supporting area for the framework while retaining the three levelling screw principle. The cores of the transducers were lightly spring loaded and this was sufficient to maintain the cores in contact with the probes and the probes in contact with the specimen.

The output from the transducers was fed to a C.N.S. multi-channel null balance read-out meter enabling large displacements to be measured with a sensitivity of the order of  $10^{-6}$  in. The system allowed a range

of 0.1 in. on each transducer and the linearity was within  $10^{-5}$  in. over the central 0.040 in. of this range. This null balance system was designed for maximum stability over long times and is ideally suited for creep strain measurement.

The reproducibility of a strain measuring system such as this which requires the transmission of specimen deformation outside the furnace before it can be measured is greatly influenced by fluctuations of ambient temperature causing expansion and contraction of the various parts of the extensometry, which is included in the apparent strain measurements. A degree of self-compensation for ambient temperature fluctuations was provided in the transducer framework by selection of materials and dimensions as described in Appendix V. It was found that the strain measurements obtained with this system exhibited a maximum deviation about a mean curve of  $\pm 2 \times 10^{-5}$ . Diagrammatic arrangements of the system are shown in figs (9 and 55).

### 3.3.6 Axial strain measurement

An attempt was made to measure axial strains which were expected to be very small. A system was devised which enabled the extensometry to be fixed directly to the specimen gauge length in a positive location, while constraining the deformation of the specimen as little as possible. Two rings were made, 1 in. deep with  $\frac{1}{4}$  in. wall thickness, and bore diameters of 2 ins. and  $2\frac{1}{2}$  ins. respectively. Titanium was chosen as the ring material because of its excellent high temperature strength-weight characteristics. Four radial holes were drilled and tapped at right angles to each other through the wall of each ring. The rings were placed round the specimen,

and titanium screws, fitted with spring loaded plungers which had conical ends, were fitted to the holes in the rings so that the ends of the plungers located in dimples, machined on the outside surface of the specimen. The axial distance between the two sets of dimples was 6 ins. The dimples were 1/16 in. deep and the plunger spring loading was fairly light. Extensometer legs made from Permant were fixed to the rings to transmit axial movement of the rings beyond the bottom of the furnace. Two pairs of legs were used, fixed at opposite ends of the specimen diameter. The relative displacement of each pair of legs was measured during the tests by means of a transducer identical to those used for diametral strain measurements. The weight of the extensometry was counter-balanced by means of a pulley system secured to the bottom furnace flange, eliminating any additional axial load on the specimen.

The arrangement of the system is shown in fig (10). This system was used, with minor modifications, in five tests and in each case one side of the cylinder apparently lengthened while the other shortened. No bending of the cylinder was detected at the end of these tests and the effect seemed to be due to creep at the dimples. The apparent changes in specimen gauge length measured in this way were very small indicating that any axial creep which must have been included in these measurements was also very small. The system was satisfactory in the one respect that very little constraint of the diametral deformation of the specimen at the location of the extensometry was observed from measurements made at the end of the tests. For the remainder of the tests fine gauge marks, similar to those used in the tensile tests, were machined on the outside

diameter of the specimens, 5 ins. apart, and an estimate of the total axial creep strain occurring during the tests was obtained from measurements of the distance between these marks before and after the tests.

### 3.4 Summary of experimental work

The history of all the test specimens prior to loading should be as similar as possible and, as discussed previously, great care was taken during manufacture of the specimens to prevent the introduction of pre-strain or structural alteration of the material due to local overheating. Care was also taken to produce a similar heating cycle before loading on all the specimens. In both tensile and internal pressure tests, the furnace circuit was switched on with the specimen in position inside the furnace. The temperature level in the specimen gauge length was brought automatically to within  $\pm 3C^{\circ}$  of the test temperature by the proportional controller. This required about 2 hours for the tensile specimens and 3 hours for the tubes. A further 6 hours, approximately, was required to achieve a satisfactory level and distribution of temperature on the specimen gauge length. Accordingly all the tests were commenced about 10 hours after the furnace circuits were switched on.

#### 3.4.1 Tensile creep tests

A preliminary series of five constant-stress tests was carried out on specimens manufactured from aluminium-0.07 percent titanium alloy remaining from the previous investigation and the results are presented in Appendix VI. An interesting feature of these results is that only primary creep was obtained, although one of the tests was continued to a

strain of 28 per cent, indicating that the tertiary stage of creep observed during constant-load tests with this material was due to thinning of the specimen section.

The main tensile creep testing programme consisted of a series of constant-stress and constant-load tests in the range 500 - 1300 lbf/in<sup>2</sup>. The material isotropy was investigated by means of constant-stress tests on specimens from the axial and two mutually perpendicular transverse directions of the billet. At the top and middle of the stress range, tests were carried out at the same constant-stress on one specimen from each of these directions. At the lower end of the range, tests were carried out on specimens from the axial and one of the transverse directions. The results of these tests are presented in figs (11 to 16).

The material behaved in an anisotropic manner during the early stages of the tests and there was a tendency for the creep-rates to increase for a very short period after loading before settling down to primary creep behaviour. This effect has been observed before with super-pure aluminium (16, 17, 3) and attributed to slight initial readjustment of the material structure produced by the applied stress, until a state of uniform strain is reached. No such tendency was observed with the aluminium-0.07 per cent titanium alloy and it is possible that the addition of 0.06 per cent titanium in the present material was too small to completely inhibit the effect. After a relatively short proportion of the test duration the initial anisotropy almost disappeared and the variation in creep rates for the three directions of the billet became small. The differences in total strains in the three directions at the end of the tests are due mainly to the effect of the early anisotropy.

An effect similar to that obtained in the early parts of these tests can be caused by non-axiality of loading. It is unlikely that this is the case in the present series of tests since reasonable precautions were taken to prevent non-axiality and the effect does not appear to be random, the axial direction of the billet being the least creep resistant in all cases. It is more likely that the initial alteration of material structure was slightly different in the three directions leading to differences in strain-rates during the early parts of the tests.

Single tests were carried out at five other stress levels, providing reasonable coverage of the stress range. In all of these constant-stress tests, only primary creep was observed at strains up to 16 per cent. With this material therefore, within the range of parameters investigated, it is illogical to divide creep curves obtained from changing stress tests into stages of primary, secondary and tertiary creep. If a time-hardening relationship holds, of the form;

$$\frac{d\epsilon}{dt} = f_1(\sigma)f_2(t)$$

the material will be in a state of primary creep governed by the time function while the creep-rate will also be influenced by the stress function which may change with time due to changes in the applied loading or specimen geometry. Increasing specimen creep-rates during primary creep of the material will be obtained when the rate of increase of the stress function is greater than the rate of decrease of the time function.

Constant-load tests were carried out at six stress levels, each initial applied stress corresponding to one of the constant-stress tests. A comparison of the creep curves obtained from the constant-stress and constant-

load tests with the same initial applied stress is presented in figs (17,18). The tensile creep data obtained from the material is presented in Tables 1 and 2. Results for constant-stress tests at the isotropy test stress levels are the average of the isotropy tests. In each of the tests, the instantaneous strain on initial application of the load was very small and creep and total strains are considered identical. Appendix VII contains the results of short time tensile tests carried out on the material at 250 °C, which indicate that the instantaneous loading strain produced at the highest stress level of the tensile creep tests was approximately  $2 \times 10^{-4}$ , which is of the order of sensitivity of the extensometry.

Examination of the tensile creep specimens after the tests indicated that the gauge length deformation was uniform although some ovality was evident on specimens subjected to large strains.

#### 3.4.2 Internal pressure creep tests

Creep tests were carried out on ten specimens in the range 600 to 1500 lbf/in<sup>2</sup> internal pressure. Due to a machining error, the outside diameter of one of the specimens was some 0.025 in. smaller than the others and this specimen was tested first at the highest pressure as a proving run for the apparatus. A severe leak occurred at the bottom end closure after only 40 minutes and the test was stopped. The strain-rates in this test were very high and the external diametral strain at the end of the tests was approximately 1 per cent. The end closure sealing arrangement was modified to include the large Viton 'O' ring. The end faces of the specimen which had been tested were machined to take this 'O' ring and a further test at the same pressure was carried out with this specimen to try

out the sealing arrangement and provide experience with the extensometry. The test was continued to an external diametral strain of almost 10 per cent and it was found that the two parts of the test combined to form one continuous smooth creep curve, indicating that the temperature and loading cycle had no effect on the material. The results of this test, therefore, are included in the main testing programme. In the remainder of the tests the modified sealing arrangement was found successful although, as discussed previously, this was not due entirely to the 'O' rings.

Creep curves obtained from the diametral extensometry exhibited scatter about a mean line of  $\pm 2 \times 10^{-5}$  which is an order of magnitude greater than the sensitivity of the transducers. To obtain a reading at any time involved the individual balancing of the outputs of two transducers by means of the read-out bridge. This operation required about 10 seconds for each transducer and in the few seconds elapsing between the two readings the position of the specimen relative to the furnace, which carried the transducer frame, could alter by a few hundred thousandths of an inch. This meant that at the time of balancing the output of the second transducer, the output of the first had altered slightly and the resulting combination of the two readings was therefore slightly in error. Ideally the output of each transducer of the pair should be combined before passing to the read-out meter and it is felt that this would increase the reproducibility of the diametral strain measurements considerably.

Using the material constants obtained from the short time tensile tests, the analysis of Allen and Sopwith (19) was applied to determine the initial stress and strain distributions occurring in the walls of the

cylinders due to the pressure loading. This indicated that the external diametral strain produced on loading in the highest pressure test was approximately  $5 \times 10^{-5}$ , i.e. of the order of magnitude of the reproducibility of the extensometry. At present, therefore, the system is not capable of measuring the small initial strains produced by the pressure load.

The external dimensions of the specimens were measured after each test and found to be in agreement with those predicted by the diametral extensometry. Some ovality was evident on all the specimens. The diametral extensometry provided some indication of the progression of ovality with strain during the tests and it appeared that most of the total ovality occurred early on in the tests. It is likely that this was due to the same mechanism as the early non-uniformity of strain in the tensile tests, the ovality being produced by early anisotropy in the transverse directions. Fig (19) shows both sets of diametral strain readings for one of the tests, indicating the progression of ovality. Measurements made after this test showed that the transducer measurements were made almost coincident with the principal axes of ovality. Non-uniformity of strain on the cylinder gauge lengths due to end effects were found to be limited to the regions within about 1.5 times the outside diameter from the ends. The diametral strain data is presented in Table 3 in which strains are the average obtained from both pairs of transducers. Table 4 presents axial strains estimated from gauge mark measurements and compares these with total diametral strains. In all cases the axial strain was small compared with the diametral strain.



TABLE 2

CONSTANT LOAD TENSILE CREEP DATA

hours	<u>Total strain (per cent) in various times for each stress level</u>					
	1153	1070	927	729	610	
						543
0.1	0.25	0.28	0.11	0.058	0.012	
0.3	0.60		0.29	0.118	0.044	
0.5	0.92	0.51	0.48	0.182	0.073	0.073
0.7	1.42	0.72	0.67	0.246	0.100	
1.0	1.57	0.99	0.94	0.355	0.142	0.130
3.0	3.17	2.10	1.42	0.508	0.211	0.173
5.0	4.12	2.81	1.87	0.642	0.276	0.208
7.0	4.87	3.40	2.73	0.860	0.396	0.265
10.0	5.87	4.17	3.50	1.042	0.500	0.310
15.0	7.32	5.23	4.78	1.338	0.669	0.381
20.0	8.62	6.15	5.32	1.465	0.736	0.410
30.0	11.10	7.78	5.83	1.576	0.795	0.436
40.0	13.46	9.30	6.76	1.778	0.906	0.483
60.0	18.55	12.29	8.58	2.124	1.079	0.559
70.0	21.32	13.82	10.28	2.416	1.236	0.619
80.0		15.42	12.09	2.680	1.361	0.668
100			14.10	2.920	1.480	0.713
140			15.68	3.088	1.566	0.742
180				3.142	1.593	0.751
220				3.685	1.846	0.837
260				4.220	2.083	0.916
290						0.993
300						1.142
400						1.289
500						1.440
600						1.594
800						
1000						
1200						
1400						

TABLE 3

INTERNAL PRESSURE CREEP TEST DATA

Mean external diametral strain (per cent) in various  
times for each pressure level

Internal pressure (lbf/in<sup>2</sup>)

hours	1530	1365	1230	1090	1030
0.05	0.074	0.013	0.006		
0.1	0.205	0.022	0.012		
0.2	0.538	0.051	0.026	0.008	0.011
0.4	1.116	0.144	0.062	0.023	0.018
0.6	1.554	0.247	0.101	0.039	0.026
0.8	1.932	0.353	0.142	0.060	0.034
1.0	2.278	0.454	0.183	0.083	0.043
1.4	2.956	0.646	0.269	0.142	0.063
1.8	3.682	0.824	0.356	0.200	0.085
2.2	4.478	0.993	0.442	0.256	0.108
2.6	5.416	1.157	0.528	0.310	0.132
3.0	6.584	1.312	0.611	0.361	0.157
3.6	9.124				
4.0		1.693	0.806	0.481	0.219
6.0		2.464	1.160	0.697	0.336
8.0		3.350	1.498	0.888	0.439
9.6					0.512
10.0		4.455	1.838	1.060	
11.0			2.014		
11.2		5.292			
14.0				1.374	
18.0				1.675	
22.0				1.964	
26.0				2.247	
30.0				2.545	
40.0				3.305	

TABLE 3 cont'd....

INTERNAL PRESSURE CREEP TEST DATA

Mean external diametral strain (per cent) in various

times for each pressure level

Internal pressure lbf/in<sup>2</sup>

Hours	910	805	720	660	620
1	0.013				
2	0.020				
4	0.044				
6	0.076				
8	0.114				
10	0.154	0.034	0.007	0.023	
15	0.258	0.052			
20	0.366	0.070	0.012	0.035	0.0010
30	0.554	0.106	0.016	0.045	0.0016
40	0.714	0.138	0.021	0.052	0.0022
60	0.994	0.198	0.029	0.063	0.0033
80	1.247	0.254	0.036	0.072	0.0044
100	1.489	0.308	0.044	0.079	0.0056
140	1.969	0.410	0.059	0.091	0.0077
180	2.457	0.508	0.073	0.102	0.0099
220	3.026	0.601	0.087	0.111	0.0121
260	3.718	0.693	0.102	0.120	0.0143
300	4.552	0.778	0.116	0.128	0.0164
350	6.004	0.895	0.134	0.138	0.0191
400		1.014	0.151	0.148	0.0217
500				0.166	0.0267
510		1.289			
520			0.194		
600				0.184	0.0315
800				0.220	0.0406
1000					0.0488
1200					0.0568
1400					0.0644

TABLE 4

AXIAL STRAINS IN INTERNAL PRESSURE TESTS

Internal pressure lbf/in <sup>2</sup>	Average strain at end of test (per cent)	
	Axial	External diametral
705	-0.02	0.19
895	-0.13	5.85
1015	0.00	0.52
1215	0.01	2.03
1345	-0.004	5.29

CHAPTER 4

ANALYSIS OF TENSILE CREEP DATA

4.1 Introduction

In Chapter 2 the equation of state was discussed and it was stated that for general loading conditions this equation must be expressed in terms of strain-rate and not strain. It was shown that many such equations of state are possible which provide different results when applied to changing stress situations, but that all of these equations lead to a common relationship when integrated with respect to time at constant stress. The integrated form of equation, may be applied, therefore, to an analysis of constant-stress creep data. For the case of uniaxial tension, this may be expressed as:

$$\epsilon = f_1(\sigma)f_2(t) \quad \dots(1)$$

where  $\sigma$  is the applied tensile stress and  $\epsilon$  is the creep strain at time  $t$ . It was found by Tapsell and Johnson (1) that  $f_1$  and  $f_2$  are separable functions and this was confirmed in later work by Johnson et al (e.g. 2). This equation has the advantage of involving only experimentally observed quantities, as opposed to equations in terms of strain-rate which must be determined from the experimental strains.

The stress function

Many forms of the function  $f_1$  have been proposed and used by many authors (e.g. 3). Most of these forms belong to one or other of the following general groups:

1. Exponential function,  $f_1(\sigma) = Ae^{b\sigma}$
2. Hyperbolic function,  $f_1(\sigma) = A \sinh(b\sigma)$

3. Power function,  $f_1(\sigma) = A\sigma^n$ .

While none of these forms has been found satisfactory under all circumstances, the power function has been applied widely and found to provide accurate representation of most data. The power function is also relatively simpler to apply to conditions of complex stress than exponential or hyperbolic functions and forms the basis for most of the creep analyses in the literature. Only this function was examined in the present investigation.

#### The time function

The time dependence of primary creep has received at least as much attention as the stress dependence and a great variety of forms of  $f_2(t)$  have been proposed. Reference (3) contains a good summary of these relationships which include logarithmic, exponential and power functions, and many combinations of these. As with stress functions, no single relationship has provided satisfactory representation of all experimental data.

Conway and Mullikin (4) have applied many of these equations to a description of experimental uniaxial tension creep data on lead at 14.5 °C, nickel at 700 °C and arc-cast tungsten at 2,400 °C. Least squares analyses were carried out by means of a digital computer and they concluded that several different equation forms provided consistently accurate representation of the experimental data. These forms were,

1.  $\epsilon = a(1 + bt^{\frac{1}{3}})e^{kt}$  proposed by Andrade (5).

2. a third degree polynomial in  $t^{\frac{1}{3}}$ , similar to the special case of Graham and Waller (6) and approximating to the Andrade equation.

3. a simple power relationship,  $\epsilon = At^P$ , which has been employed extensively in the literature and shown by Johnson et al (e.g. 2) to provide an accurate representation of primary creep behaviour for a wide range of materials.

4.  $\epsilon = at^P + bt^Q$  proposed by De Lacombe (7) to provide a description of the entire creep curve when  $0 < p < 1$  and  $q > 1$ .

#### 4.2 Constant-stress data

The selection of a time function was considered first and the graphical method of Johnson (8) was used. For any single stress level equation (1) becomes,

$$\epsilon = Af_2(t).$$

This may be written,

$$k_1 \epsilon = k_2 f_2(t)$$

and a common curve of the data drawn by suitable choice of the scaling constants  $k_1$  and  $k_2$ . Both constants were chosen as 1 at the intermediate stress level of 927 lbf/in<sup>2</sup> and the rest of the data scaled to suit. This composite curve is shown in fig (20) and demonstrates the geometrical similarity of the creep curves over the stress range. The mean curve obtained from the composite plot is shown in fig (21) providing a good straight line relationship on double logarithmic strain-time co-ordinates. This indicates that a simple power function of time is suitable for representing the experimental data,

$$\text{i.e. } f_2(t) = t^P$$

$$\text{and } \epsilon = At^P \quad \dots(2)$$

where  $p$  is the slope of the line in fig (21) and is approximately 0.51.

Equation (1) is a creep strain relationship and measurements made during creep tests are of total strain. The initial time-independent strain occurring on loading must, therefore, be subtracted from the measured strains to provide creep strains for use in the analyses. The assessment of initial loading strain from creep data presents difficulties (9) and various methods have been adopted (10, 11, 12, 7) to determine this quantity. Equation (2) should be written,

$$\epsilon = \epsilon_0 + At^P \quad \dots\dots(3)$$

where  $\epsilon_0$  is the loading strain.

The simplest method of overcoming the difficulty is to use strain-rate data rather than strain data. Equation (3) then becomes,

$$\frac{d\epsilon}{dt} = pAt^{p-1}$$

and  $\epsilon_0$  is eliminated. However, strain-rate data exhibit considerably more scatter than strain data and their use is likely to swamp the advantage of eliminating  $\epsilon_0$ . The method of analysis presented by De Lacombe and subsequently used by Crussard (13) overcomes this by eliminating  $\epsilon_0$  from the analysis while retaining the advantage of strain data. Although in the present creep tests the initial loading strains are very small compared with creep strains, this method of analysis was investigated. The method assumes that equation (3) holds for primary creep. Then, at different times in the same test,

$$\begin{aligned} \epsilon_1 &= \epsilon_0 + At_1^P \\ \text{and } \epsilon_2 &= \epsilon_0 + At_2^P \\ \therefore \epsilon_2 - \epsilon_1 &= A(t_2^P - t_1^P) \end{aligned}$$

If the times are selected in geometric progression with ratio  $r$ ,  
then

$$t_2 = t_1 \times r$$

$$\text{and } \epsilon_2 - \epsilon_1 = At_1^P (r^P - 1)$$

$$\therefore \log (\epsilon_2 - \epsilon_1) = \log [A(r^P - 1)] + p \log t_1$$

$$\text{i.e. } \log \frac{\Delta \epsilon}{n - (n-1)} = \log [A(r^P - 1)] + p \log t_{(n-1)}$$

For any test, therefore, a graph of  $\log \Delta \epsilon - \log t$  should provide a straight line of slope  $p$  and ordinate  $A(r^P - 1)$  at  $\log t = 0$ . This allows  $A$  to be determined and hence  $\epsilon_0$  since,

$$\epsilon_0 = \epsilon + At^P \text{ at any time.}$$

The method places heavy weighting on data obtained from the early parts of the tests and was rather unsatisfactory with the present data because of the unsettled creep behaviour observed early in the tests, as discussed in Chapter 3. In many cases the best straight line to be drawn through the points was not obvious and a random selection of  $p$  values was obtained, ranging between 0.36 and 0.58.

The experimental creep curves were drawn on double logarithmic co-ordinates, fig (22) and reasonable straight line relationships were obtained after the initial low creep-rate portion. A computer programme, employing the method of least squares was used to fit the relationship,

$$\epsilon = At^P$$

to each set of data. From each experimental creep curve points were chosen, at equal intervals of time, to provide uniform weighting over

the duration of each test. It was found that this form of equation provided a good representation of the data, but the exponent "p" varied unsystematically with stress to some extent.

The creep curves on fig (22) exhibited downward curvature at short times and an attempt was made to include this in the analysis by adjustment of the time function. A procedure, similar to that before, was used to fit a relationship of the form,

$$\epsilon = A \left[ (t + 1)^{\frac{1}{2}} - 1 \right]^P$$

to the experimental data. This improved the description of the short time data, but the variation of "p" from test to test was greater than before. In a correlation of the data obtained from the preliminary tests on aluminium-0.07 per cent titanium alloy (Appendix VI) it was found that variation of the time exponent from test to test could be greatly reduced by the use of the equation

$$\epsilon = A \left[ (t + 1)^2 - 1 \right]^P$$

and this equation was also fitted to the data. The variation of "p" was greatly reduced by this means but the description of the short time data was rather poor.

By comparing the standard deviations obtained for each test using these three equations it was found that the best fit to the data was provided by the simple power function and an average value of the exponent "p" was calculated, providing the relationship,

$$\epsilon = At^{0.484}.$$

In this equation,  $A = f_1(\sigma)$ . A simple power law relationship was investigated

in which

$$A = B\sigma^n \dots\dots(4)$$

where A is the value of the coefficient for each creep test obtained from the computer.

A least squares analysis was carried out on the computer, using the values of A and  $\sigma$  for each test, to obtain values of B and n. Only eight data points were available (one for each stress level) and this was found to be insufficient for such an analysis. Recourse was made, therefore, to graphical methods.

Taking logarithms of each side, equation (4) becomes,

$$\log A = \log B + n \log \sigma$$

and a graph of  $\log \sigma$  against  $\log A$  should provide a straight line of slope "n". This plot is shown in fig (23). Two straight lines were obtained of slopes,

$$n_1 = 4.8$$

$$\text{and } n_2 = 9.7$$

There appeared to be a fairly sharp transition in the stress dependence of the material, occurring at approximately 600 lbf/in<sup>2</sup>.

Another graphical method was used to check this relationship. The creep equation has the assumed form,

$$\epsilon = B\sigma^n t^P$$

and for any two constant-stress tests,

$$\frac{\epsilon_1}{\epsilon_2} = \left(\frac{\sigma_1}{\sigma_2}\right)^n \left(\frac{t_1}{t_2}\right)^P$$

Then, if  $\epsilon_1 = \epsilon_2$ ,

$$\left(\frac{\sigma_1}{\sigma_2}\right)^n = \left(\frac{t_2}{t_1}\right)^p$$

$$\therefore n \log \left(\frac{\sigma_1}{\sigma_2}\right) = p \log \left(\frac{t_2}{t_1}\right)$$

$$\therefore \log \left(\frac{t_2}{t_1}\right) = \frac{n}{p} \log \left(\frac{\sigma_1}{\sigma_2}\right).$$

By selecting pairs of constant-stress tests and plotting  $\log \sigma_r$  against  $\log t_r$  at the same strain a straight line of slope  $\frac{n}{p}$  should be obtained. In addition when  $t_1 = t_2$ ,  $\sigma_1 = \sigma_2$ , therefore the line must pass through the origin. This analysis was carried out and the results are shown in fig (24). Two straight lines were obtained, and using the value of "p" = 0.484, the slopes of these lines provided,

$$n_1 = 4.6$$

$$n_2 = 9.3,$$

confirming the approximate values obtained previously.

The stress range was divided into high and low stress groups with the transition stress taken as 610 lbf/in<sup>2</sup> so that the test at this stress level could be placed in both groups. Average values from the two graphical analyses were taken as,

$$n = 4.7 \quad \text{high stress group}$$

$$\text{and } n = 9.5 \quad \text{low stress group.}$$

Using equation (4) with these values of "n" and the computed values of A, values of B were calculated. The values of "n" were adjusted to produce values of B with minimum scatter. The equations arrived at finally were,

$$\epsilon = 3.40 \times 10^{-17} \sigma^{4.8} t^{0.484}, \quad \sigma \geq 610 \text{ lbf/in}^2$$

$$\epsilon = 1.38 \times 10^{-30} \sigma^{9.6} t^{0.484}, \quad \sigma \leq 610 \text{ lbf/in}^2.$$

The representation of experimental data obtained with these equations is shown in figs (22, 25, 26 and 27).

#### 4.3 Constant load data

In these tests the applied stress increased continuously due to thinning of the cross sections of the specimens. The applied stress at any time  $t$  is given by,

$$\sigma = \sigma_0(1 + \epsilon) \quad \dots\dots(5)$$

where  $\sigma_0$  is the initial stress and  $\epsilon$  is the strain at time  $t$ .

The constant-stress equation has the form,

$$\epsilon = B\sigma^n t^P \quad \dots\dots(6)$$

and the simplest method of allowing for the increase of stress in the constant-load tests is to modify equation (6) accordingly. Combining equations (5) and (6),

$$\epsilon = B\sigma_0^n(1 + \epsilon)^n t^P \quad \dots\dots(7)$$

from which the strain at any time in a constant-load test can be calculated. Equation (7) is an approximation, similar to the deformation theory of plasticity, and states that the strain at any instant depends upon the current values of stress and time and is independent of the previous loading of the specimen. As discussed in Chapter 2 this cannot be true under conditions of general loading. The use of equation (7) in an analysis of constant-load data is probably justifiable since the increase in stress is monotonic and relatively small, and such an equation has provided good agreement with experimental data (Appendix VI).

However, during redistribution of stress due to creep in the wall of

a thick-cylinder under internal pressure the stress changes are considerable and the stress ratios alter so that use of a strain-rate form of equation of state is essential. The constant-load data were used, therefore, to determine a strain-rate form of equation of state which would apply to conditions of varying stress.

Constant-stress creep data give some indication of the form of equation suitable for a representation of creep behaviour. Data collected from tests in which the stresses vary do not, and an equation form must be assumed at the outset and checked against the data. Time-hardening and strain-hardening relationships were examined.

For the time-hardening relationships, differentiating equation (6) with respect to time at constant stress

$$\frac{d\varepsilon}{dt} = pB\sigma^n t^{p-1} \dots\dots(8)$$

For the strain-hardening relationship, from equation (6)

$$\begin{aligned} \frac{1}{\varepsilon^p} &= B^p \sigma^{\frac{n}{p}} t \\ \therefore \frac{1}{p\varepsilon} \frac{1-p}{p} \frac{d\varepsilon}{dt} &= B^p \sigma^{\frac{n}{p}} \\ \therefore \frac{d\varepsilon}{dt} &= \frac{pB^p \sigma^{\frac{n}{p}}}{\varepsilon^{\frac{1-p}{p}}} \dots\dots(9) \end{aligned}$$

Combining equations (5) and (8),

$$\begin{aligned} \frac{d\varepsilon}{dt} &= pB\sigma_o^n (1 + \varepsilon)^n t^{p-1} \\ \therefore \int_0^\varepsilon \frac{d\varepsilon}{(1 + \varepsilon)^n} &= \int_0^t pB\sigma_o^n t^{p-1} dt \end{aligned}$$

$$\begin{aligned} \therefore \left[ \frac{1}{(1-n)(1+\epsilon)^n - 1} \right]^\epsilon &= B\sigma_o^{n_t P} \\ \therefore \frac{1}{1-n} \left[ \frac{1}{(1+\epsilon)^{n-1}} - 1 \right] &= B\sigma_o^{n_t P} \\ \therefore \epsilon &= \left[ \frac{1}{[1 - (n-1)B\sigma_o^{n_t P}]^{\frac{1}{n-1}}} - 1 \right] \dots\dots(10) \end{aligned}$$

Combining equations (5) and (9),

$$\begin{aligned} \frac{d\epsilon}{dt} &= \frac{pB^{1/p} \sigma_o^{n/p} (1+\epsilon)^{n/p}}{\epsilon^p} \\ \therefore \int_0^\epsilon \frac{1-p}{\epsilon^p} \frac{d\epsilon}{(1+\epsilon)^{n/p}} &= \int_0^t pB^{1/p} \sigma_o^{n/p} dt \\ &= pB^{1/p} \sigma_o^{n/p} t \\ \therefore t &= \frac{\int_0^\epsilon \frac{1-p}{\epsilon^p} \frac{d\epsilon}{(1+\epsilon)^{n/p}}}{pB^{1/p} \sigma_o^{n/p}} \dots\dots(11) \end{aligned}$$

Equations (10) and (11) were solved, for the six constant-load stress levels, by means of the computer. The values of B, n and p obtained from the constant-stress data were used in the equations and a numerical procedure was employed to evaluate the integral in equation (11). The representation of the experimental data obtained by the time-hardening and

strain-hardening relationships is shown in figs (28, 29 and 30). The strain-hardening form provides a slightly better fit to the experimental data but there is little to choose between the theories and the simpler time-hardening relationship was employed in the thick-cylinder analyses.

CHAPTER 5

ANALYSIS OF THICK-WALLED CYLINDER CREEP DATA

5.1 Introduction

Apparent tertiary creep was observed in some of the experimental creep curves, e.g. fig (19). As discussed in Chapter 3 the results of the constant-stress tensile creep tests indicated that this behaviour is unlikely to be a true form of tertiary creep and is probably caused by the increase in stress level in the wall of the cylinders due to wall-thinning with increasing creep strains. Accordingly the general method of analysis adopted is similar to that applied to the constant-load tensile creep data. It is considered that the material is in the primary stage of creep at all times and that the cylinder creep-rates are influenced by the primary time function and stress changes due to changes in cylinder geometry. Within the framework of this concept two approaches are possible.

(a) A method of analysis similar to that of Bailey (1). Elastic strains are neglected and it is assumed that the steady-state stress distribution is set up in the cylinder wall immediately on loading. Subsequent creep deformation is governed by this stress distribution in conjunction with the primary time function. The stress level will increase with time as the cylinder dimensions change but the form of the stress distribution remains unaltered.

(b) An analysis which takes into account the interaction of elastic and creep strains during stress redistribution. Several analyses of this type have been described in Chapter 2. The starting point in this approach is the initial stress distribution which occurs on loading at time zero.

Depending upon the test material, cylinder diameter ratio and internal pressure, the conditions of the cylinder on loading may be elastic, elastic-plastic or completely plastic. This stress distribution is modified by creep, and the creep behaviour at any time after loading is governed by the current stress distribution and the primary time function. After the steady-state stress distribution is arrived at the analysis becomes identical to (a).

Although method (a) is essentially an approximation it is a good approximation when creep strains are large compared with elastic strains. If creep and elastic strains are of comparable order, or if stresses rather than strains at any time are to be determined an approach similar to method (b) is essential.

In what follows it is assumed that,

1) the creep behaviour of the material under uniaxial stress conditions is described by an equation of state of the form,

$$\dot{\epsilon} = A\sigma^n t^p$$

2) creep behaviour of the material under multiaxial stress conditions is described by an equation of state of the form,

$$\dot{\epsilon}_E = A\sigma_E^n t^p$$

where  $\epsilon_E$  and  $\sigma_E$  are an effective creep-rate and effective stress respectively.

3) the creep-rates in any direction of the material under a multiaxial stress system may then be derived in a manner based on the theory of time-independent plasticity.

It is considered, therefore, that creep-rates under multiaxial stress systems are governed by a "stress criterion" and a "flow rule". Three stress criteria are considered,

- (i) the von Mises criterion
- (ii) the Tresca criterion
- (iii) the criterion of Berman and Pai (2) which is a general anisotropic surface represented by a piecewise linear model.

The representation of these three criteria on the reduced plane is shown in fig (31). The surfaces connect all points in stress space having equal values of effective creep-rate. (i) and (ii) are isotropic surfaces and (iii) is an anisotropic surface, introduced for secondary creep, which can be completely defined by means of uniaxial tension and compression creep tests in the principal stress directions. All three criteria may be applied to primary creep if it is assumed that the form of the stress surface does not change during creep. This amounts to assumptions of isotropy in cases (i) and (ii) and of a consistent form of anisotropy in case (iii).

The effective stress and effective creep-rate at any point on the stress surface is defined as follows,

$$\left. \begin{aligned} \text{(i) } \sigma^* &= \frac{1}{\sqrt{2}} [(\sigma_1 - \sigma_2)^2 + (\sigma_2 - \sigma_3)^2 + (\sigma_3 - \sigma_1)^2]^{\frac{1}{2}} \\ \dot{\epsilon}^* &= \frac{\sqrt{2}}{3} [(\epsilon_1 - \epsilon_2)^2 + (\epsilon_2 - \epsilon_3)^2 + (\epsilon_3 - \epsilon_1)^2]^{\frac{1}{2}} \end{aligned} \right\} \dots\dots(1)$$

$$\left. \begin{aligned} \text{(ii) } \bar{\sigma} &= \sigma_1 - \sigma_3 \quad \text{for} \quad \sigma_1 \geq \sigma_2 \geq \sigma_3 \\ \dot{\epsilon} &= \frac{2}{3}(\epsilon_1 - \epsilon_3) \quad \text{etc.} \end{aligned} \right\} \dots\dots(2)$$

(iii)  $\sigma_e$  given by the equation of each sector of the surface, e.g. side AB, in fig (31),

$$\frac{\sigma_1 - \sigma_3}{a} + \frac{\sigma_3 - \sigma_2}{b} = 1$$

$$\text{if } m = \frac{b}{a}$$

$$\sigma_e = \sigma_1 - (1 - \frac{1}{m})\sigma_3 - (\frac{1}{m})\sigma_2 \quad \dots\dots(3)$$

Therefore the isotropic form of (iii), i.e. with  $m = 1$ , is identical to (ii). In the Berman and Pai paper it was not necessary to define the particular form of the effective creep-rate.

A flow-rule is required in conjunction with the stress criterion to determine the creep-rates in the principal directions. The general form of flow rule given by Prager (3) is,

$$\dot{\epsilon}_1 : \dot{\epsilon}_2 : \dot{\epsilon}_3 = \frac{\partial f}{\partial \sigma_1} : \frac{\partial f}{\partial \sigma_2} : \frac{\partial f}{\partial \sigma_3} \quad \dots\dots(4)$$

where  $f$  is the stress criterion. The flow-rule specifies a direction at each point of the yield surface, the three direction cosines being proportional to  $\dot{\epsilon}_1$ ,  $\dot{\epsilon}_2$ , and  $\dot{\epsilon}_3$ . The direction specified by equation (4) is the normal to the stress surface at the point. Equation (4) becomes,

$$\dot{\epsilon}_1 = S \frac{\partial f}{\partial \sigma_1} ; \quad \dot{\epsilon}_2 = S \frac{\partial f}{\partial \sigma_2} ; \quad \dot{\epsilon}_3 = S \frac{\partial f}{\partial \sigma_3} \quad \dots\dots(5)$$

where  $S$  is a function of the principal stresses. If  $f$  is the von Mises criterion,

$$\frac{\partial f}{\partial \sigma_1} = \frac{[\sigma_1 - \frac{1}{2}(\sigma_2 + \sigma_3)]}{\sigma^*}$$

$$\begin{aligned} \text{and } \dot{\epsilon}_1 - \dot{\epsilon}_2 &= \frac{S}{\sigma^*} [\sigma_1 - \frac{1}{2}\sigma_2 - \frac{1}{2}\sigma_3 - \sigma_2 + \frac{1}{2}\sigma_1 + \frac{1}{2}\sigma_3] \\ &= \frac{3}{2} \frac{S}{\sigma^*} [\sigma_1 - \sigma_2] \end{aligned}$$

$$\therefore \frac{\dot{\epsilon}_1 - \dot{\epsilon}_2}{\sigma_1 - \sigma_2} = \frac{\dot{\epsilon}_2 - \dot{\epsilon}_3}{\sigma_2 - \sigma_3} = \frac{\dot{\epsilon}_3 - \dot{\epsilon}_1}{\sigma_3 - \sigma_1} \quad \dots\dots(6)$$

This is the usual form of the von Mises flow rule and these equations are the Levy Mises equations.

If  $f$  is taken as the Tresca criterion, then for  $\sigma_1 \geq \sigma_2 \geq \sigma_3$ ,

$$\begin{aligned}\dot{\epsilon}_1 &= S \frac{\partial f}{\partial \sigma_1} = S \\ \dot{\epsilon}_2 &= S \frac{\partial f}{\partial \sigma_2} = 0 \\ \dot{\epsilon}_3 &= S \frac{\partial f}{\partial \sigma_3} = -S \\ \therefore \dot{\epsilon}_1 : \dot{\epsilon}_2 : \dot{\epsilon}_3 &= 1 : 0 : -1 \quad \dots\dots(7)\end{aligned}$$

Six different combinations are obtained for the possible principal stress ratios and the flow rule is undefined at the corners of the stress surface. Prager (3) suggests a method of obviating this difficulty by the introduction of a constant  $\lambda$  which may be determined for a given stress system from considerations of symmetry.

e.g. Consider a uniaxial tension test,

$$\bar{\sigma} = \sigma_1, \quad \sigma_2 = \sigma_3 = 0$$

and the stress condition is at a corner on the stress surface. From symmetry  $\dot{\epsilon}_2 = \dot{\epsilon}_3$ , and assuming constant volume creep deformation,

$$\begin{aligned}\dot{\epsilon}_1 + \dot{\epsilon}_2 + \dot{\epsilon}_3 &= 0 \quad \dots\dots(8) \\ \therefore \dot{\epsilon}_2 = \dot{\epsilon}_3 &= -\frac{1}{2}\dot{\epsilon}_1 \quad \text{and } \lambda = \frac{1}{2} \\ \dot{\epsilon}_1 : \dot{\epsilon}_2 : \dot{\epsilon}_3 &= 1 : -\lambda : -(1 - \lambda) \\ &= 1 : -\frac{1}{2} : -\frac{1}{2}.\end{aligned}$$

A simpler method of defining the direction of the creep-rate vector at corners on the stress surface is to assume that the von Mises flow rule

applies regardless of the stress criterion employed. This amounts to an assumption that the Lévy Mises equations are valid for creep and has been verified experimentally, (e.g. 4, 5). The direction of the creep-rate vector at any point on the stress surface is in the direction of a line produced from the hydrostatic stress axis as origin and passing through the point.

Combining equations (6) and (8) we obtain,

$$\dot{\epsilon}_1 = \frac{S}{\sigma} \left[ \sigma_1 - \frac{1}{2}(\sigma_2 + \sigma_3) \right] \text{ etc.....(9)}$$

The form of S depends upon the selected stress criterion.

von Mises criterion with associated flow rule

Combining equations (1) and (6),

$$\frac{\dot{\epsilon}^*}{\sigma^*} = \frac{S}{\sigma}$$

$$\therefore S = \frac{\sigma^* \dot{\epsilon}^*}{\sigma}$$

$$\text{and } \dot{\epsilon}^* = A \sigma^{*n} t^p$$

$$\therefore S = A \sigma^{*n} t^p$$

and equation (9) becomes,

$$\dot{\epsilon}_1 = A \sigma^{*(n-1)} \left[ \sigma_1 - \frac{1}{2}(\sigma_2 + \sigma_3) \right] t^p \text{ etc.....(10)}$$

Tresca criterion with von Mises flow rule

Combining equations (2) and (6),

$$\frac{\dot{\epsilon}}{\bar{\sigma}} = \frac{S}{\sigma}$$

$$\dot{\epsilon} = \frac{\sigma^* \dot{\epsilon}}{\bar{\sigma}}$$

$$\text{and } \dot{\epsilon} = A \bar{\sigma}^n t^p$$

$$\dot{\epsilon} = A \bar{\sigma}^{*n} (n-1) t^p$$

and equation (8) becomes,

$$\dot{\epsilon}_1 = A \bar{\sigma}^{(n-1)} \left[ \sigma_1 - \frac{1}{2}(\sigma_2 + \sigma_3) \right] t^p \text{ etc.} \quad \dots(11)$$

Berman and Pai criterion with von Mises flow rule

The following expressions are derived by these authors for secondary creep-rates.

$$\dot{\epsilon}_1 = \frac{A \bar{\sigma}^n \left[ \sigma_1 - \frac{1}{2}(\sigma_2 + \sigma_3) \right]}{\sigma^*} \text{ etc.} \quad \dots(12)$$

In the isotropic case the Berman and Pai criterion is identical to the Tresca criterion and equation (12) becomes,

$$\dot{\epsilon}_1 = \frac{A \bar{\sigma}^n \left[ \sigma_1 - \frac{1}{2}(\sigma_2 + \sigma_3) \right]}{\sigma^*} \text{ etc.} \quad \dots(13)$$

Equation (13) should be identical to equation (11) modified for secondary creep (as stated by Pai (6)) but in fact is different. Berman and Pai begin their analysis by introducing the relationship,

$$\dot{\epsilon}_1 = AM^n \frac{\partial D}{\partial \sigma_1} \text{ etc.} \quad \dots(14)$$

where M is a magnitude function which defines the stress surface and D is a direction function to which the flow-rule provides normality.

$$M = \sigma_e = \bar{\sigma} \text{ in isotropic case}$$

$$\text{and } D = \sigma^*$$

From equations (14) and (5),

$$AM^n = S$$

Therefore in the isotropic case,

$$\begin{aligned} AM^n &= \frac{\sigma^* \dot{\epsilon}}{\bar{\sigma}} \\ &= A \sigma^* \bar{\sigma}^{(n-1)} \\ \therefore M^n &= \sigma^* \sigma_e^{(n-1)} \\ &\neq \sigma_e^n \end{aligned}$$

Therefore the initial relationship, equation (14), should be,

$$\dot{\epsilon}_1 = AM^{(n-1)} D \frac{\partial D}{\partial \sigma} \text{ etc.}$$

Equation (12) then becomes,

$$\dot{\epsilon}_1 = A \sigma_e^{(n-1)} \left[ \sigma_1 - \frac{1}{2}(\sigma_2 + \sigma_3) \right] \text{ etc.,}$$

and for primary creep

$$\dot{\epsilon}_1 = A \sigma_e^{(n-1)} \left[ \sigma_1 - \frac{1}{2}(\sigma_2 + \sigma_3) \right] t^p \text{ etc.} \quad \dots(15)$$

Equations (10), (11), or (15) then may be applied to determine the creep-rates in the principal directions in a material under a general system of stress. The constants A, n and p are those obtained from constant-stress creep tests in uniaxial tension.

## 5.2 Application of general relationships to thick-cylinder creep data

Method a) Elastic strains neglected and steady-state stress distribution set up on loading.

The steady-state stresses are obtained from the following equations,

(e.g. refs. (1), (7)).

$$\left. \begin{aligned}
 \sigma_r &= \frac{-P\left[\left(\frac{b}{r}\right)^{2/n} - 1\right] - Q\left[\left(\frac{b}{a}\right)^{2/n} - \left(\frac{b}{r}\right)^{2/n}\right]}{\left(\frac{b}{a}\right)^{2/n} - 1} \\
 \sigma_\theta &= \frac{P\left[1 - \left(\frac{n-2}{n}\right)\left(\frac{b}{r}\right)^{2/n}\right] - Q\left[\left(\frac{b}{a}\right)^{2/n} - \left(\frac{n-2}{n}\right)\left(\frac{b}{r}\right)^{2/n}\right]}{\left(\frac{b}{a}\right)^{2/n} - 1} \\
 \sigma_z &= \frac{P\left[1 - \left(\frac{n-1}{n}\right)\left(\frac{b}{r}\right)^{2/n}\right] - Q\left[\left(\frac{b}{a}\right)^{2/n} - \left(\frac{n-1}{n}\right)\left(\frac{b}{r}\right)^{2/n}\right]}{\left(\frac{b}{a}\right)^{2/n} - 1}
 \end{aligned} \right\} \dots\dots(16)$$

where  $\sigma_r$ ,  $\sigma_\theta$  and  $\sigma_z$  are the principal stresses in the cylinder wall in the radial, tangential and axial directions respectively; a, b and r are the inside, outside and reference radii respectively; P and Q are the internal and external pressures respectively and n is the material stress exponent.

The general creep-rate/stress relationships, equations (10), (11) and (15), applied to the cylinder become,

$$\left. \begin{aligned}
 \dot{\epsilon}_r &= A\sigma_E^{(n-1)} \left[ \sigma_r - \frac{1}{2}(\sigma_\theta + \sigma_z) \right] t^P \\
 \dot{\epsilon}_\theta &= A\sigma_E^{(n-1)} \left[ \sigma_\theta - \frac{1}{2}(\sigma_z + \sigma_r) \right] t^P \\
 \dot{\epsilon}_z &= A\sigma_E^{(n-1)} \left[ \sigma_z - \frac{1}{2}(\sigma_r + \sigma_\theta) \right] t^P
 \end{aligned} \right\} \dots\dots(17)$$

where  $\sigma_E$  is the stress criterion employed. Equations (16) provide,

$$\sigma_z = \frac{\sigma_r + \sigma_\theta}{2} \dots\dots(18)$$

leading to  $\dot{\epsilon}_z = 0$  in equations(17). The assumption of zero axial creep therefore is inherent in this form of analysis but should not lead to appreciable errors since the axial creep is certainly very small compared with creep in the tangential and radial directions.

For a thick-cylinder under internal pressure and carrying its own pressure end load,

$$\begin{aligned} \sigma_\theta &> \sigma_z > \sigma_r \\ \therefore \bar{\sigma} &= \sigma_\theta - \sigma_r \end{aligned} \quad \dots\dots(19)$$

Eliminating  $\sigma_z$  by means of equation (18),

$$\sigma^* = \frac{\sqrt{3}}{2}(\sigma_\theta - \sigma_r) \quad \dots\dots(20)$$

For the Berman and Pai criterion, the portion of the stress surface of interest is sector AB.

$$\therefore \sigma_e = \left(\frac{1}{2} + \frac{1}{2m}\right)(\sigma_\theta - \sigma_r) \quad \dots\dots(21)$$

Also 
$$\sigma_\theta - \frac{1}{2}(\sigma_z + \sigma_r) = \frac{3}{4}(\sigma_\theta - \sigma_r)$$

and 
$$\begin{aligned} \sigma_r - \frac{1}{2}(\sigma_\theta + \sigma_z) &= \frac{3}{4}(\sigma_r - \sigma_\theta) \\ &= -\frac{3}{4}(\sigma_\theta - \sigma_r) \end{aligned}$$

and equations (17) become,

$$\left. \begin{aligned} \dot{\epsilon}_\theta &= \frac{3}{4}A\sigma_E^{(n-1)}(\sigma_\theta - \sigma_r) t^P \\ \dot{\epsilon}_r &= -\dot{\epsilon}_\theta \\ \dot{\epsilon}_z &= 0 \end{aligned} \right\} \quad \dots\dots(22)$$

(i) von Mises criterion and flow-rule

$$\dot{\epsilon}_\theta = \frac{3}{4}A\left(\frac{\sqrt{3}}{2}\right)^{(n-1)}(\sigma_\theta - \sigma_r)^{(n-1)}(\sigma_\theta - \sigma_r) t^P$$

$$\therefore \dot{\epsilon}_{\theta} = \left(\frac{\sqrt{3}}{2}\right)^{(n+1)} A (\sigma_{\theta} - \sigma_r)^n t^P \quad \dots\dots(23)$$

(ii) Tresca criterion with von Mises flow-rule

$$\dot{\epsilon}_{\theta} = \frac{3}{4} A (\sigma_{\theta} - \sigma_r)^n t^P \quad \dots\dots(24)$$

(iii) Berman and Pai criterion with von Mises flow-rule

$$\dot{\epsilon}_{\theta} = \frac{3}{4} A \left(\frac{1}{2} + \frac{1}{2m}\right)^{(n-1)} (\sigma_{\theta} - \sigma_r)^{(n-1)} (\sigma_{\theta} - \sigma_r) t^P$$

$$\therefore \dot{\epsilon}_{\theta} = \frac{3}{4} \left(\frac{1}{2} + \frac{1}{2m}\right)^{(n-1)} (\sigma_{\theta} - \sigma_r)^n t^P \quad \dots\dots(25)$$

The use of a Tresca criterion and associated flow-rule under these conditions will lead to relationships identical to (24) since from equations (7),

$$\dot{\epsilon}_{\theta} : \dot{\epsilon}_z : \dot{\epsilon}_r = 1 : 0 : -1$$

which is identical to equations (22).

From equations (16),

$$(\sigma_{\theta} - \sigma_r) = \frac{2(P - Q) \left(\frac{b}{r}\right)^{2/n}}{n \left[\left(\frac{b}{a}\right)^{2/n} - 1\right]} \quad \dots\dots(26)$$

Diametral creep strains at the outside surface of the cylinder were measured during the tests and,

$$\epsilon_D = \frac{D - D_o}{D_o}$$

where D is the instantaneous outside diameter during the test and D<sub>o</sub> is the initial outside diameter

$$\therefore \epsilon_D = \frac{\pi(D - D_o)}{\pi D_o}$$

$$= \epsilon_{\theta} \text{ at the outside surface.}$$

At the outside surface, r = b, and putting <sup>b</sup>/<sub>a</sub> = K, equation (26) becomes,

$$(\sigma_{\theta} - \sigma_r) = \frac{2(P - Q)}{n [K^{2/n} - 1]}$$

where (P - Q) is the pressure in the cylinders in excess of atmospheric, i.e. the measured gauge pressure

$$\therefore (\sigma_{\theta} - \sigma_r)^n = 2^n \left(\frac{P - Q}{n}\right)^n (K^{2/n} - 1)^{-n}$$

and the tangential creep-rate at the outside surface becomes,

$$\dot{\epsilon}_{\theta} = C \left(\frac{P - Q}{n}\right)^n (K^{2/n} - 1)^{-n} t^p \quad \dots\dots(27)$$

where C is a constant depending upon the stress criterion employed.

Equation (27) was used as the basis for an incremental analysis carried out by means of the computer to obtain external diametral creep curves for each of the experimental pressures. The effect of wall-thinning was included in the analysis. The increment of creep strain  $d\epsilon_{\theta}$  occurring over a small time interval dt is obtained from,

$$d\epsilon_{\theta} = C \left(\frac{P - Q}{n}\right)^n (K^{2/n} - 1)^{-n} t^p dt (1 + \epsilon_{\theta})$$

where K is the diameter ratio of the cylinder and  $\epsilon_{\theta}$  is the tangential strain at the beginning of the time interval. The term  $(1 + \epsilon_{\theta})$  is required to refer the strain increment to the original dimensions of the cylinder maintaining the analysis within the context of "engineering strain". The total creep strain at the end of the time interval is then the sum of  $\epsilon_{\theta}$  and  $d\epsilon_{\theta}$ . The change in diameter ratio dK during the time interval is given by,

$$dK = \frac{K(1 - K^2)d\epsilon_{\theta}}{1 + \epsilon_{\theta}} \quad \dots\dots(28)$$

The diameter ratio at the beginning of the next time interval is then  $K + dK$ .

The derivation of equation (28) is due to Mr. W. W. Mackie and is presented in Appendix VIII.

The incremental analysis was carried out for each of the test pressures using the four forms of equation (27) obtained from the possible combinations of the von Mises and Tresca criteria with the creep constants obtained from the tensile data for high and low stresses. It was found that the high stress constants in conjunction with the Tresca criterion provided the best representation of the data at pressures from 805 lbf/in<sup>2</sup> upwards while the low stress constants in conjunction with the von Mises criterion provided the best representation of the data at pressures from 805 lbf/in<sup>2</sup> downwards. This representation of the experimental data is shown in figs. (32, 33, 34 and 35). Fig (32) shows clearly that the initial period of creep in these tests was not of the classical primary creep form. This was similar to the behaviour observed in the tensile creep tests but was of much longer duration, extending over almost the entire testing period at low pressures. The Berman and Pai criterion was not investigated fully since it was clear that although any single set of experimental data could be better represented by the selection of a suitable adjusting constant "m" in equation (27), no single value of "m" would improve the representation over the entire pressure range.

Another form of steady-state analysis has been presented by Marriott and Leckie (8) who observed that during stress redistribution in the wall of a thick cylinder there is a point in the wall called the "skeletal point" at which the effective stress  $\sigma^*$  remains almost constant. At this position in the wall therefore during stress redistribution the following may be stated,

- 1)  $(\sigma_{\theta} - \sigma_r)$  remains constant, so the cylinder creep rates are governed by a constant stress;
- 2) there is little difference to be expected from the use of time-hardening or strain-hardening equations of state;
- 3) there will be little error incurred by making use of steady-state stresses at time zero;
- 4) because of the strong strain compatibility conditions imposed on thick cylinder deformation it is expected that points 2) and 3) will apply throughout the cylinder wall.

Although the skeletal point is defined by Marriott and Leckie as the position in the cylinder wall at which the elastic and steady-state distributions of effective stress cross over, it is to be expected that a similar closely related point should exist for the tangential stress distributions since

$$\sigma^* \propto (\sigma_{\theta} - \sigma_r)$$

and changes in radial stress distribution during creep are very small compared with changes in tangential stress distribution. This effect is observed in several instances in the literature. Coffin, Shepler and Cherniak (9) have produced a graph of tangential stress redistribution in the wall of a 12 per cent chromium-steel cylinder of diameter ratio 2 which illustrates a skeletal point at  $r/R_0 \doteq 1.4$ , where  $R_0$  is the outside radius of the cylinder. Johnson, Henderson and Khan (7) applying their non steady-state analysis to cylinders of diameter ratio 2 of various materials remarked that the tangential stresses remained almost constant during stress redistribution at  $r/R_0 \doteq 1.4$  also. This indicates that the position of the skeletal point may be independent of material properties. Further evidence of this is contained in a graph of tangential stress distri-

butions in the wall of a cylinder of diameter ratio 2 presented by Finnie and Heller (10). The elastic distribution is shown together with steady-state distributions for various values of material stress exponent "n". Again a skeletal point is observed at  $r/R_o \doteq 1.4$ .

The existence of a skeletal point, the position of which is relatively independent of material creep properties leads to a simplified method of predicting thick-cylinder creep-rates. In concept the method is identical to that proposed by Soderberg (11) for thin-walled cylinders. The Soderberg analysis allows the prediction of tangential creep-rates at the outside surface of a thin-cylinder under internal pressure from creep-rates obtained from a single test in uniaxial tension, thus dispensing with the need for a programme of creep tests in uniaxial tension to determine material creep properties. This is an important feature since such a programme of tests could require the use of several tests units for a long period of time and the accuracy of cylinder creep-rate prediction obtained would depend to a great extent on the degree of correlation achieved with the tensile data. The Soderberg analysis only requires the use of a stress criterion and flow-rule and does not depend upon such a correlation. The Soderberg method depends essentially upon the assumption that the redistribution of stress due to creep in the wall of a thin-cylinder under internal pressure is very small compared with the level of stress and therefore the effective stress at the mean diameter of the cylinder may be taken as constant during this redistribution and calculated from initial loading conditions using thin-walled cylinder formulae.

Soderberg shows that if a uniaxial tension creep test is carried out at the same stress as the effective stress at the mean diameter, the tangential

creep-rate at the outside diameter of the cylinder is related to the tensile creep-rate by,

$$\dot{\epsilon}_{\theta} = \frac{\sqrt{3}}{2} \left(\frac{D_m}{D_o}\right)^2 \dot{\epsilon}_1$$

where  $D_m$  and  $D_o$  are the mean and outside diameters of the cylinder respectively. The von Mises criterion and flow-rule was assumed to apply to the material.

When applied to a thick-walled cylinder, this analysis is open to objection on two main grounds.

1) The mean diameter is no longer a suitable reference position since in general the effective stress at this point will change during creep.

2) The method of calculation of the effective stress from thin-cylinder equations of equilibrium is no longer valid and produces a stress which is neither the initial loading stress nor the steady-state stress at the mean diameter.

The skeletal point concept provides a method of analysis for thick-walled cylinders which overcomes these objections while retaining the essential features of the Soderberg analysis. This analysis is presented in Appendix IX which is the typescript of a note shortly to be published. The skeletal point is taken as the reference diameter in the cylinder at which the effective stress remains constant during stress redistribution. The position of this diameter is calculated from the intersection of the elastic and steady-state effective stress distributions as,

$$\frac{D_o}{D} = \left[ \frac{K^2 - 1}{n(K^{1/n} - 1)} \right]^{\frac{n}{2(n-1)}}$$

where D is the reference diameter. It is shown that  $\frac{D_o}{D}$  is insensitive to "n" and may be obtained to a good approximation from an assumed value of "n". The effective stress at this reference diameter may then be calculated from the elastic solution. If a uniaxial tension creep test is carried out at the same stress as this effective stress it is shown that, as in the Soderberg analysis, the tangential creep rate at the outside diameter of the cylinder is given by,

$$\dot{\epsilon}_\theta = \frac{\sqrt{3}}{2} \left(\frac{D}{D_o}\right)^2 \dot{\epsilon}_1$$

An experimental check on this analysis requires a tensile creep test to be carried out at the appropriate stress level for each pressure creep test. Unfortunately the testing programme was almost completed when the analysis was devised, however, in the pressure region where the von Mises criterion was found applicable one of the internal pressures and one of the tensile stress levels corresponded suitably and the results of the analysis applied to these experimental data is contained in Appendix VIII.

The position of the skeletal point is unaffected by the use of an effective stress defined by the Tresca criterion which was applicable to cylinders in the higher pressure regions. For "n" = 5, the skeletal point is,

$$\frac{D_o}{D} = 1.885$$

and from the elastic solution,

$$\begin{aligned} \bar{\sigma} &= \frac{2}{\sqrt{3}} \sigma^* = \frac{2}{\sqrt{3}} \frac{\sqrt{3} P}{(K^2 - 1)} \left(\frac{D_o}{D}\right)^2 \\ &= 0.982 P. \end{aligned}$$

Considering the cylinder test at an internal pressure of 1090 lbf/in<sup>2</sup>

$$\bar{\sigma} = 0.982 \times 1090 = 1070 \text{ lbf/in}^2$$

which corresponds exactly to one of the tension test stress levels. For the Tresca criterion,

$$\begin{aligned}\epsilon_{\theta} &= \frac{3}{4} \left( \frac{D}{D_0} \right)^2 \epsilon_1 \\ &= 0.211 \epsilon_1\end{aligned}$$

The results of this analysis are presented in fig (36) which compares the tangential creep-rates at the outside surface of the cylinder with 0.211 times the tensile creep-rates obtained from constant-stress and constant-load tests at an initial stress of 1070 lbf/in<sup>2</sup>. Although the creep-rates compare favourably at short times, after two or three hours the cylinder creep-rate becomes much higher than predicted by the constant-stress tensile data.

However, the tangential creep strain at the outside diameter of the cylinder is 0.36 per cent at three hours and is beyond the strain limitation placed on the analysis by wall-thinning. It can also be seen that the effect of wall-thinning in the tube is more severe than the effect of specimen thinning in the constant-load test. This strain limitation is present in the Soderberg analysis which also takes no account of changes in cylinder dimensions.

Skelton and Crossland (12) have found the Soderberg analysis provides good agreement with their thick-walled cylinder experimental data. Fig (37) shows the difference in creep-rates predicted by the Soderberg method and the skeletal point analysis for a material with "n" = 5 and diameter ratios up to 3. As the diameter ratio increases, the Soderberg creep rates are increasingly greater than those predicted by the skeletal point method. The uniaxial tension creep-tests of Skelton and Crossland were carried out under conditions of constant load and the Soderberg method was used to compare

minimum creep-rates of the cylinders and tension specimens. From fig (36) it is seen that from constant-load data, the skeletal point analysis predicts a minimum cylinder creep-rate of approximately  $3 \times 10^{-4}$ /hr. From fig (37) it is found that for a cylinder of diameter ratio 2.87 as in the present tests, the Soderberg method predicts a minimum cylinder creep rate of 2.16 times this,

$$\begin{aligned} \text{i.e. } \dot{\epsilon}_{\theta \text{ min}} &= 3 \times 10^{-4} \times 2.16 \\ &= 6.5 \times 10^{-4} / \text{hr.} \end{aligned}$$

This value is within about 7 per cent of the actual cylinder minimum creep-rate.

This is a fortuitous result and is due to the high levels of strain present in the specimens when the minimum creep-rates are attained. At low strains the skeletal point analysis predicts accurate values of cylinder creep-rate from the constant-load tensile test and the Soderberg analysis predicts values approximately 100 per cent high. The minimum creep-rates in these tests are brought about by increases in stress due to wall-thinning in the tube and decreasing cross sectional area in the constant-load tensile specimen. The effect of increasing stress is more severe in the tube than in the tensile specimen and the minimum creep-rate occurs earlier in the tube. The skeletal point analysis therefore predicts a very low value of cylinder minimum creep-rate. The error in the Soderberg analysis due to the large diameter ratio of the tube is in the correct direction and of approximately the correct magnitude to compensate for this. For a material which exhibited a very short primary stage of creep and entered the secondary stage while creep strains were still small, the Soderberg analysis would predict very high values of secondary creep-rate for tubes of appreciable wall thickness.

Method b) Elastic strains taken into account and stress redistribution in the cylinder wall considered.

The analysis of Johnson, Henderson and Khan (7), discussed briefly in Chapter 2, was examined. This analysis was devised to determine total strain-rates occurring in the cylinder wall in the region where creep and elastic strains are of comparable magnitude, i.e. in the region where stress redistribution is occurring. Johnson et al employed a von Mises criterion and flow-rule in a time-hardening form of equation. The equations for total strain-rate were,

$$\dot{\lambda}_{\theta} = \frac{2}{3} A (J_2)^{\frac{n}{2}} \left[ \sigma_{\theta} - \frac{1}{2} (\sigma_r + \sigma_z) \right] f(t) + \frac{1}{E} \frac{d[\sigma_{\theta} - \mu(\sigma_r + \sigma_z)]}{dt} \quad \text{etc.}$$

Originally plane cylinder cross sections were assumed to remain plane during creep and three relationships possible, on general grounds, between the elastic and creep components of axial strain were stated.

(i) That axial creep strain is zero at all times, and is accompanied by constant elastic strain.

(ii) That axial creep strain is zero at all times, and is allied with changing elastic axial strain.

(iii) That both axial creep strain and elastic strain may change but that the total axial strain remains constant in value at all times.

It was shown that (iii) deteriorates into (i). Although relations (i) and (ii) both fail to satisfy all the necessary conditions, relation (i) was taken in preference to (ii) which fails to satisfy constancy of axial strain across the tube section.

The axial strain relationship required to fulfil all the necessary conditions is that both axial creep strain and elastic strain may change

while the total axial strain may vary with time but not with radius. In an analysis designed for manual computation, however, the assumption of zero axial creep is almost essential because then,

$$\dot{\epsilon}_z = A\sigma_E^{n-1} \left[ \sigma_z - \frac{1}{2}(\sigma_r + \sigma_\theta) \right] = 0$$

$$\therefore \sigma_z = \frac{1}{2}(\sigma_r + \sigma_\theta)$$

and the axial stress can be eliminated from the subsequent analysis.

It was pointed out by Johnson et al that relations (i) and (ii) lead to the same forms for  $\sigma_\theta$ ,  $\sigma_r$ ,  $\sigma_z$ ,  $\dot{\lambda}_\theta$ , and  $\dot{\lambda}_r$  but lead to different forms of  $\dot{\lambda}_z$ . In fact the relation used in the subsequent analysis is relation (ii), since if relation (i) is applied, the following condition is necessary in the analysis,

$$\epsilon_z = \frac{1}{E} [\sigma_z - \mu(\sigma_r + \sigma_\theta)] = C$$

where  $\epsilon_z$  is the axial elastic strain and C is a constant with respect to time and radius.

$$\therefore \sigma_z = CE + \mu(\sigma_r + \sigma_\theta)$$

$$\text{Also } \sigma_z = \frac{1}{2}(\sigma_r + \sigma_\theta)$$

$$\therefore \sigma_r + \sigma_\theta = \frac{CE}{\left(\frac{1}{2} - \mu\right)} = \text{Constant.}$$

Therefore if relation (i) is applied, no change of tangential stress can occur at the bore and outside surfaces of the cylinder unless there is a change in the radial stresses at these positions which can only take place if the applied pressure changes. The analysis of Johnson et al applies therefore to a cylinder in which originally plane cross sections are distorting during creep. This can be observed from the results presented in the Johnson paper

if axial strains at any radius at a given time are calculated from,

$$e_z = \frac{1}{E} [\sigma_z - \mu(\sigma_r + \sigma_\theta)]$$

Setting  $(\sigma_r - \sigma_\theta) = x$ , and making use of the equations of radial force equilibrium and total strain compatibility, Johnson et al derived the following equation,

$$\frac{d}{dr} \left[ \frac{EAf(t)}{2^n(2-\mu)} + r^2 x^{(n+1)} + r^2 \frac{dx}{dt} \right] = 0$$

Integrating this equation with respect to radius introduces an unknown function of time  $f(t)$  into the right hand side of the equation. It was shown that the equation is satisfied by the elastic stresses at time zero and the steady-state stresses at infinite time and Johnson et al concluded that  $f(t)$  applies between these limits. The equation is then,

$$\frac{EAf(t)r^2 x^{(n+1)}}{2^n(2-\mu)} + \frac{d(r^2 x)}{dt} = \frac{KEAf(t)}{2^n(2-\mu)}$$

which becomes,

$$\int_0^t \frac{EAf(t)dt}{2^n(2-\mu)} = - \int_{x_0}^x \frac{dx}{[x^{(n+1)} - x_\infty^{(n+1)}]}$$

where  $x_0$  and  $x_\infty$  are the values of  $x$  obtained from the elastic and steady-state stress distributions respectively.  $f(t)$  is taken as  $t^{m-1}$  and the equation becomes,

$$\frac{EA t^m}{m 2^n(2-\mu)} = - \int_{x_0}^x \frac{dx}{[x^{(n+1)} - x_\infty^{(n+1)}]} \dots\dots(29)$$

Johnson et al then introduce a complex graphical procedure to determine the stress and total strain-rate distributions at any time in the cylinder. The analysis can be carried out fairly simply if only the inside and outside surfaces of the cylinder are considered since at these positions  $\sigma_r$  remains constant. For the present tests equation (29) was used to determine the redistribution of tangential stress with time at the inside and outside surfaces of the cylinders. Equation (29) was solved, by means of the computer using a numerical method of integration, for the four lowest pressure tests for which it was estimated that the initial stress distribution would be completely elastic. The results are shown in figs (38, 39, 40, and 41). It is seen that stress redistribution is completed in an extremely short time, with redistribution at the bore being quicker than at the outside surface. The longest time required for stress redistribution was some 3 hours at the outside surface of the cylinder at the lowest pressure. The results of this analysis indicate that at the pressures above  $805 \text{ lbf/in}^2$ , in which it was estimated that some time-independent plasticity would occur on pressure loading, the time required for complete redistribution of the stresses would be of the order of the few seconds required to apply the pressure, and a steady-state stress distribution would in effect be set up at time zero.

As stated in Chapter 2 the analysis of Johnson et al was examined by Larke and Parker (13) and compared with the Bailey (1) analysis which neglects elastic components of strain and considers the steady-state stress distribution to be set up in the cylinder wall from time zero. These solutions have in common the assumption of zero axial creep and determine creep-rates from time-

hardening equations based on the von Mises criterion and flow-rule. Larke and Parker demonstrate that the equations for circumferential strain at the inside and outside surfaces of the cylinder inherent in both theories are mathematically identical. If this were true the relatively simple method of analysis adopted in the first part of this chapter would provide an accurate description of the total circumferential strains occurring at the outside surface of a thick-cylinder in the region where creep and elastic strains are of comparable magnitude. Complex analyses would then have value only if knowledge of stresses rather than strains at any time was of importance. Unfortunately this is not the case.

Larke and Parker, considering the analysis of Johnson et al, show that at the bore and outside surface of the cylinder where  $\sigma_r$  does not change, and therefore  $\frac{d\sigma_r}{dt} = 0$ , the expression for total tangential strain-rate becomes,

$$\dot{\lambda}_\theta = - \frac{Ax^{(n+1)}_t^{(m-1)}}{2^{(n+1)}} - \frac{(2 - \mu)}{2E} \frac{dx}{dt} \quad \dots\dots(30)$$

where  $x = (\sigma_r - \sigma_\theta)$  as in the Johnson analysis. Substituting for  $\frac{dx}{dt}$  in equation (30) from the relationship,

$$\left[ x^{(n+1)} - x_\infty^{(n+1)} \right] \frac{EA t^{(m-1)}}{2^n (2 - \mu)} + \frac{dx}{dt} = 0$$

contained in the Johnson paper, Larke and Parker obtain,

$$\dot{\lambda}_\theta = \frac{Ax^{(n+1)}_t^{(m-1)}}{2^{(n+1)}} + \frac{(2 - \mu)EA t^{(m-1)} (x^{(n+1)} - x_\infty^{(n+1)})}{2E(2 - \mu)2^n} \quad \dots\dots(31)$$

which reduces to,

$$\dot{\lambda}_{\theta} = - \frac{Ax_{\infty}^{(n+1)} t^{(m-1)}}{2^{(n+1)}} \dots\dots(32)$$

Equation (32) is then integrated to provide,

$$\lambda_{\theta} = - \frac{Ax_{\infty}^{(n+1)} t^m}{m 2^{(n+1)}} \dots\dots(33)$$

The remainder of the paper is devoted to obtaining equivalence of the Johnson and Bailey creep constants from which it is shown that equation (33) is identical to the Bailey equation for tangential creep-strain.

Equation (33) is an erroneous relationship. The right hand side of equation (31) is in two parts. The first is the creep component of strain-rate and the second is the elastic strain-rate component. If these components are combined into one term as in equation (32), the equation cannot be integrated to provide total strain. The creep strain is cumulative and can therefore be obtained by integration of the creep-rate component from time zero, but the elastic strain is not cumulative and depends only upon the instantaneous values of the principal stresses and is not obtained therefore by integration of an elastic strain-rate component from time zero. The expression for total circumferential strain at time t inherent in the Johnson analysis is in fact,

$$\lambda_{\theta} = \int_0^t \frac{Ax^{(n+1)} t^{(m-1)} dt}{2^{(n+1)}} + \frac{1}{E} [\sigma_{\theta} - (\sigma_r + \sigma_z)] \quad \text{at time } t$$

which will, in general, be different from the Bailey circumferential creep strain equation.

The incremental analysis of Smith (14), discussed in Chapter 2, was examined. A simplified form was taken considering isothermal conditions, complete pressure loading at zero time, and zero external pressure. The basic relationships in the Smith analysis are:

- 1) radial equilibrium of force

$$\frac{d\sigma_r}{dr} - \frac{1}{r}(\sigma_\theta - \sigma_r) = 0 \quad \dots\dots(1)$$

- 2) radial equilibrium of total strain

$$\frac{d\lambda_\theta}{dr} - \frac{1}{r}(\lambda_r - \lambda_\theta) = 0 \quad \dots\dots(2)$$

- 3) axial equilibrium of force

$$\int_a^b r \sigma_z dr = \frac{P}{2} (b^2 - a^2) \quad \dots\dots(3)$$

- 4) axial compatibility of total strain

$$\lambda_z = \text{constant with respect to radius} \quad \dots\dots(4)$$

Total strains at any time are the sum of elastic and creep components. If the creep strains,  $\epsilon_\theta$ ,  $\epsilon_r$  and  $\epsilon_z$  at any time are known, equations (1) to (4) form a set of four simultaneous equations which may be solved for the four unknowns  $\sigma_\theta$ ,  $\sigma_r$ ,  $\sigma_z$  and  $\lambda_z$ .

Small intervals of time are considered during which the stresses remain constant. Increments of creep strain occurring during a time interval are calculated from the assumed equation of state, e.g.,

$$\dot{\epsilon}_\theta = A\sigma^{*n-1} \left[ \sigma_\theta - \frac{1}{2}(\sigma_r + \sigma_z) \right] t^P$$

The total creep strains at the end of the time interval are the sums of the total creep strains at the beginning of the time interval and the creep strain

increments. The creep strains at the end of the time interval are used in equations (1) to (4) which are solved simultaneously for  $\sigma_{\theta}$ ,  $\sigma_r$ ,  $\sigma_z$  and  $\lambda_z$ . This allows determination of the complete stress and strain distributions in the cylinder wall at the end of the time interval which provides the starting point for the next time interval.

This analysis was carried out by means of the computer for the internal pressure test at the lowest pressure (620 lbf/in<sup>2</sup>). Nine radial positions in the wall were taken and the first time interval was selected as  $10^{-12}$  hours, as redistribution of stress appeared to start at times of this order from the results of the Johnson analysis at this pressure.

The distributions of the principal stresses in the cylinder wall at various times obtained from the Smith analysis are shown in fig (42) and the redistributions of tangential stress with time at the bore and outside surfaces are compared with the Johnson analysis in fig (43). As in the Johnson analysis redistribution of stress is faster initially at the bore than at the outside surface but the results of the Smith analysis show that redistribution of the stresses is completed at approximately the same time throughout the wall. Fig (44) shows the distributions in the cylinder wall of total axial strain, and the elastic and creep components, at a time of 1 hour, when stress redistribution is almost completed. Although the creep component of axial strain is not zero during stress redistribution, the results of the analysis show that it is always very small compared with the tangential and radial creep strains. Fig (45) shows tangential and axial creep strains against time occurring at the bore of the cylinder. Similar results were obtained at each of the radial stations.

CHAPTER 6

DISCUSSION OF THE RESULTS OF THE INVESTIGATION

6.1 Choice of strain system

Normal strain may be defined as,

1) engineering strain,

$$\epsilon = \frac{l - l_0}{l_0},$$

where  $l$  and  $l_0$  are the instantaneous and original lengths respectively, or

2) natural or logarithmic strain,

$$e = \ln \frac{l}{l_0}.$$

The definition of engineering strain is more convenient to use and was adopted in the work described here. The concept of natural strain has been made use of in the analysis of thick-cylinder creep behaviour by Rimrott (1).

The advantage of natural strain is that strain increments may be added directly,

$$\text{i.e. } e = e_1 + e_2 + e_3 \dots \dots\dots(1)$$

while within the definition of engineering strain the same relationship is,

$$1 + \epsilon = (1 + \epsilon_1)(1 + \epsilon_2)(1 + \epsilon_3) \dots$$

Similarly the condition that creep occurs at constant volume may be expressed in terms of natural strain as,

$$e_1 + e_2 + e_3 = 0 \dots\dots(2)$$

while in engineering strain form this becomes,

$$(1 + \epsilon_1)(1 + \epsilon_2)(1 + \epsilon_3) = 1$$

Up to moderate strain levels the strain values calculated by these two

methods are very similar and there is little error caused by using engineering strains in equations of the form of (1) and (2).

## 6.2 Tensile creep tests

The isotropy of the material was investigated by means of constant-stress tensile creep tests on specimens from three mutually perpendicular directions of the billet. This method was far from exhaustive and only the tensile specimens taken from the axial direction of the billet were truly representative of a cylinder principal direction. It has also been indicated (2) that the compressive creep properties of materials should be included in an investigation of isotropy. However a rigorous determination of material isotropy would be a major investigation in its own right and it was felt that the isotropy test results presented in figs (11 to 16 inclusive) indicated that reasonably isotropic behaviour could be expected within the range of test conditions.

The method of investigating the uniaxial tension creep behaviour of the material by means of a series of constant-stress tests proved to be most useful. In this type of test stress becomes a parameter rather than a test variable and the functions of stress and time can be separated and determined individually. The equation of state can then be built up from a combination of these functions. This approach is not possible with data obtained from conventional constant-load creep tests since stress, strain and time must be considered together. Therefore the form of the equation of state must be selected first and its suitability determined from the experimental data.

While, as discussed in Chapter 2, the existence of an equation of

state for the material is unlikely, the correlation of the constant-stress tensile creep data shown in figs (25, 26 and 27) indicated that the equation of state approach should be valid within the stress range of the tests. This correlation also indicated that the irregular creep behaviour observed during the early parts of these tests had little effect on the overall creep behaviour.

Another important feature of the constant-stress data was the occurrence of primary creep only during the tests indicating, as discussed previously, that any increasing creep-rates in the constant load and tube tests would be caused by stress increases.

If stages of creep other than primary are observed during constant-stress creep tests it is possible to represent the data by suitable choice of the time function. Bailey (3) suggested the use of a time function of the form

$$f(t) = t^p$$

where  $p < 1$  for primary creep,  $p = 1$  for secondary creep and  $p > 1$  for tertiary creep. This method leads to discontinuities due to the abrupt changes in  $f(t)$  at each stage and methods providing complete continuity have been proposed by de Lacombe (4) in which,

$$f(t) = at^p + bt^q$$

where  $p < 1$  and  $q > 1$ , and Graham and Wallis (5) who suggested the particular series

$$f(t) = at^{1/3} + bt + ct^3$$

Both these methods lead to fairly complex analysis.

The representation of the constant-load data shown in figs (29 and 30) obtained from time-hardening and strain-hardening equations using the creep constants obtained from the constant-stress data indicates that

both forms of equation provide a satisfactory fit to the experimental data. This prediction of the constant-load data from the constant-stress correlation was used as an intermediate step in the prediction of the thick-cylinder data. The results show that for such a step to be most useful the stress would be required to vary much more than in the constant-load tests. A continuously increasing stress system would be more valuable than one providing abrupt changes in stress and such a system could be arranged by means of a cam similar to that used in the constant-stress tests which caused the load applied to the specimen to increase as creep took place. The instantaneous stress during a constant-load test is given by,

$$\sigma = \sigma_0 (1 + \epsilon)$$

and the cam could be produced to provide

$$\sigma = \sigma_0 (1 + A\epsilon)$$

where  $A = 3$  perhaps, providing a more seriously changing stress system.

### 6.3 Internal pressure creep tests

Because of the low creep resistance of the test material creep strains of a large order compared with elastic strains were produced very quickly, even at low pressures. Redistribution of stress in the walls of the cylinders was extremely rapid therefore, as shown in figs (38 to 43) and the steady state stress distribution was set up almost instantaneously in all but the lowest pressure tests. The material therefore was unsuitable for an experimental investigation of thick-walled cylinder creep behaviour in the strain range in which stress redistribution occurs. Within this strain range the changes in specimen outside diameter occurring were of

the order of microinches and as discussed in Chapter 3 this order of sensitivity was not obtained from the diametral extensometry. In any case strains of a much larger order were required before the initial irregularities in creep behaviour were eliminated.

However, apart from this irregular creep behaviour at low strains, which unfortunately was more pronounced in the cylinder tests than the tensile tests, the test material was ideally suited to an experimental investigation involving creep strains of a finite magnitude. Due to the low creep resistance, large creep strains could be obtained in short times at pressures low enough to ensure negligible plastic strain on loading. In the test at the highest pressure in which 10 per cent strain was obtained at the outside diameter of the cylinder in less than 4 hours, the analysis of Allen and Sopwith (6) showed that, on initial loading, the cylinder was not yet fully plastic and the tangential strain at the outside diameter due to the pressure loading was calculated to be only  $5 \times 10^{-5}$ . This means not only that the measured strains may be taken as creep strains eliminating the necessity of subtracting the initial loading strains, but also that no severe prestraining of the specimens due to a large initial plastic component is caused. Such prestraining can alter greatly the subsequent creep behaviour (7) and reduce the possibility of correlation of the data over the stress range.

The representation of the experimental data shown in figs (32 to 35) provided by the modified Bailey form of analysis is fairly good although this analysis describes creep behaviour by means of a simple power law function of time and creep behaviour of this variety was not obtained

during the early stages of the tests. This representation of the experimental data indicates that the approach adopted in the modified Bailey analysis, of considering cylinder creep-rates to be governed by a primary time function together with an increasing function of stress due to wall-thinning is realistic, within the experimental range investigated.

The apparent transition in stress dependence from the von Mises criterion at low pressures to the Tresca criterion at higher pressures is interesting. It is possible that this effect could be due to the form of anisotropy referred to by Berman and Pai (2) occurring after moderate creep strains. This form of anisotropy would not be evident from the isotropy tests carried out in uniaxial tension. The von Mises and Tresca criteria were taken to be equivalent in uniaxial tension, i.e. on the reduced plane the corners of the Tresca hexagon coincide with the von Mises circle, as shown in fig (46). With the assumption of zero axial creep used in the analysis, the stress state in the wall of the cylinder becomes one of pure shear indicated in fig (46) by  $\sigma$ . A third possible form of yield criterion which is isotropic in uniaxial tension but for which different creep behaviour will occur in tension and compression is shown in the figure and it can be seen that for a material actually governed by this criterion, the Tresca criterion will provide a better description of thick-cylinder creep behaviour than the von Mises criterion. The apparent transition in stress criterion obtained in the present investigation therefore could be due to this form of anisotropy occurring after moderate cylinder creep strains.

The poorest representation of the experimental data was obtained in the region where the transition of both the stress criterion and the stress exponent

took place. Although a fairly abrupt change in stress exponent was found in the tensile tests, the change in the cylinder tests will be more gradual because of the large range of effective stress present in the wall of each cylinder. A pressure range exists within which the material towards the bore of a cylinder will be in the high stress range while the material towards the outside surface will be in the low stress range. Because of the strong compatibility conditions to be satisfied by cylinder deformation the creep behaviour will be governed by a compromise value of stress exponent somewhere between the high and low values. The determination of this pressure range is complicated by the apparent change in stress criterion, since the effective stress at any point in the cylinder depends upon the stress criterion.

The prediction of creep-rates at the outside diameters of the cylinders by means of the skeletal point analysis shown in figs (36 and 58) indicates that this method can be expected to provide reasonable accuracy before the effect of cylinder wall-thinning becomes too great. In the present investigation it is estimated that this form of analysis is limited to tangential creep strains at the outside diameter of the cylinders up to about 0.2 per cent. It is also evident from fig (36) that the use of constant-load rather than constant-stress uniaxial tension creep test data would not increase the useful strain range to any worthwhile extent. Section 6.3.1, following, presents a possible modification of the skeletal point analysis to extend the strain range for which the method is applicable.

The degree of success achieved in the prediction of thick-walled cylinder creep behaviour by a Bailey type of analysis depends to a great extent upon a satisfactory correlation of uniaxial tension creep data. The skeletal point type of analysis requires only the use of a satisfactory form of

stress criterion and flow rule since,

$$\dot{\epsilon}_1 = A\sigma_1^n f(t)$$

in uniaxial tension and,

$$\dot{\epsilon}_E = A\sigma_E^n f(t)$$

in the thick-walled cylinder. "A", "n" and f(t) are identical in both cases allowing the elimination of "A" and f(t) from the analysis. Although the stress exponent "n" appears in the analysis, its accurate determination is not required as shown in Appendix VIII.

The results of the analyses of Johnson et al (7) and Smith (8) of the test at the internal pressure of 620 lbf/in<sup>2</sup> show that the rate of stress redistribution is extremely high and that the redistribution is almost complete after about an hour. This is a direct consequence of the low creep resistance of the test material allowing creep strains of the same order as the elastic strains to be accumulated in a very short time. Fig (43) shows that the forms of redistribution of stress with time obtained from these analyses are in qualitative agreement. The Johnson analysis, however, indicates that stress redistribution in the cylinder is completed at the bore earlier than at the outside surface while the Smith analysis shows completion of the redistribution at about the same time throughout the wall. A similar result has been described by Mackie and King in discussion of (8). It is likely that this difference is due to the simplifying axial creep assumption made in the Johnson analysis. As discussed in Chapter 5 the axial strain condition imposed in the Johnson analysis causes initially plane cross sections of the cylinder to distort during stress redistribution and therefore the analysis provides a form of stress redistribution with time which will differ to some extent from that of a

cylinder in which plane cross sections remain plane during creep. This form of error can be eliminated only if the axial creep, which takes place during stress redistribution, is accounted for in the analysis. If this is done, an incremental approach similar to that of Smith is required and manual computation is no longer possible.

Even if computer time is readily available the approximate method of Johnson et al is of considerable value since it provides results for stress redistribution, which are in reasonable agreement with the results of the incremental analysis, with an enormous saving in computer time.

### 6.3.1 Possible extension of the skeletal point analysis to finite strain range

The position of the skeletal point is obtained from,

$$\frac{D_o}{D} = \left\{ \frac{(K^2 - 1)}{n(K^{2/n} - 1)} \right\}^{\frac{n}{2(n-1)}} = S \quad \dots(1)$$

and the effective stress at the skeletal point is,

$$\sigma^* = \frac{\sqrt{3} P}{(K^2 - 1)} S^2 \quad \dots(2)$$

As the cylinder dimensions change during creep, K decreases and the position of the skeletal point therefore changes. Creep deformation of the cylinder is considered as a series of small increments of creep, during each of which creep-rates are determined from the effective stress at the current position of the skeletal point which is determined from the current value of the cylinder K ratio.

Equations (1) and (2) may be used to determine the effective stress at the skeletal point for any value of K during creep. The tangential creep-rate at the skeletal point is,

$$\dot{\epsilon}_S = \frac{\sqrt{3}}{2} A\sigma^{*n} f(t)$$

This creep-rate is related to the instantaneous cylinder dimensions. The tangential creep-rate at the outside diameter of the cylinder must be related to the initial dimensions of the cylinder, to remain within the definition of engineering strain, and becomes,

$$\dot{\epsilon}_b = \frac{\dot{\epsilon}_S}{S^2} (1 + \epsilon_b)$$

As before,

$$\dot{\epsilon}_S = \frac{\sqrt{3}}{2} \dot{\epsilon}_1$$

where  $\dot{\epsilon}_1$ , is the creep-rate of a tension specimen tested at

$$\sigma = \sigma^*$$

$$\dot{\epsilon}_1 = A\sigma^{*n} f(t)$$

$$\begin{aligned} \text{and } \dot{\epsilon}_b &= \frac{\sqrt{3}}{2} \frac{\dot{\epsilon}_1 (1 + \epsilon_b)}{S^2} \\ &= \frac{\sqrt{3}}{2} \frac{A\sigma^{*n} f(t) (1 + \epsilon_b)}{S^2} \end{aligned}$$

$$= \frac{\sqrt{3}}{2} A\sigma_1^n f(t)$$

$$\text{where } \sigma_1 = \sigma^* \left\{ \frac{(1 + \epsilon_b)}{S^2} \right\}^{\frac{1}{n}}$$

Therefore if a uniaxial tension creep specimen is tested with

$$\sigma_1 = \sigma^* \left\{ \frac{(1 + \epsilon_b)}{S^2} \right\}^{\frac{1}{n}}$$

the tangential creep-rate at the outside surface of the cylinder is,

$$\dot{\epsilon}_b = \frac{\sqrt{3}}{2} \dot{\epsilon}_1$$

As discussed previously, the equation of state may apply over only a limited range of stress. It is important therefore that the tensile stress  $\sigma_1$  be as close as possible to the effective stress  $\sigma^*$  and therefore that the ratio

$$\frac{1 + \epsilon_b}{S^2} \doteq 1$$

At any time the change in the position of the skeletal point from the initial position at time zero may be defined as,

$$\begin{aligned} \Delta S &= S - S_0 \\ \therefore S &= S_0 + \Delta S \\ &= S_0 \left( 1 + \frac{\Delta S}{S_0} \right) \end{aligned}$$

Equation (3) may then be written as,

$$\sigma_1 = \sigma^* \left\{ \frac{(1 + \epsilon_b)}{\left( 1 + \frac{\Delta S}{S_0} \right)^2} \right\}^{\frac{1}{n}}$$

and the tangential creep-rate at the outside surface of the cylinder becomes,

$$\dot{\epsilon}_b = \frac{\sqrt{3}}{2} \frac{\dot{\epsilon}_1}{S_0^2}$$

The ratio,

$$\frac{(1 + \epsilon_b)}{\left( 1 + \frac{\Delta S}{S_0} \right)^2} \doteq 1$$

and the tensile stress  $\sigma_1$  will always be close to the effective stress  $\sigma^*$ .

The following procedure could be carried out by means of a simple

computer programme.

Initial values of cylinder inside and outside radii,  $a_0$  and  $b_0$  and hence  $K_0$  are known.  $S_0$  and  $\sigma_0^*$  are calculated from equations (1) and (2). Then, at  $t = 0$ ,  $\sigma_1 = \sigma_0^*$  and  $\epsilon_1 = \epsilon_b = 0$ .

Values of  $\epsilon_b$  are chosen in small increments. At any  $\epsilon_b$  say  $\epsilon_{b_n}$ ,

$$b_n = b_0 (1 + \epsilon_{b_n})$$

$$\epsilon_{a_n} = K^2 \epsilon_{b_n} = \frac{a_n}{a_0} - 1, \text{ hence } a_n$$

$$K_n = \frac{b_n}{a_n}$$

$S_n$  and  $\sigma_n^*$  are calculated from equations (1) and (2), then,

$$\Delta S_n = S_n - S_0$$

$$\sigma_{1_n} = \sigma_n^* \left\{ \frac{(1 + \epsilon_{b_n})}{\left(1 + \frac{\Delta S_n}{S_0}\right)^2} \right\}^{\frac{1}{n}}$$

$$\epsilon_{1_n} = \epsilon_{1_{n-1}} + \frac{2S_0^2}{\sqrt{3}} (\epsilon_{b_n} - \epsilon_{b_{n-1}})$$

In this way, corresponding values of  $\sigma_1$  and  $\epsilon_1$  are obtained.

For a uniaxial tension creep specimen, if constant volume creep deformation is assumed,

$$l \times A = l_0 \times A_0$$

where  $l$  and  $A$  are the length and cross sectional area respectively.

Also

$$\sigma_1 = \frac{W}{A}$$

where  $W$  is the applied load,

and

$$\epsilon_1 = \frac{l}{l_0} - 1$$

Combining these equations leads to the following expression,

$$W = \frac{A_0 \sigma_1}{(1 + \epsilon_1)}$$

Therefore the required tensile load  $W$  corresponding to any strain  $\epsilon_1$  can be calculated.  $W$  should be found to increase with increasing strain. The required increase in  $W$  can be obtained by means of a cam system similar to that used in the constant-stress tests with a profile causing an increasing load rather than a decreasing load. The general form of profile which would be suitable is shown in fig (47). The same profile could be used for any pressure since the pressure is directly proportional to  $\sigma_1$  but would be restricted to a single value of stress exponent.

CONCLUSIONS

While the cylinder diametral extensometry performed satisfactorily, the sensitivity of the system was about an order of magnitude less than that of each individual transducer and measurement of the very small initial loading strains was not possible. It is felt that summation of the outputs of opposing transducers to provide a combined reading would increase the sensitivity of the system considerably. Continuous axial strain measurement in the internal pressure tests was not accomplished. With a material as soft as the present test material the only feasible method of continuous axial strain measurement appears to be by direct observation of the specimen through windows in the furnace. It is doubtful, however, if measurements of sufficient sensitivity could be made in this way.

In an investigation involving moderate or high levels of creep strain, uniaxial tension creep data obtained from constant-stress tests provides a clearer indication of material creep behaviour than data obtained from constant-load tests in which stress becomes a test variable. In the present investigation constant-load tests served the useful secondary function of providing creep data for a system of simply varying stress.

Only primary creep was observed during the constant-stress tests leading to the conclusion that creep rates in the constant-load and internal pressure tests, in which the specimen stresses increase continuously due to decreasing cross sectional area and wall thinning respectively, would be determined by the combination of an increasing stress function and a decreasing time function. This approach provided a realistic description of the creep behaviour observed in the constant-load and internal pressure tests.

The skeletal point concept leads to an extension of the Soderberg analysis which is applicable to thick-walled cylinders and provides accurate prediction of the diametral creep rates of a cylinder from the results of a single creep test in uniaxial tension, provided the total strain is small. An analysis has been presented which removes this strain limitation by taking account of the stress increase due to wall thinning.

Comparison of the results of the analyses of Smith and Johnson et al shows that, although the axial creep strain occurring during stress redistribution is very small compared with the tangential and radial creep strains, Johnson's assumption of zero axial creep leads to a difference in the form of the stress redistribution obtained from the two analyses. Incremental analyses such as the Smith analysis, however, lead to great computational complexity compared with the Johnson analysis and the difference in the results is small compared with these difficulties.

APPENDIX I

THE TEST MATERIAL

The material was received in the form of a continuously cast billet, 24 ins. long and  $9\frac{5}{8}$  ins. diameter, together with a transverse slice, taken from the end of the billet, which had been machined and etched to reveal the macrostructure. Examination of this slice indicated that the material had a fairly uniform grain structure with some radial elongation of the grains, probably due to the casting process. The grain size was approximately 1-2 mm. The composition of the material obtained by spectrographic analysis is given below:

titanium	0.06%
iron	0.004%
silicon	0.003%
copper	0.002%
boron	0.001%
remainder aluminium.	

The billet was cut up to produce specimen blanks, as shown in figs (48, 49 and 50). Manufacture of the blanks was carried out in a horizontal mill fitted with a thin circular saw. Very light cuts were taken at each stage and a liberal flow of cutting fluid was used to prevent any alteration of the uniform material structure.

Further examination of the material macrostructure was carried out as follows.

1) On tensile specimen 12 from the axial direction of the billet in the prior to creep test condition. The structure was examined in the axial

direction of the specimen and in three transverse directions at  $120^{\circ}$  to each other.

2) In the axial directions of tensile specimens A3, B4 and 4 after the creep tests. These specimens were used for the isotropy creep tests at  $927 \text{ lbf/in}^2$  and had been subjected to about 10 per cent strain and held at the test temperature for about 500 hours.

3) In the axial direction of tubular specimen 1 after the internal pressure creep test at  $1525 \text{ lbf/in}^2$  during which the external diametral strain obtained was about 10 per cent and the time at temperature was of the order of 20 hours.

The final polishing of these sections was limited to a fine grade of silicon carbide paper since finer polishing might have caused smearing of the surfaces. The following etching solution was found to reveal the macrostructure suitably:

75 ml. concentrated hydrochloric acid

25 ml. concentrated nitric acid

5 ml. 40 per cent hydrofluoric acid.

The surfaces prepared from the unstrained tensile specimen confirmed the observations made on the etched end piece of the billet and showed that the grain elongation was, in fact, in a combined radial and axial direction. Examination of the sectioned surfaces of the tested specimens revealed little apparent change in the macrostructure to have taken place during the tests.

APPENDIX II

DESIGN OF CONSTANT STRESS MECHANISM

To maintain constancy of uniaxial tensile stress in a specimen during creep it is necessary to reduce the applied load as the cross sectional area of the specimen decreases. The method adopted in the present series of tests is shown diagrammatically in fig (4). As the specimen length increases, the wheel and cam assembly rotates clockwise and the load applied to the specimen

$$W = \frac{R_1}{R_2} \times (\text{applied weights})$$

decreases as  $R_1$  decreases while  $R_2$  remains constant. Since the proposed creep tests involved only moderate stresses no mechanical advantage was required and  $R_2$  and the initial value of  $R_1$  were both selected as 9 ins, which was the maximum size permitted by workshop machine capacity. In the design of the cam profile it was assumed that creep deformation would take place at constant volume and that strain along the effective length of the specimen would be uniform. The analytical approach of Garofalo et al (1) was adopted for an effective specimen length of 6 ins. The following equations were obtained providing the rectangular coordinates of the cam profile for any angle of rotation  $\theta$ .

$$x = \frac{9}{1 + 1.5 \theta} \left[ \cos \theta + \frac{1.5 \sin \theta}{1 + 1.5 \theta} \right] \dots\dots(1)$$

$$y = \frac{9}{1 + 1.5 \theta} \left[ \sin \theta - \frac{1.5 \cos \theta}{1 + 1.5 \theta} \right]$$

To manufacture the working cam a template was made by jig-boring  $\frac{1}{8}$  in.

diameter holes close together in a mild steel sheet so that when hardened steel pins were fitted in the holes the required profile was a tangent to the pins and could be produced by filing the mild steel away until the pins were just reached. This template was used to produce two cams, designed for strains up to 35 per cent, from  $\frac{1}{2}$  in. mild steel plate. One cam was the working cam and the other was a counter balance. The load was applied to the specimen via the cam by means of a steel strip, 0.020 in. thick and the basic cam profile equations were adjusted to allow for this. The co-ordinates supplied to the jig borer were calculated from equations (1) modified to allow for pin diameter and strip thickness:-

$$\begin{aligned}x' &= x - 0.0725 \cos \theta \\y' &= y - 0.0725 \sin \theta.\end{aligned}$$

The cams were bolted to the constant radius wheel and keyed to a 1 in. diameter shaft supported in self-aligning bearings. The assembly was bolted to the top-plate of the framework and balanced finally. The assembly was tested for functional accuracy by fitting a proving ring, which had been calibrated and found to provide dial gauge readings which varied linearly with applied load, in place of a specimen, loading the weight carrier and noting the proving ring reading for various angles of rotation of the cam.

For constant volume creep deformation,

$$A \times l = \text{constant},$$

where A and l are the instantaneous values of cross sectional area and effective length of the specimen.

If  $l_0$  = initial effective length,

$$l = l_0 + R_2 \theta$$

$$= 6 + 9\theta$$

$$\therefore A(6 + 9\theta) = \text{constant}$$

$$\text{also } A = \frac{W}{\text{stress}} = \frac{W}{\text{constant}}$$

$$\therefore \text{Load } W \propto A \propto \frac{1}{6 + 9\theta}$$

Therefore a straight line relationship should exist between the proving ring dial gauge reading and the function  $\frac{1}{6 + 9\theta}$  as the cam is rotated. This relationship is shown in fig (51).

### Possible errors in the system

#### a) Effective specimen length

If effective length of specimen is in error by 0.1 in., i.e. say

$l_0 = 5.9$  in., then after 30 per cent strain,

$$l = 1.3 \times 5.9 \text{ in.} = 7.67 \text{ in.},$$

and 
$$\theta = \frac{7.67 - 5.9}{9} = 0.197 \text{ radians.}$$

The basic cam profile equation (ref (1)) is,

$$R_1 = \frac{9 l_0}{l_0 + R_2 \theta}$$

$$\therefore R_1 = \frac{9 \times 6}{6 + 9 \times 0.197} = 6.94 \text{ in.}$$

$$\text{Load on specimen} = \frac{6.94}{9} W.$$

If effective length is correct,

$$l = 1.3 \times 6 = 7.80 \text{ in.},$$

$$\theta = \frac{7.8 - 6}{9} = 0.200 \text{ radians,}$$

$$R_1 = \frac{9 \times 6}{6 + 9 \times 0.2} = 6.92 \text{ in.}$$

$$\text{Load on specimen} = \frac{6.92}{9} W.$$

∴ Error in stress =  $\frac{0.02}{6.92} \times 100 = 0.29$  per cent,

i.e. for error in effective length of specimen of 0.1 in., error in stress after 30 per cent strain is less than 0.3 per cent.

b) Initial zero setting of cam

If initial setting is  $+ 1^\circ$  i.e.  $+ 0.0175$  radians in error, then at 30 per cent strain,  $\theta$  is 0.2175 radians instead of 0.200 radians.

$$\text{Then } R_1 = \frac{9 \times 6}{6 + 9 \times 0.2175} = 6.78 \text{ in.}$$

$$\text{Load on specimen} = \frac{6.78}{9} W.$$

$$\text{Error in stress} = \left\{ \frac{6.92 - 6.78}{6.92} \right\} \times 100 = 2.02 \text{ per cent,}$$

i.e. an error of  $\pm 1^\circ$  in initial cam setting leads to a stress error of approximately 2 per cent at 30 per cent strain. The initial cam setting could be adjusted to within  $\pm 0.1^\circ$  ensuring correspondingly smaller errors from this source.

c) Constant load error

In addition to the load applied via the cam, the specimen supports a small load due to the "chain-effect" of pull rods and associated items which hang below the specimen. Although this load is accounted for in the calculation of total load initially, it does not decrease along with the main applied load as the specimen extends and therefore leads to an error in stress which increases with strain. This constant portion of load was 3.78 lb. and since initially  $R_1 = R_2$ , the total load applied to the specimen at the start of a test

$$= 3.78 + (\text{weight on load carrier}) \text{ lb.}$$

If initial weight on load carrier is  $W_0$ , the cam is designed so that

when specimen creep strain is  $\epsilon$ ;

$$W = \frac{W_0}{1+\epsilon}$$

e.g. test in which  $\sigma = 1153 \text{ lbf/in}^2$ .

Initial load applied to the specimen,

$$= 3.78 + 141.12 = 144.90 \text{ lb.}$$

Final strain  $\epsilon = 16$  per cent.

∴ Final applied load

$$= 3.78 + \frac{141.12}{1.16} = 125.44 \text{ lb.}$$

Correct final applied load

$$= \frac{144.90}{1.16} = 124.91 \text{ lb.}$$

Error in stress

$$= \left\{ \frac{125.44 - 124.91}{124.91} \right\} \times 100$$

$$= 0.42 \text{ per cent.}$$

The maximum errors caused by this constant load effect are tabulated for each stress level below.

Nominal Stress	Maximum error per cent
1287	0.29
1153	0.42
1070	0.40
927	0.43
729	0.18
610	0.08
543	0.03
487	0.01

From considerations of these sources of error in stress constancy

it is estimated that the maximum variation of stress in any one test was less than 1 per cent.

Reference

(1) Garofalo, F., Richmond, O., Domis, W.F., "Design of apparatus for constant-stress or constant-load creep tests," Trans. A.S.M.E., J. Basic Eng., 1962, 84 (Series D), 287.

APPENDIX IIIINVESTIGATION OF CREEP OCCURRING IN FILLETRADII OF TENSILE SPECIMENS

Typical tensile specimen fig (52a) has fillet radius  $r$  and gauge length diameter  $D$ . If primary creep is neglected and a secondary creep relationship is assumed of the form,

$$\dot{\epsilon} = A\sigma^n$$

where  $\dot{\epsilon}$  and  $\sigma$  are the creep-rate and applied stress respectively and  $A$  and  $n$  are constants, then the axial creep-rate in the parallel length of the specimen is,

$$\dot{\epsilon}_P = A \left\{ \frac{W}{\frac{\pi D^2}{4}} \right\}^n$$

where  $W$  is the applied load.

∴ Axial creep strain after time  $t$  is

$$\begin{aligned} \dot{\epsilon}_P &= A \left\{ \frac{W}{\frac{\pi D^2}{4}} \right\}^n t \\ &= \frac{l - l_0}{l_0} \end{aligned}$$

where  $l_0$  is the original gauge length and  $l$  is the gauge length after time  $t$ .

∴ Increase in length of parallel section in time  $t$

$$\begin{aligned} \Delta l &= l - l_0 \\ &= A \left\{ \frac{W}{\frac{\pi D^2}{4}} \right\}^n t l_0 \end{aligned}$$

Specimen cross sectional area at fillet

$$= \frac{\pi}{4} \{D + 2r(1 - \cos \theta)\}^2$$

Axial creep rate at a point in the fillet

$$\dot{\epsilon}_F = A \left\{ \frac{W}{\frac{\pi}{4} [D + 2r(1 - \cos \theta)]^2} \right\}^n$$

and axial creep strain at the point after time t

$$\epsilon_F = A \left\{ \frac{W}{\frac{\pi}{4} [D + 2r(1 - \cos \theta)]^2} \right\}^n t$$

∴ Increase in axial length of fillet in time t

$$\Delta F = \int_0^L A \left\{ \frac{W}{\frac{\pi}{4} [D + 2r(1 - \cos \theta)]^2} \right\}^n t dL$$

$L = r \sin \theta$  and  $dL = r \cos \theta d\theta$

$$\begin{aligned} \therefore \Delta F &= A \left[ \frac{4W}{\pi} \right]^n t r \int_0^\theta \frac{\cos \theta d\theta}{[D + 2r(1 - \cos \theta)]^{2n}} \\ &= A r t \left[ \frac{4W}{\pi} \right]^n D^{-2n} \int_0^\theta \frac{\cos \theta d\theta}{\left[ 1 + \frac{2r}{D}(1 - \cos \theta) \right]^{2n}} \end{aligned}$$

∴ Ratio of axial creep in parallel portion of specimen, to axial creep in fillets

$$R = \frac{\Delta \ell_p}{2\Delta F} = \frac{\ell}{2r} \left[ \frac{1}{\int_0^\theta \frac{\cos \theta d\theta}{\left[ 1 + \frac{2r}{D}(1 - \cos \theta) \right]^{2n}}} \right]$$

A value of  $n = 3.5$  was assumed since this  $n$  value had been found to apply to a material very similar in composition to that used in the present investigation (1). The integral was evaluated graphically in the range  $0 \leq \theta \leq \frac{\pi}{2}$  for various values of  $r/D$  and the results are shown in fig (53).

For a large value of R the following conditions should be met,

1)  $l$  should be large

2)  $r$  should be small

3)  $\int_0^\theta \frac{\cos \theta \, d\theta}{\left[1 + \frac{2r}{D}(1 - \cos \theta)\right]^{2n}}$  should be small.

Condition 3) requires therefore that  $r/D$  should be large and since  $r$  should be small from condition 2)  $D$  should be as small as possible.

The maximum size of  $l$  is limited by the dimensions of the billet and the minimum size of  $D$  is limited by the difficulty of machining long thin specimens of very ductile material. In view of these requirements, the following optimum dimensions were chosen,

$$l = 5.75 \text{ in}; \quad D = 0.4 \text{ in}; \quad \text{and } r = 0.125 \text{ in.},$$

and the specimen had the form shown in fig (2). This design of specimen provides  $R = 41.4$ .

∴ Proportion of total creep strain occurring in fillets = 2.4 per cent.

Proportion of total creep strain occurring in parallel portion 0.25 in. long = 4.3 per cent. The effective length of the specimen was taken as 6 in. which is in error by less than 2 per cent.

An attempt was made to check the analysis by means of experimental data. Eight tensile creep specimens which had been used in a previous testing programme (1) and which had been subjected to various known creep strains were selected and the axial deformation which had taken place in the fillets was estimated from measurements made by means of a projection microscope. The original fillet form of these specimens is shown in fig (52b). The specimen dimensions were,  $r = 0.5 \text{ in}; D = 0.437 \text{ in}; \theta = 40^\circ$  and  $l_0 = 4.6 \text{ in}$ .

From an analysis similar to that described a value of  $R = 13$  was obtained. The estimated values of  $R$  from the measurements varied from 3 to 50 providing an average value of about 19.

Reference

- (1) King, R.H., "Creep of thick-walled cylinders under internal pressure," Ph.D. Thesis, University of Glasgow, 1964.

APPENDIX IV

TENSILE SPECIMEN LOADING JACK

A diagrammatic arrangement of the jack is shown in fig (54). A  $\frac{1}{4}$  h.p. electric motor fitted with a gear box providing an output shaft speed of 12 r.p.m. is connected via a pair of 1 : 1 ratio bevel gears to the vertical screw. The screw runs in a circular nut which is a sliding fit in the cylinder. The nut is fitted with a key which runs in a vertical keyway cut in the cylinder. Rotation of the screw therefore moves the nut axially in the cylinder. The load is initially supported by the platform which is lowered at a constant rate by the electric motor until the load is completely applied to the specimen. The system is reversible and the electric motor can be used to return the platform to its initial position. The time taken for complete application of the load depends upon the "slack" to be taken up. This is in the form of elastic strain in the system and consists mainly of strain in the steel loading strip. It also includes the "instantaneous" specimen strain.

If applied load = W, then displacement during loading,

$$d = W \left[ \frac{L_1}{A_1 E_1} + \frac{L_2}{A_2 E_2} + \dots \right]$$

where L, A, and E are the length, cross sectional area and Young's modulus respectively of the constituent elements of the system

$$\therefore d \propto W$$

d is also directly proportional to the time taken to apply the load, therefore the loading rate is constant for all specimens and is independent of the magnitude of the load.

Estimate of approximate loading rate

Assuming all the displacement is due to elastic strain in the loading strip,

$$W = 150 \text{ lb. (say); } L = 6 \text{ ft; } A = 0.01 \text{ in}^2; E = 30 \times 10^6 \text{ lbf/in}^2.$$

$$\delta = \frac{150 \times 6 \times 12}{0.01 \times 30 \times 10^6} = 3.6 \times 10^{-2} \text{ in.}$$

Screw has 20 t.p.i. and r.p.m. = 12.

$$\therefore \text{Loading time} = \frac{20 \times 3.6 \times 10^{-2} \times 60}{12}$$

$$= 3.6 \text{ seconds.}$$

$$\therefore \text{Loading rate} = 42 \text{ lb/sec.}$$

The actual loading rate will be slightly less than this due to smaller contributions to the displacement from other parts of the system.

APPENDIX V

THERMAL COMPENSATION OF TRANSDUCER FRAMEWORK

The approximate coefficients of thermal expansion at room temperature of the various components and materials are listed below.

Transducer bobbin	$5 \times 10^{-6}$ in/in $^{\circ}\text{C}$
Transducer core	$11 \times 10^{-6}$ in/in $^{\circ}\text{C}$
"Permant" low expansion alloy	$1.5 \times 10^{-6}$ in/in $^{\circ}\text{C}$
Mild steel	$11 \times 10^{-6}$ in/in $^{\circ}\text{C}$ .

Referring to fig (55) and considering a  $1^{\circ}\text{C}$  rise in ambient temperature.

It is required to maintain the centre line of transducer bobbin and core in the same relative positions as before.

Considering movement of bobbin relative to core

Relative movement towards centre of furnace taken as positive

1) Expansion of bobbin and core.

$$\begin{aligned} \text{Bobbin moves } & 2 \times (2 \times 11 - 1 \times 5) 10^{-6} \text{ in.} \\ & = 34 \times 10^{-6} \text{ in. +ve.} \end{aligned}$$

2) Expansion of "Permant" frame

$$\begin{aligned} \text{Bobbin moves } & 19 \times 1.5 \times 10^{-6} \text{ in.} \\ & = 29 \times 10^{-6} \text{ in. -ve.} \end{aligned}$$

3) Expansion of "Permant" transducer slide

$$\begin{aligned} \text{Bobbin moves } & 2 \times (3 \times 1.5 \times 10^{-6}) \text{ in.} \\ & = 9 \times 10^{-6} \text{ in. +ve.} \end{aligned}$$

4) Expansion of steel micrometer baseplate

$$\begin{aligned} \text{Bobbin moves } & 2 \times (1.25 \times 11 \times 10^{-6}) \text{ in.} \\ & = 25 \times 10^{-6} \text{ in. -ve.} \end{aligned}$$

5) Expansion of micrometer anvil

$$\begin{aligned} \text{Bobbin moves } & 2 \times (0.5 \times 11 \times 10^{-6}) \text{ in.} \\ & = 11 \times 10^{-6} \text{ in +ve.} \end{aligned}$$

Approximate positive movement

$$\begin{aligned} & = (34 + 9 + 11) 10^{-6} \text{ in.} \\ & = 54 \times 10^{-6} \text{ in.} \end{aligned}$$

Approximate negative movement

$$\begin{aligned} & = (29 + 25) 10^{-6} \text{ in.} \\ & = 54 \times 10^{-6} \text{ in.} \end{aligned}$$

The degree of thermal compensation achieved is approximate since

- 1) No account is taken of the effect of thermal fluctuations on the lengths of the quartz probes because of the complex nature of the thermal gradient along the lengths of the probes. This effect should be small since the coefficient of thermal expansion of quartz is only  $5 \times 10^{-7}$  in/in  $^{\circ}\text{C}$ .
- 2) The effect of temperature changes on the actual specimen diameter are also neglected since these temperature changes are small and do not occur in phase with ambient temperature changes.
- 3) The calculated "free lengths" of the various components are approximate.

APPENDIX VI

# COMPARISON OF CONSTANT-LOAD AND CONSTANT-STRESS TENSILE CREEP DATA FOR AN ALUMINIUM-0.07 PER CENT TITANIUM ALLOY AT 250°C

By J. Fairbairn\*

Constant-stress tensile creep data were obtained from an aluminium-0.07 per cent titanium alloy at 250°C and correlated using a power law of the form:

$$\epsilon = A\sigma^n t^p$$

To obtain a better fit to the experimental data in the higher strain regions a modified time function was selected and the experimental data correlated using an equation of the form:

$$\epsilon = A\sigma^n(t^2 + 2t)^p$$

This equation was used to obtain theoretical constant-load curves which are compared with experimental constant-load data previously obtained from the same billet of material.

## INTRODUCTION

RECENT INVESTIGATIONS here concern the creep behaviour of thick-walled cylinders under internal pressure. The material used in the experimental programme is an aluminium-titanium alloy which has been described previously (1)†.

Creep tests are carried out at 250°C on cylinders and plate specimens machined from the same billet of material. The tensile test stress range is selected to cover a range of stresses occurring in the cylinder internal pressure tests. The tensile data are correlated to obtain an expression describing the creep behaviour of the material in this stress range.

Tensile data were obtained from constant-load tests and were found to correlate well with a 'time-hardening' power law of the form:

$$\frac{d\epsilon_L}{dt} = A\sigma^n t^p \quad . \quad . \quad . \quad (1)$$

This is an instantaneous relationship and the stress varies continuously during a constant-load test.

Assuming constant-volume creep deformation, uniform gauge length cross-section and neglecting elastic strains, the instantaneous effective stress  $\sigma$  is related to the initial stress  $\sigma_0$  by the expression:

$$\sigma = \sigma_0(1 + \epsilon_L) \quad . \quad . \quad . \quad (2)$$

*MS. of this paper was first received at the Institution on 3rd August 1966 and in its revised form, as accepted by the Council for publication, on 16th September 1966. 34  
Mechanical Engineering Research Annexe, University of Glasgow.  
Graduate of the Institution.  
References are given in the Appendix.*

Equation (1) may then be written

$$\frac{d\epsilon_L}{dt} = A\sigma_0^n(1 + \epsilon_L)^n t^p$$

Integrating from time  $t = 0$ , making use of the condition  $\epsilon_L = 0$  at  $t = 0$ , this equation becomes

$$\left\{ 1 - \frac{1}{(1 + \epsilon_L)^{n-1}} \right\} = \frac{(n-1)A}{p+1} \sigma_0^n t^{p+1}$$

and involves only experimentally measured quantities.

This equation was used to obtain the constants  $A$ ,  $n$  and  $p$ .

Constant-stress tests were carried out on tensile specimens from the same billet of material to eliminate the stress variable and perhaps provide a clearer indication of the best 'creep law'.

## Notation

- $A, a, m, n, p$  Constants.
- $t$  Time from initial application of tensile stress.
- $\epsilon$  Creep strain.
- $\epsilon_L$  Creep strain under constant-load conditions.
- $\epsilon_S$  Creep strain under constant-stress conditions.
- $\sigma$  Instantaneous applied tensile stress.
- $\sigma_S$  Applied tensile stress during constant-stress test.
- $\sigma_0$  Initial applied tensile stress in constant-load test.

## APPARATUS

The constant-load apparatus has been described previously (1).

The constant-stress machine utilized a cam arrangement of the Andrade Chalmers type, similar to that of Garofalo *et al.* (2). The cam profile was computed for a specimen of 1/4-in parallel length, assuming constant-volume creep deformation and uniform specimen cross-section, and was designed for strains up to 35 per cent. The specimens were 1/4-in diameter with a 5-in gauge length.

A five zone electric furnace with proportional temperature control provided a gauge length temperature of

$250^{\circ}\text{C} \pm 0.5 \text{ degC}$  throughout each test. Initial loading was carried out by means of an electric screw-jack arrangement providing a constant loading rate on all specimens.

Strains were measured by means of telescopes, attached to a small cathetometer, sighting through holes in the furnace wall on gauge marks on the specimen surface. Glass windows sealed the holes in the furnace wall allowing continuous observation of the specimen without loss of temperature distribution. The sensitivity of the strain measuring system was approximately  $2 \times 10^{-4}$  and the stress remained constant during each test to better than 1 per cent.

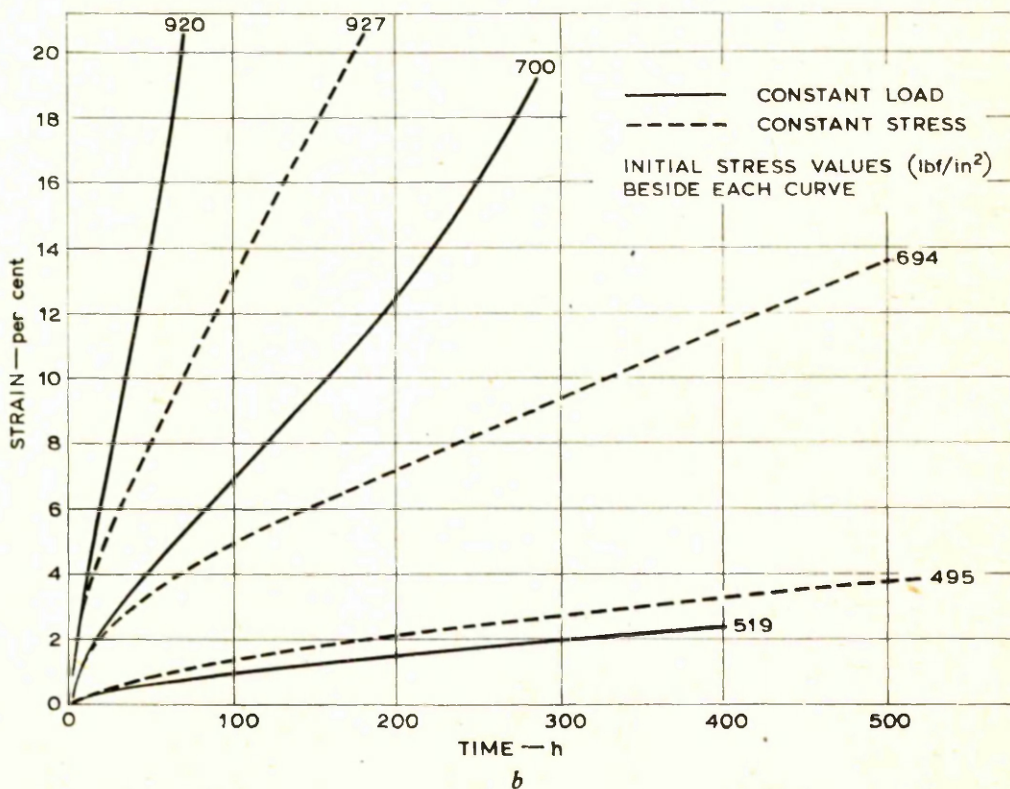
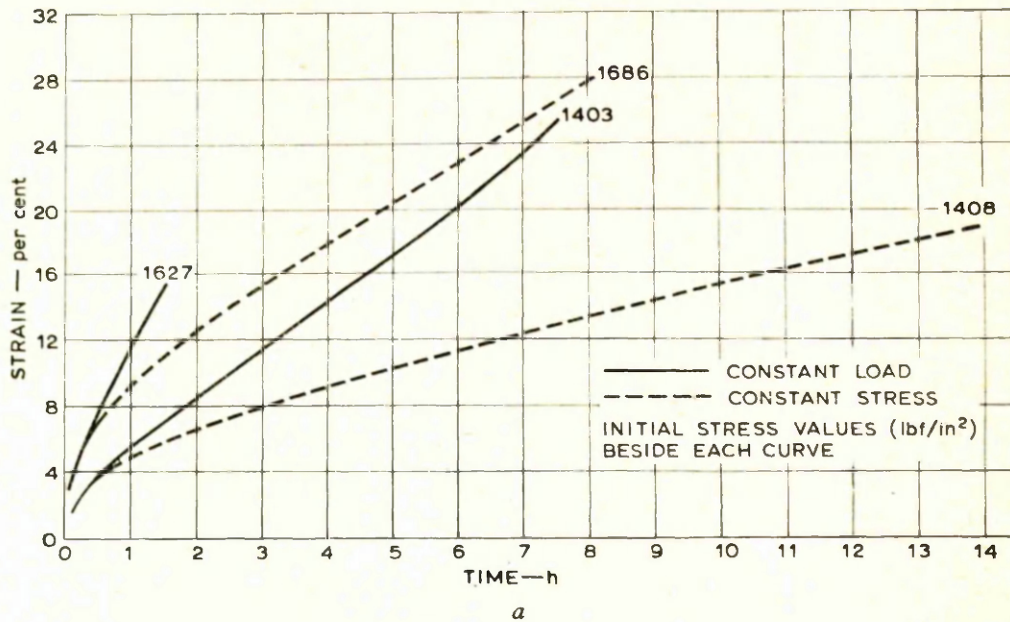


Fig. 1. Comparison between constant-load and constant-stress experimental data with approximately the same value of initial stress

**RESULTS**

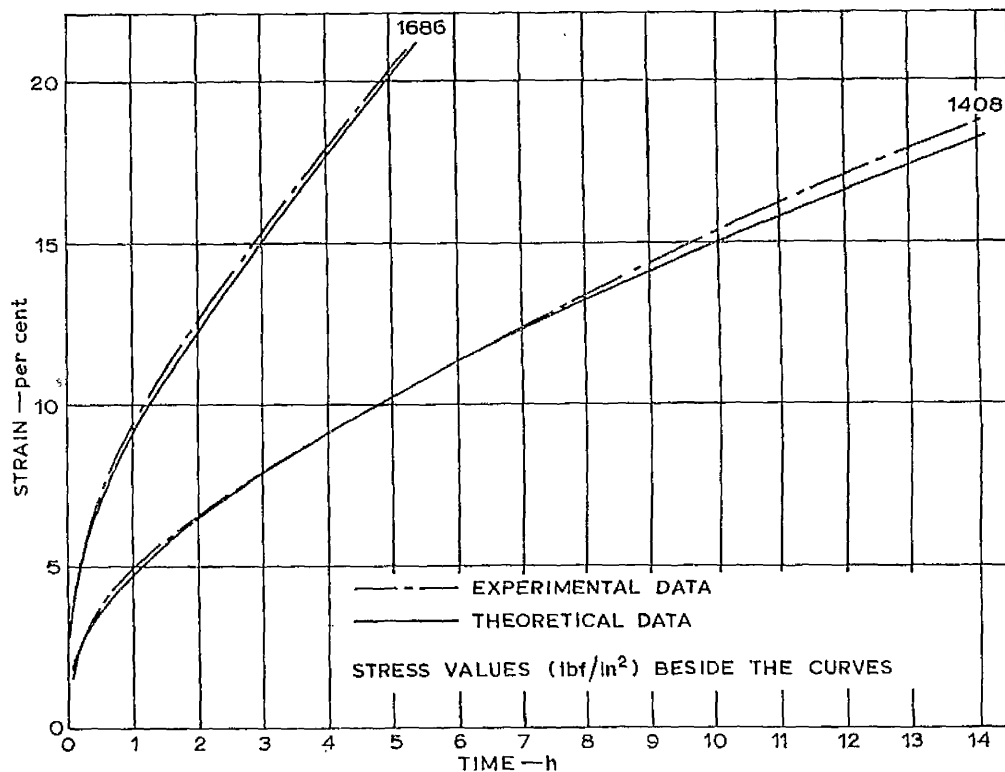
Experimental data from both constant-load and constant-stress tests are shown in Fig. 1. The effect of the continuous stress increase occurring during a constant-load test is observed by comparing constant-load and constant-stress curves having approximately the same value of initial

stress. It can also be seen that in all of the constant-stress tests the creep rate decreased continuously.

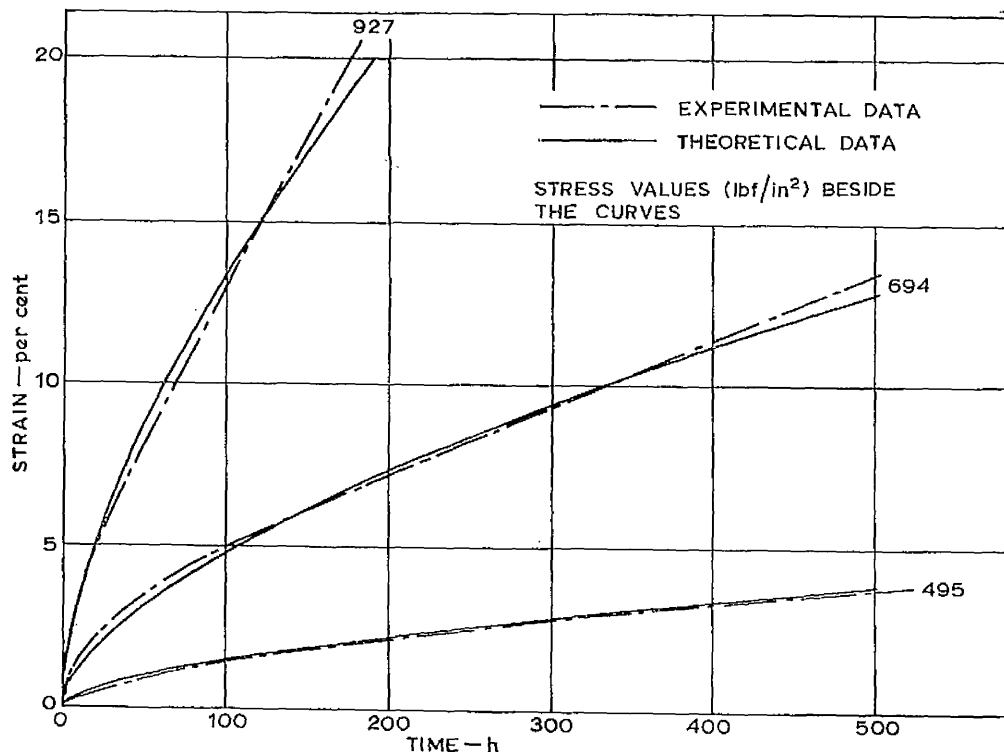
**Constant-stress data**

A power law of the form

$$\epsilon = A\sigma^n t^p$$



a



b

Fig. 2. Correlation of constant-stress data with equation  $\epsilon = 1.56 \times 10^{-13} \sigma^{3.6} (t^2 + 2t)^{0.313}$

was fitted to the constant-stress data. Initial instantaneous deformation was very small compared with creep strain and was included in the latter. The constants  $A$ ,  $n$  and  $p$  were obtained by graphical and 'least squares' analyses of the experimental data. It was found that one set of constants could not be used to cover the complete stress range owing to stress dependence exhibited by  $p$ . The stress range was divided into two parts (above and below 1000 lbf/in<sup>2</sup>) and a set of constants derived for each range.

The relationships obtained were:

$$\epsilon = 5.09 \times 10^{-12} \sigma^{3.17} t^{0.44} \quad (\sigma > 1000 \text{ lbf/in}^2)$$

$$\epsilon = 3.60 \times 10^{-12} \sigma^{3.17} t^{0.55} \quad (\sigma \leq 1000 \text{ lbf/in}^2)$$

This form of equation did not describe adequately creep behaviour in the higher strain regions and for this reason a modified time function was used to provide the creep equation:

$$\epsilon = A\sigma^n(t^2 + 2t)^p \quad (3)$$

The constant  $p$  in this modified time function was independent of stress and one equation was obtained to cover the entire stress range, namely

$$\epsilon = 1.56 \times 10^{-13} \sigma^{3.6} (t^2 + 2t)^{0.313}$$

This correlation is shown in Fig. 2.

### Constant-load data

Substituting the relationship between instantaneous stress  $\sigma$  and initial stress  $\sigma_0$  during a constant-load test into equation (3)

$$\begin{aligned} \frac{\epsilon_L}{(1 + \epsilon_L)^n} &= A\sigma_0^n(t^2 + 2t)^p \\ &= \epsilon_S \quad \text{for } \sigma_S = \sigma_0 \end{aligned}$$

It is assumed here that the stress is constant at  $\sigma_0(1 + \epsilon_L)$  from the beginning of the test by analogy with the 'deformation theory' of plasticity.

This provides a method of calculating constant-load creep curves for any value of initial stress. A comparison of theoretical constant-load creep curves obtained in this way with the experimental constant-load data is shown in Fig. 3.

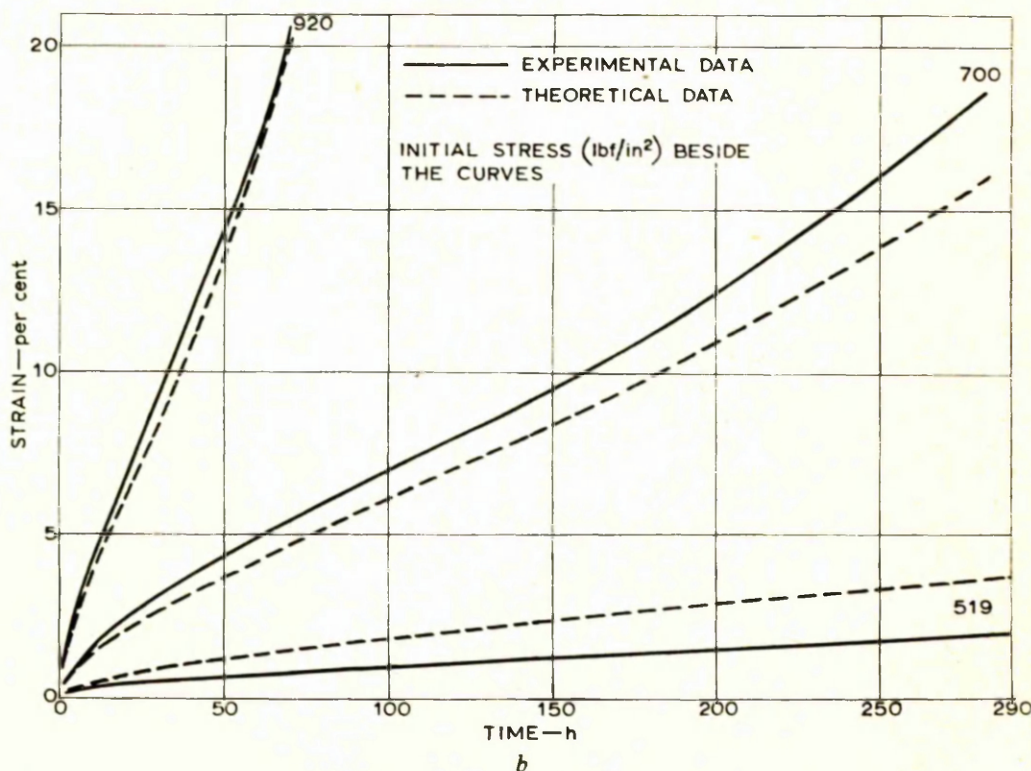
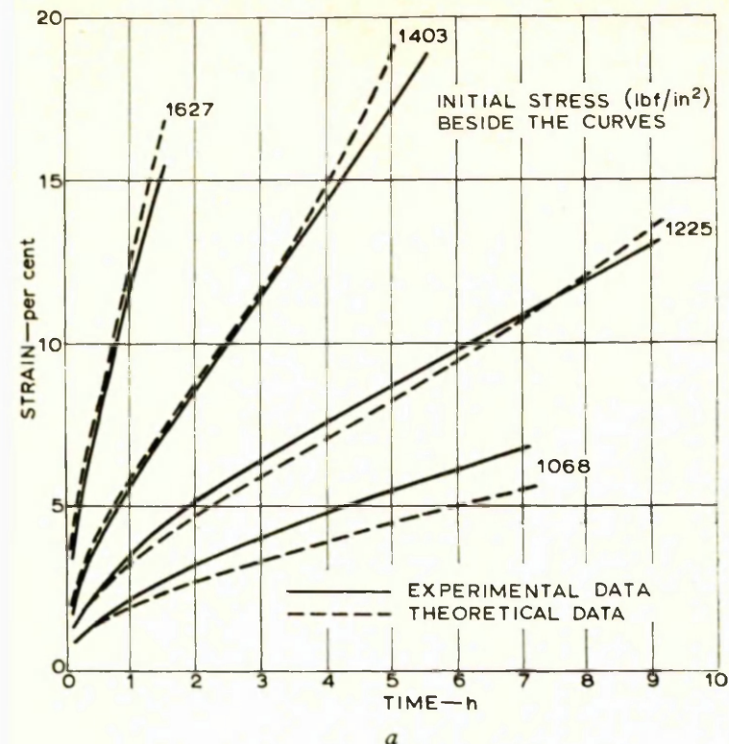


Fig. 3. Correlation of constant-load data with equation  $\frac{\epsilon_L}{(1 + \epsilon_L)^n} = 1.56 \times 10^{-13} \sigma_0^{3.6} (t^2 + 2t)^{0.313}$

can be seen from these graphs that the experimental strain observed during the constant-load test with initial stress of 519 lbf/in<sup>2</sup> is much lower than the theoretical strain from the analysis. However, the experimental strain is so lower than the experimental strain observed during 495 lbf/in<sup>2</sup> constant-stress test and it is felt that the 495 lbf/in<sup>2</sup> constant-load test results are not significant.

### CONCLUSIONS

Primary creep (decreasing creep rate) was observed during constant-stress tests, on one occasion at 28 per cent strain.

Use of the time function  $(t^2 + 2t)^p$  provided a good relation with the experimental data and eliminated the dependence of  $p$ , enabling one equation to cover the entire stress range considered.

The constant-stress data provided a better indication of the constant-load data of the best form of 'creep

equation' for the material. When this equation was modified to take account of the variation of stress during a constant-load test, good predictions of the constant-load experimental data were obtained.

### ACKNOWLEDGEMENT

The present research programme is supported by the Science Research Council and Imperial Chemical Industries Ltd.

### APPENDIX

#### REFERENCES

- (1) KING, R. H. 'Creep of thick-walled cylinders under internal pressure', Ph.D. thesis, University of Glasgow, May 1964.
- (2) GAROFALO, F., RICHMOND, O. and DOMIS, W. F. 'Design of apparatus for constant-stress and constant-load creep tests', *Trans. Am. Soc. mech. Engrs, J. basic Engng* 1962 84 (Series D), 287.

APPENDIX VII

SHORT TIME TENSILE PROPERTIES OF THE MATERIAL

Two short time tensile tests at 250 °C were carried out at the National Engineering Laboratory, East Kilbride, and conformed with B.S. 1094:1943. The tests were carried out at constant strain-rates of 0.1/min for test "A" and 0.05/min for test "B". The results are shown in figs (56) and (57) and from these results the following material properties were evaluated.

$$\text{Young's Modulus} = 7.8 \times 10^6 \text{ lbf/in}^2$$

$$\text{Limit of Proportionality} = 660 \text{ lbf/in}^2$$

$$\text{Approximate yield point} = 1,700 \text{ lbf/in}^2.$$

It can be observed from fig (57) that the stress/strain curve depends upon the strain-rate to some extent.

APPENDIX VIII

DERIVATION OF WALL-THINNING EQUATION

In a thick-walled cylinder, for constant volume creep deformation, and zero axial creep,

$$b^2 - a^2 = b_o^2 - a_o^2$$

where b and a are the external and bore radii respectively and the subscripts o refer to initial values.

$$\therefore 2b \frac{db}{dt} - 2a \frac{da}{dt} = 0 \quad \dots(1)$$

$$\epsilon_{\theta b} = \frac{b - b_o}{b_o} = \frac{b}{b_o} - 1$$

$$\therefore \dot{\epsilon}_{\theta b} = \frac{1}{b_o} \frac{db}{dt} \quad \dots(2)$$

similarly  $\dot{\epsilon}_{\theta a} = \frac{1}{a_o} \frac{da}{dt} \quad \dots(3)$

Substituting equations (2) and (3) in (1),

$$b b_o \dot{\epsilon}_{\theta b} = a a_o \dot{\epsilon}_{\theta a}$$

$$\therefore \dot{\epsilon}_{\theta a} = K K_o \dot{\epsilon}_{\theta b} \quad \dots(4)$$

where K is the cylinder diameter ratio and

$$K = \frac{b}{a}$$

$$\therefore \frac{dK}{dt} = \frac{1}{a} \frac{db}{dt} - \frac{b}{a^2} \frac{da}{dt}$$

$$= \frac{b_o}{a} \dot{\epsilon}_{\theta b} - \frac{b a_o}{a^2} \dot{\epsilon}_{\theta a}$$

$$= \frac{b_o}{b} K \dot{\epsilon}_{\theta b} - \frac{b b_o K^2}{K_o b^2} K K_o \dot{\epsilon}_{\theta b}$$

$$= \frac{b_o}{b} K \dot{\epsilon}_{\theta b} (1 - K^2)$$

$$\therefore dK = \frac{b_o}{b} K \dot{\epsilon}_{\theta b} (1 - K^2) dt$$

$$= \frac{b}{b} k(1 - k^2) d\varepsilon_{\theta b}$$

$$= \frac{k(1 - k^2) d\varepsilon_{\theta b}}{1 + \varepsilon_{\theta b}}$$

APPENDIX IX

A SIMPLE METHOD OF OBTAINING CREEP RATES  
OF A THICK-WALLED CYLINDER UNDER INTERNAL PRESSURE

J. Fairbairn and W. W. Mackie

During creep deformation of a thick-walled cylinder under internal pressure, the distributions of the principal stresses in the wall change with time from the initial distribution produced on loading to the "steady-state" distribution. If creep deformation is of concern, creep rates can be calculated with little error by assuming that the "steady-state" stress distribution is set up immediately after loading. However, in order to calculate creep rates in the cylinder, "creep constants" for the material must be determined. These can generally be obtained from a series of uniaxial tension tests.

In the recent paper by Skelton and Crossland (1) on the correlation of tension and thick-walled cylinder creep tests the Soderberg (2) method of analysis was applied with some success. In this analysis a characteristic "steady-state" stress in the cylinder wall is determined without prior knowledge of material "creep constants" by assuming that if the cylinder wall thickness is small compared with the radius, the change in stress during stress redistribution is negligible. The "steady-state" stresses at the mean diameter of the cylinder are then identical to those obtained on initial pressure loading, and are calculated from the thin cylinder equations of equilibrium. This method of calculation of the effective creep stress and the use of the mean diameter as the reference position in the cylinder wall has little justification however when dealing with tubes of appreciable wall thickness.

In a thick-walled tube the change of stress at the mean diameter during stress redistribution is not negligible and the Soderberg analysis becomes increasingly inaccurate at greater diameter ratios.

The attraction of the Soderberg method is that only a single tensile creep test is required and in this note a method is presented for prediction of cylinder creep behaviour which is valid for thick-walled cylinders and still preserves this feature. Experimental data are presented for one creep test on a thick-walled cylinder under internal pressure and two corresponding constant uniaxial tensile stress creep tests.

NOTATION

$\sigma^*$	Effective stress associated with the von Mises criterion.
$\sigma_\theta, \sigma_r, \sigma_z$	Principal stresses in thick cylinder in tangential, radial and axial direction respectively
$\sigma_1$	Uniaxial tensile stress.
$\dot{e}^*$	Effective strain-rate associated with von Mises criterion.
$\dot{e}_\theta, \dot{e}_r, \dot{e}_z$	Strain-rates in thick cylinder in tangential, radial and axial directions respectively.
$\dot{e}_1$	Strain-rate in uniaxial tension.
A, n	Creep constants
f(t)	Time function
$D_o$	External diameter of cylinder
D	Diameter of cylinder at position of representative stress.
K	Diameter ratio of cylinder = $\frac{\text{External diameter}}{\text{bore diameter}}$
P	Internal pressure

ASSUMPTIONS

The material is isotropic and creep behaviour is governed by the von Mises criterion and associated flow rule

$$\text{i.e. } \sigma^* = \frac{1}{\sqrt{2}} [(\sigma_\theta - \sigma_r)^2 + (\sigma_r - \sigma_z)^2 + (\sigma_z - \sigma_\theta)^2]^{\frac{1}{2}}$$

$$\dot{\epsilon}^* = \frac{\sqrt{2}}{3} [(\dot{\epsilon}_\theta - \dot{\epsilon}_r)^2 + (\dot{\epsilon}_r - \dot{\epsilon}_z)^2 + (\dot{\epsilon}_z - \dot{\epsilon}_\theta)^2]^{\frac{1}{2}}$$

$$\frac{\dot{\epsilon}_\theta - \dot{\epsilon}_r}{\sigma_\theta - \sigma_r} = \frac{\dot{\epsilon}_r - \dot{\epsilon}_z}{\sigma_r - \sigma_z} = \frac{\dot{\epsilon}_z - \dot{\epsilon}_\theta}{\sigma_z - \sigma_\theta}$$

Creep deformation occurs at constant volume.

Elastic strains are negligible compared with creep strains.

The creep-rate in the axial direction of the cylinder is zero.

A power law relationship exists between creep rate and stress for the material i.e.

$$\dot{\epsilon}^* = A\sigma^{*n}f(t)$$

ANALYSIS

Marriot and Leckie (3) have shown that during stress redistribution in a thick cylinder there is a position in the wall at which the effective stress  $\sigma^*$  remains almost constant. If this effective stress is considered as a representative stress (4), stress redistribution will have little effect on the creep rates at this position and, therefore, little effect elsewhere in the wall since creep rates at any position may be calculated from the creep rates at the representative stress position using the assumptions of constancy of volume and zero axial creep.

The position of the representative stress is the point of intersection in the wall of the effective stress distributions obtained for elastic and "steady-state" conditions.

$$\text{Then } \frac{\sqrt{3} P}{K^2 - 1} \left(\frac{D_o}{D}\right)^2 = \frac{\sqrt{3} P}{n(K^{2/n} - 1)} \left(\frac{D_o}{D}\right)^{2/n}$$

$$\therefore \frac{D_o}{D} = \left\{ \frac{K^2 - 1}{n(K^{2/n} - 1)} \right\}^{n/2} \frac{n}{2(n-1)}$$

It is found as shown in table 1 that  $D_o/D$  is not sensitive to "n" and may be obtained to good approximation from an assumed value of "n".

n	$D_o/D$
2	1.500
3	1.490
4	1.486
5	1.483
6	1.481

Table 1

for  $K = 2$

The representative stress may then be obtained from the elastic solution

$$\sigma^* = \frac{\sqrt{3} P}{K^2 - 1} \left(\frac{D_o}{D}\right)^2$$

The tangential creep-rate at the position of the representative stress becomes

$$\begin{aligned} \dot{\epsilon}_\theta &= A \sigma^{*(n-1)} \left[ \sigma_\theta - \frac{1}{2} (\sigma_r + \sigma_z) \right] f(t) \\ \sigma^* &= \frac{\sqrt{3}}{2} (\sigma_\theta - \sigma_r) ; \sigma_\theta - \frac{1}{2} (\sigma_r + \sigma_z) = \frac{3}{4} (\sigma_\theta - \sigma_r) \\ \therefore \dot{\epsilon}_\theta &= \frac{\sqrt{3}}{2} A \sigma^{*n} f(t) = \frac{\sqrt{3}}{2} \dot{\epsilon}_1 \end{aligned}$$

where  $\dot{\epsilon}_1$  is the creep-rate of a tensile test carried out at  $\sigma_1 = \sigma^*$

The tangential creep-rate at the external surface of the cylinder becomes

$$\begin{aligned} \dot{\epsilon}_{\theta o} &= \dot{\epsilon}_\theta \left(\frac{D}{D_o}\right)^2 \\ \therefore \dot{\epsilon}_{\theta o} &= \frac{\sqrt{3}}{2} \left(\frac{D}{D_o}\right)^2 \dot{\epsilon}_1 \end{aligned}$$

Therefore if a uniaxial tensile stress creep test is carried out at a stress given by the representative stress for the cylinder, the creep-rate at the external surface of the cylinder can be obtained at any time.

#### EXPERIMENTAL DATA

Tensile creep tests at constant stress and thick cylinder creep tests under internal pressure have been carried out in our laboratory on an Aluminium/0.06 per cent Titanium alloy at 250 °C. It was found that the test pressure applied to one cylinder corresponded suitably to the stress applied to two tensile specimens used as part of a series of isotropy tests.

#### Cylinder creep test

$K = 2.87$ ;  $P = 660 \text{ lbf/in}^2$ ; "n" for the material was found to be 4.8 so a value of 5 is taken here providing  $D_o/D = 1.885$ .

$$\therefore \text{representative stress } \sigma^* = 561 \text{ lbf/in}^2.$$

#### Tensile creep tests at constant stress

$$\sigma_1 = 543 \text{ lbf/in}^2 \text{ in both tests.}$$

$$\therefore \dot{\epsilon}_{\theta o} = \frac{\sqrt{3}}{2} \left(\frac{D}{D_o}\right)^2 \dot{\epsilon}_1 = 0.244 \dot{\epsilon}_1$$

Fig (58) is a graph of 0.244 times the tensile creep-rates and the tangential creep-rate at the outside surface of the cylinder against time on logarithmic scales. The agreement is good although it is seen that the cylinder creep-rate tends to be higher than the creep-rate predicted from the tensile tests as the deformation continues since the simple analysis can make no allowance for the increase of effective stress due to thinning of the cylinder wall.

The limiting cylinder creep strain beyond which the effect of wall

thinning becomes intolerable depends to a great extent upon the stress sensitivity of the material, characterised by the value of stress exponent "n". In the present tests the analysis is probably limited to external diametral strains of approximately 0.3 per cent.

#### CONCLUSION

The analysis provides a method of determining creep-rates in a thick-walled cylinder under internal pressure from the results of a single uniaxial tension test. Fair agreement is shown with limited experimental data.

#### ACKNOWLEDGEMENT

The present research is supported by the Science Research Council.

#### REFERENCES

- (1) Skelton, W.J., Crossland, B., "Correlation of tension and thick-walled cylinder creep based on experimental data." Paper 7 Conference on High Pressure Engineering, London, September 1967.
- (2) Soderberg, C.R., "Interpretation of creep tests on tubes." Trans. Am. Soc. Mech. Engrs., 1941, 63.
- (3) Marriot, D.L., Leckie, F.A., "Some observations on the deflections of structures during creep." Proc. Instn. Mech. Engrs., 1963-64, vol.178, part 3L.
- (4) Anderson, R.G., Discussion of (3).

BIBLIOGRAPHY

CHAPTER 1

- (1) Bridgeman, P.W., "Flow and fracture", Trans.A.S.M.E., 1945, 162, 569.
- (2) Ros, M., Eichinger, A., "The liability of solids to fracture under steady state static conditions", Eidgenossische Material prugungs Versuchsanstalt fur Industrie, Bericht No. 172, Surich: Bauwesen und Gewerbe, 1949.
- (3) Crossland, B., "The effect of fluid pressure on the shear properties of metals", Proc. Instn. Mech. Engrs., 1954, 168(4), 935.
- (4) Nadai, A.L., "Review of recent research work in plasticity", J. Appl. Mech. 1936, 3(3), 104.
- (5) Cox, H.L., Sopwith, D.G., "The effect of orientation on stresses in single crystals and of random orientation on strength of polycrystalline aggregates", Proc. Phys. Soc., 1937, 49, 134.
- (6) Beeching, R., "Communications on yield and stress-strain relations", Proc. Instn. Mech. Engrs., 1948, 159 (39), 113.
- (7) Taylor, G.I., Quinney, H., "The plastic distortion of metals", Phil. Trans., 1931, 230, 323.
- (8) Lessels, J.M., MacGregor, C.W., "Combined stress experiments on a nickel-chrome-molybdenum steel", J. Franklin Inst., 1940, 230, 163.
- (9) Davis, E.A., "Yielding and fracture of a medium carbon steel under combined stress", J. Appl. Mech., 1945, 12 (1), 13.
- (10) Morrison, J.L.M., "Criterion of yield of gun steels", Proc. Instn., Mech. Engrs., 1948, 159 (39), 81.
- (11) Hill, R., "The mathematical theory of plasticity", 1950, Clarendon Press, Oxford.
- (12) Fraenkel, S.J., "Experimental studies in biaxially stressed mild steel in plastic range", J. Appl. Mech., 1948, 15 (3), 193.
- (13) Prager, W., "Theory of plastic flow versus theory of plastic deformation", J. Appl. Phys., 1948, 19, 540.
- (14) Gill, S.S., Parker, J., "Plastic stress-strain relationships - some experiments on the effect of loading path and loading history", Trans. A.S.M.E., J. Appl. Mech., 1959, 26, 77.

- (15) Budianski, B., "A Reassessment of deformation theories of plasticity", Trans A.S.M.E., J. Appl. Mech. 1959, 26, 259.
- (16) Manson, S.S., "Thermal stress and low cycle fatigue", 1966, McGraw-Hill, New York.
- (17) Hill, R., Lee, E.H., Tupper, S.J., "The theory of combined plastic and elastic deformation with particular reference to a thick tube under internal pressure", Proc. Roy. Soc., 1947, A191, 278.
- (18) Hill, R., Lee, E.H., Tupper, S.J., "Plastic flow in a closed ended tube with internal pressure", Proc. 1st. Nat. Congr. (U.S.) Appl. Mech., 1951, 561.
- (19) Allen, D.N. DeG., Sopwith, D.G., "The stresses and strains in a partly plastic thick tube under internal pressure and end load", Proc. Roy. Soc., 1951, A205, 69.
- (20) Berman, I., Pai, D.H., "Elevated temperature autofrettage", Trans. A.S.M.E., J. of Engng. for Power, July 1967, 369.
- (21) Bailey, R.W., "The utilisation of creep test data in engineering design", Proc. Instn., Mech. Engrs. 1935, 131, 131.
- (22) Soderberg, C.R., "The interpretation of creep tests for machine design", Trans. A.S.M.E., 1936, 58, 733.
- (23) Marin, J., "Design of members subject to creep at high temperatures", J. Appl. Mech., 1937, 4(2), 55.
- (24) Nadai, A., "On the creep of solids at elevated temperatures", J. Appl. Phys. 1937, 8(6), 418.
- (25) Bailey, R.W., "Creep of steel under simple and compound stresses". The Engineer, 1929, 148, 528, and Engineering, 1930, 129, 265 and 327.
- (26) Johnson, A.E., "Complex stress creep of metals", Met. Rev., 1960, 5(20), 447.
- (27) Johnson, A.E., "Creep under complex stress systems at elevated temperatures", Proc. Instn. Mech. Engrs., 1951, 164(4), 432.
- (28) Johnson, A.E., Henderson, J., Khan, B., "Complex-stress creep, relaxation, and fracture of metallic alloys", Edinburgh 1962, H.M.S.O.
- (29) Stowell, E.Z., Gregory, R.K., "Steady-state biaxial creep", Trans A.S.M.E., J. Appl. Mech., 1965, 32, 37.
- (30) Nadai, A., "Theory of flow and fracture of solids", McGraw-Hill Book Co. Inc., New York, 1950, 236.

- (31) Soderberg, C.R., "Interpretation of creep tests on tubes", Trans. A.S.M.E., 1941, 63, 737.
- (32) Norton, F.H., "Creep in tubular pressure vessels", Trans. A.S.M.E., 1939, 61, 239.
- (33) Rowe, G.H., Stewart, J.R., Burgess, K.N., "Capped end, thin-wall tube creep-rupture behaviour for type 316 stainless steel", Trans. A.S.M.E., J. Basic Eng., 1963, 85, 71.
- (34) Kennedy, C.R., Harms, W.O., Douglas, D.A., "Multiaxial creep studies on inconnel at 1500°F", Trans. A.S.M.E., J. Basic Eng., 1959, 81, 599.
- (35) Wahl, A.M., "Analysis of creep in rotating discs based on the Tresca criterion and associated flow rule", J. Appl. Mech., 1956, 23, 231.
- (36) Wahl, A.M., Sankey, G.O., Manjoine, M.J., Shoemaker, E., "Creep tests of rotating discs at elevated temperature and comparison with theory", J. Appl. Mech., 1954, 21, 225.
- (37) Finnie, I., "An experimental study of multiaxial creep in tubes", Jt. Int. Conf. on creep, Proc. Instn. Mech. Engrs., 1963-64, 178 (Pt. 3A), 2-21.
- (38) Orowan, E., "The creep of metals", J. West of Scotland Iron and Steel Inst., 1946-47, 54, 45.
- (39) Zener, C. Hollomon, J.H., "Problems in non-elastic deformation in metals", J. Appl. Phys., 1946, 17, 69.
- (40) Dorn, J.E., "Some fundamental experiments on high temperature creep", Symp. on creep and fracture of metals at high temperatures, N.P.L., 1954, H.M.S.O., London, 1956, 89.
- (41) Sherby, O.D., Dorn, J.E., "Correlations of high temperature creep data", M.R.L. report No. 41, University of California, 1955.
- (42) Kennedy, A.J., "Processes of creep and fatigue in metals", Oliver and Boyd Ltd., Edinburgh, 1962, 215.
- (43) Graham, A., Discussion, Conf. thermal loading and creep, Proc. Instn. Mech. Engrs., 1963-64, 178 (Pt. 3L), 171.
- (44) Lubahn, J.D., Felgar, R.P., "Plasticity and creep of metals", John Wiley & Sons, Inc., New York, 1961, 239.
- (45) Roberts, I., "Prediction of relaxation of metals from creep data", Proc. A.S.T.M., 1951, 51, 811.
- (46) Johnson, A.E., Henderson, J., Mather, V.D., "Creep under changing complex stress systems", The Engineer, 1958, 206, 209, 251, 287.

- (47) Johnson, A.E., Khan, B., "Creep under changing complex stress systems in copper at 250°C, N.E.L. Report No. 203, Ministry of Technology, 1965.
- (48) Namestnikov, V.S., "Combined-stress creep under changing loads", Jt. Int. Conf. on creep, Proc. Instn. Mech. Engrs., 1963-64, 178 (Pt.3A), 2-109.

CHAPTER 2

- (1) Allen, D.N.deG., Sopwith, D.G., "The stresses and strains in a partly plastic thick tube under internal pressure and end load", Proc. Roy. Soc., A. 205, 1951, 69.
- (2) Bailey, R.W., "The utilisation of creep test data in engineering design", Proc. Instn. Mech. Engrs., 1935, 131, 131.
- (3) Skelton, J., Crossland, B., "Creep of thick-walled cylinders subjected to internal pressure: review of literature", Paper 4, Conf. High Pressure Engineering, Instn. Mech. Engrs., Sept. 1967.
- (4) Johnson, A.E., Henderson, J., Khan, B., "Complex-stress creep, relaxation, and fracture of metallic alloys", H.M.S.O., Edinburgh, 1962.
- (5) Bailey, R.W., "Thick-walled tubes and cylinders under high pressure and temperature", Engineering, 1930, 29, 772, 785, 818.
- (6) Johnson, A.E., "Creep under complex stress systems at elevated temperatures", Proc. Instn. Mech. Engrs., 1951, 164(4), 432.
- (7) Coffin, L.F., Shepler, P.R., Cherniak, G.S., "Primary creep in the design of internal pressure vessels", J. Appl. Mech., 1949, 19, 229.
- (8) Traexler, J.F., "Design of pressurised cylinders for high temperature applications", Trans. A.S.M.E., J. Basic Eng., 1960, 82 (Series D), 477.
- (9) Weir, C.D., "The creep of thick tubes under internal pressure", Trans A.S.M.E., J. Appl. Mech. 1957, 179, 464.
- (10) Finnie, I., "Steady-state creep of a thick-walled cylinder under combined axial load and internal pressure", Trans. A.S.M.E., J. Basic Eng., 1960, 82 (Series D), 689.
- (11) Rimrott, F.P.J., "Creep of thick-walled tubes under internal pressure considering large strains", Trans. A.S.M.E., J. Appl. Mech., 1959, 81, 271.
- (12) Soderberg, C.R., "The interpretation of creep tests for machine design", Trans. A.S.M.E., 1936, 58, 733.
- (13) Skelton, W.J., Crossland, B., "Correlation of tension and thick-walled cylinder creep based on experimental data", Paper 7, Conf. High Pressure Engineering, Instn. Mech. Engrs., September 1967.
- (14) Poritsky, H., Fend, F.A., "Relief of thermal stresses through creep", J. Appl. Mech., 1958, 25, 589.

- (15) Mendelson, A., Hirschberg, M.H., Manson, S.S., "A general approach to the practical solution of creep problems", Trans. A.S.M.E., J. Basic Eng., 1959, 81 (Series D), 585.
- (16) Wilson, W.K., Davis, E.A., "Creep and relaxation of heavy walled cylinders with specific axial boundary conditions", Jt. Int. Conf. on creep, Proc. Instn. Mech. Engrs., 1963-64, 178 (Pt.3A), 2-69.
- (17) Mendelson, A., Manson, S.S., "Practical solution of plastic deformation problems in the elastic-plastic range", A.S.M.E., Paper 56-A-202.
- (18) Davis, E.A., "Creep and relaxation of oxygen free copper", J. Appl. Mech., 1943, 10, A 101.
- (19) Smith, E.M., "Primary creep behaviour of thick tubes", Conf. Thermal Loading and Creep, Proc. Instn. Mech. Engrs., 1963-64, 178 (Pt.3L), 135.
- (20) Johnson, A.E., Henderson, J., Khan, B., "Behaviour of metallic thick-walled cylindrical vessels or tubes subject to high internal or external pressures at elevated temperatures", Proc. Instn. Mech. Engrs., 1961, 175, 1043.
- (21) Voorhees, H.R., Sliepcevich, C.M., Freeman, J.W., "Thick walled pressure vessels", Ind. and Eng. Chem., 1956, 48, 872.
- (22) Smith, E.M., "Primary creep design of thick tubes", Trans. A.S.M.E., J. Basic Eng., 1965, 87, (Series D), 379.
- (23) King, R.H., "Creep of thick-walled cylinders under internal pressure", Ph.D. Thesis, University of Glasgow, 1964.
- (24) Larke, E.C., Parker, R.J., "Circumferential creep strain of cylinders subjected to internal pressure: a comparison of the theories of Johnson and Bailey", J. Mech. Eng. Sci., 1966, 8, 22.
- (25) Marriott, D.L., Leckie, F.A., "Some observations of the deflections of structures during creep", Conf. Thermal Loading and Creep, Proc. Instn., Mech. Engrs., 1963-64, 178 (Pt. 3L), 115.
- (26) Moore, H.F., Alleman, N.J., "Creep of lead and lead alloys used for cable sheathing", University Illinois Eng. Exper. Stn. Bull. No. 243, 1932.
- (27) Moore, H.F., Betty, B.B., Dollins, C.W., "Investigation of creep and fracture of lead and lead alloys for cable sheathing". University of Illinois Eng. Exper. Stn. Bull No. 306, 1938.
- (28) McKeown, J., "Creep of lead and lead alloys", J. Inst. Metals, 1937, 60, 201.

- (29) Nakahara, M., "New theories of creep of metals", Japanese Soc. Mech. Eng., 1939 2, 55.
- (30) Latin, A., "Creep of tubes under internal pressure (pressure and creep at constant hoop stress on lead and alloy "E" pipes)", J. Inst. Metals, 1948, 74, 259.
- (31) Smith, E.M., "Creep of thick tubes subjected to internal pressure", Ph.D. Thesis, University of Glasgow, 1962.
- (32) King, R.H., Mackie, W.W., "Creep of thick-walled cylinders", Trans. A.S.M.E., J. Basic. Eng., 1967, 89 (Series D), 877.
- (33) White, A.E., Clark, C.L., "Properties of boiler tubing at elevated temperatures determined by expansion tests", Trans. A.S.M.E., 1926, 48, 1075.
- (34) White, A.E., Clark, C.L., "Properties of ferrous metals at elevated temperatures as determined by short-time tensile and expansion tests", Trans. A.S.M.E., 1928, 50, 263.
- (35) Norton, F.H., "Creep in tubular pressure vessels", Trans. A.S.M.E., 1939, 61, 239.
- (36) Norton, F.H., "Progress report on tubular creep tests", Trans. A.S.M.E., 1941, 63, 735.
- (37) Norton, F.H., Soderberg, C.R., "Report on tubular creep tests", Trans. A.S.M.E., 1942, 64, 769.
- (38) Davis, E.A., "Creep rupture tests for design of high pressure steam equipment", Trans. A.S.M.E., J. Basic Eng., 1960, 82 (Series D), 453.
- (39) Ohnami, M., Awaya, Y., "Creep and creep rupture of cylindrical tube under combined axial tension and internal pressure", Proc. 6th Japan Cong. Test. Mater., 1963, 61.
- (40) Taira, S., Koterazawa, R., Ohtani, R., "Creep of thick-walled cylinders under internal pressure at elevated temperature", Proc. 8th Japan Cong. Test. Mater., 1965, 53.
- (41) Parker, R.J., "Equipment for creep testing pressurised thick-walled metal cylinders", Conv. Machines for Materials and Environmental Testing, Proc. Instn. Mech. Engrs. 1965-66, 180, (Pt.3A), 113.
- (42) Skelton, W.J., Crossland, B., "Results of high sensitivity tensile creep tests on a 0.19% carbon steel used for thick-walled cylinder creep tests", Paper 3, Conf. High Press. Eng., Inst. Mech. Engrs., September, 1967, and "Creep of thick-walled cylinders: development of a testing machine and preliminary results", Paper 6, Conf. High Press. Eng. Inst. Mech. Engrs., September, 1967.

- (43) Johnson, A.E., "The behaviour of a nominally isotropic 0.17% carbon cast steel under complex stress systems at elevated temperatures", Proc. Instn. Mech. Engrs., 1949, 161, 182.
- (44) Chitty, A. Duval, D., "The creep-rupture properties of tubes for high temperature steam power plant", Jt. Int. Conf. on Creep, Proc. Instn. Mech. Engrs., 1963-64, 178, (Pt. 3A), 4-1.
- (45) Voorhees, H.R., Ph.D. Thesis, University of Michigan, 1956.
- (46) Berman, I., Pai, D.H., "A theory of anisotropic steady-state creep", Int. J. Mech. Sci., 1966, 8, 341.
- (47) Pai, D.H., "Steady-state creep analysis of thick-walled orthotropic cylinders", Int. J. Mech. Sci., 1967, 9, 335.
- (48) Finnie, I., "A tester for creep rupture under multiaxial stress", Proc. Soc. Exp. Stress Anal., 1959, 16, 49.
- (49) Kooistra, L.F., Blaser, R.U., Tucker, J.T., "High temperature stress rupture testing of tubular specimens", Trans. A.S.M.E., 1952, 74, 783.
- (50) Tucker, J.T., Coulter, E.E., Kooistra, L.F., "Effect of wall thickness on stress rupture life of tubular specimens", Trans. A.S.M.E., J. Basic Engng., 1960, 82 (Series D), 465.
- (51) Smith, E.M., "Axial deformation in thick tubes creeping under internal pressure", J. Mech. Eng. Sci., 1964, 6, 418.

CHAPTER 3

- (1) Smith, E.M., "Creep of thick tubes subjected to internal pressure", Ph.D. Thesis, University of Glasgow, 1962.
- (2) Smith, E.M., "Axial deformation in thick tubes creeping under internal pressure", J. Mech. Eng. Sci., 1964, 6, 418.
- (3) King, R.H., "Creep of thick-walled cylinders under internal pressure", Ph.D. Thesis, University of Glasgow, 1964.
- (4) King, R.H., Mackie, W.W., "Creep of thick-walled cylinders", Trans. A.S.M.E., J. Basic Engng. 1967, 89 (series D), 877.
- (5) Norton, F.H. "Creep in tubular pressure vessels", Trans. A.S.M.E. 1939, 61, 239.
- (6) Andrade, E.N. Da C., "On the viscous flow in metals, and allied phenomena", Proc. Roy. Soc. 1910, 84A, 1.
- (7) Andrade, E.N. Da C., Chalmers, B., "The resistivity of polycrystalline wires in relation to plastic deformation and the mechanism of plastic flow", Proc. Roy. Soc., 1932, 138 A, 348.
- (8) Andrade, E.N. Da C., "A new device for maintaining constant stress in a rod undergoing plastic extension", Proc. Phys. Soc., 1948, 60, 304.
- (9) Ward, A.G., Marriott, R.R., "A constant stress apparatus for the study of the creep properties of plastics", J. Sci. Inst., 1948, 25, 147.
- (10) Kennedy, A.J., "A constant stress device adjustable for specimen length" J. Sci. Inst. 1952, 29, 40.
- (11) Fullman, R.L., Carrerer, R.P., Fisher, J.C., "Simple devices for approximating constant stress during tensile creep tests", Trans. A.S.M.E., 1953, 197, 657.
- (12) Garofalo, F., Richmond, O., Domis, W.F., "Design of apparatus for constant-stress or constant-load creep tests", Trans. A.S.M.E., J. Basic. Eng., 1962, 84, (Series D), 287.
- (13) Kinsey, H.V., "An evaluation of the effective gauge length equivalent of the shoulder and fillet of the gauge length portion of a tensile test bar under creep and stress rupture conditions", A.S.T.M. Bull., Jan. 1951, 60.
- (14) Laubitz, M.J., "Design of gradientless furnaces", Canad. J. Phys., 1957, 37, 1114.
- (15) "Wiggin Electrical Resistance Materials", Henry Wiggin and Co. Ltd., Publication No. 2246, March, 1961.

- (16) Bhattacharya, S., Congreve, W.K.A., Thompson, F.C., "The creep/time relationship under constant tensile stress", J. Inst. of Metals, 1952-53, 81, 83.
- (17) Sherby, O.D., Trozera, T.A., Dorn, J.E., "Effects of creep stress history at high temperatures on the creep of aluminium alloys", Proc. A.S.T.M., 1956, 56, 789.
- (18) Allen, D.N.de G., Sopwith, D.G., "The stresses and strains in a partly plastic thick tube under internal pressure and end load", Proc. Roy. Soc., 1951, A205, 69.

CHAPTER 4

- (1) Tapsell, H.J., Johnson, A.E., "Creep under combined tension and torsion", Engineering, 1940, 150, 24.
- (2) Johnson, A.E., Henderson, J., Khan, B., "Complex-stress creep, relaxation and fracture of metallic alloys", Edinburgh, 1962, H.M.S.O.
- (3) Kennedy, A.J. - "Processes of creep and fatigue in metals". Oliver and Kennedy, A.J., "Processes of creep and fatigue in metals", Oliver and Boyd Ltd., Edinburgh, 1962.
- (4) Conway, J.B., Mullikin, M.J., "An evaluation of various equations for 1966, 236, 1496.
- (5) Andrade, E.N. daC., "On the viscous flow in metals, and allied phenomena, Proc. Roy. Soc., 1910, 84A, 1.
- (6) Graham, A., Bates, G.J., "On the shape of the creep curve particularly of nimonic alloys", N.G.T.E. Report No. R.233, April, 1959.
- (7) de Lacombe, M.J., "Un Mode de Representation des courbes de fluage", Revue de Metallurgie, 1939, 36, 178.
- (8) Johnson, A.E., "The creep of a nominally isotropic aluminium alloy under combined stress systems at elevated temperatures", Metallurgia 1949, 40, 125.
- (9) Lubahn, J.D., Felgar, R.P., "Plasticity and creep of metals", John Wiley & Sons, Inc., New York, 1961, 133.
- (10) Bhattacharya, S., Congreve, W.K.A., Thompson, F.C., "The creep/time relationship under constant tensile stress", J. Inst. of Metals, 1952-53, 81, 83.
- (11) Sturm, R.G., Dumont, C., Howell, F.M., "A method of analysing creep data", J. Appl. Mech., 1936, A-62.
- (12) Hazlett, T.H., Parker, E.R., "Nature of the creep curve", Trans. A.I.M.E. J. of Metals, Feb. 1953, 318.
- (13) Crussard, C., "Etude rheologique du fluage et de l'hysteresis mecanique des materiaux", Metaux Corrosion Industries, 1963, No. 457, 299, No. 458, 357, No. 459, 395.

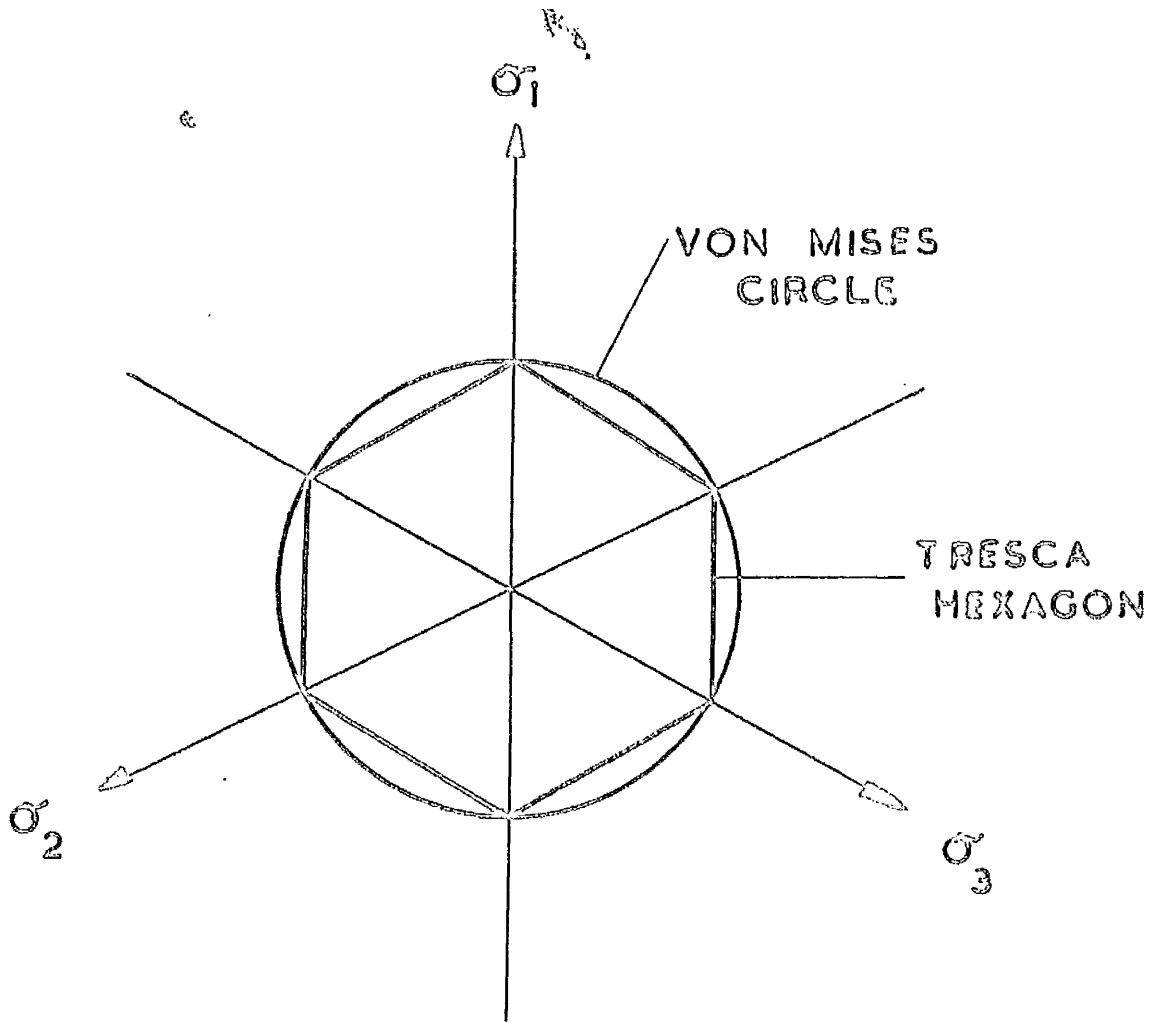
CHAPTER 5

- (1) Bailey, R.W., "Creep relationships and their application to pipes, tubes, and cylindrical parts under pressure," Proc. Instn. Mech. Engrs., 1951, 164, 425.
- (2) Berman, I., Pai, D.H., "A theory of anisotropic steady-state creep", Int. J. Mech. Sci., 1966, 8, 341.
- (3) Prager, W., "On the use of singular yield conditions and associated flow rules", Trans. A.S.M.E., J. Appl. Mech., 1953, 20, 317.
- (4) Johnson, A.E., Henderson, J., Khan, B., "Complex-stress creep, relaxation, and fracture of metallic alloys", Edinburgh 1962, H.M.S.O.
- (5) Stowell, E.Z., Gregory, R.K., "Steady-state biaxial creep", Trans. A.S.M.E., J. Appl. Mech., 1965, 32, 37.
- (6) Pai, D.H., "Steady-state creep analysis of thick-walled orthotropic cylinders," Int. J. Mech. Sci., 1967, 9, 335.
- (7) Johnson, A.E., Henderson, J., Khan, B., "Behaviour of metallic thick-walled cylindrical vessels or tubes subject to high internal or external pressures at elevated temperatures", Proc. Instn. Mech. Engrs., 1961, 175, 1043.
- (8) Marriot, D.L., Leckie, F.A., "Some observations of the deflections of structures during creep", Conf. Thermal loading and creep, Proc. Instn. Mech. Engrs., 1963-64, 178, (Pt. 3L), 115.
- (9) Coffin, L.F., Shepler, P.R., Cherniak, G.S., "Primary creep in the design of internal pressure vessels", J. Appl. Mech., 1949, 19, 229.
- (10) Finnie, I., Heller, W.R., "Creep of engineering materials", McGraw-Hill Book Company, Inc., New York, 1959.
- (11) Soderberg, C.R., "Interpretation of creep tests on tubes", Trans. A.S.M.E., 1941, 63, 737.
- (12) Skelton, W.J., Crossland, B., "Correlation of tension and thick-walled cylinder creep based on experimental data", Paper 7, Conf. High Pressure Engineering, Instn. Mech. Engrs., September, 1967.
- (13) Larke, E.C., Parker, R.J., "Circumferential creep strain of cylinders subjected to internal pressure: a comparison of the theories of Johnson and Bailey", J. Mech. Eng. Sci., 1966, 8, 22.
- (14) Smith, E.M., "Primary creep behaviour of thick tubes", Conf. Thermal Loading and Creep, Proc. Instn. Mech. Engrs., 1963-64, 178, (Pt. 3L), 135.

CHAPTER 6

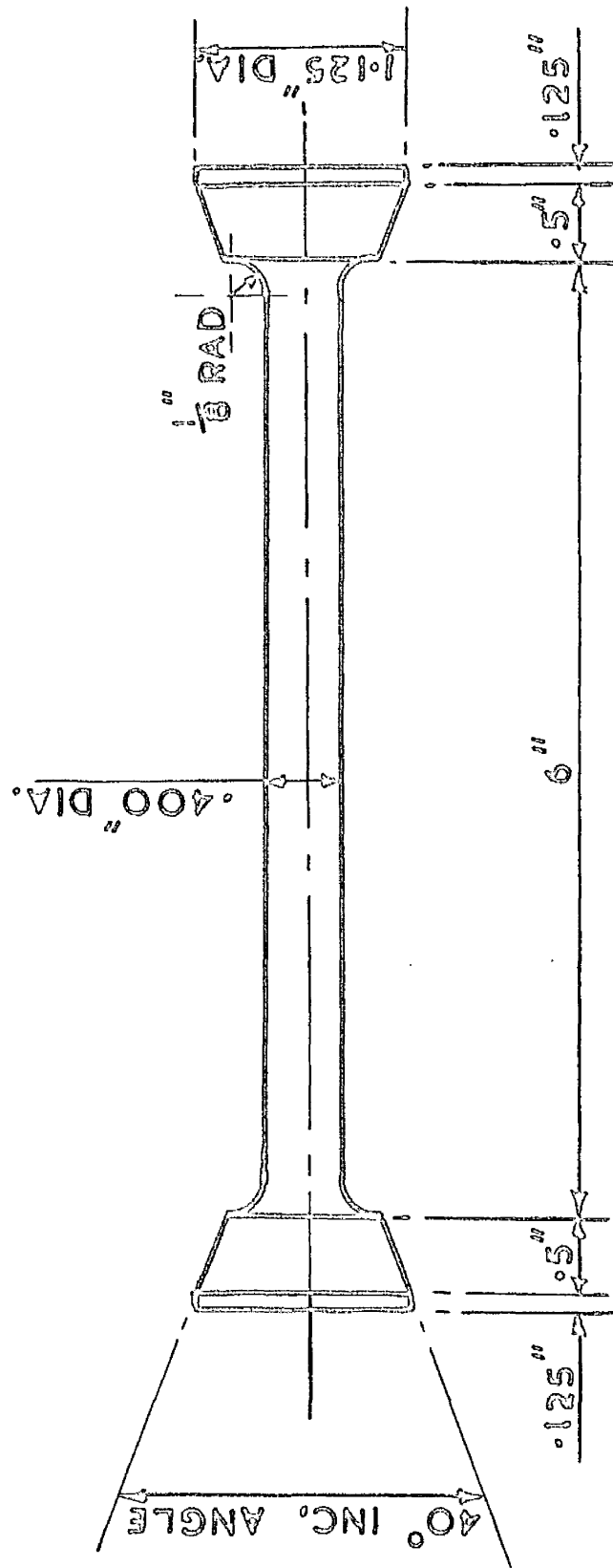
- (1) Rimrott, F.P.J., "Creep of thick-walled tubes under internal pressure considering large strains", Trans. A.S.M.E., J. Appl. Mech., 1959, 81, 271.
- (2) Berman, J., Pai, D.H., "A theory of anisotropic steady-state creep", Int. J. Mech. Sci., 1968, 8, 341.
- (3) Bailey, R.W., "Creep relationships and their application to pipes, tubes, and cylindrical parts under internal pressure", Proc. Instn. Mech. Engrs., 1951, 164, 324.
- (4) de Lacombe, M.J., "Un mode de representation des courbes de fluage", Revue de Metallurgie, 1939, 36, 178.
- (5) Graham, A., Wallis, K.F.A., "Regularities in creep and hot-fatigue data, Parts I and II", N.G.T.E. Reports Nos. 189 and 190, December 1956.
- (6) Allen, D.N.de G., Sopwith, D.G., "The stresses and strains in a partly plastic thick tube under internal pressure and end load," Proc. Roy. Soc., 1951, A205, 69.
- (7) Johnson, A.E., Henderson, J., Khan, B., "Behaviour of metallic thick-walled cylindrical vessels or tubes subject to high internal or external pressures at elevated temperatures", Proc. Instn. Mech. Engrs., 1961, 175, 1043.
- (8) Smith, E.M., "Primary creep behaviour of thick tubes", Conf. Thermal Loading and Creep, Proc. Instn. Mech. Engrs., 1963-64, 178 (Pt.3L), 135.

FIGURES



VON MISES AND TRESCA CRITERIA ON  
REDUCED PLANE

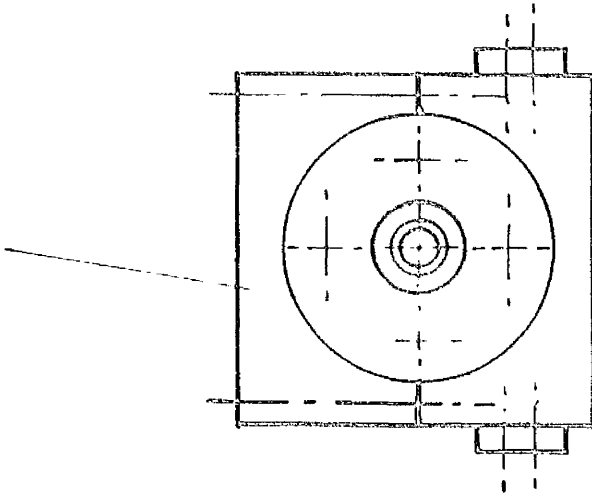
fig 1



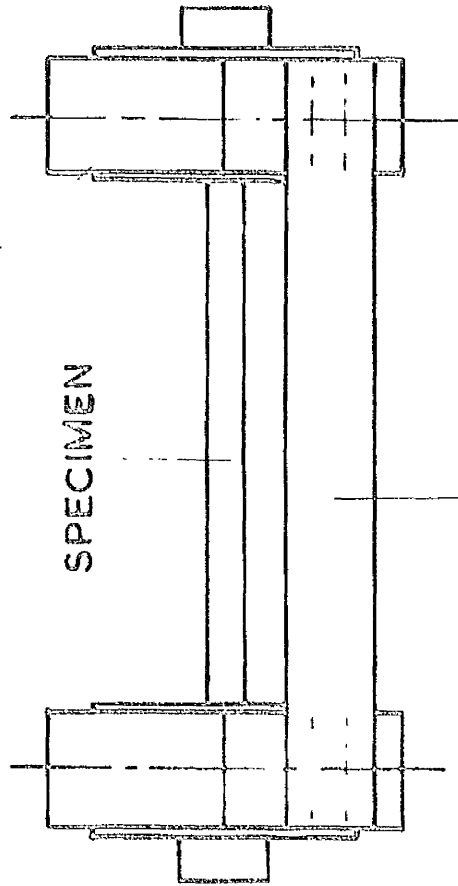
DETAIL OF TENSILE SPECIMENS

fig 2

SPECIMEN GRIPS



END PIECES

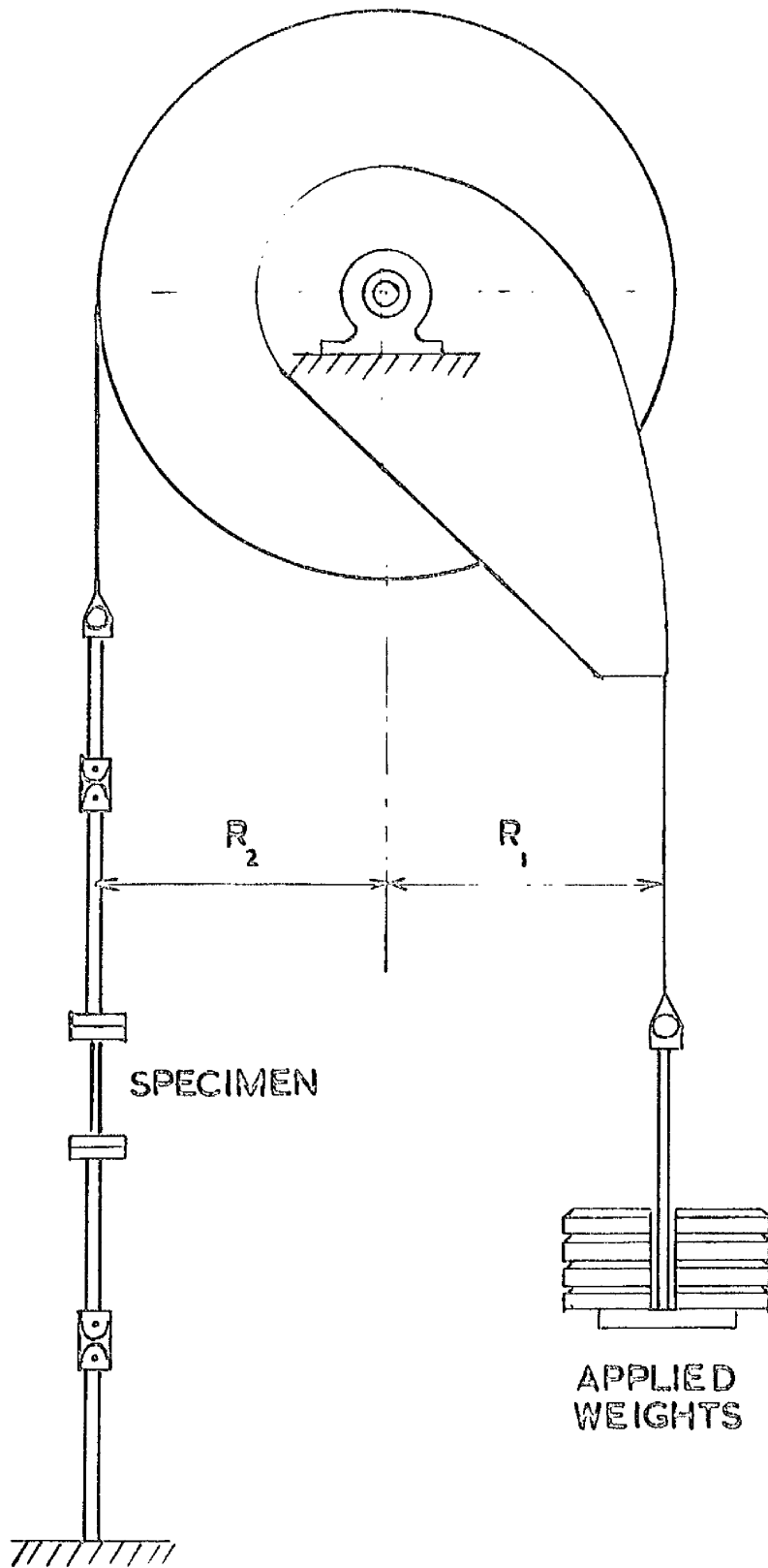


SPECIMEN

STRAPS

TENSILE SPECIMEN JIG

fig 3



ARRANGEMENT OF CONSTANT  
TENSILE STRESS SYSTEM

fig 4

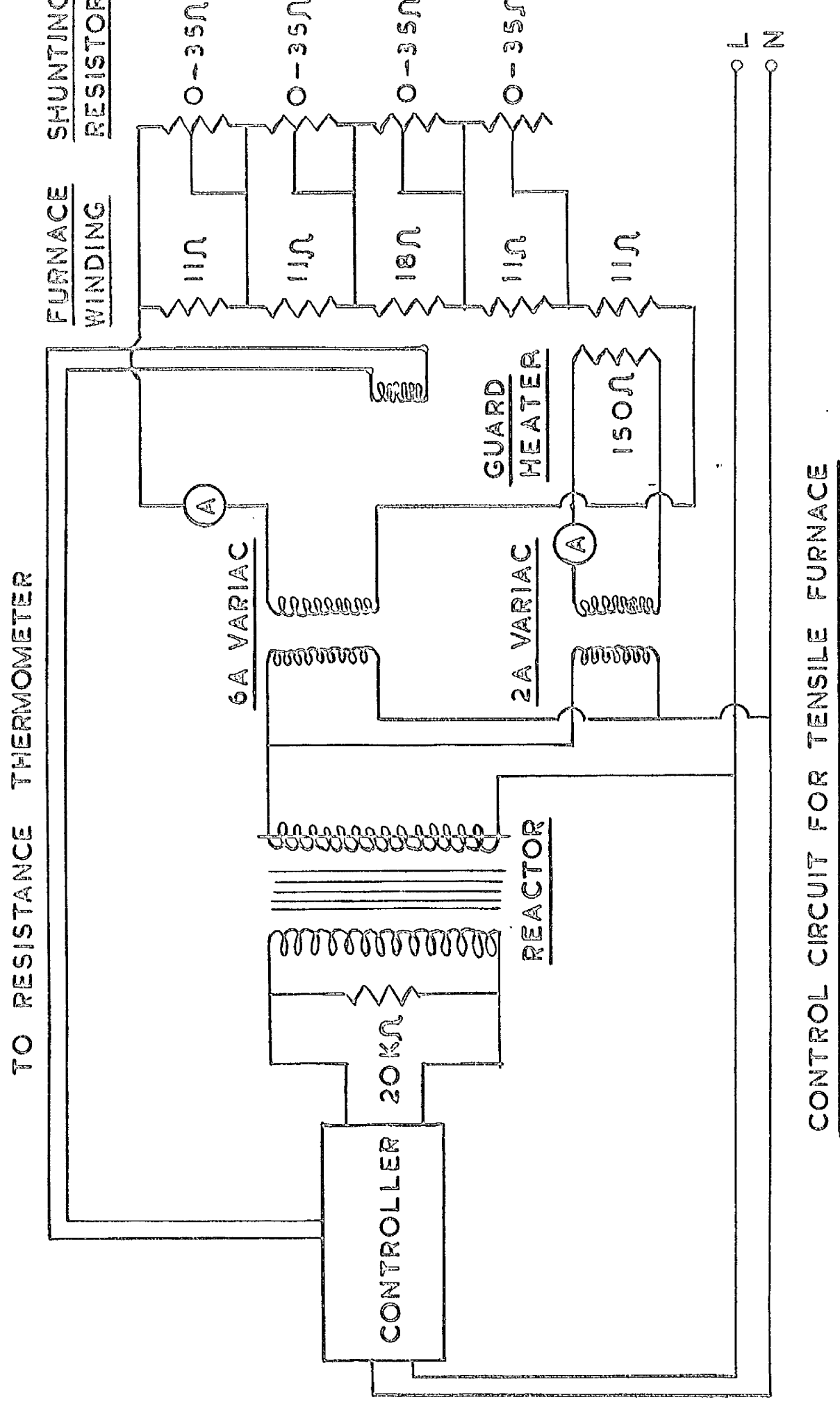
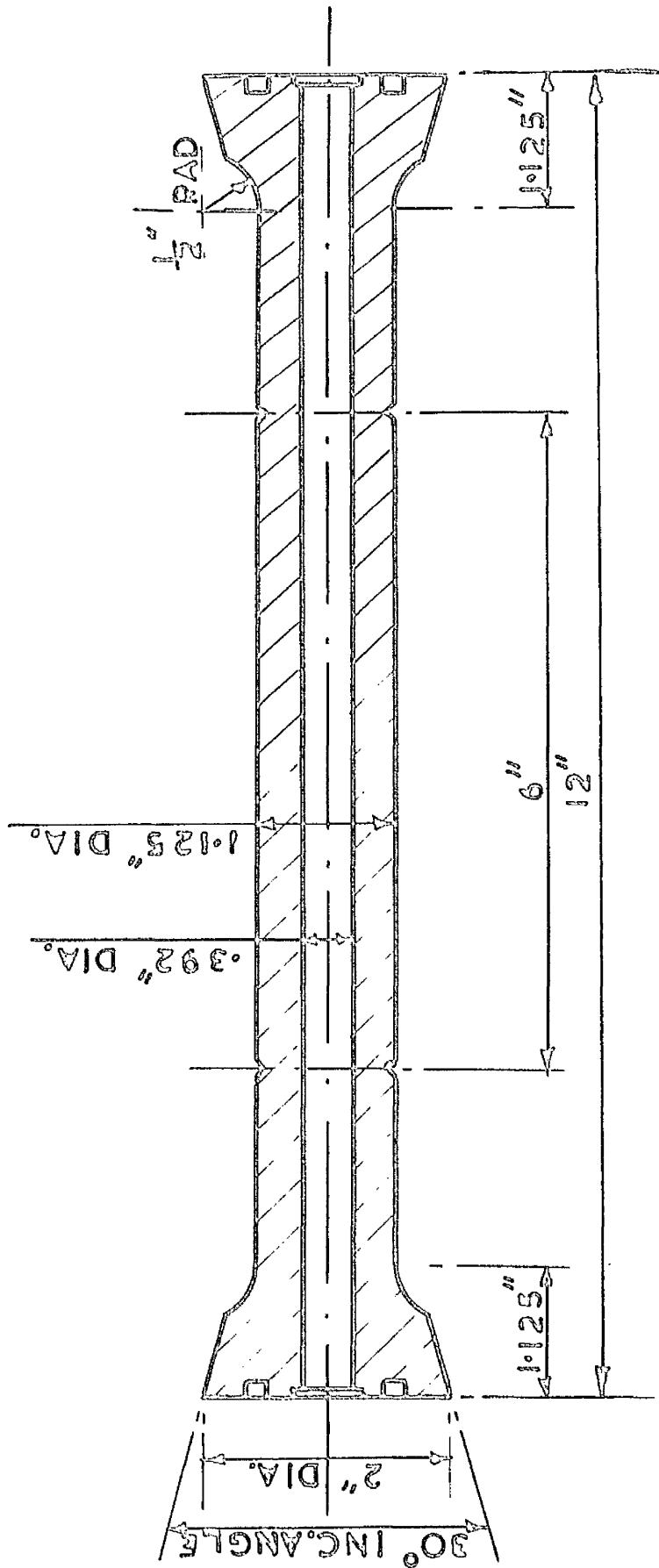
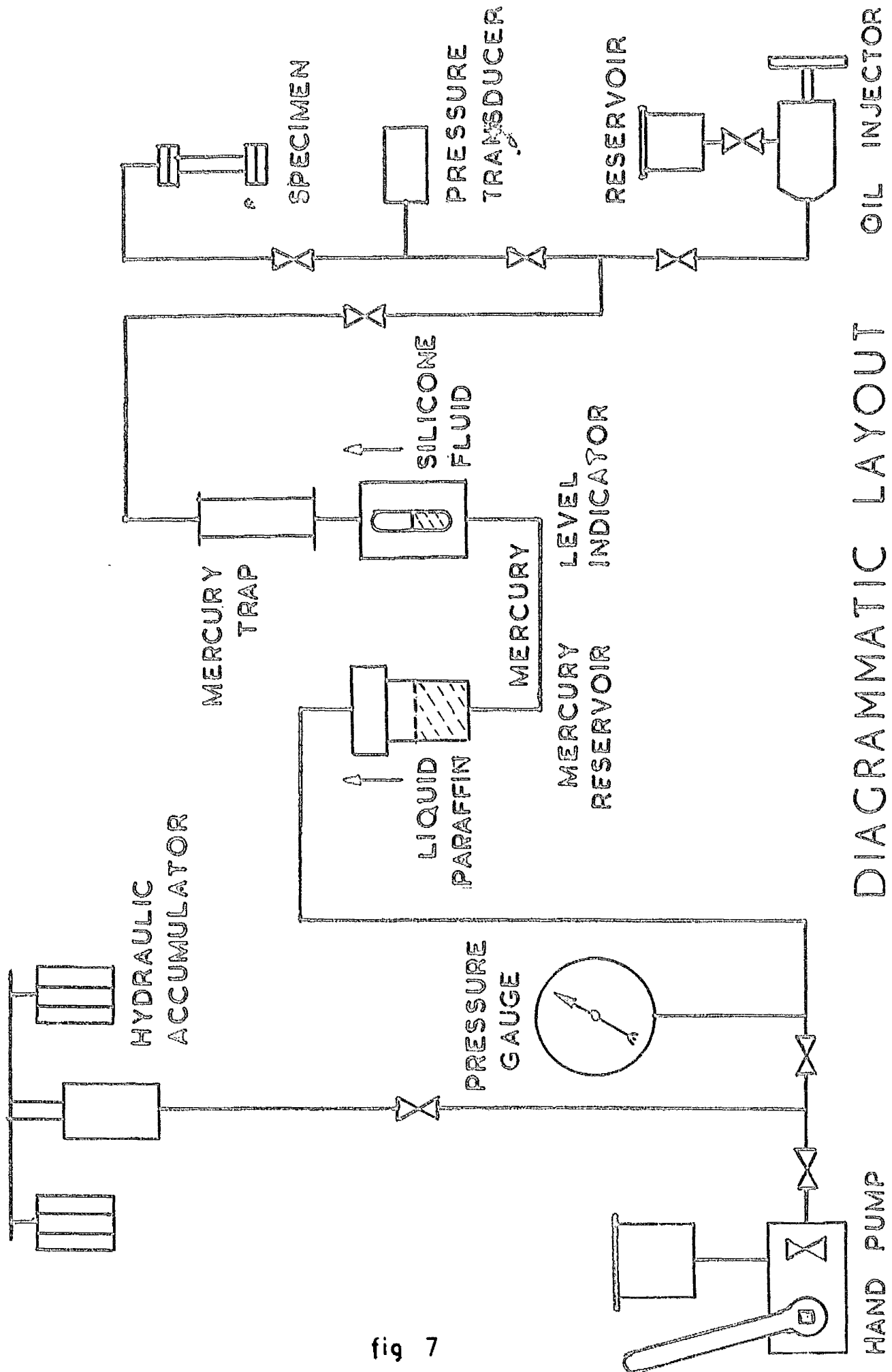


fig 5



DETAIL OF TUBULAR SPECIMENS

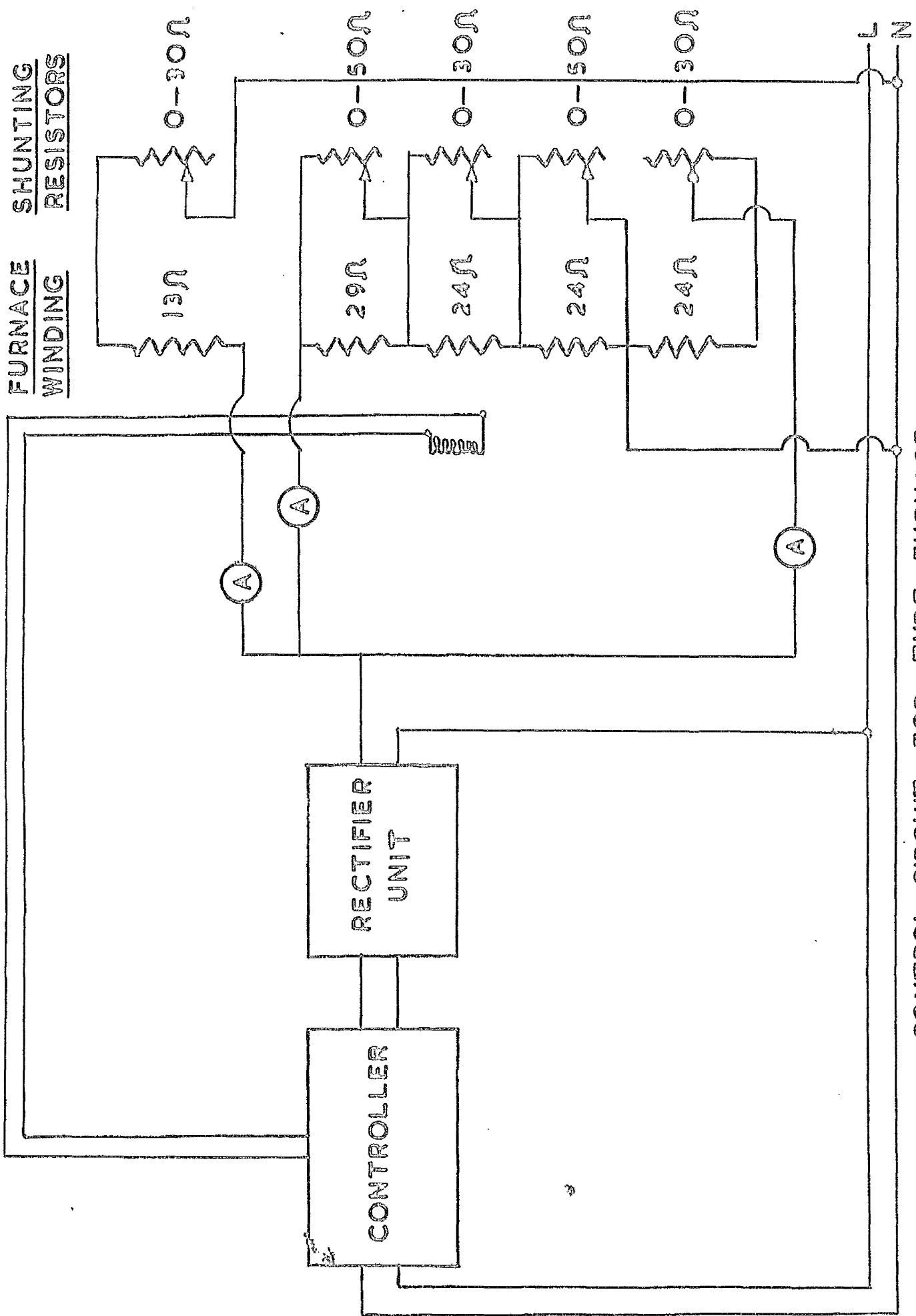
fig 6



DIAGRAMMATIC LAYOUT OF PRESSURE SYSTEM

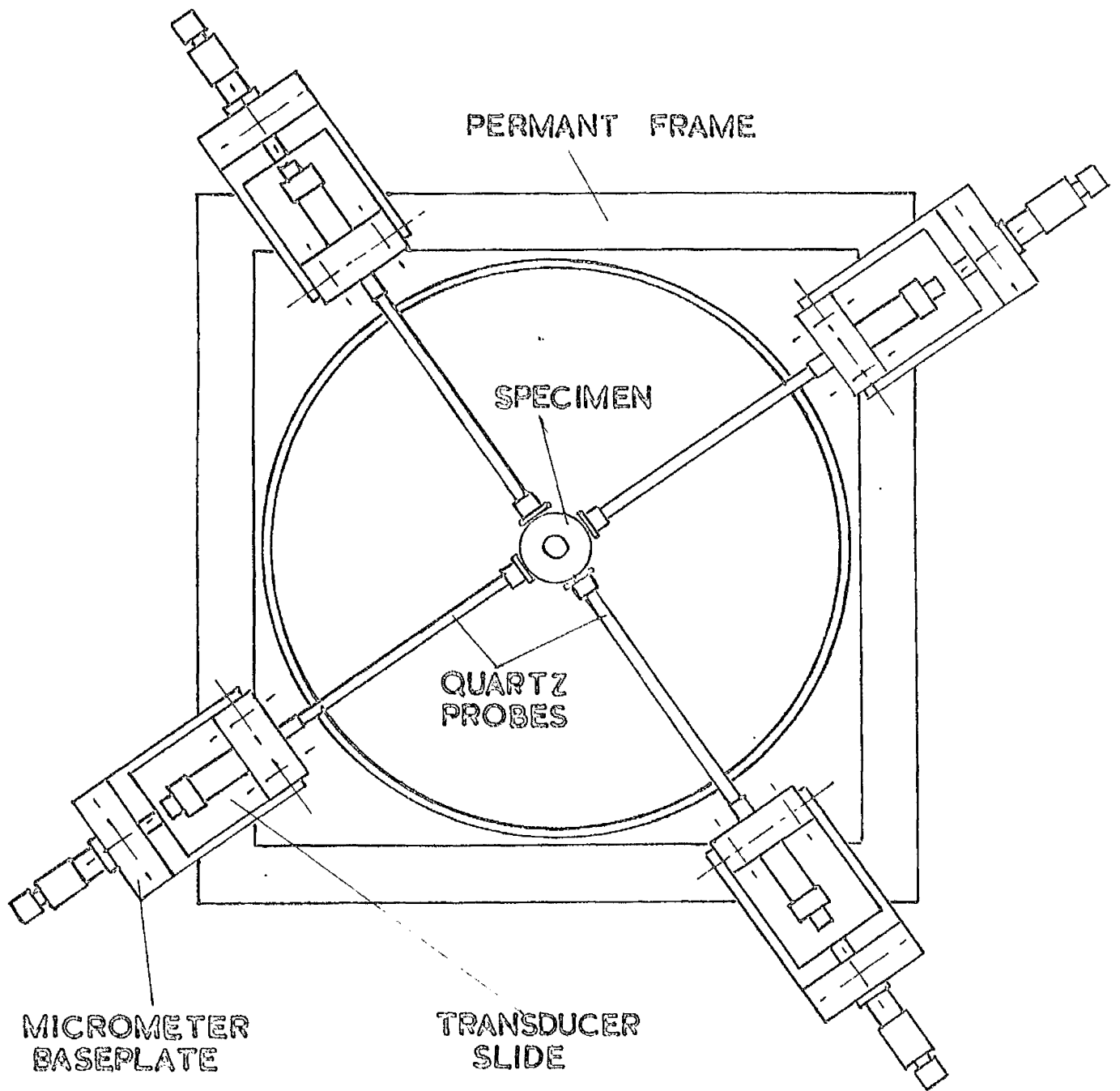
fig 7

TO RESISTANCE THERMOMETER



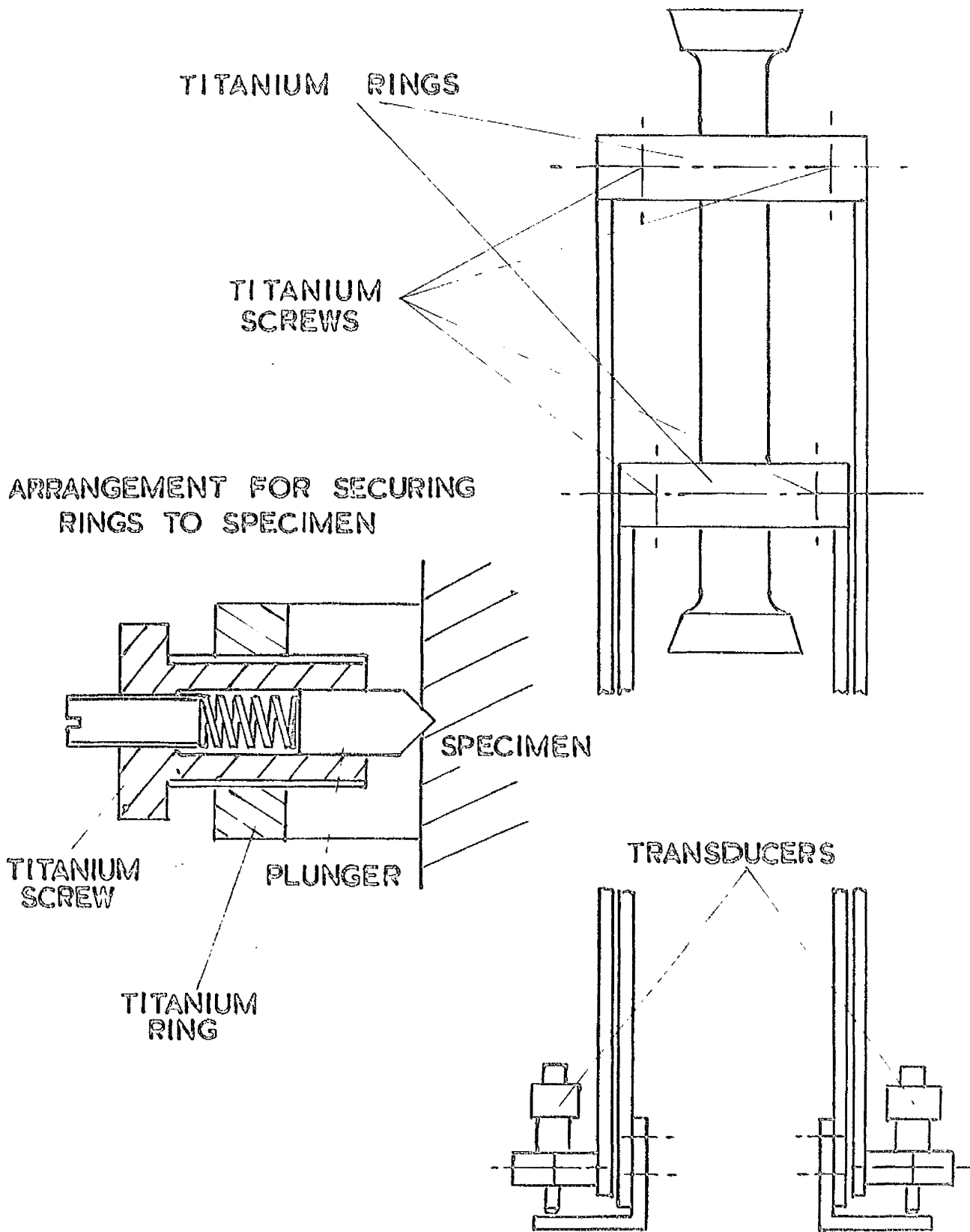
CONTROL CIRCUIT FOR TUBE FURNACE

fig 8



ARRANGEMENT OF DIAMETRAL EXTENSOMETRY

fig 9



ARRANGEMENT OF AXIAL EXTENSOMETRY

fig 10

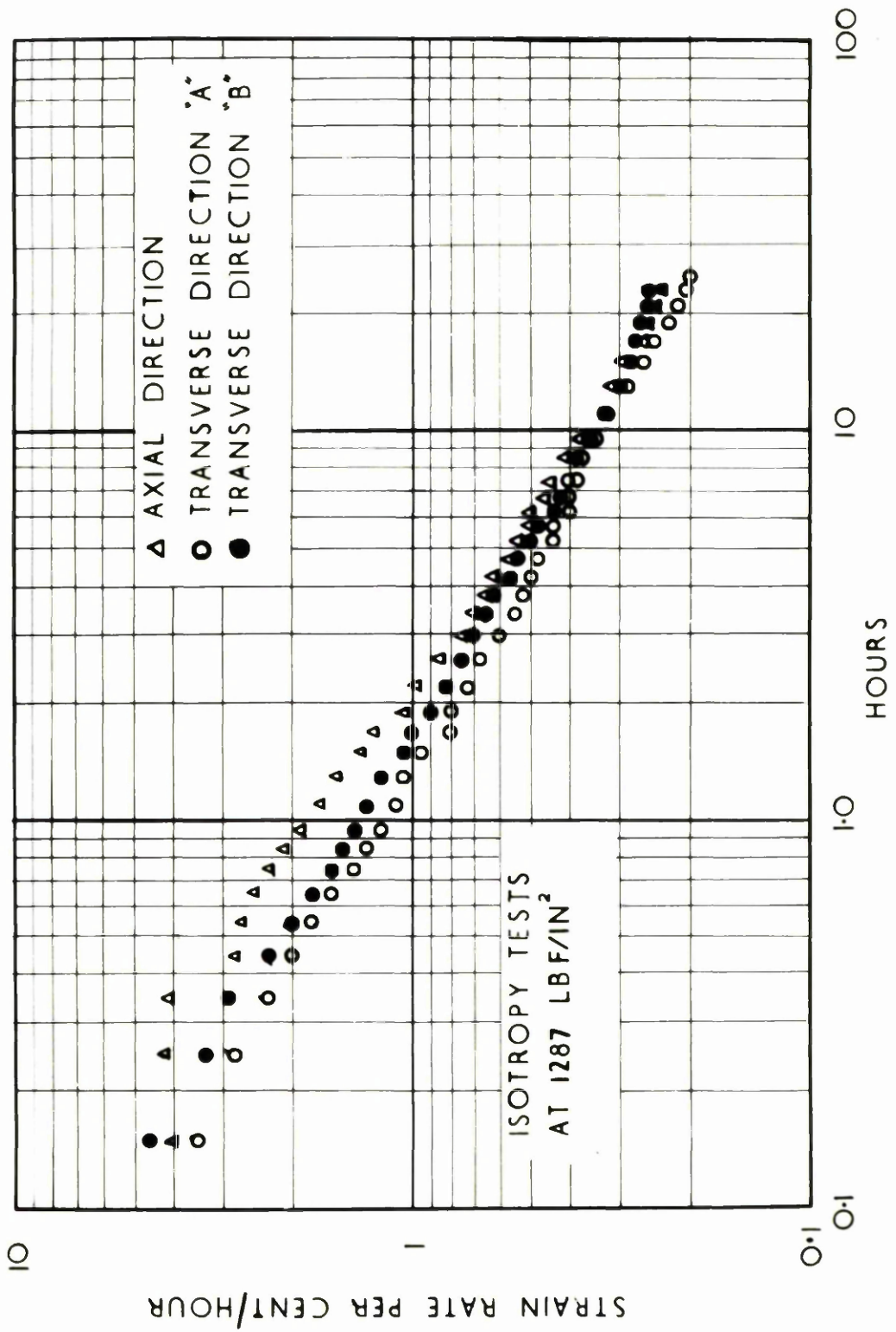


fig 11

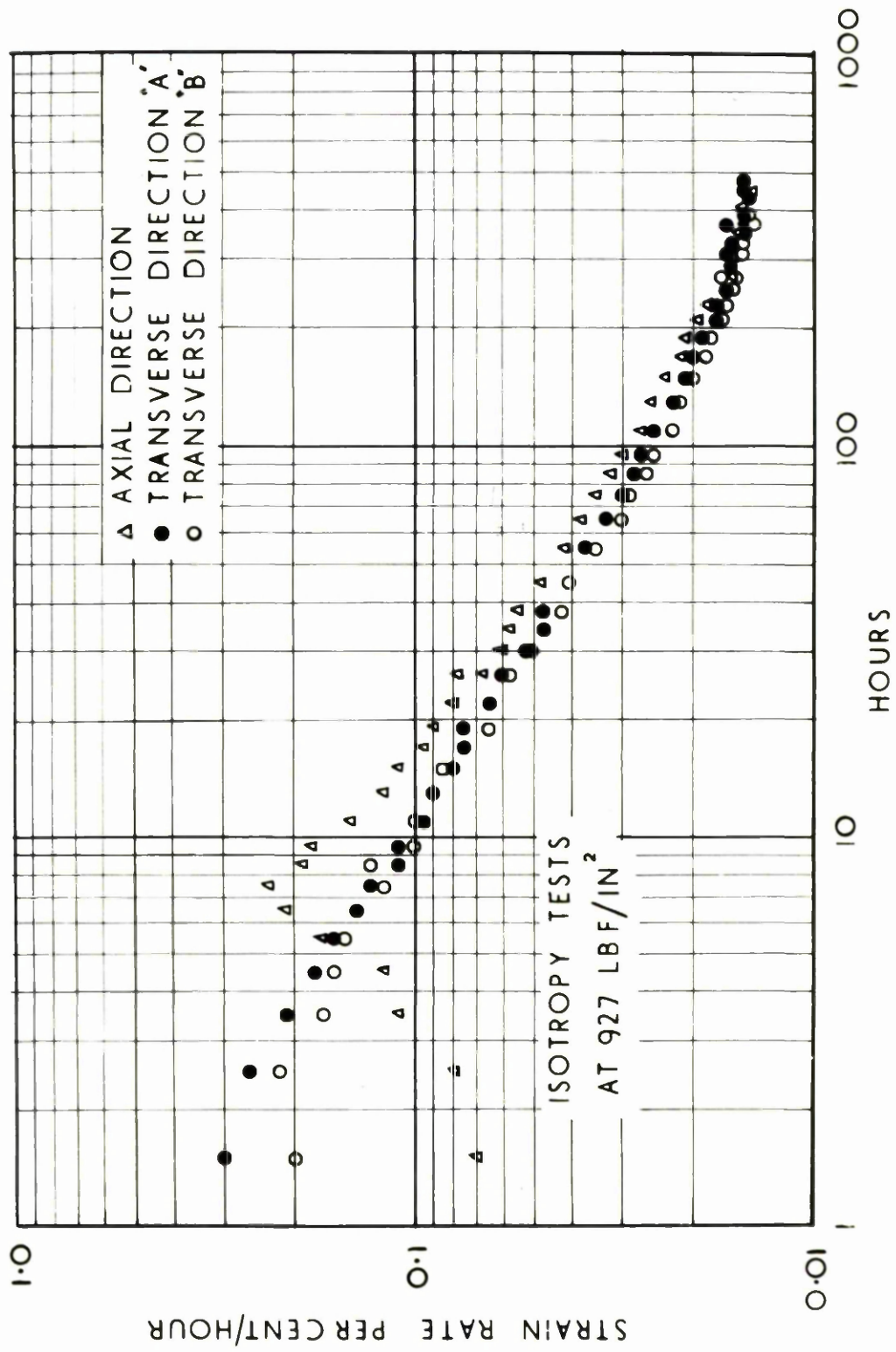


fig 12

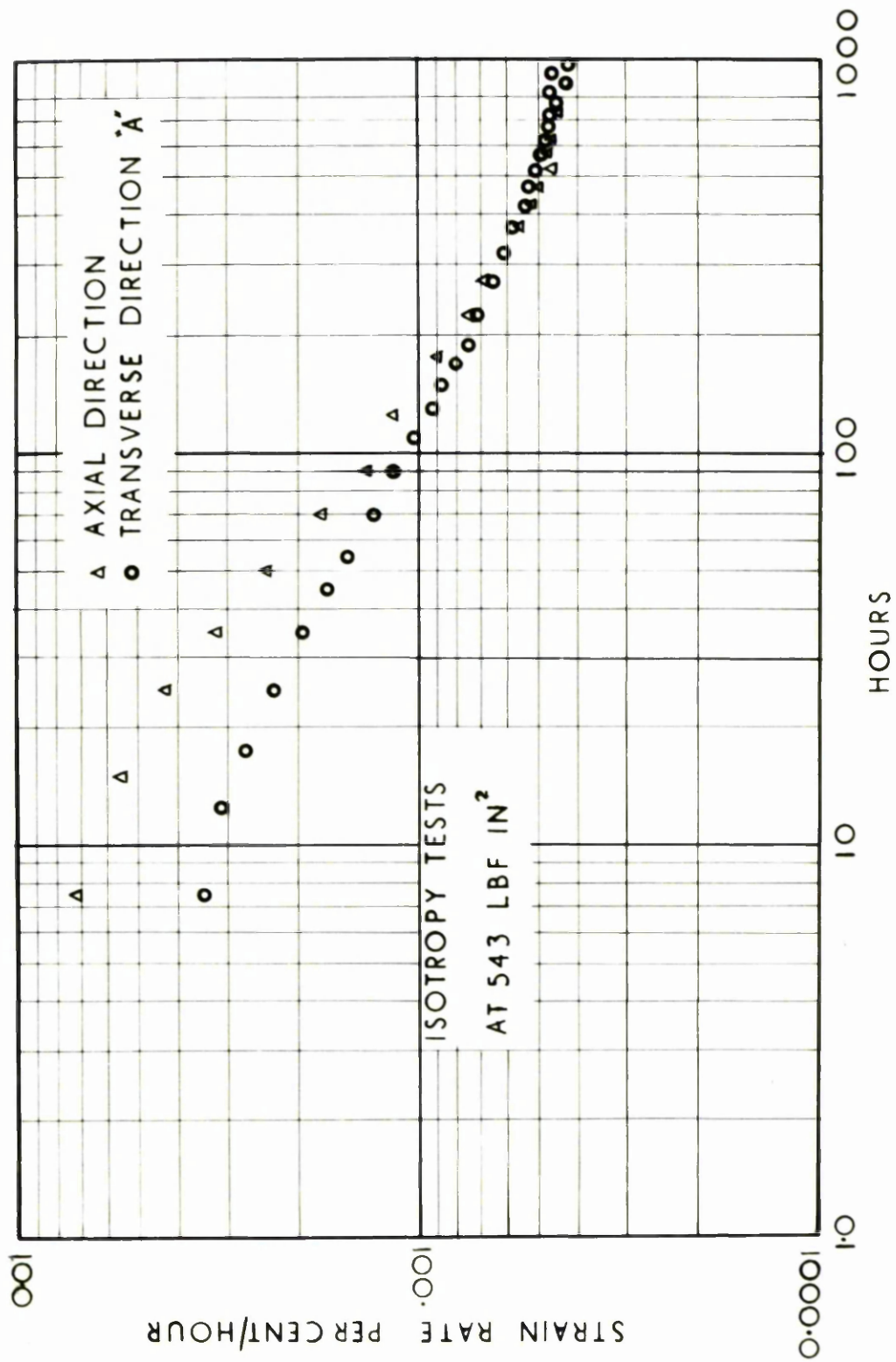


fig 13

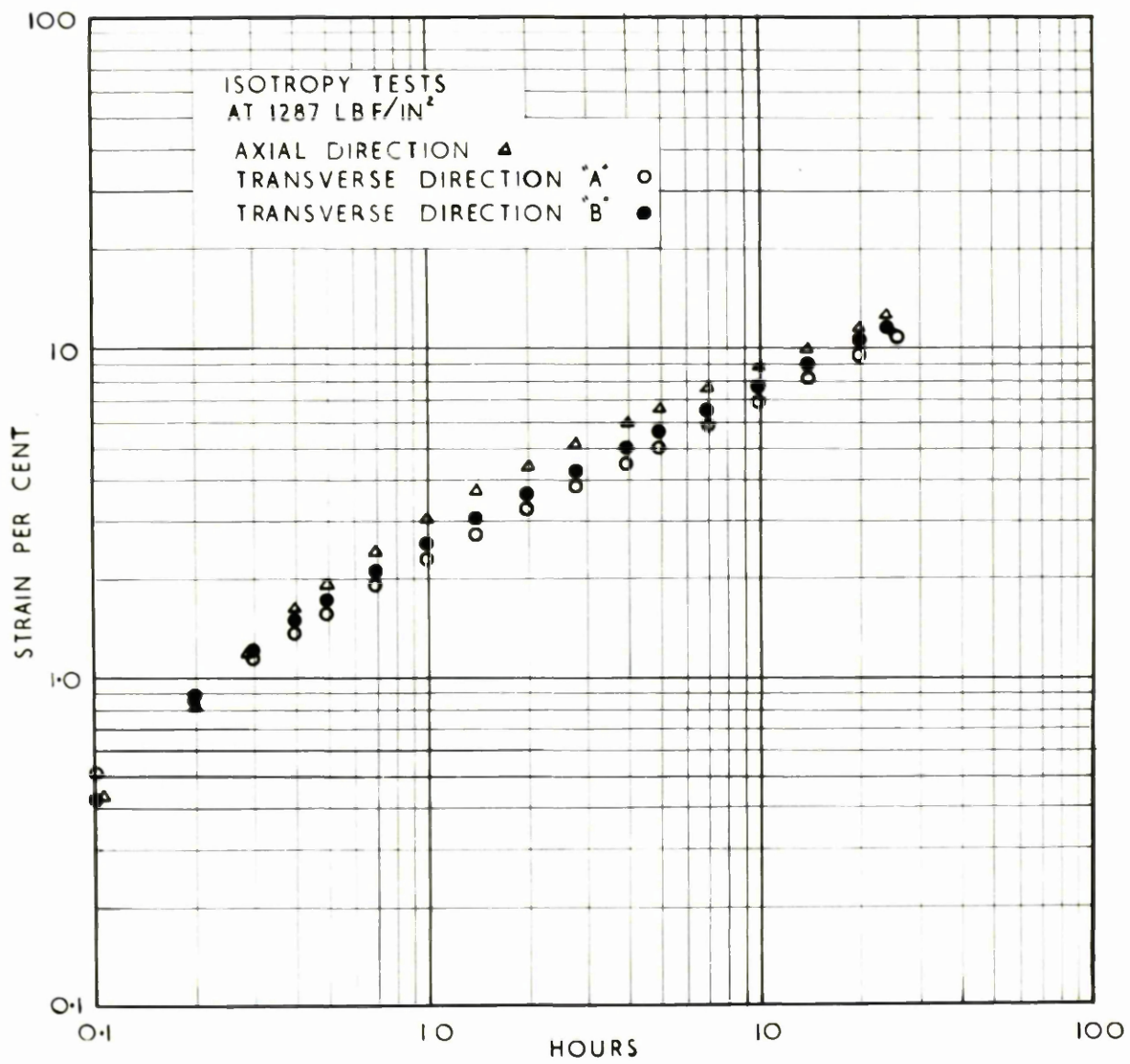


fig 14

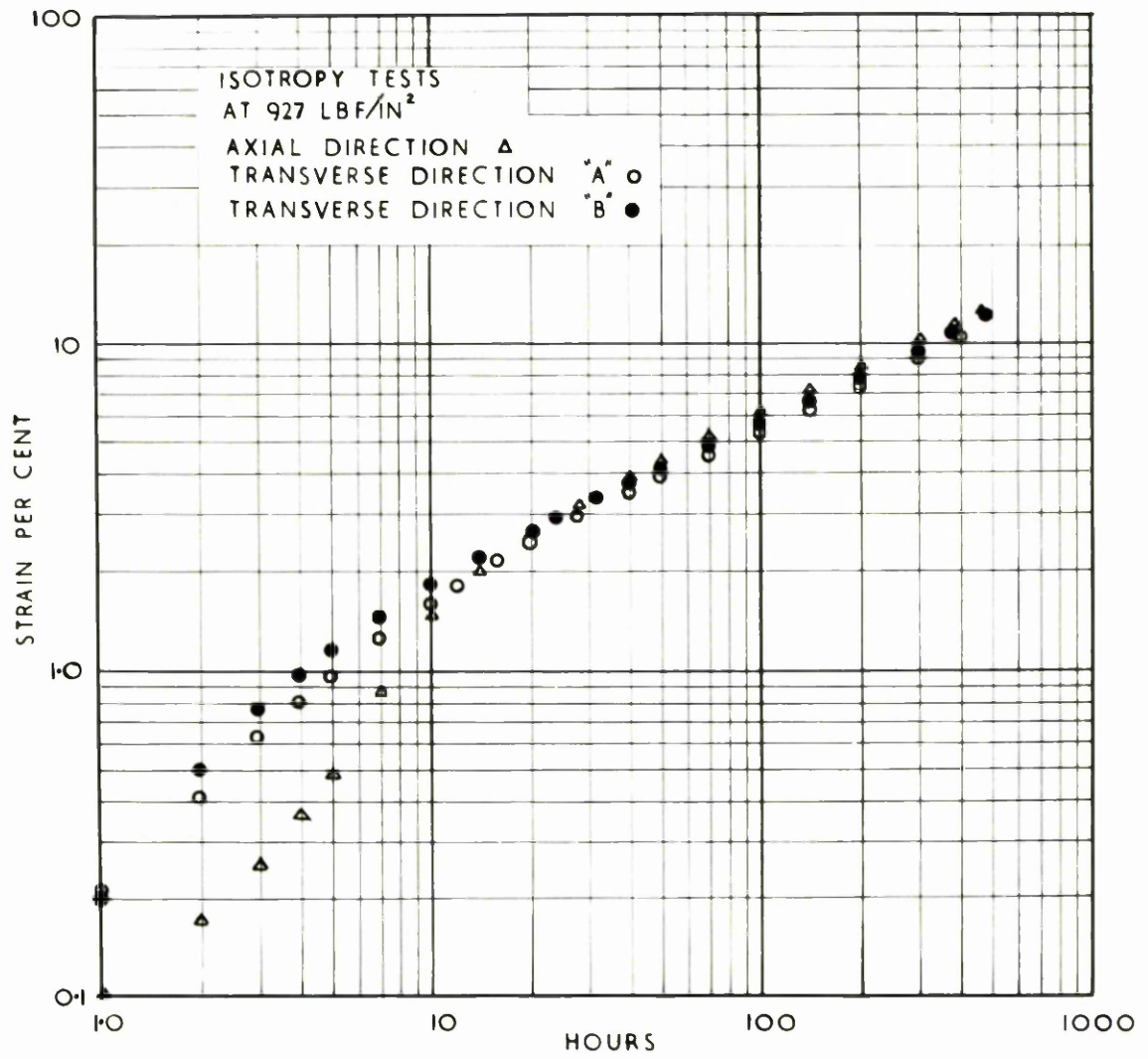


fig 15

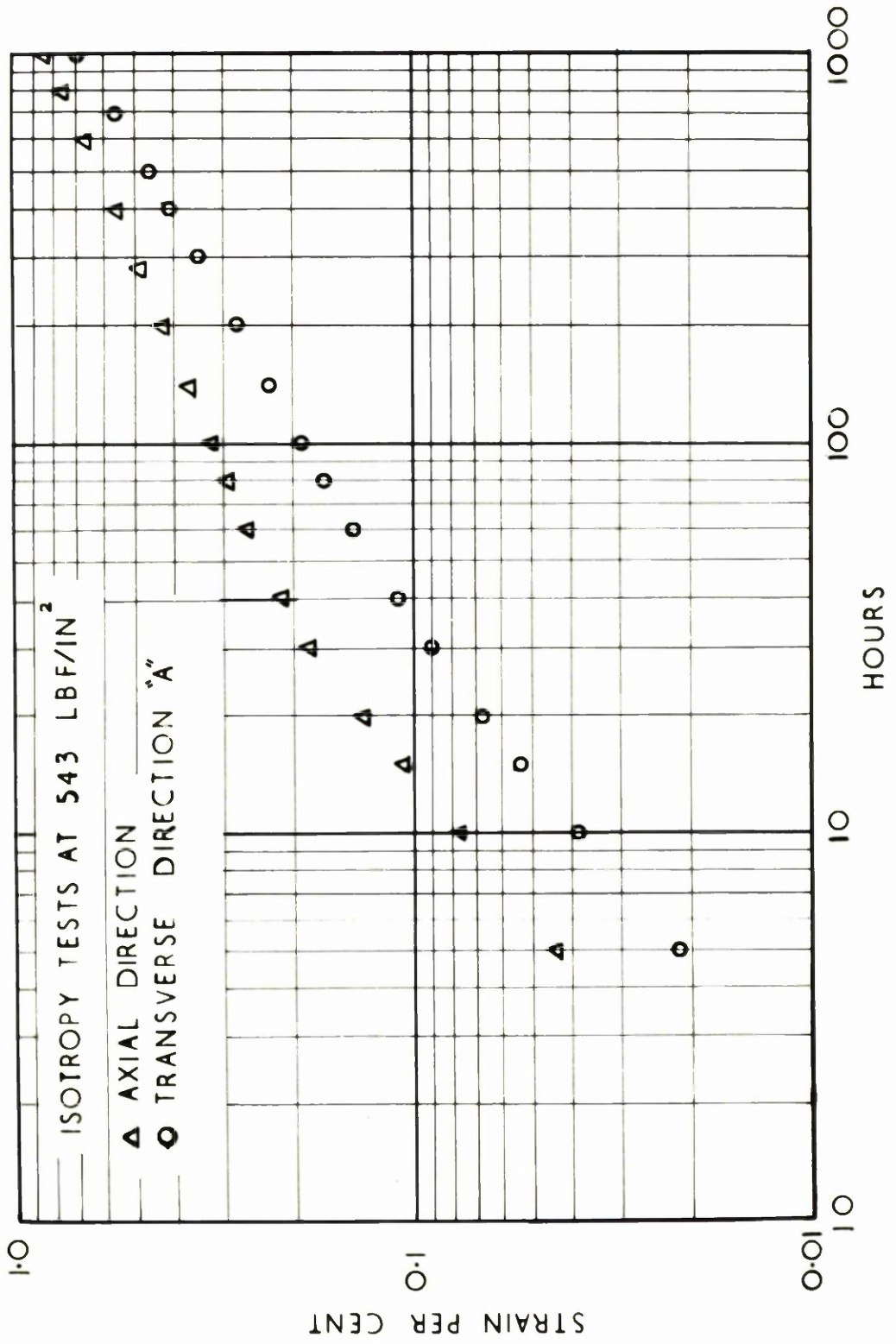


fig 16

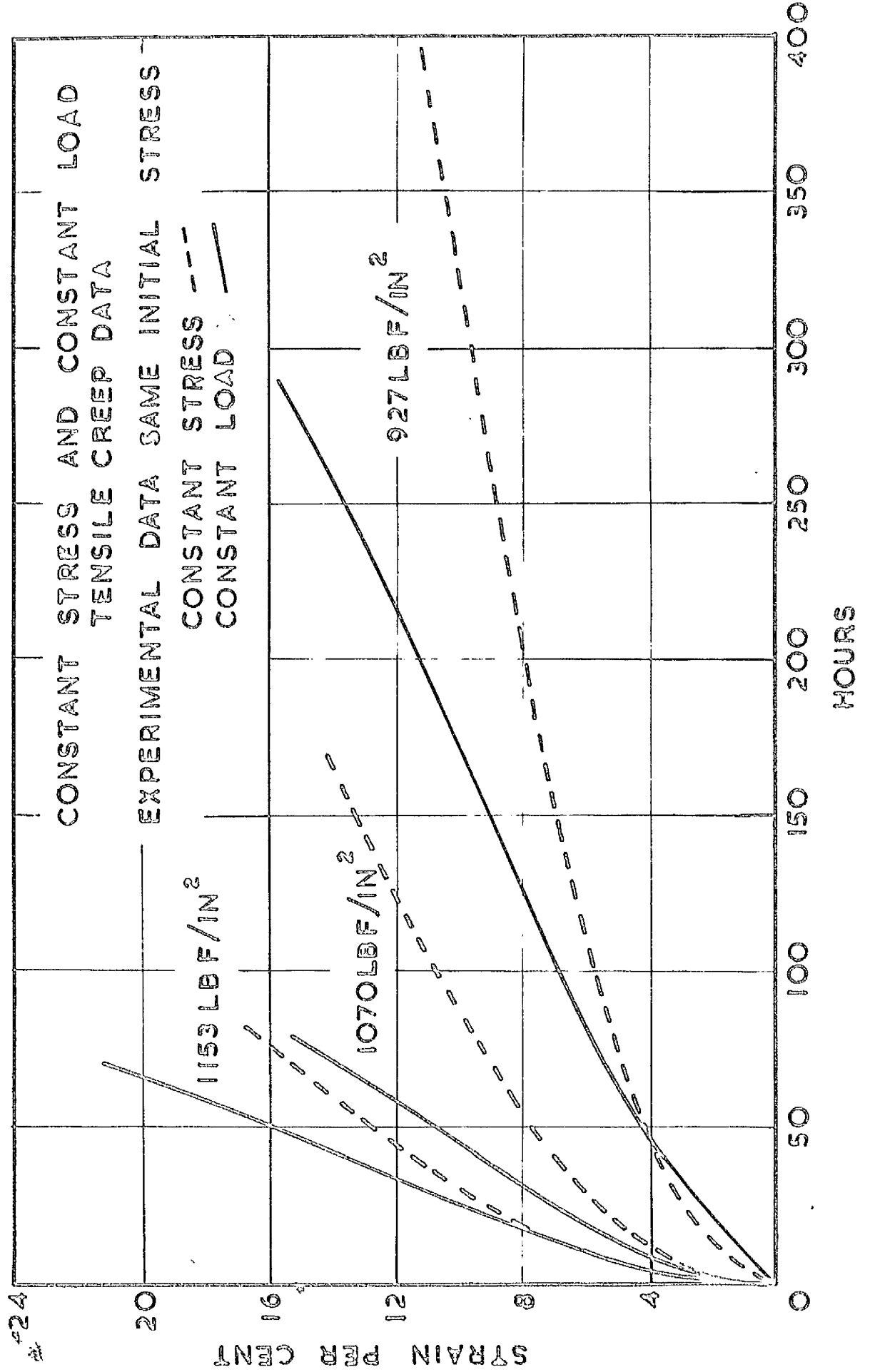


fig 17

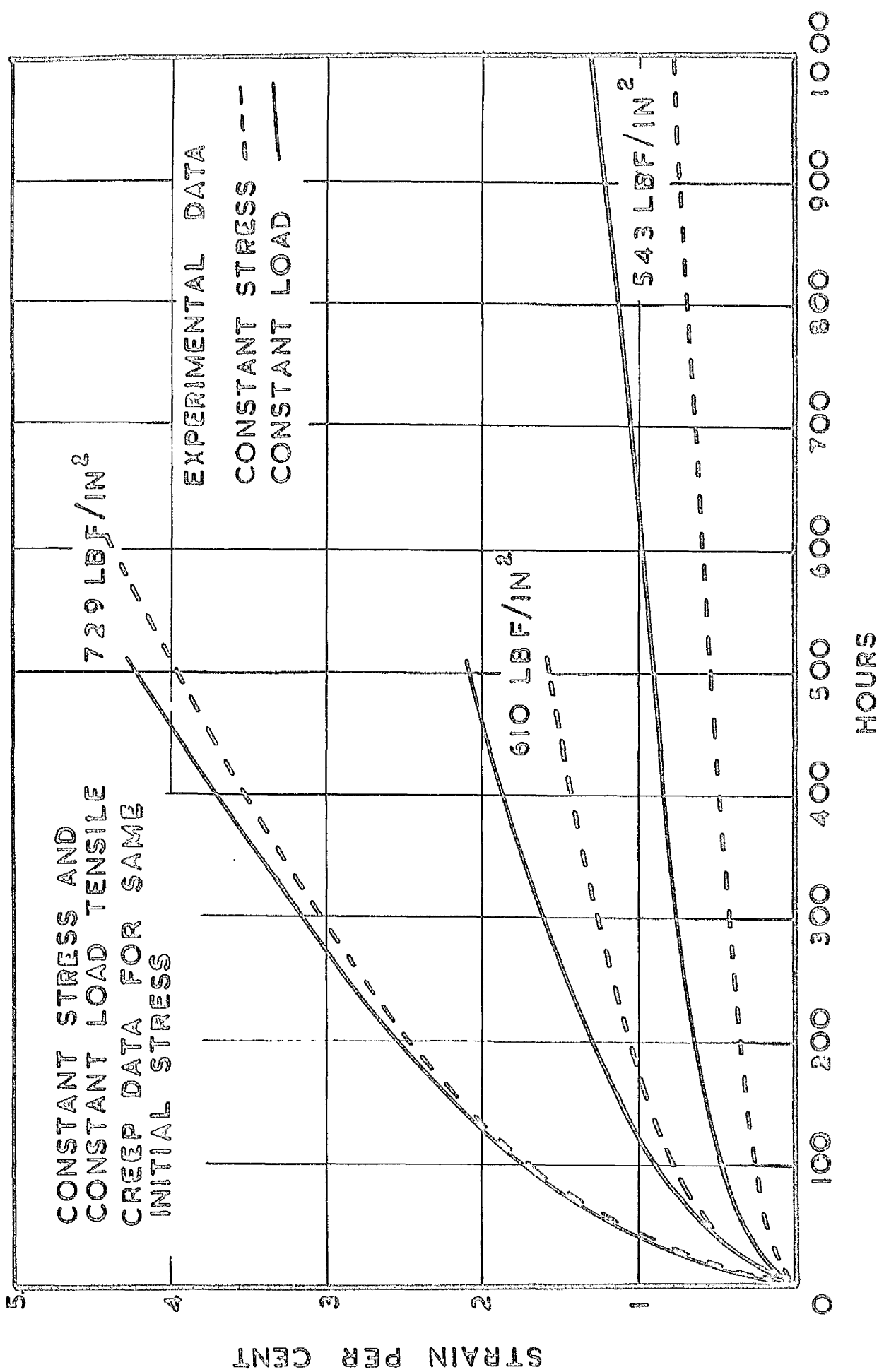


fig 18

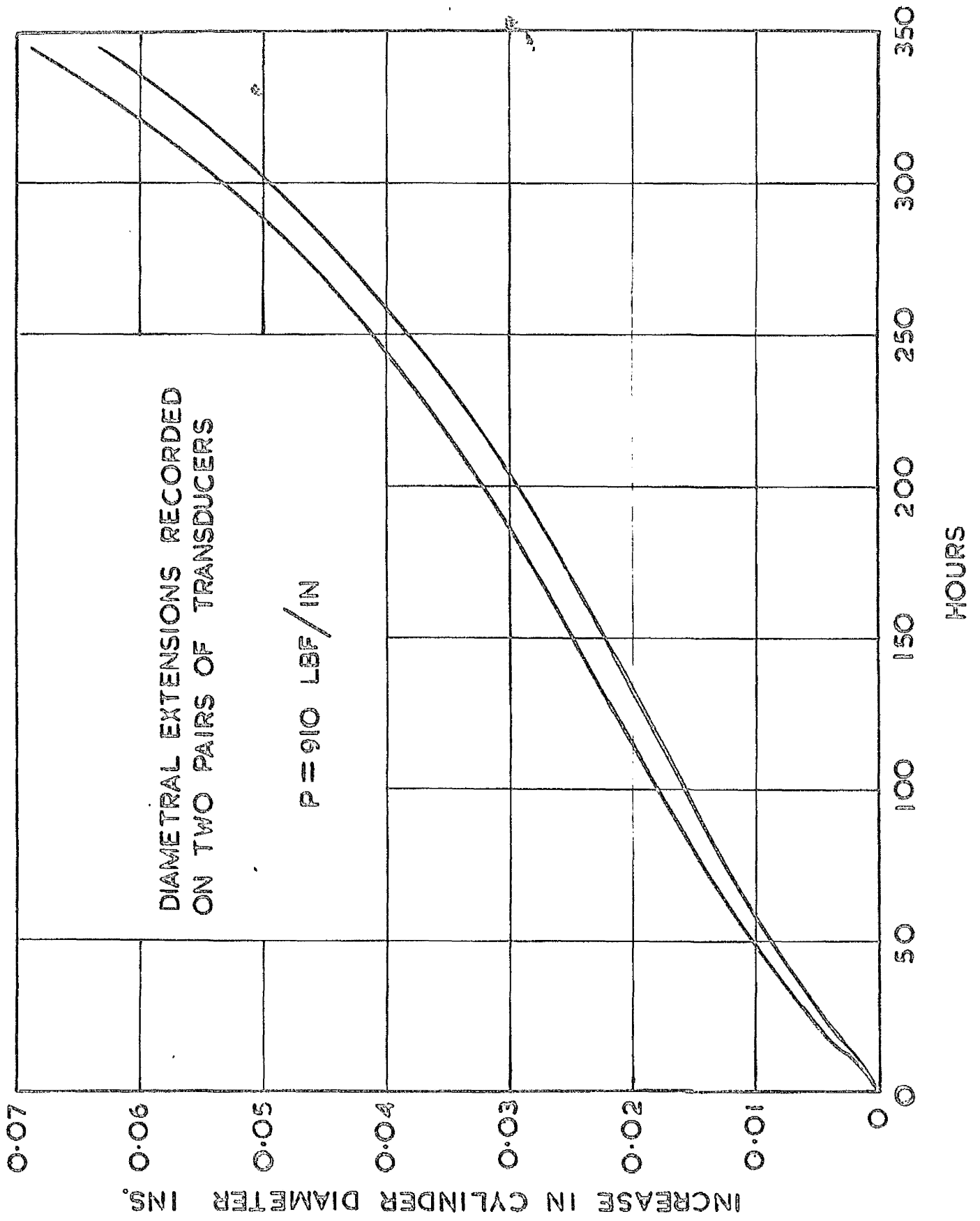


fig 19

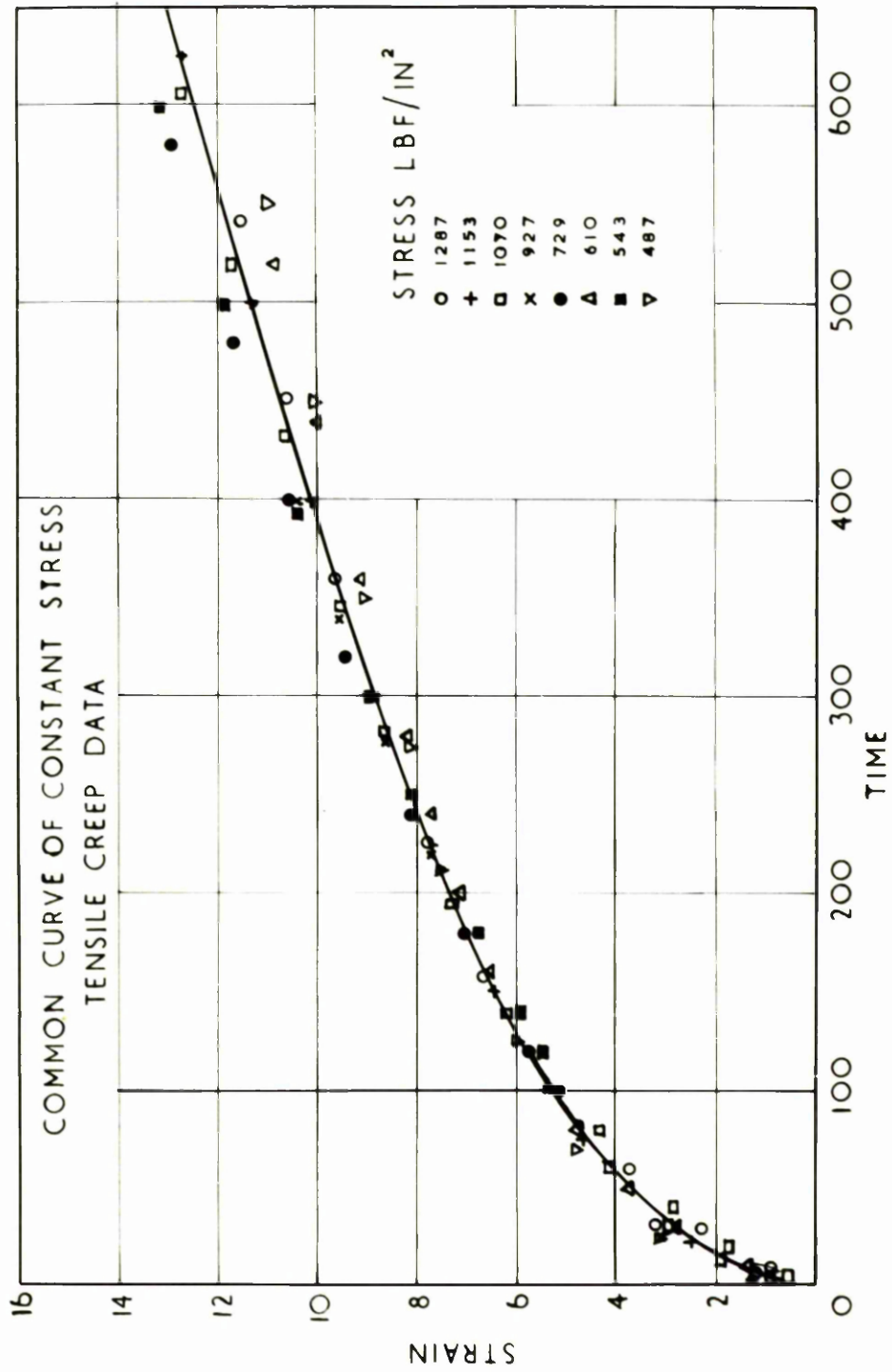


fig 20

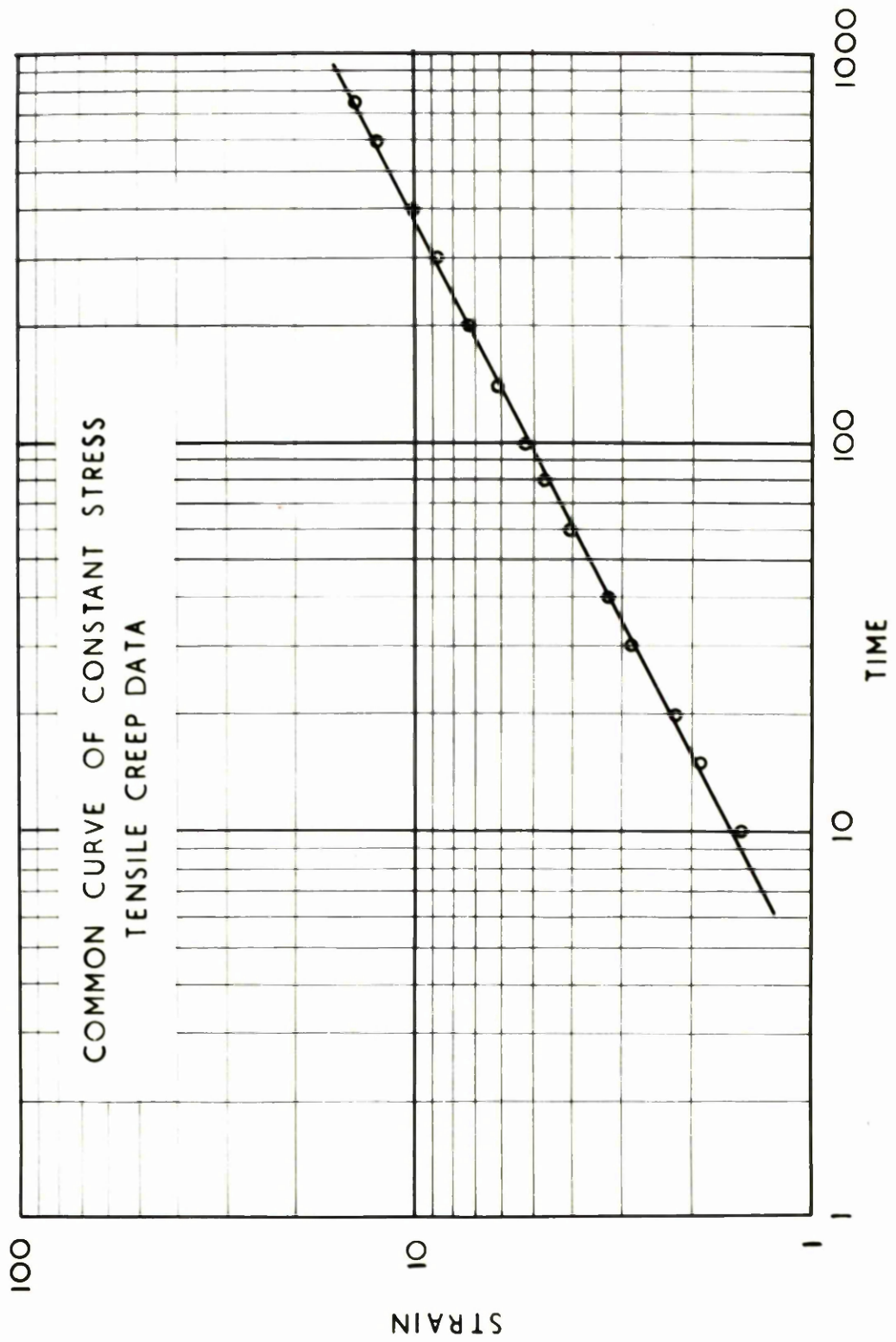


fig 21

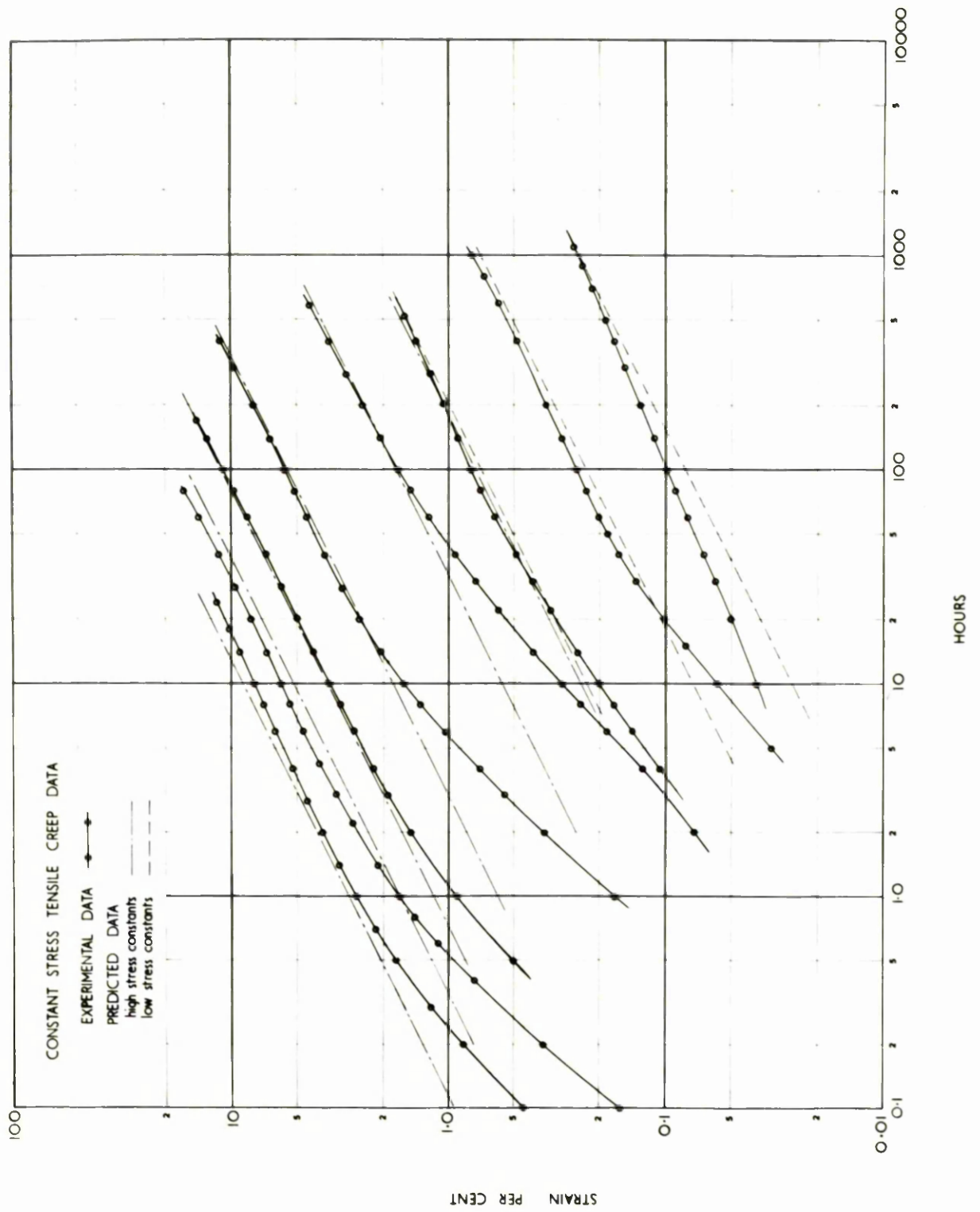


fig 22

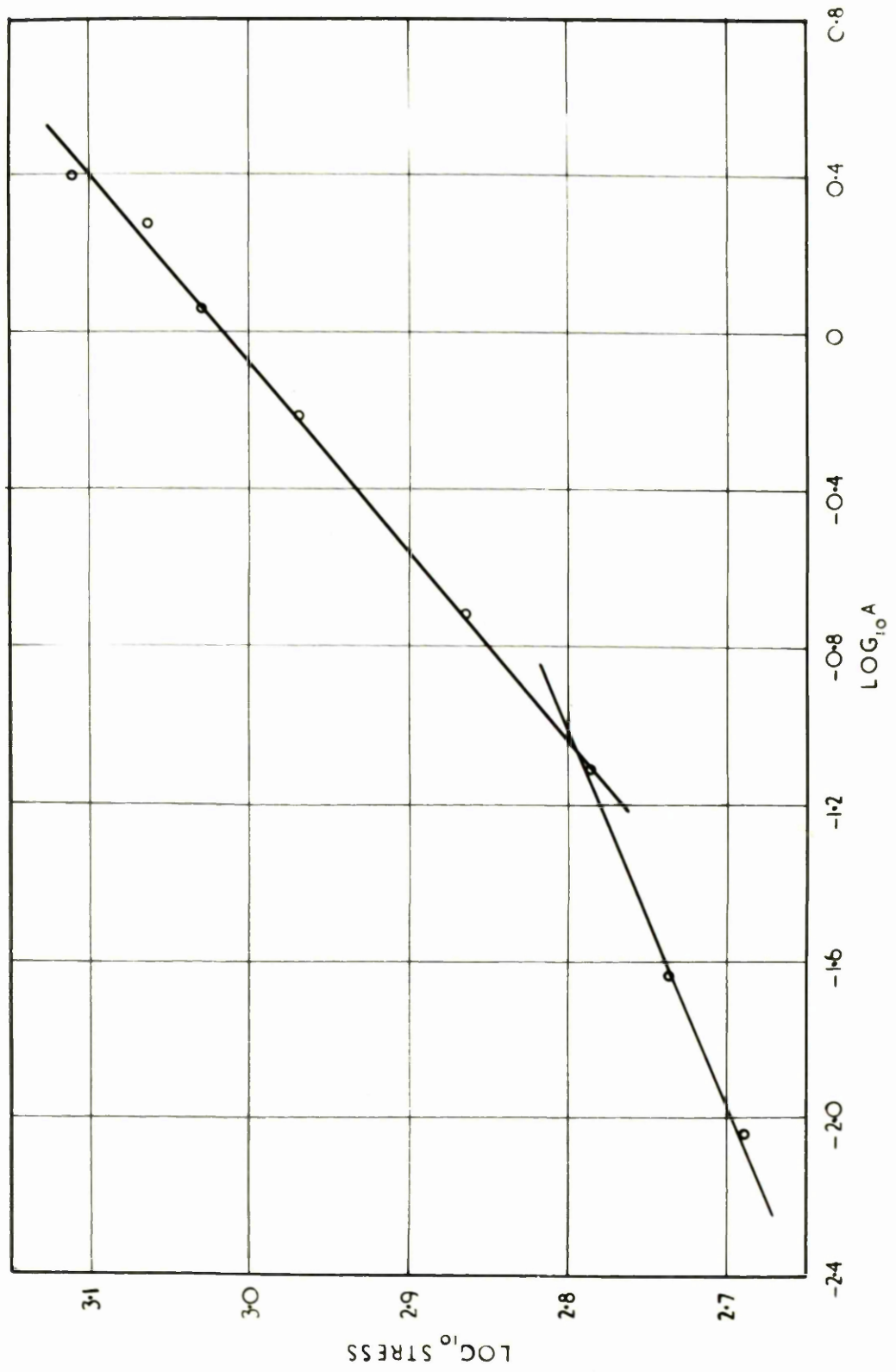


fig 23

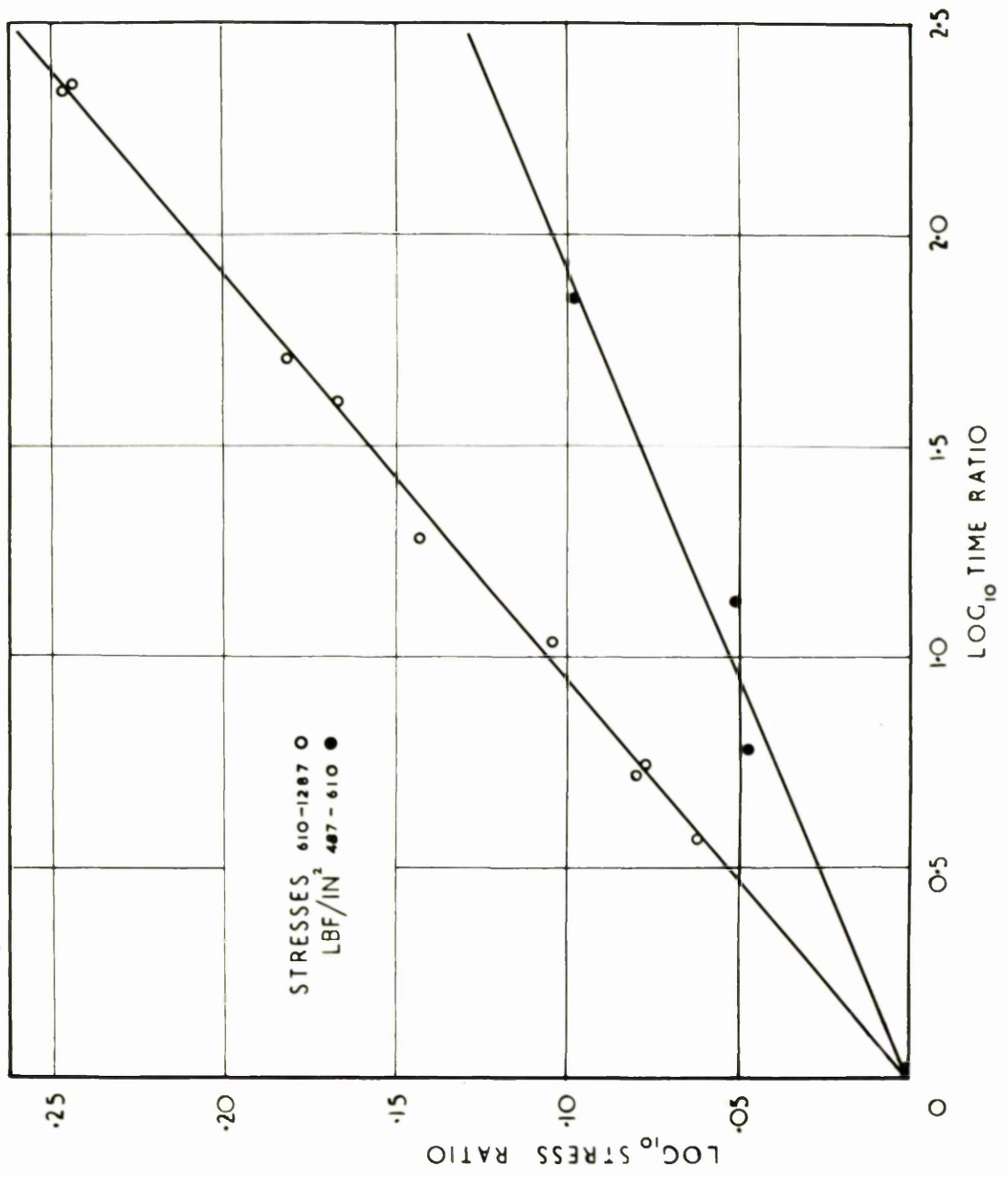


fig 24

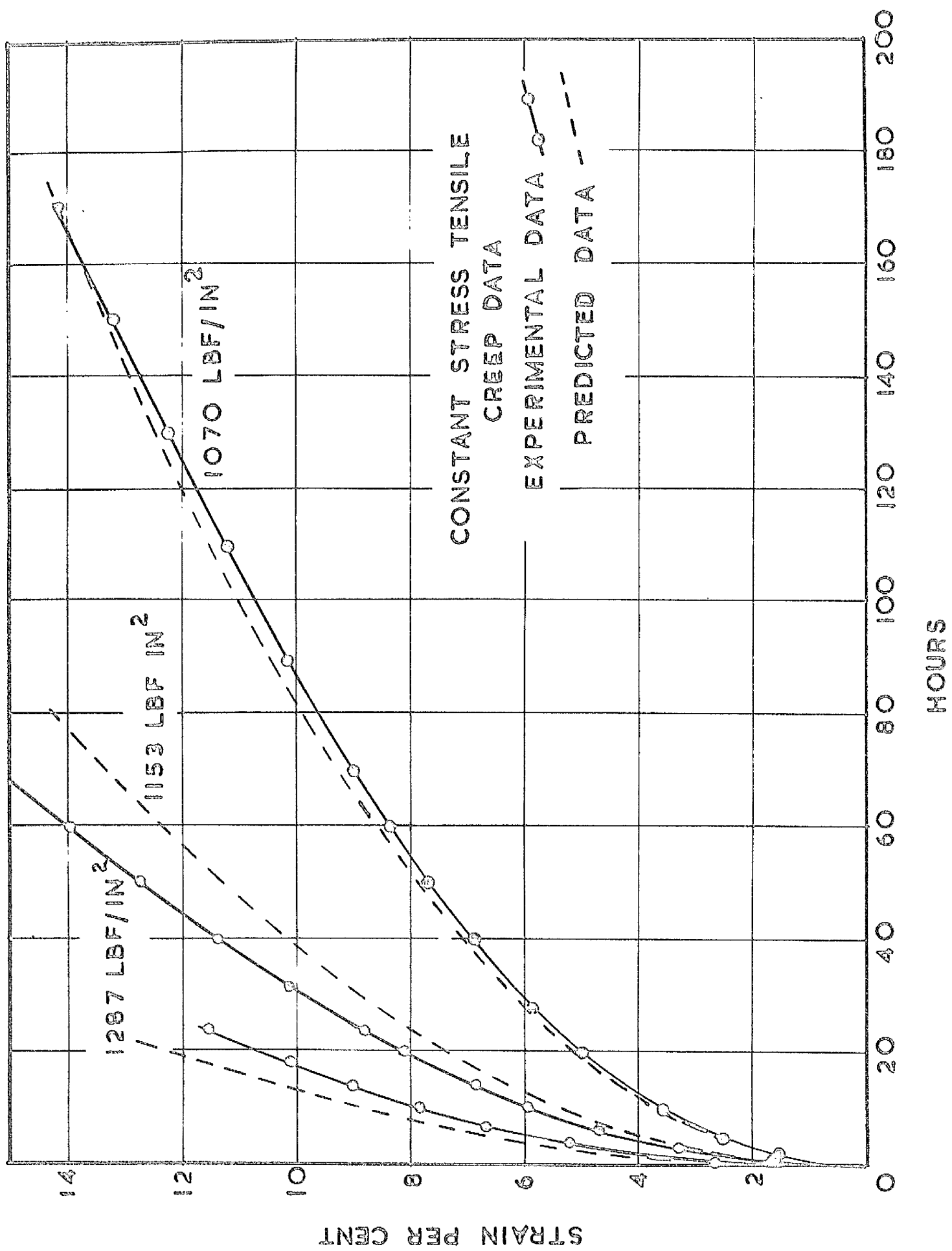


fig 25

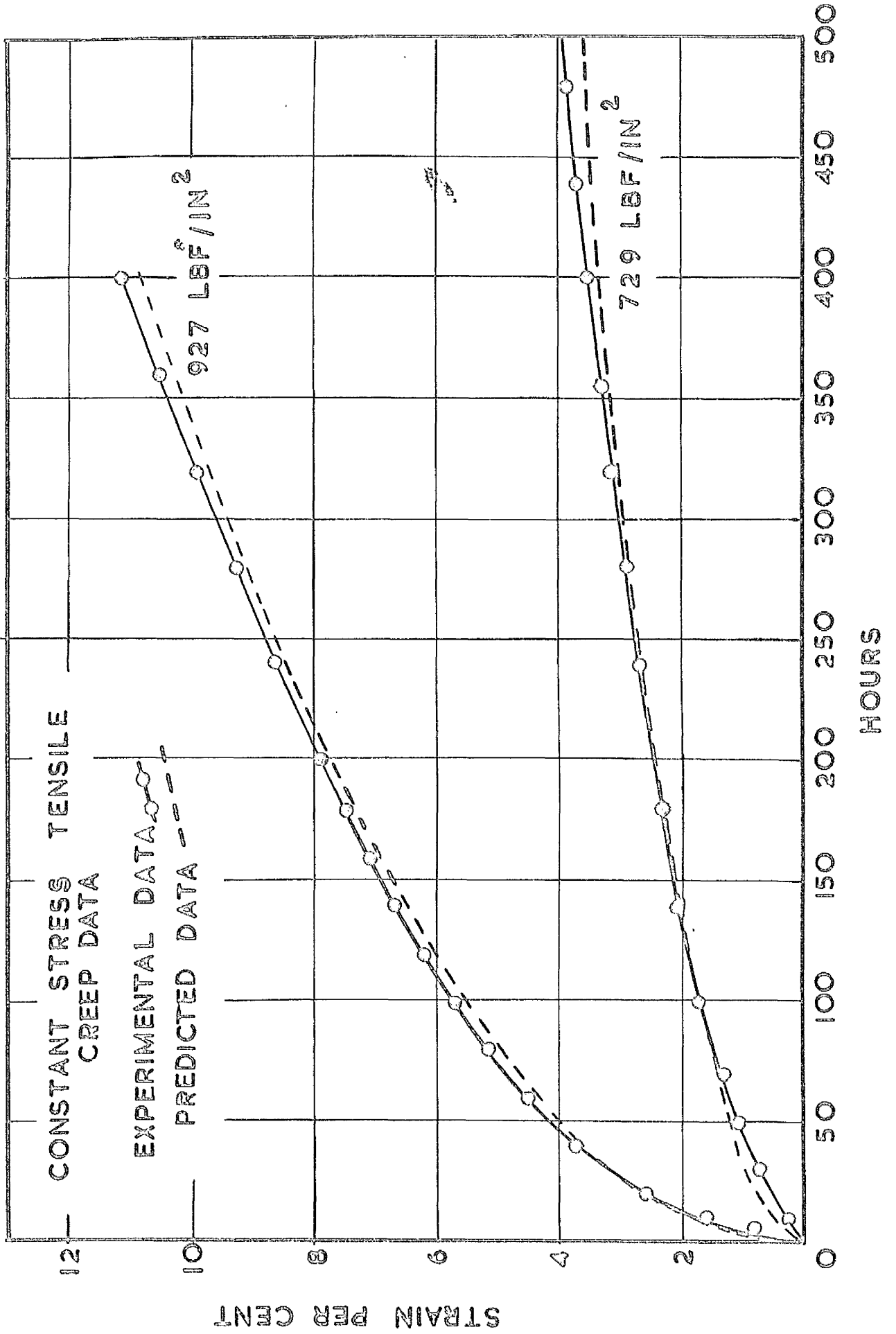


fig 26

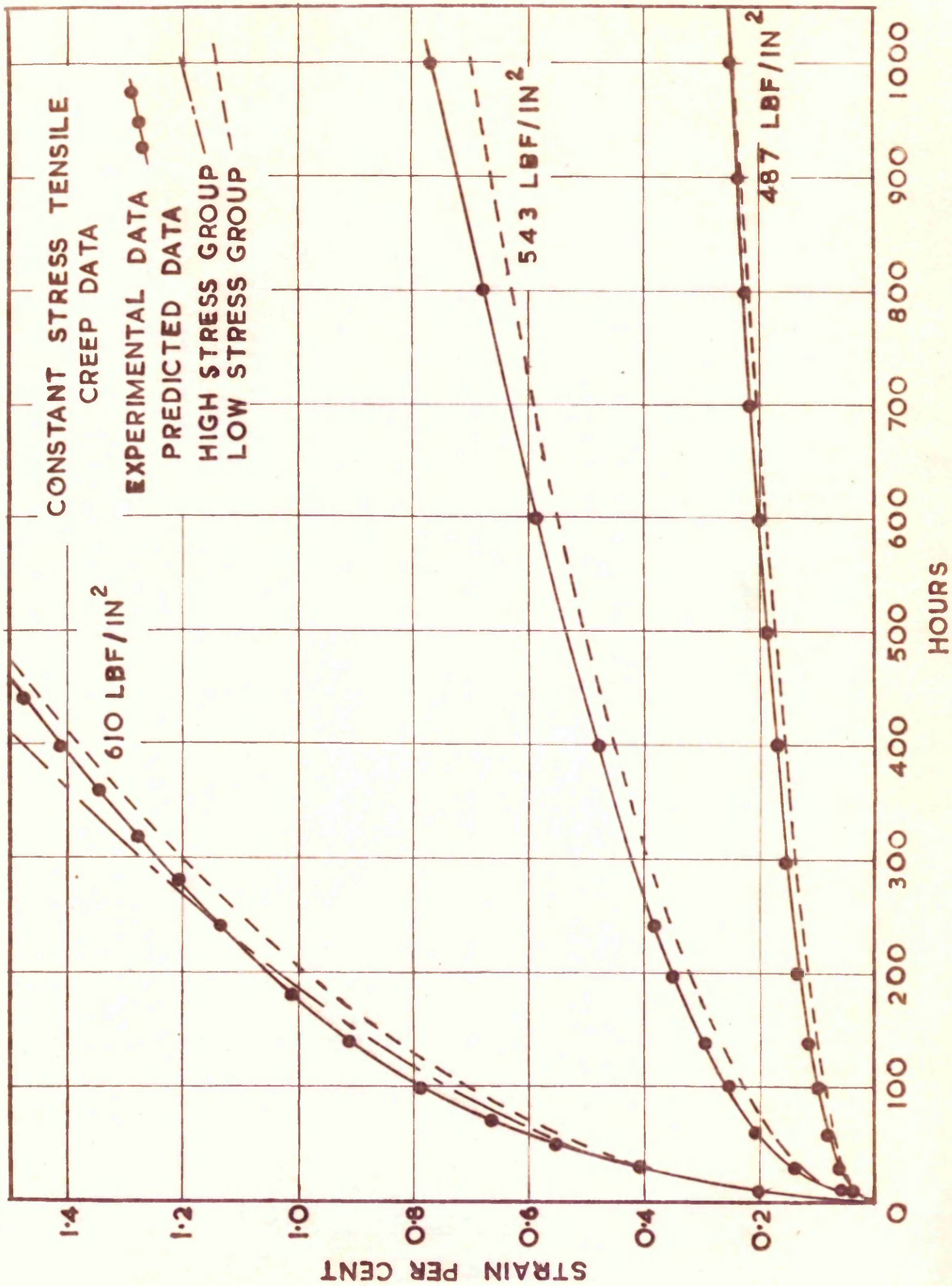


fig 27

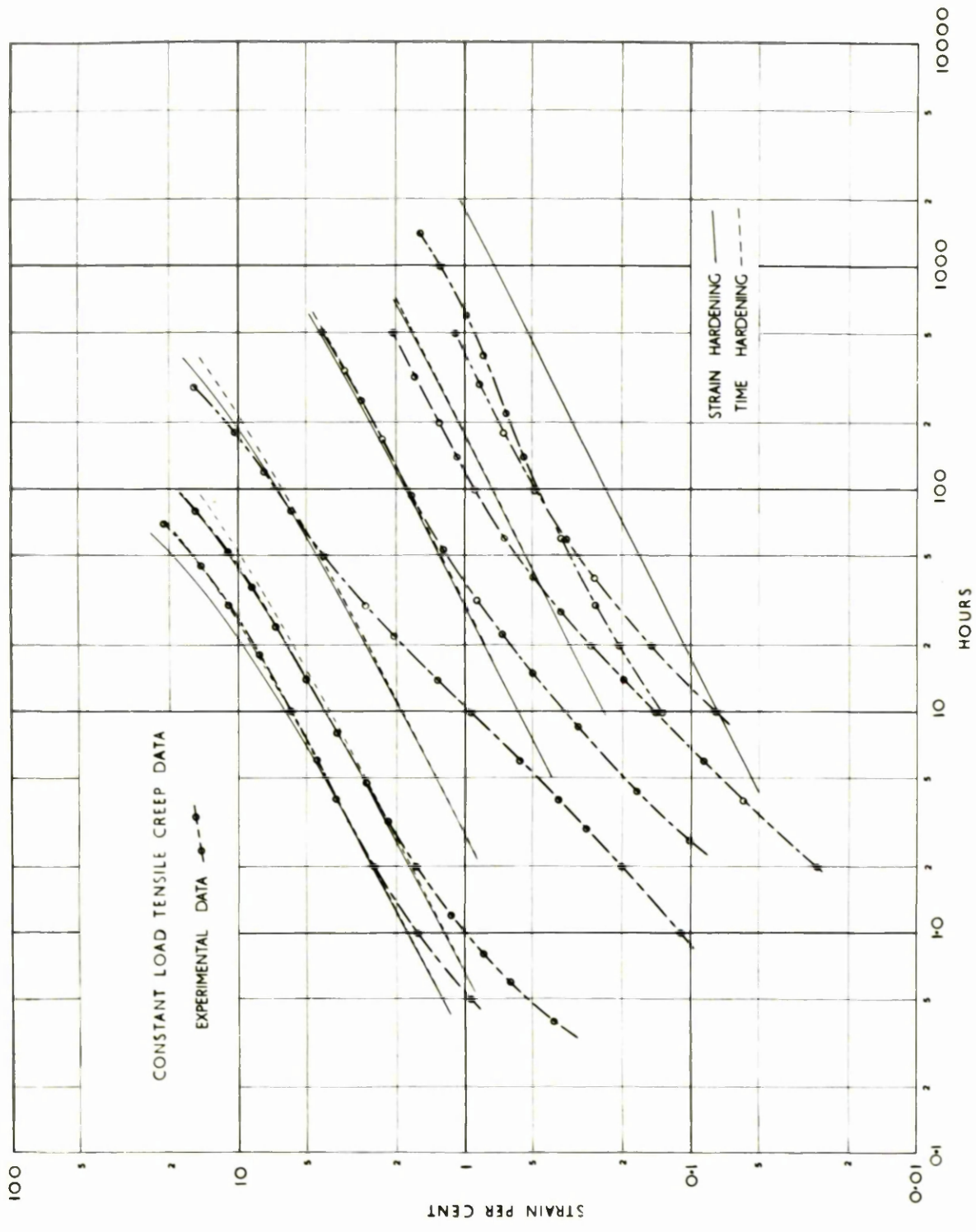


fig 28

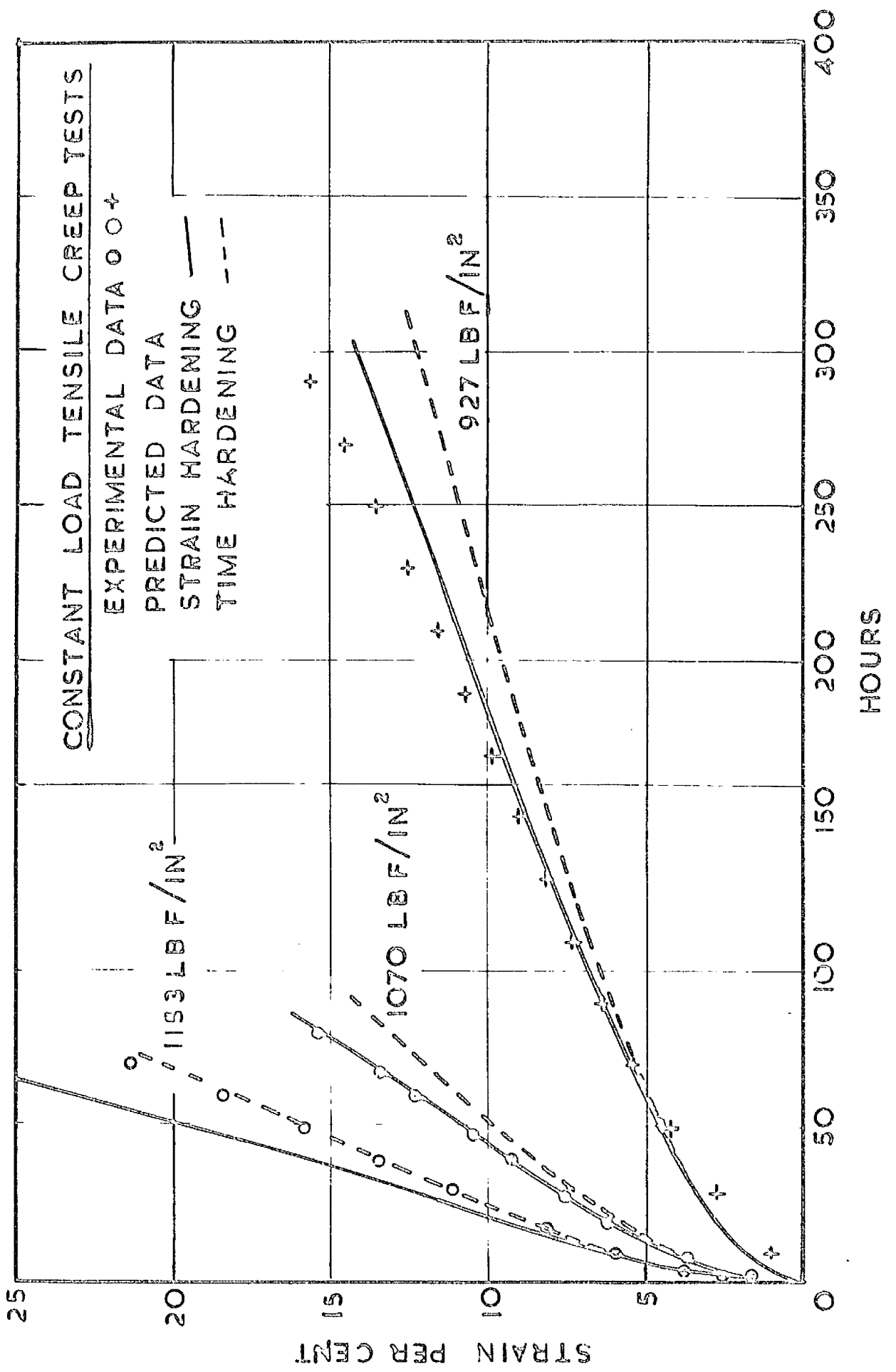


fig 29

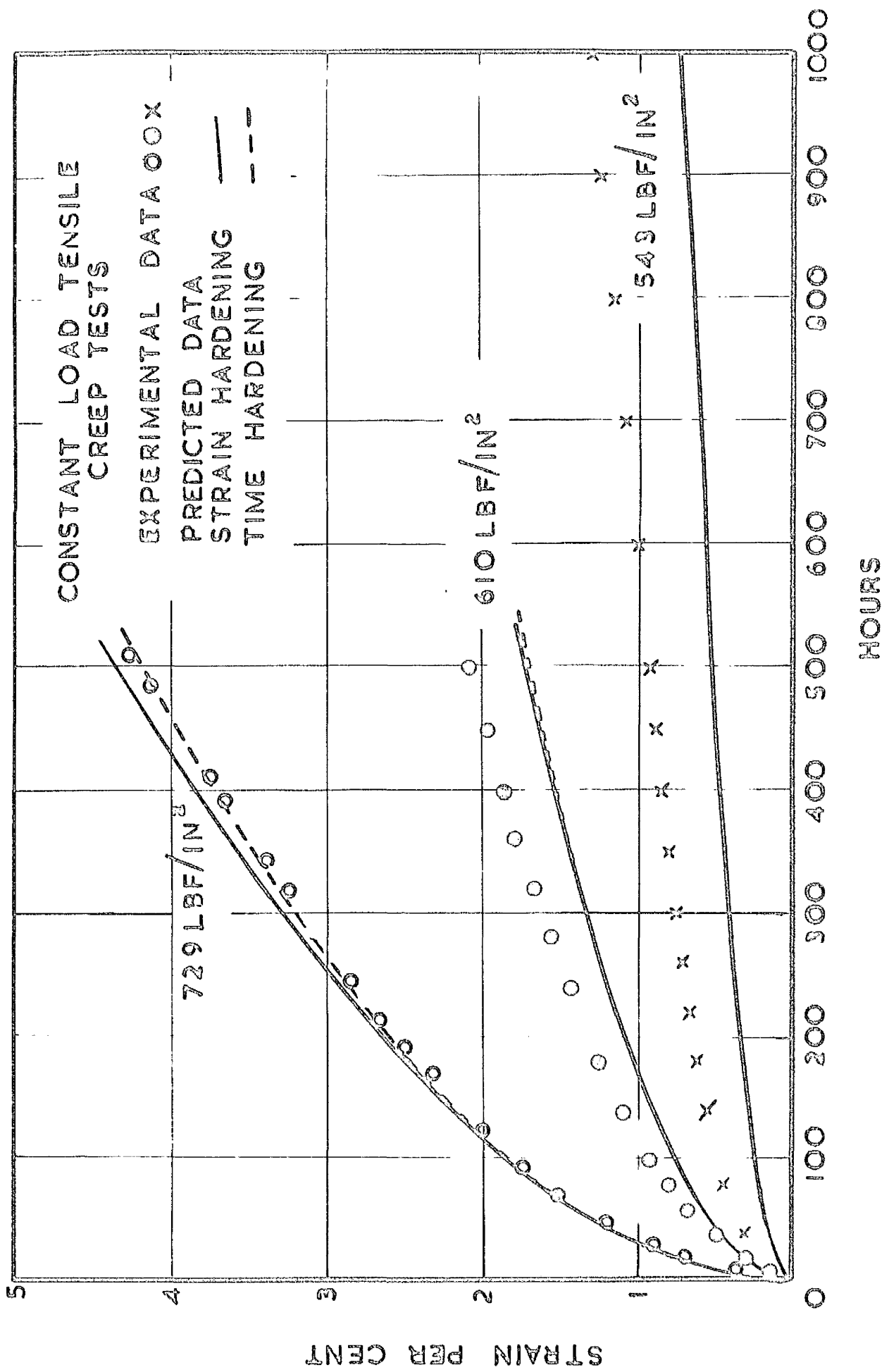
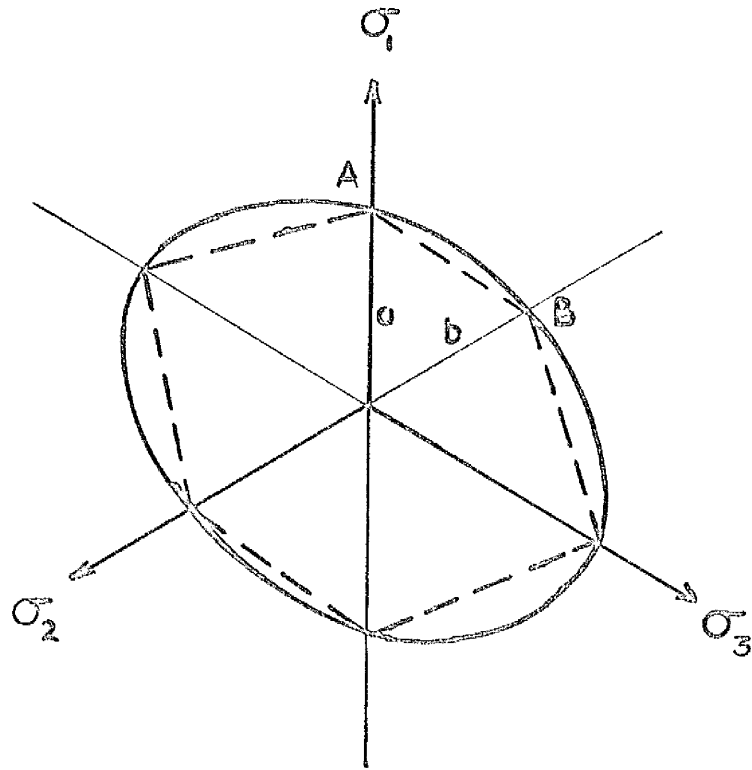
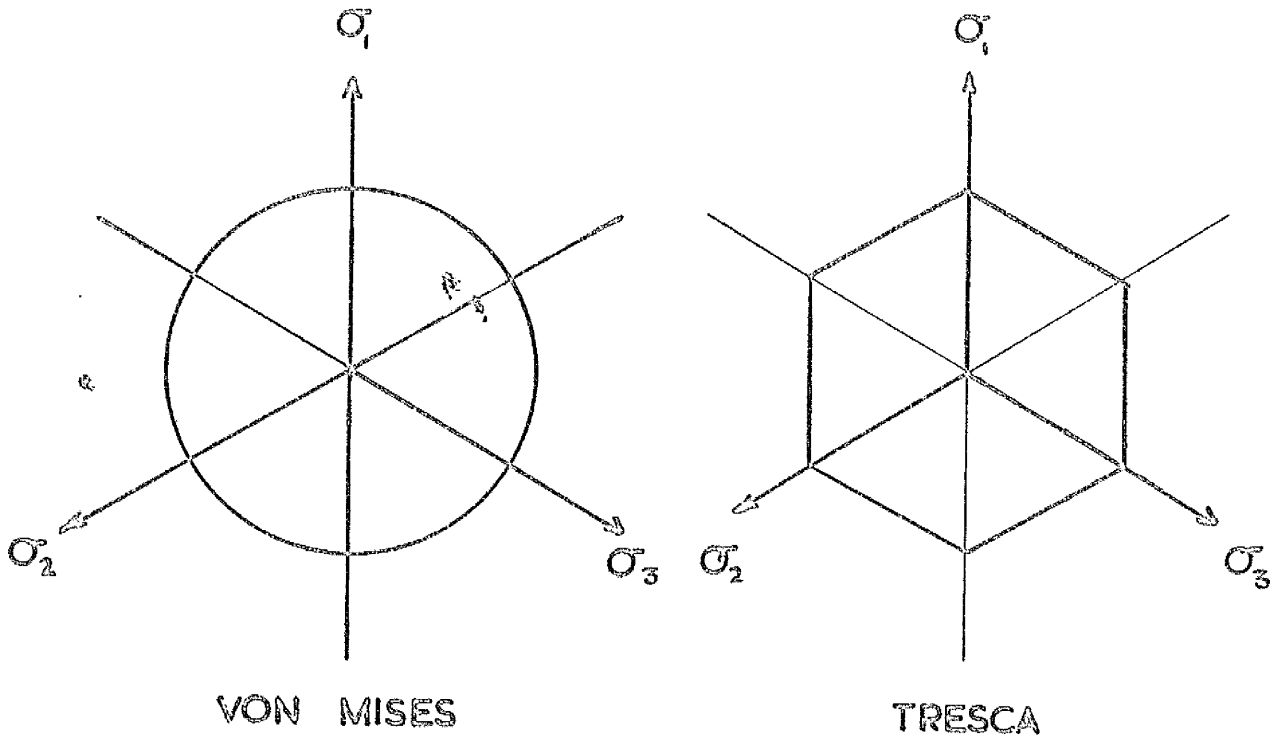


fig 30



BERMAN & PAI ANISOTROPIC

fig 31

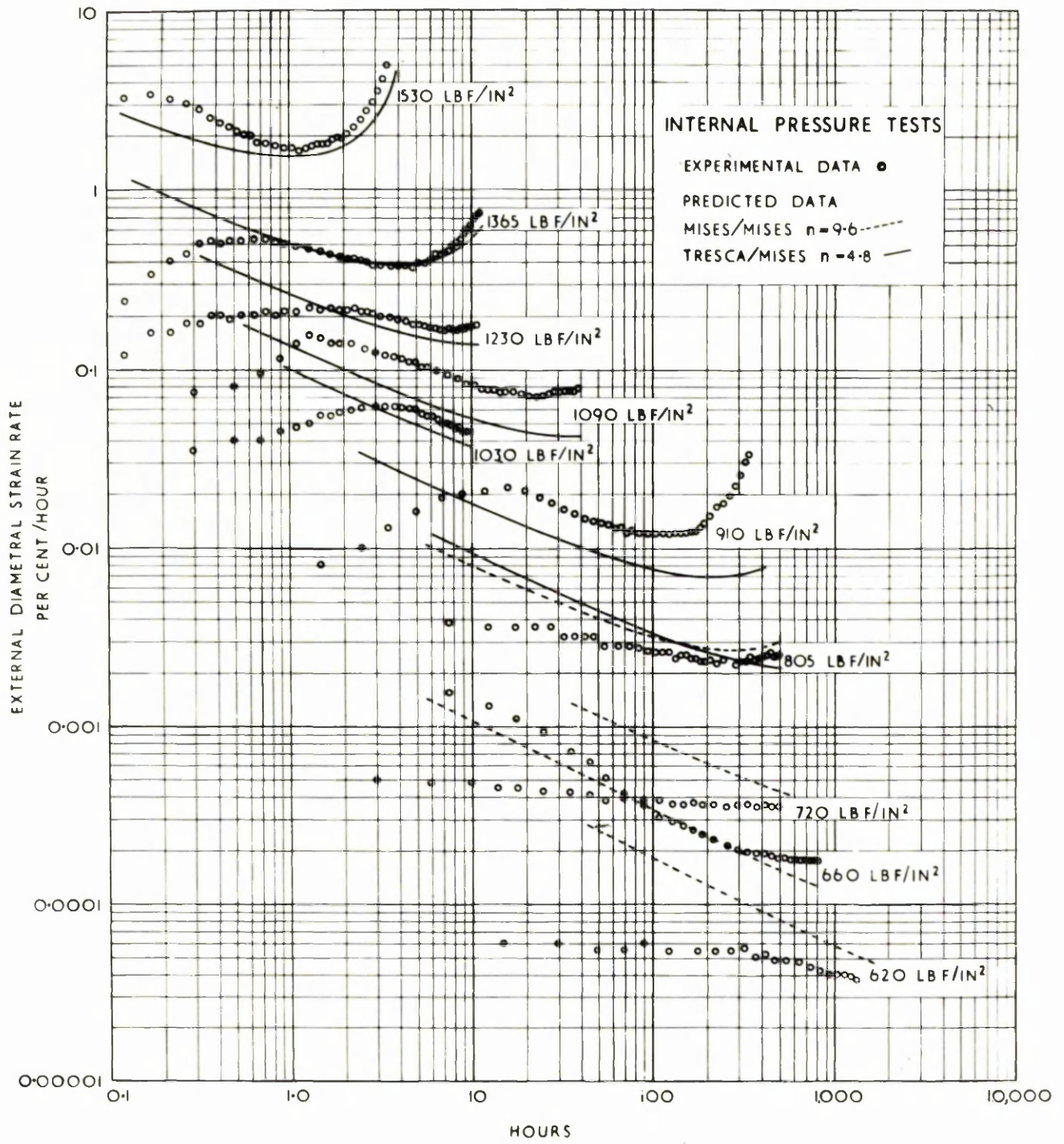


fig 32

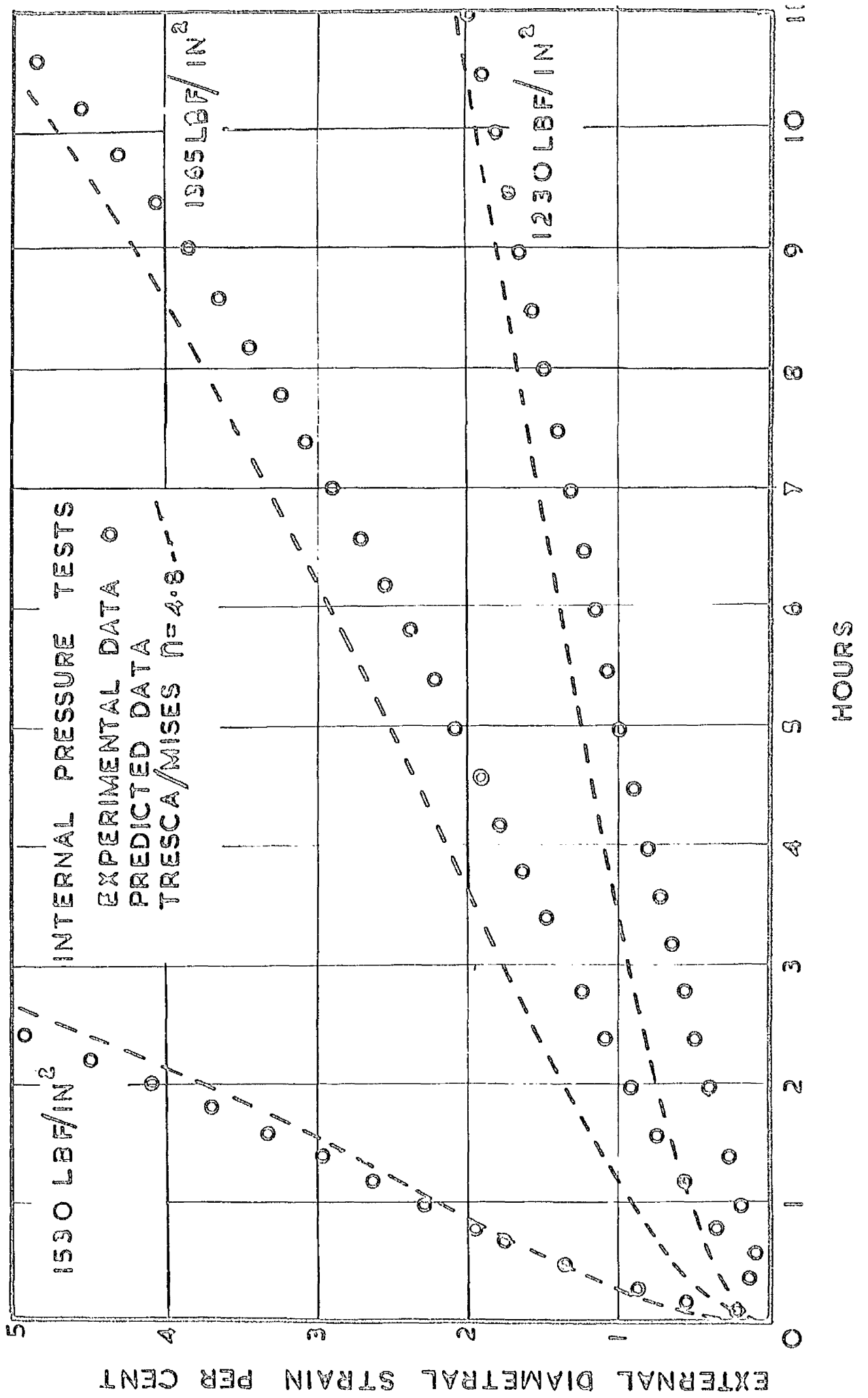


fig 33

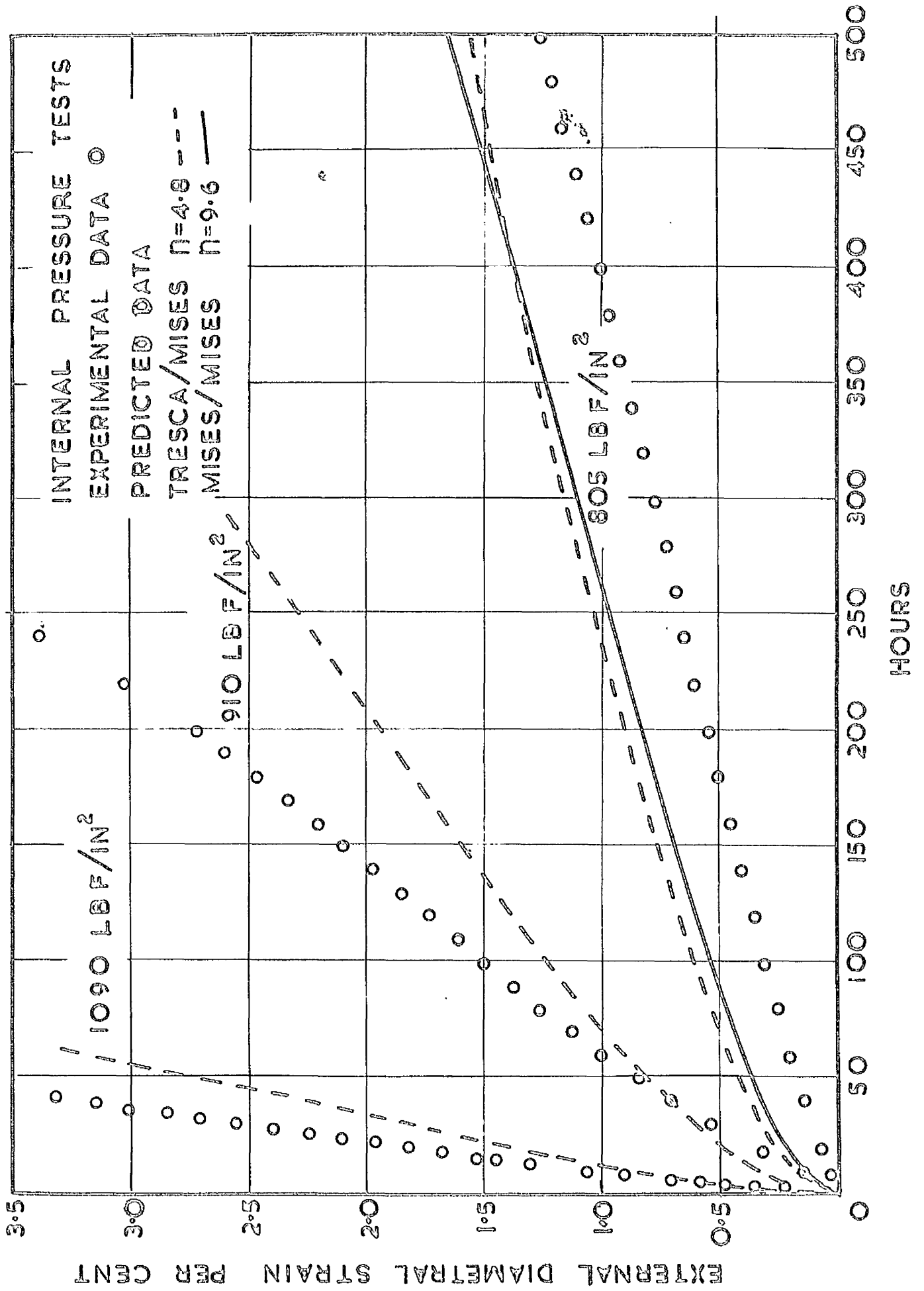


fig 34

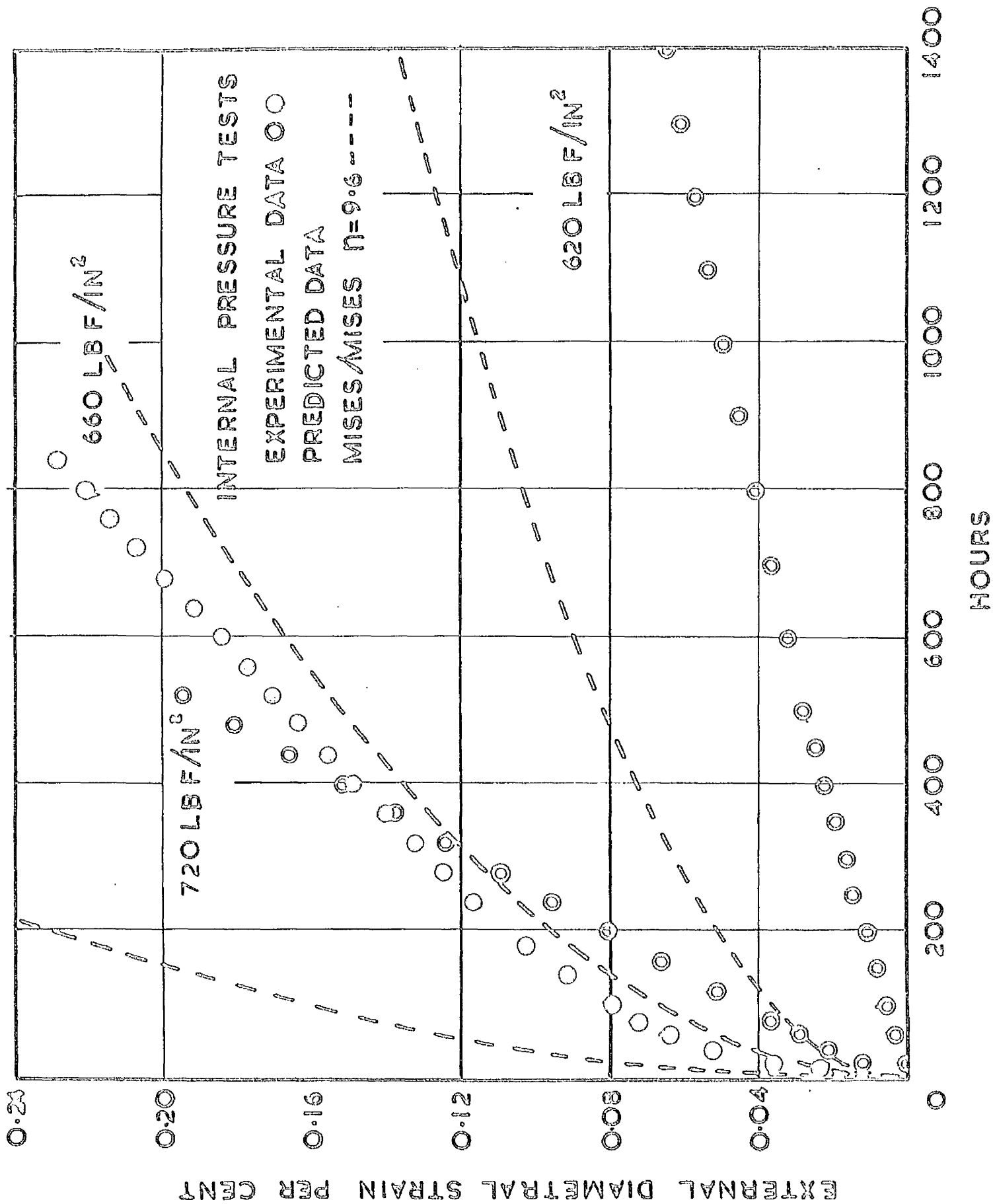


fig 35

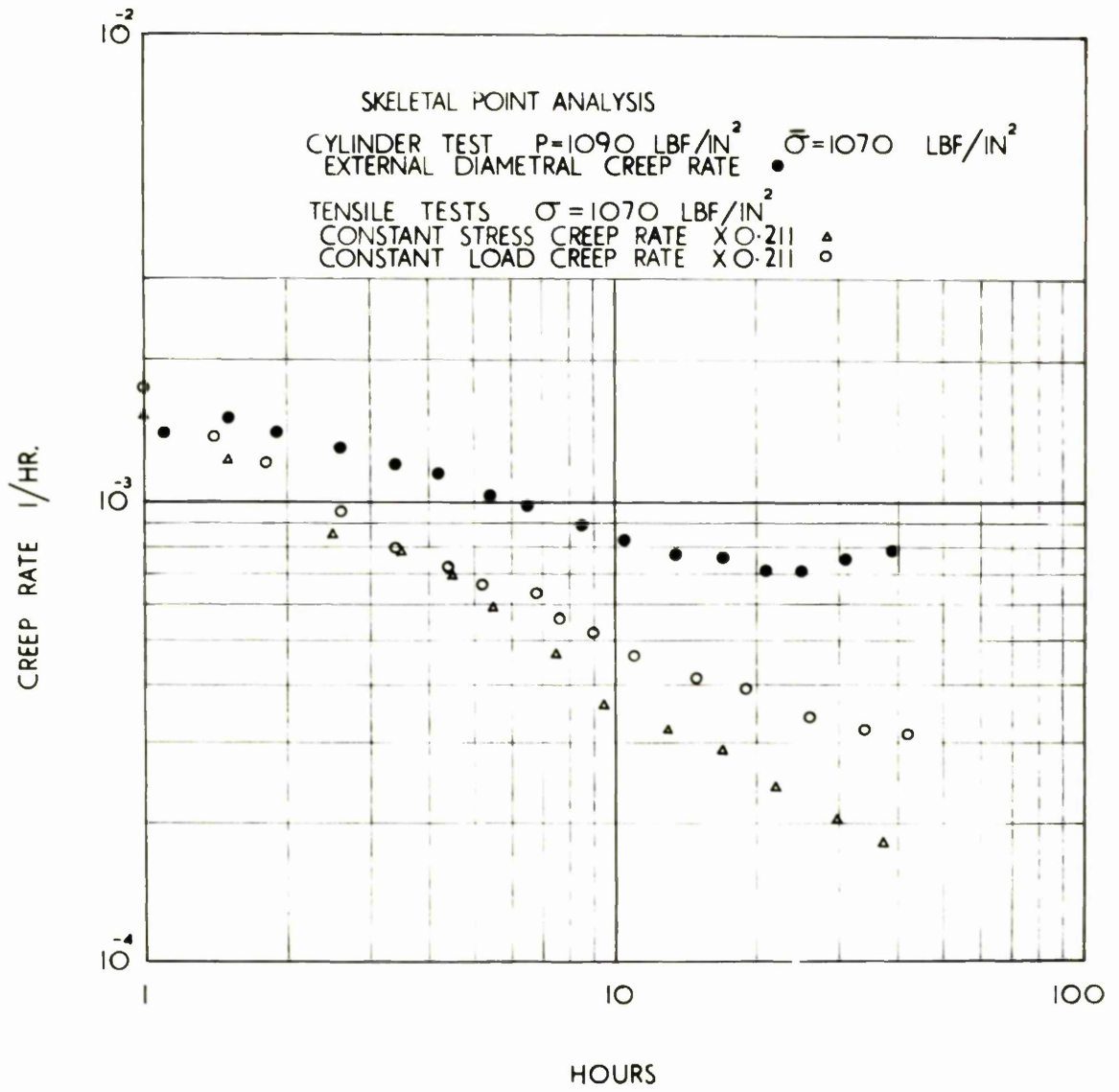


fig 36

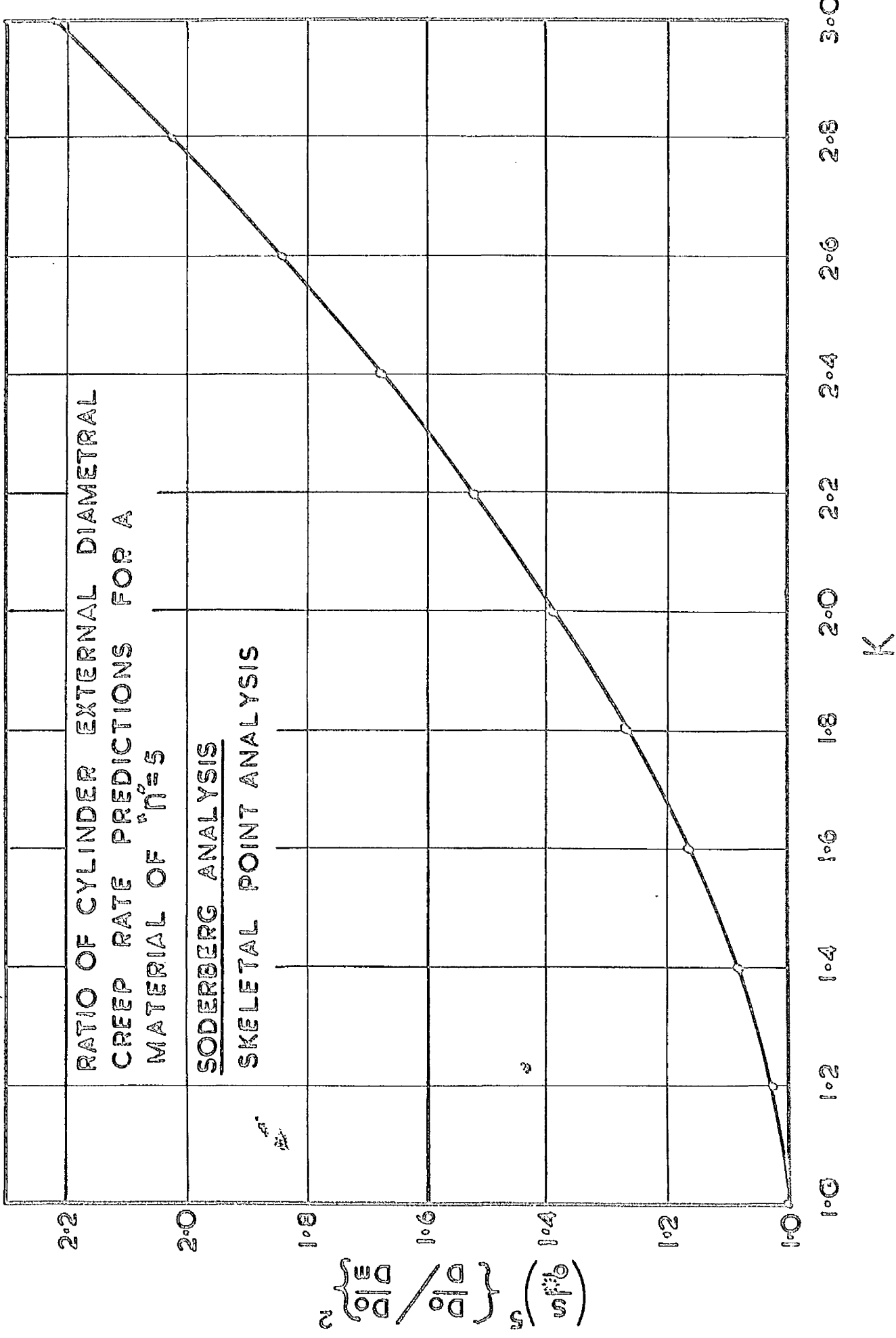


fig 37

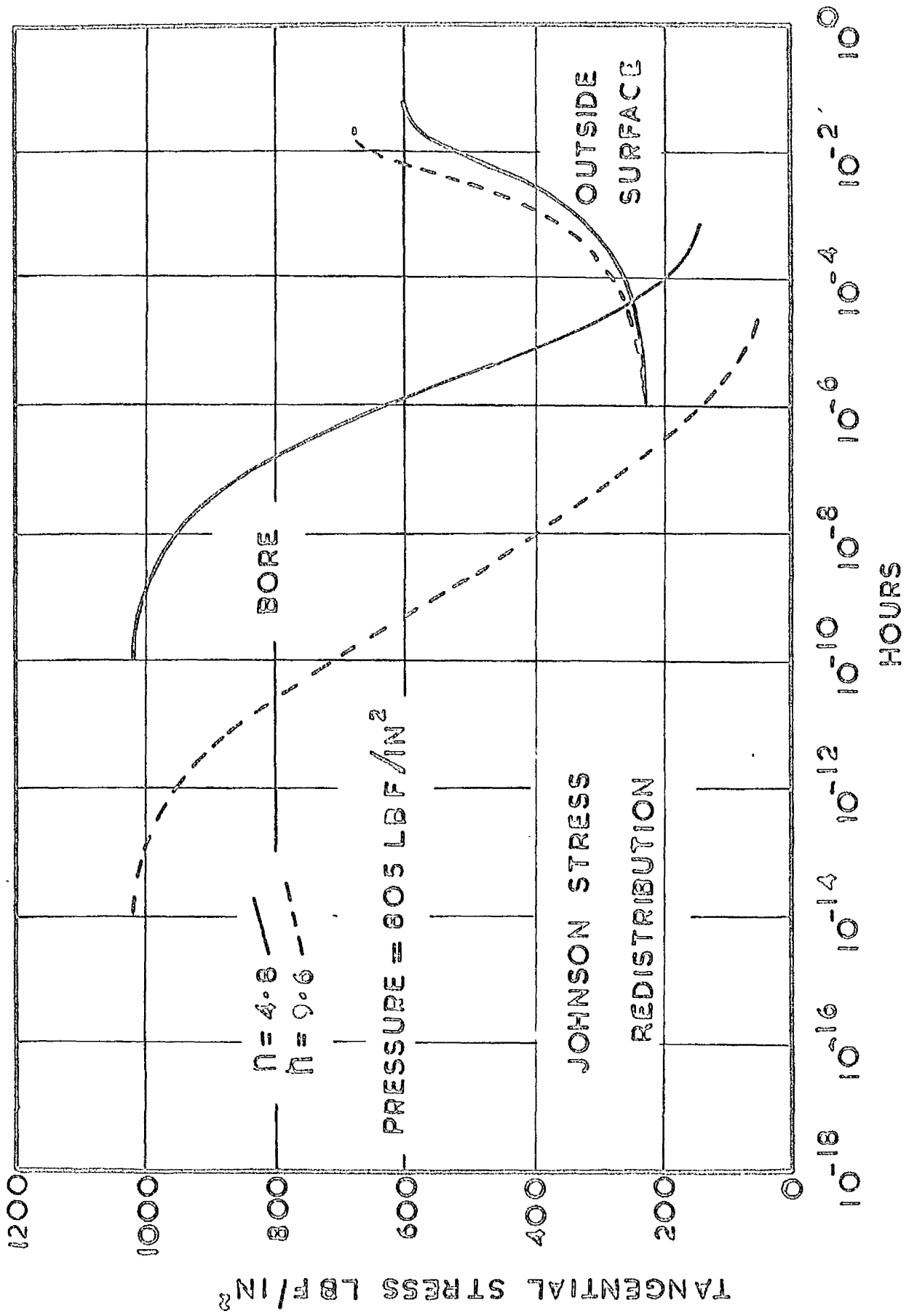


fig 38

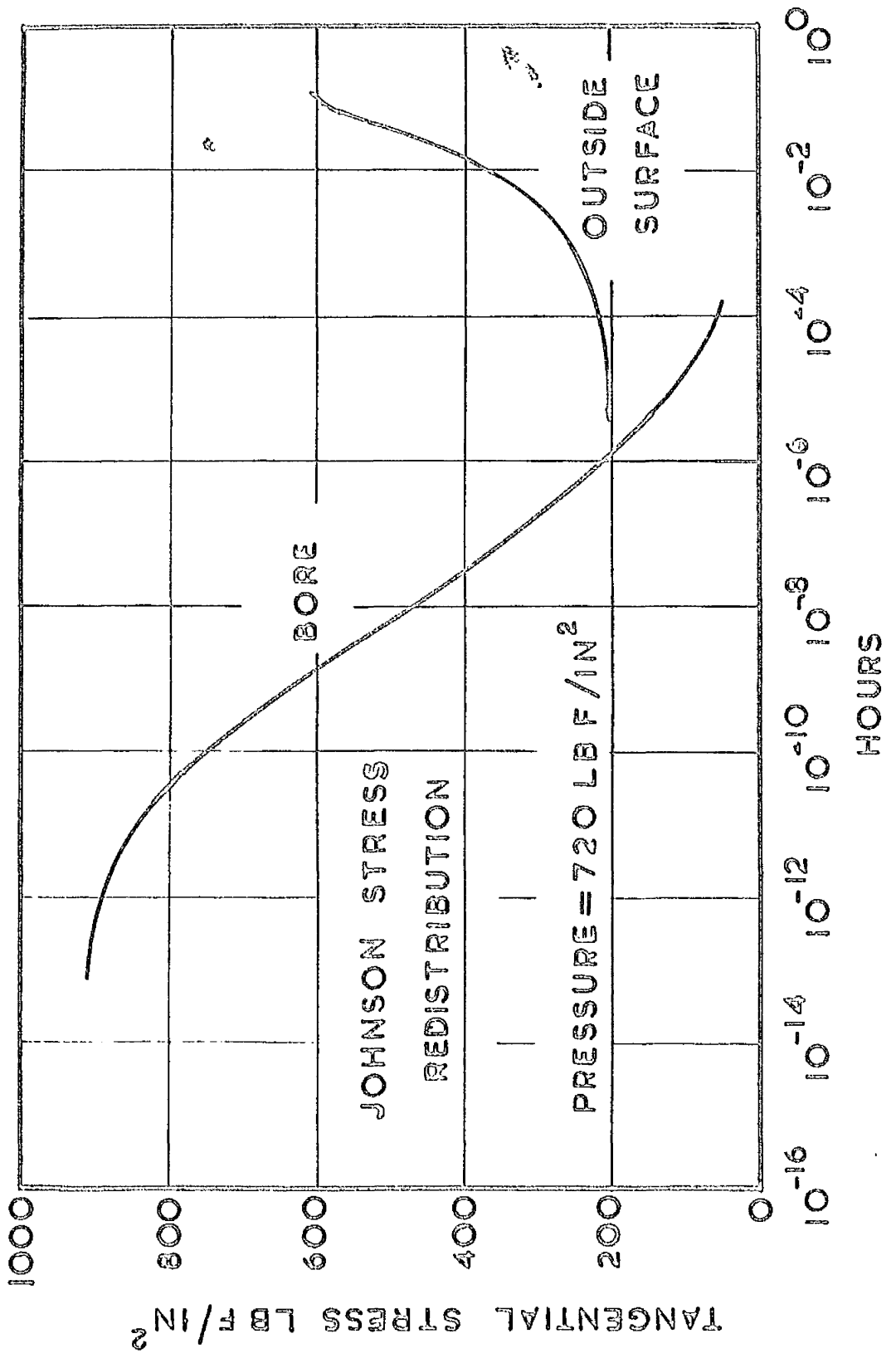


fig 39

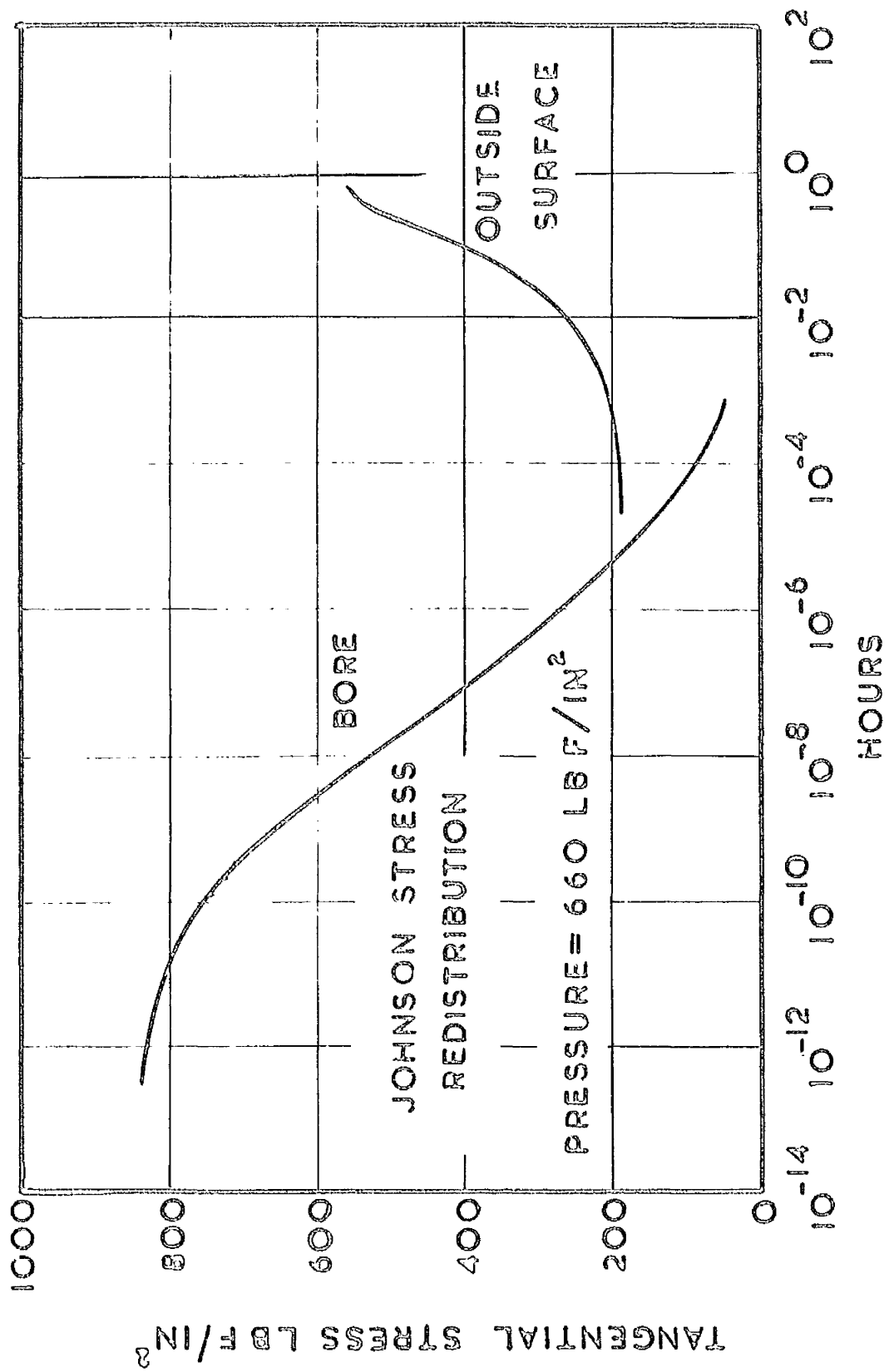


fig 40

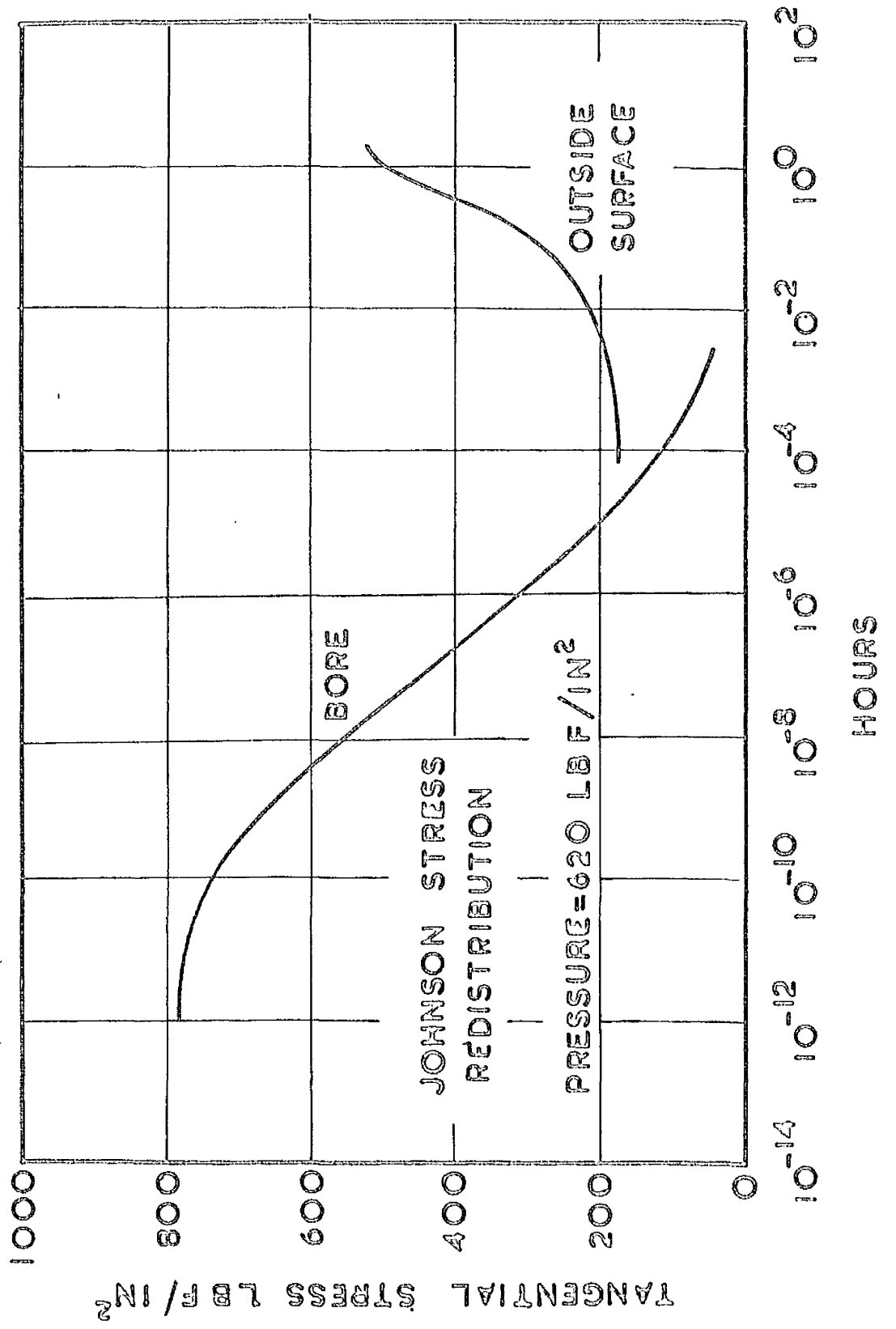


fig 41

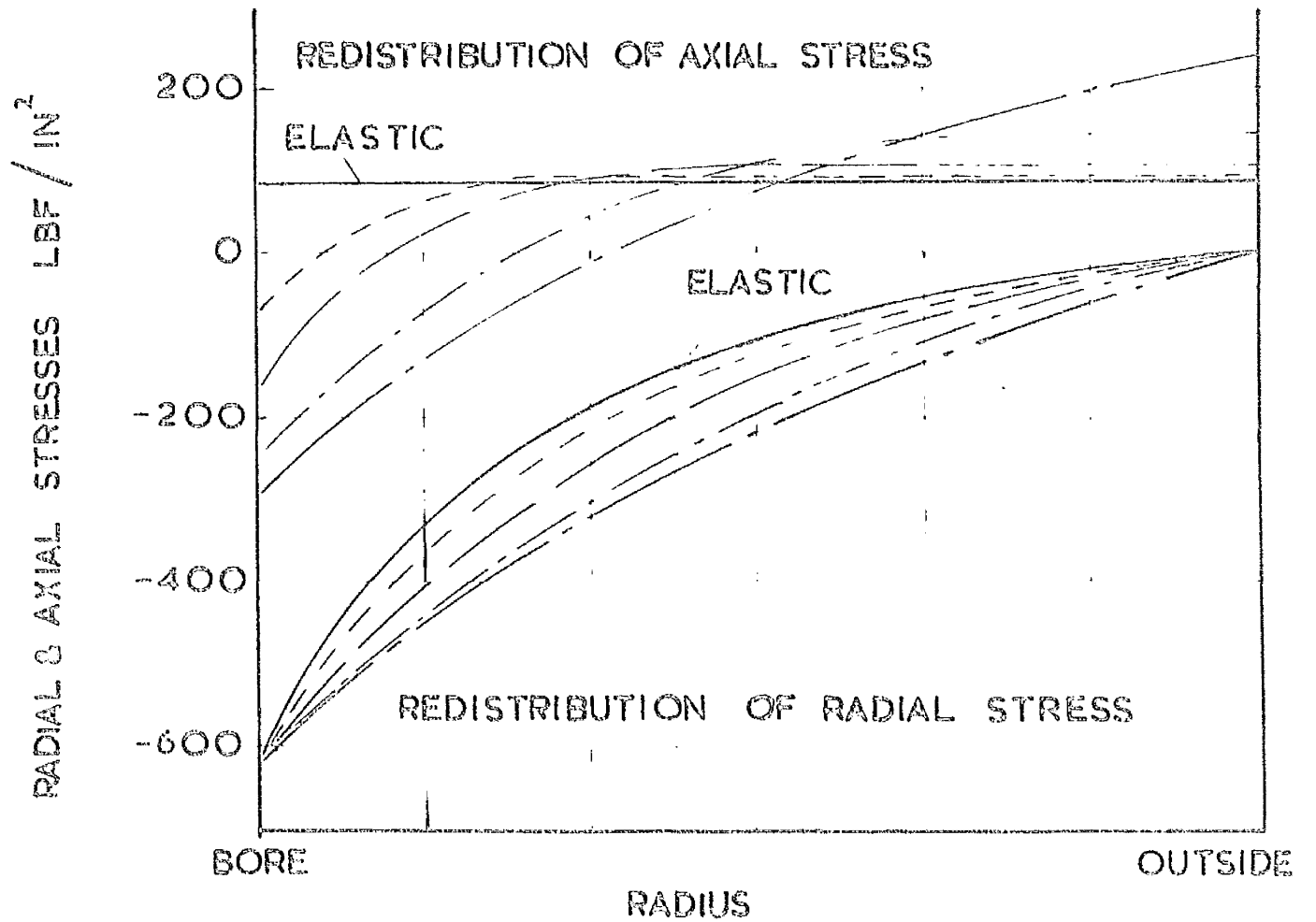
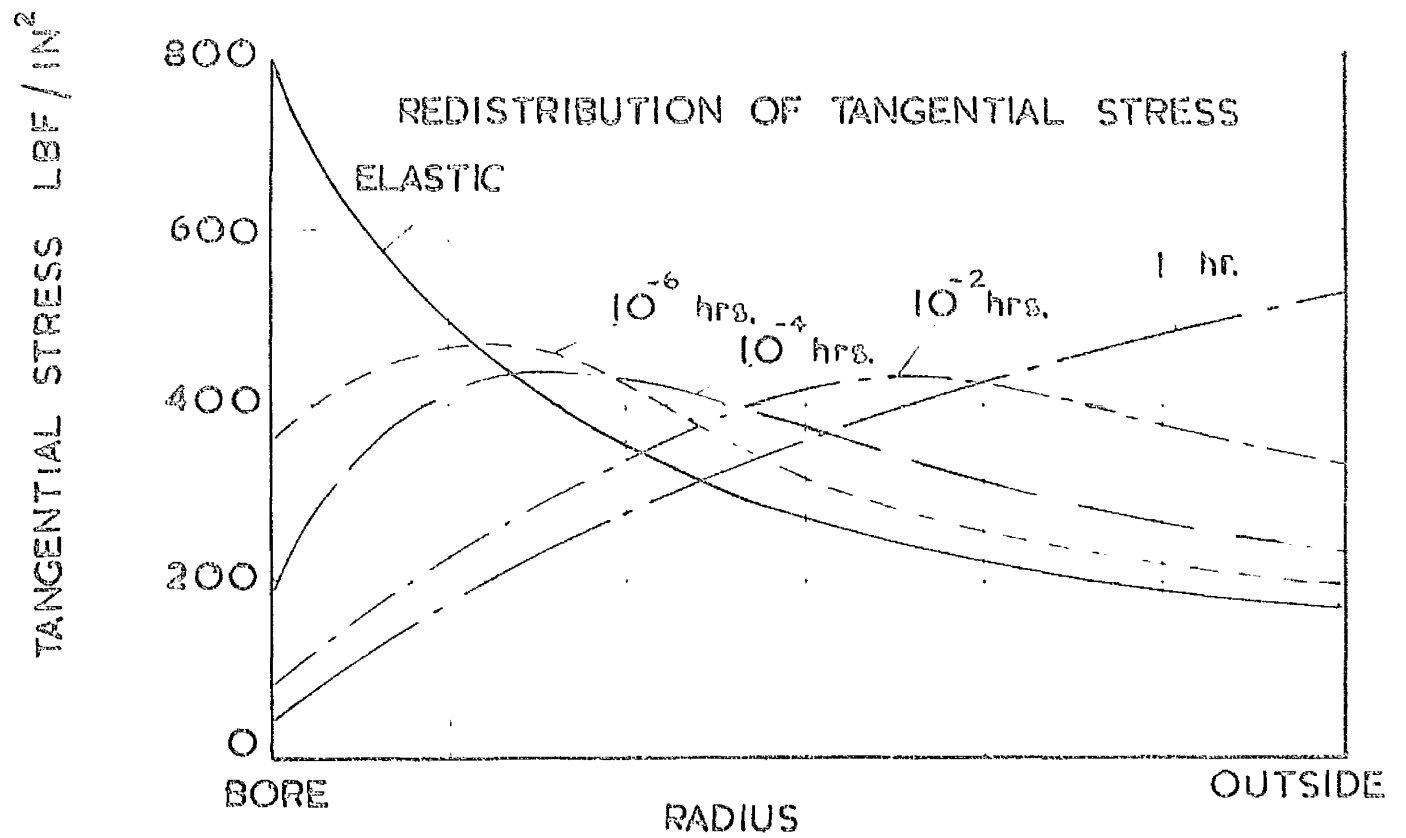


fig 42

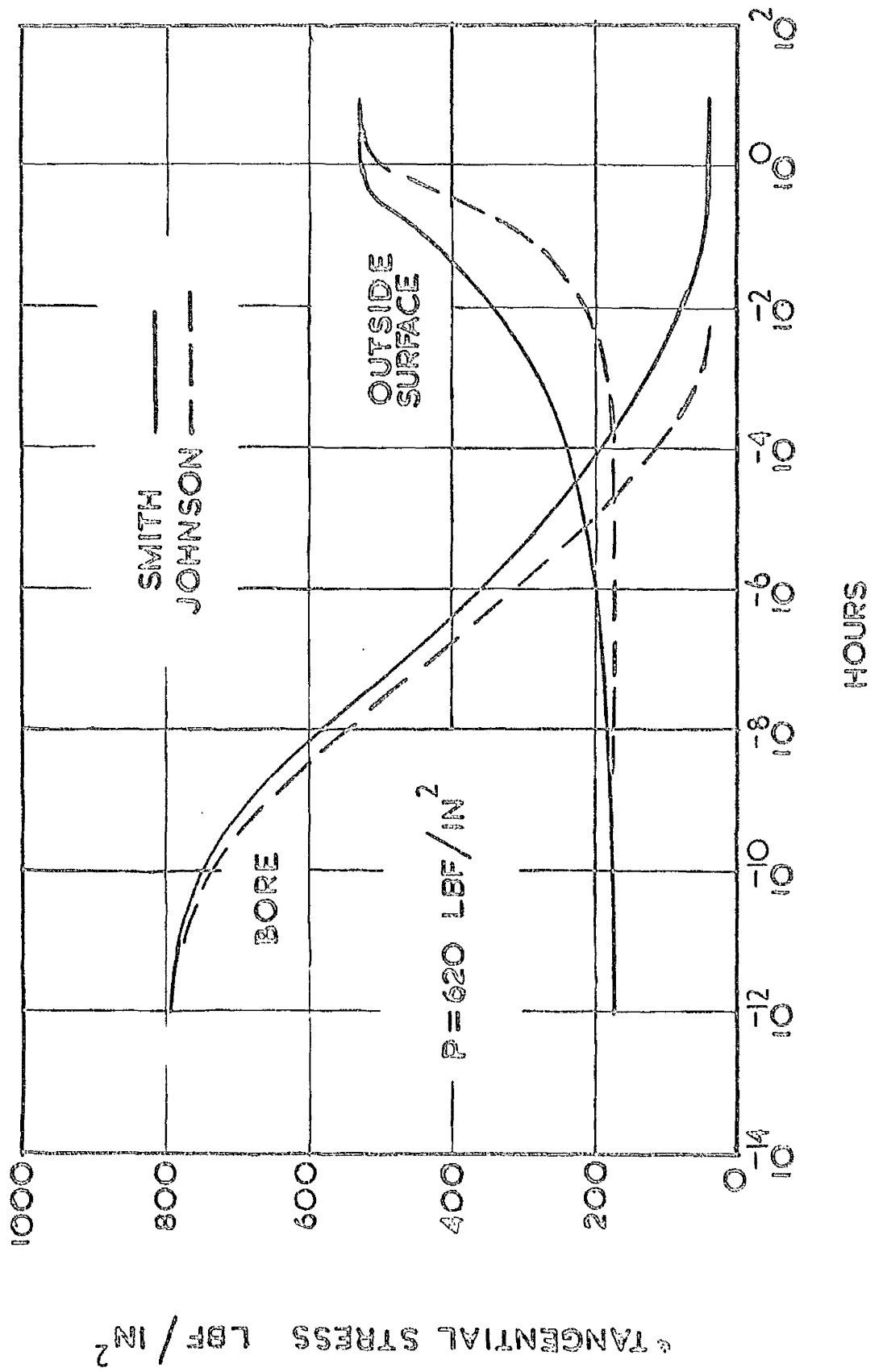


fig 43

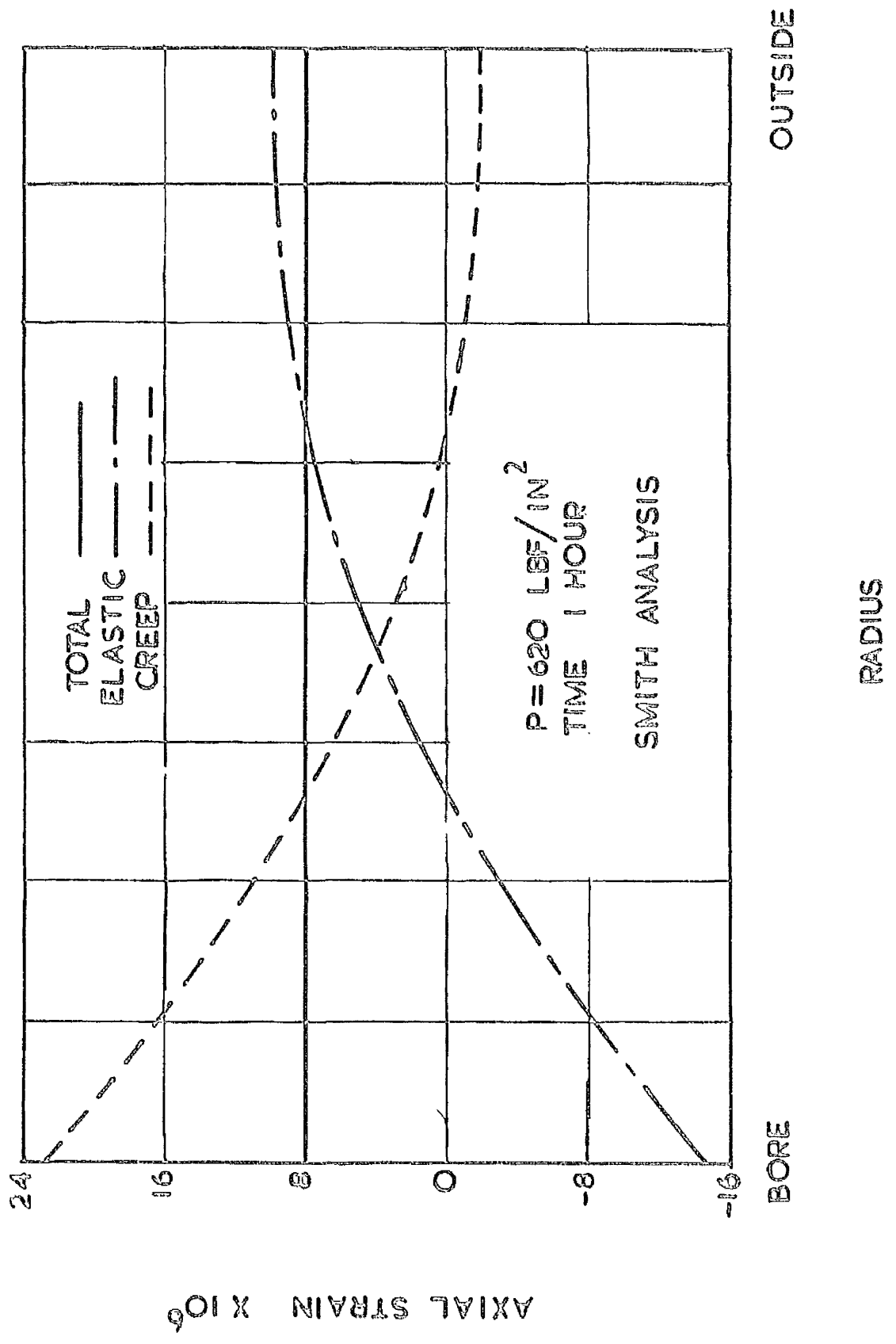


fig 44

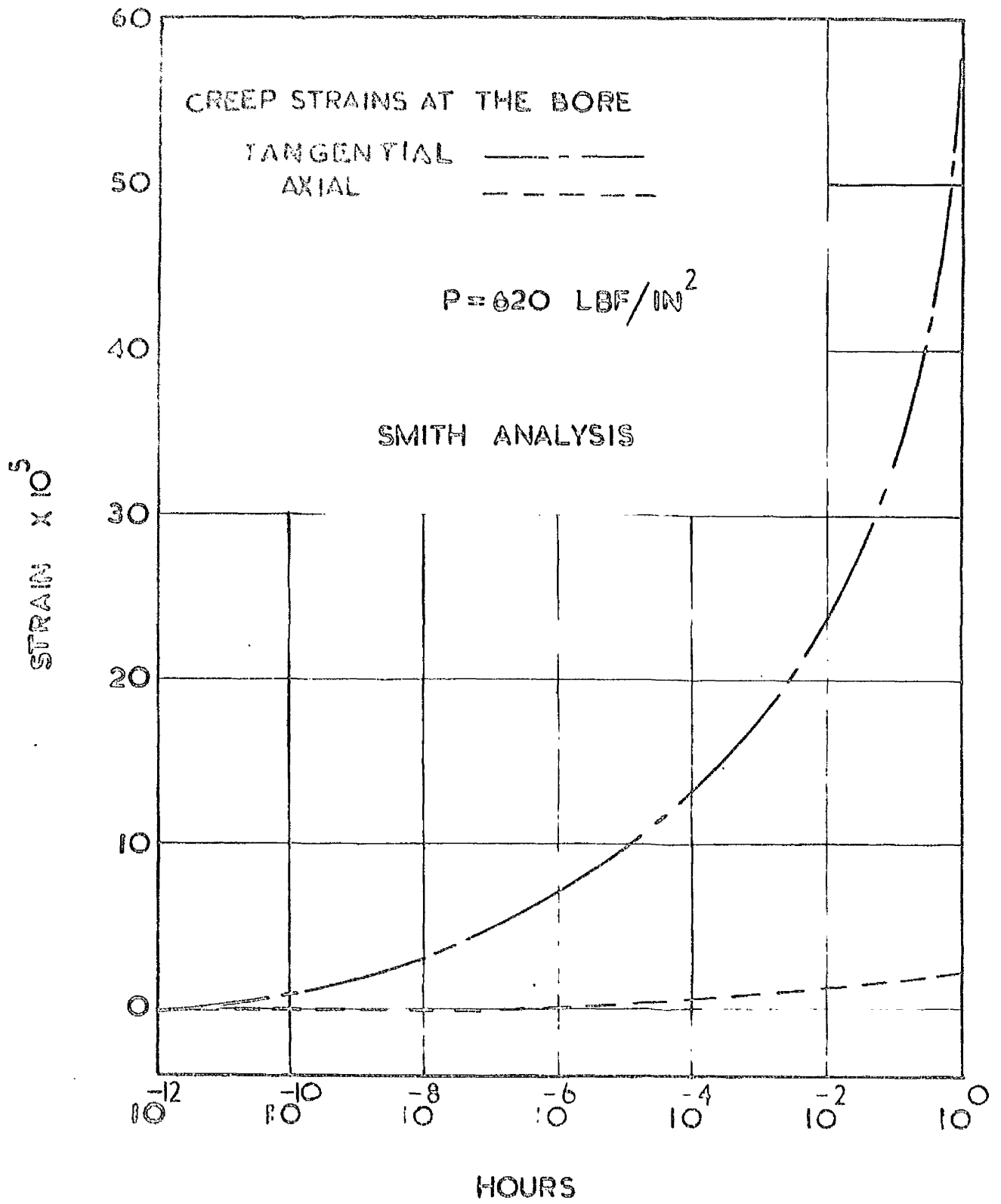


fig 45

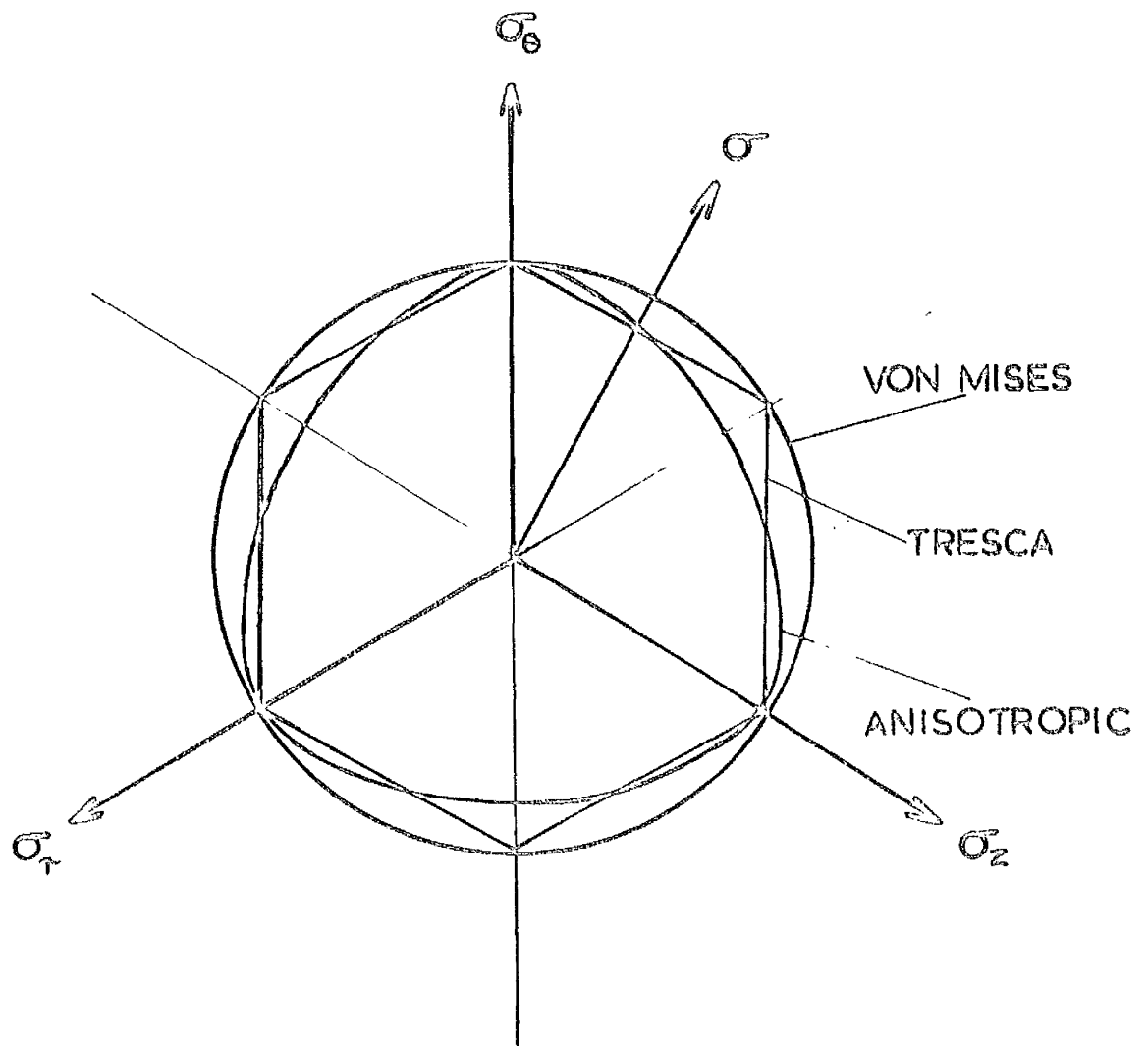
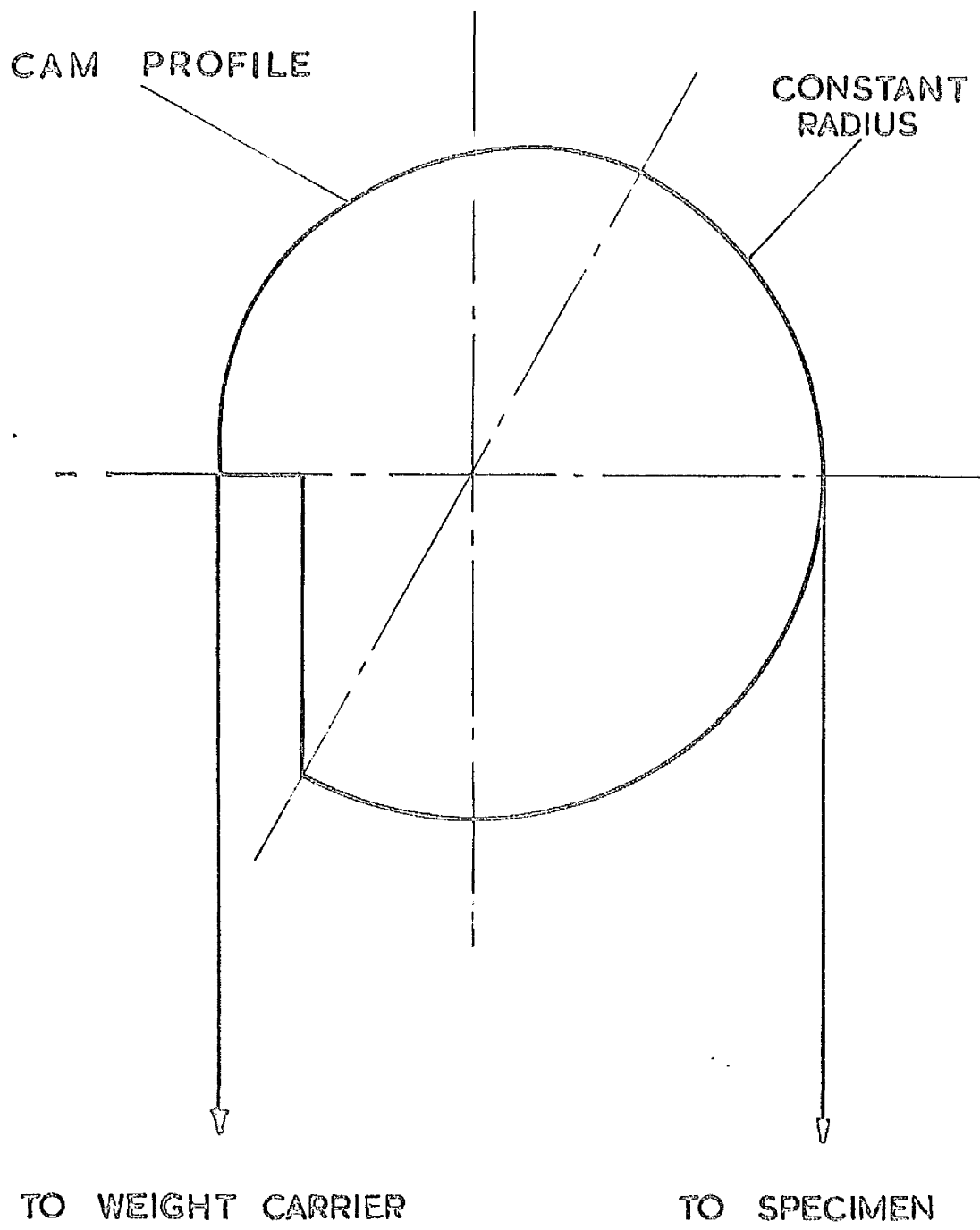


fig 46



GENERAL FORM OF CAM PROFILE FOR INCREASING TENSILE STRESS

BILLET "CUTTING UP" DIAGRAM

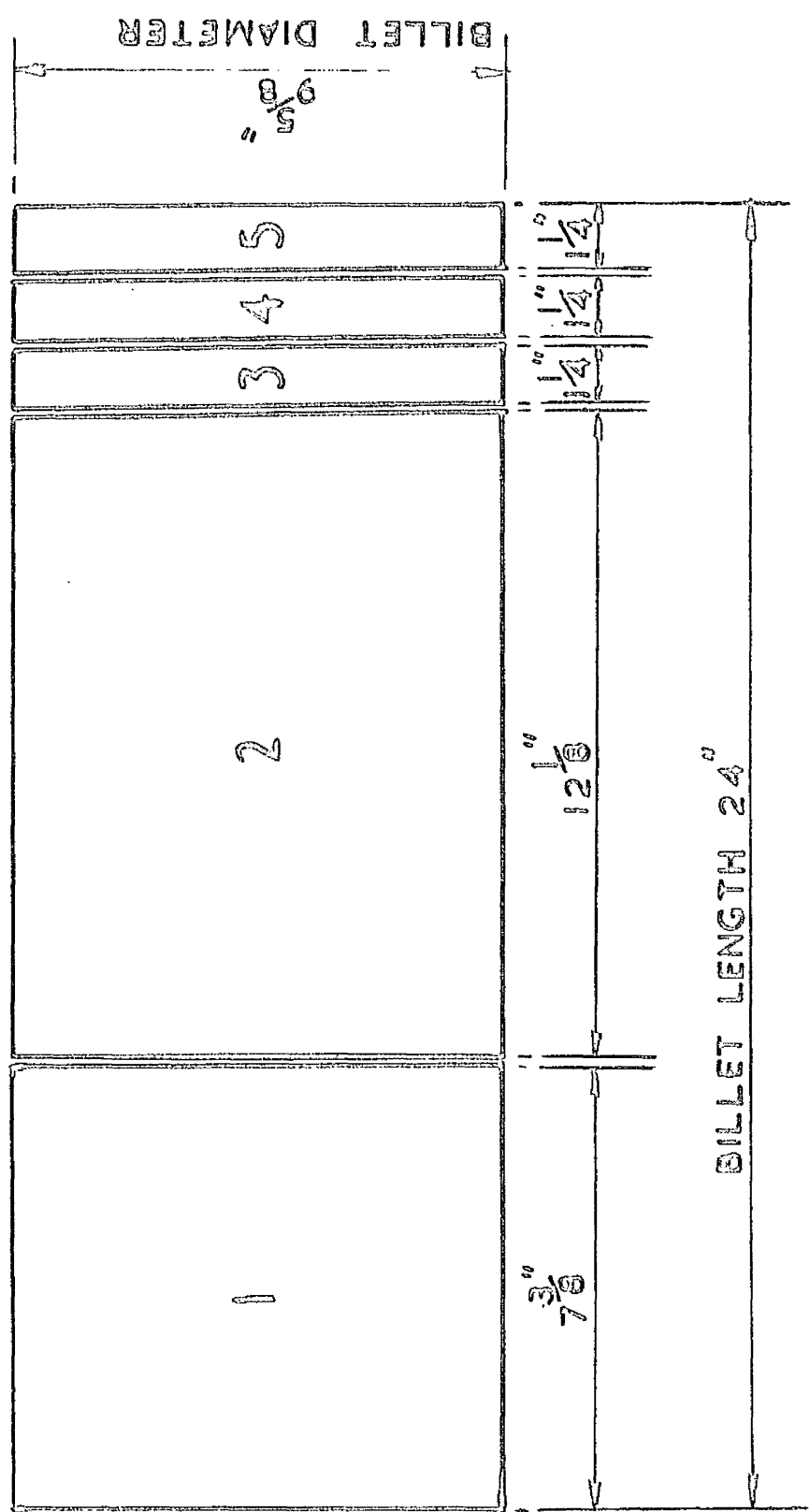
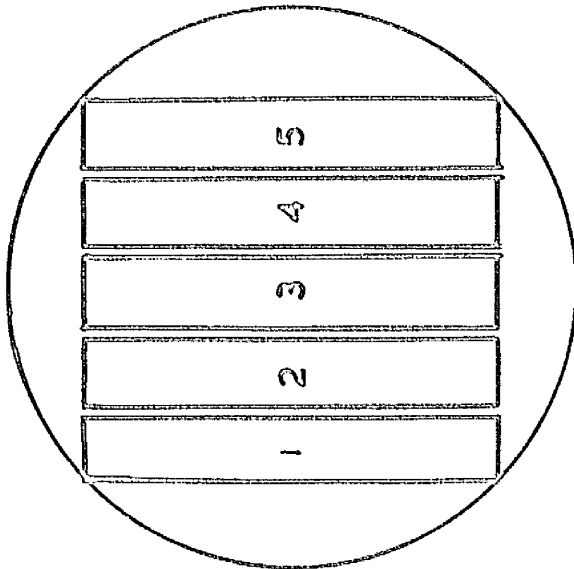
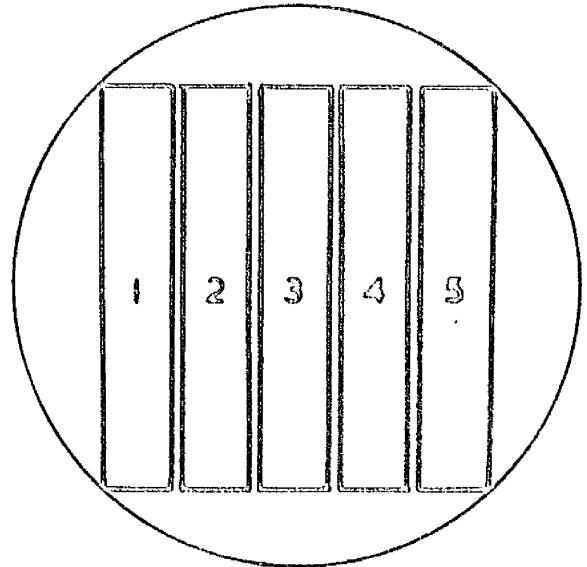


fig 48

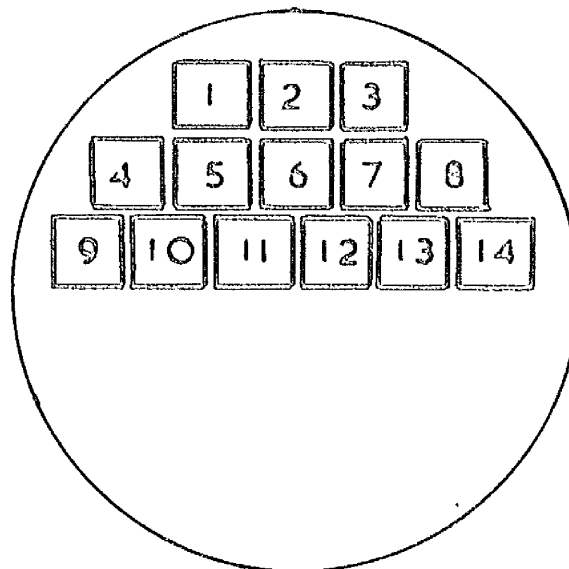
POSITION OF TENSILE SPECIMEN BLANKS IN BILLET



SLICE 4  
"B" DIRECTION



SLICES 3 & 5  
"A" DIRECTION



CROSS SECTION  
OF BLANKS

$1\frac{3}{16}$ " X  $1\frac{3}{16}$ "

SLICE 1  
AXIAL DIRECTION

POSITION OF TUBULAR SPECIMEN BLANKS CUT  
FROM SECTION 2 OF BILLET

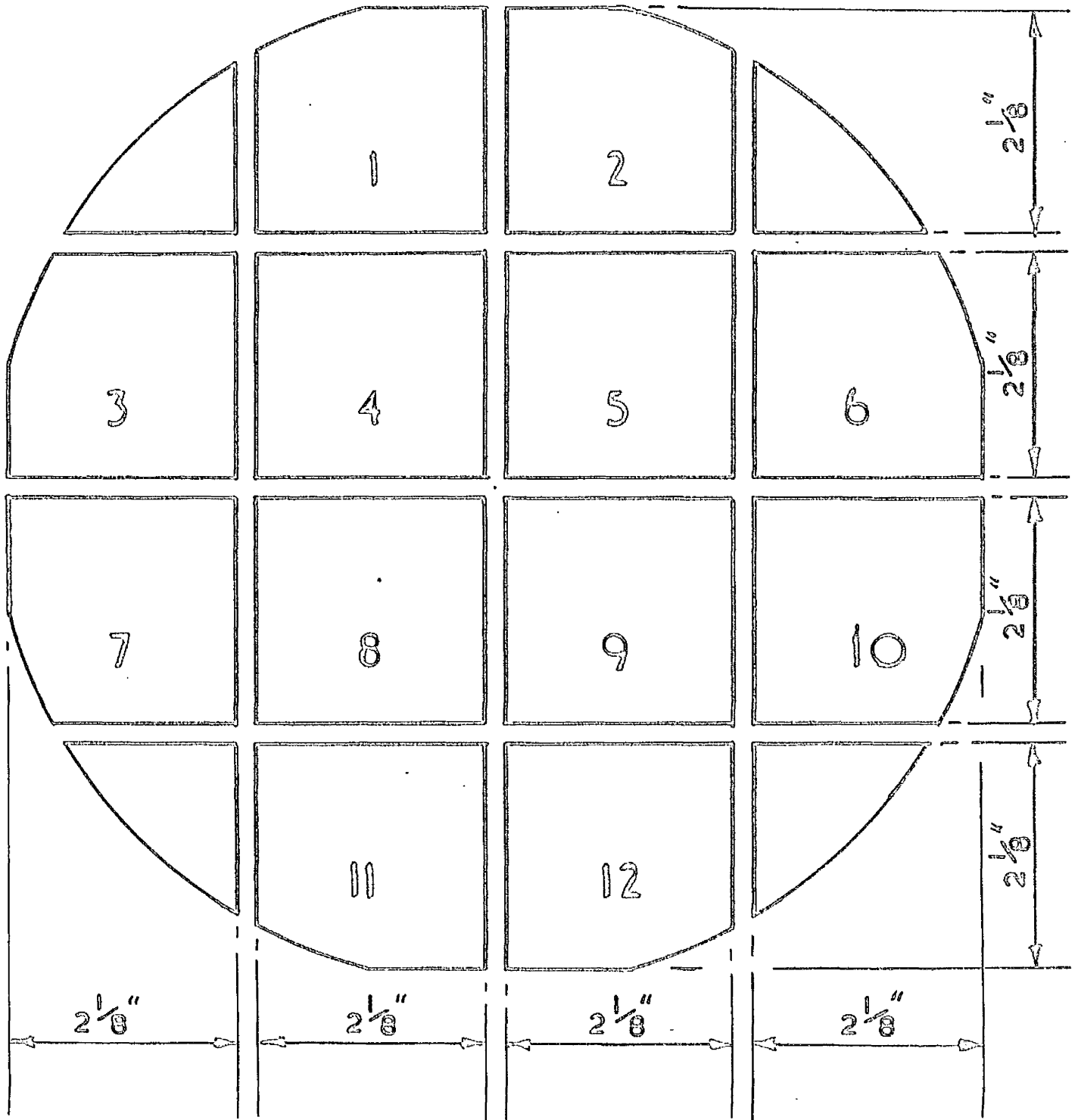


fig 50

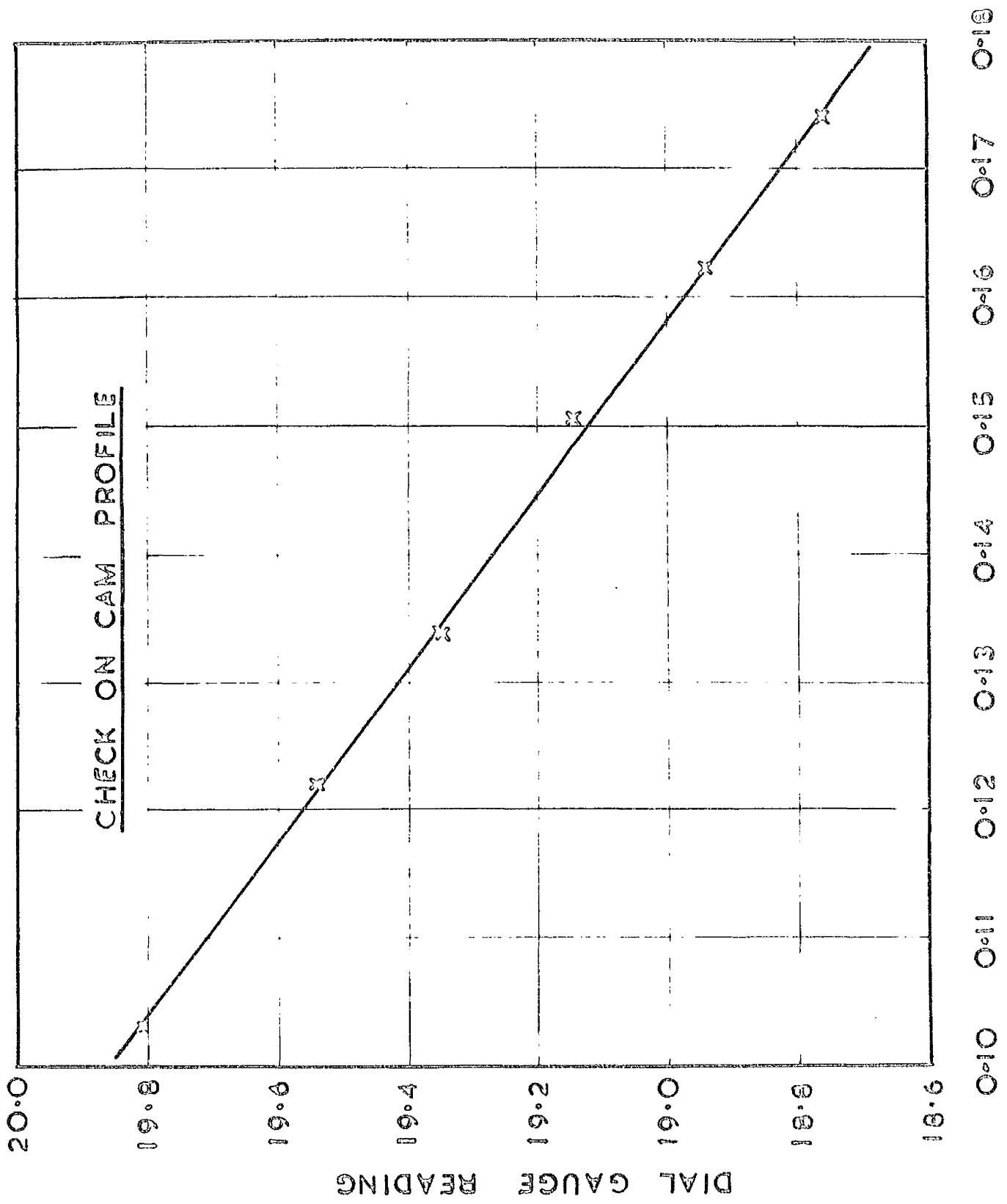
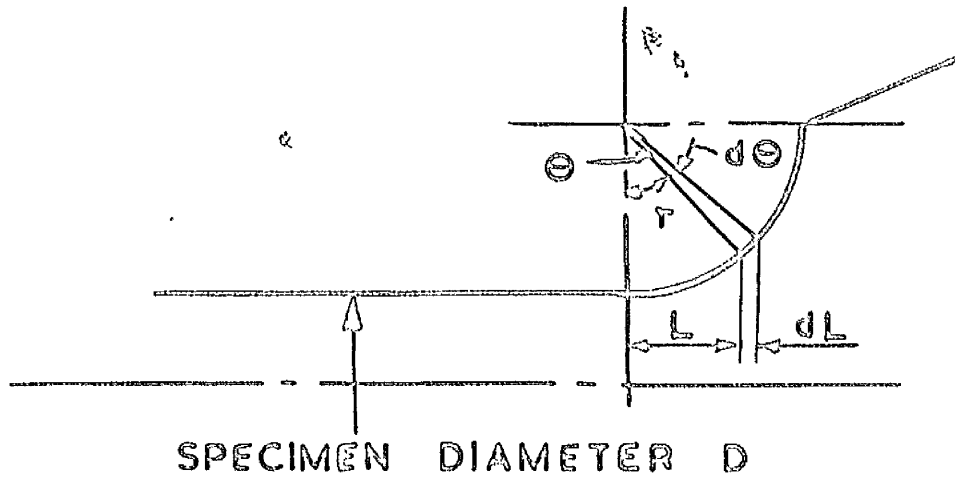
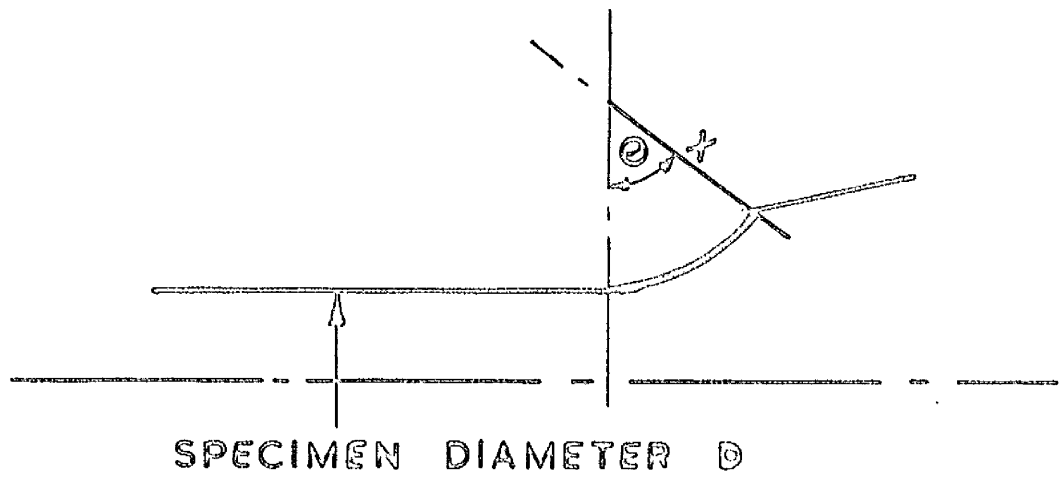


fig 51



(d) TYPICAL SPECIMEN FILLET RADIUS



(b) FILLET RADIUS OF MEASURED  
SPECIMENS

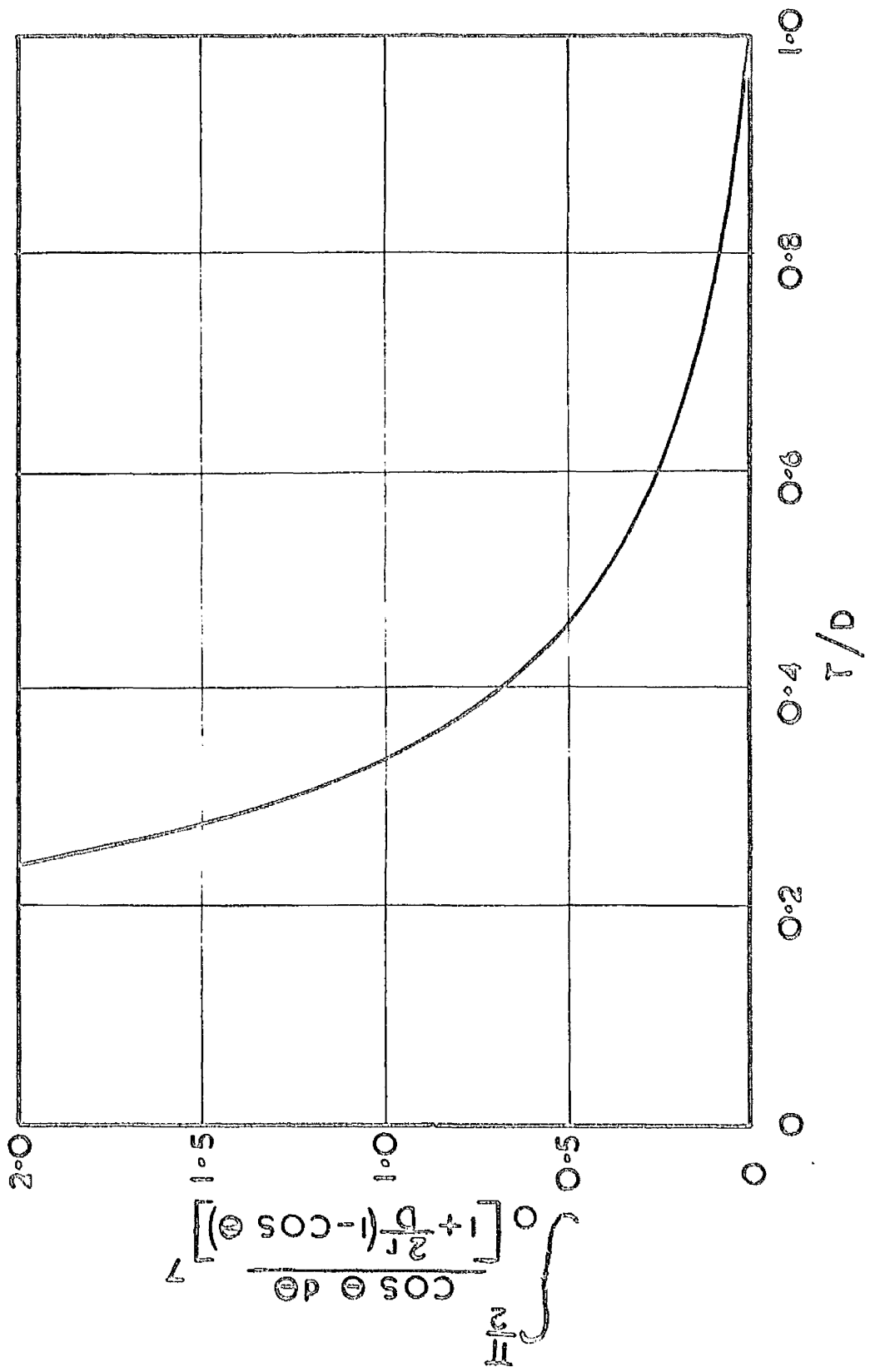
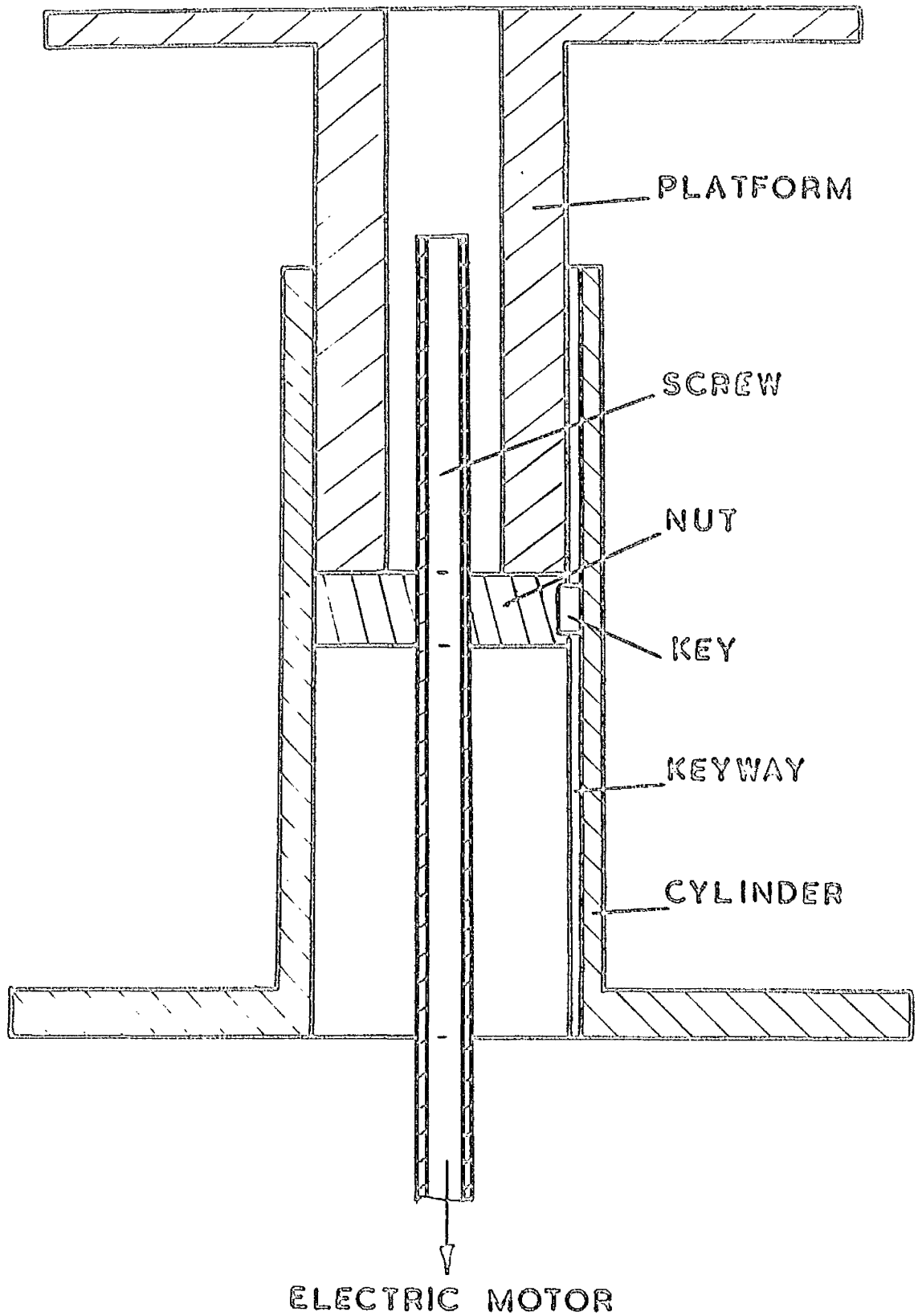
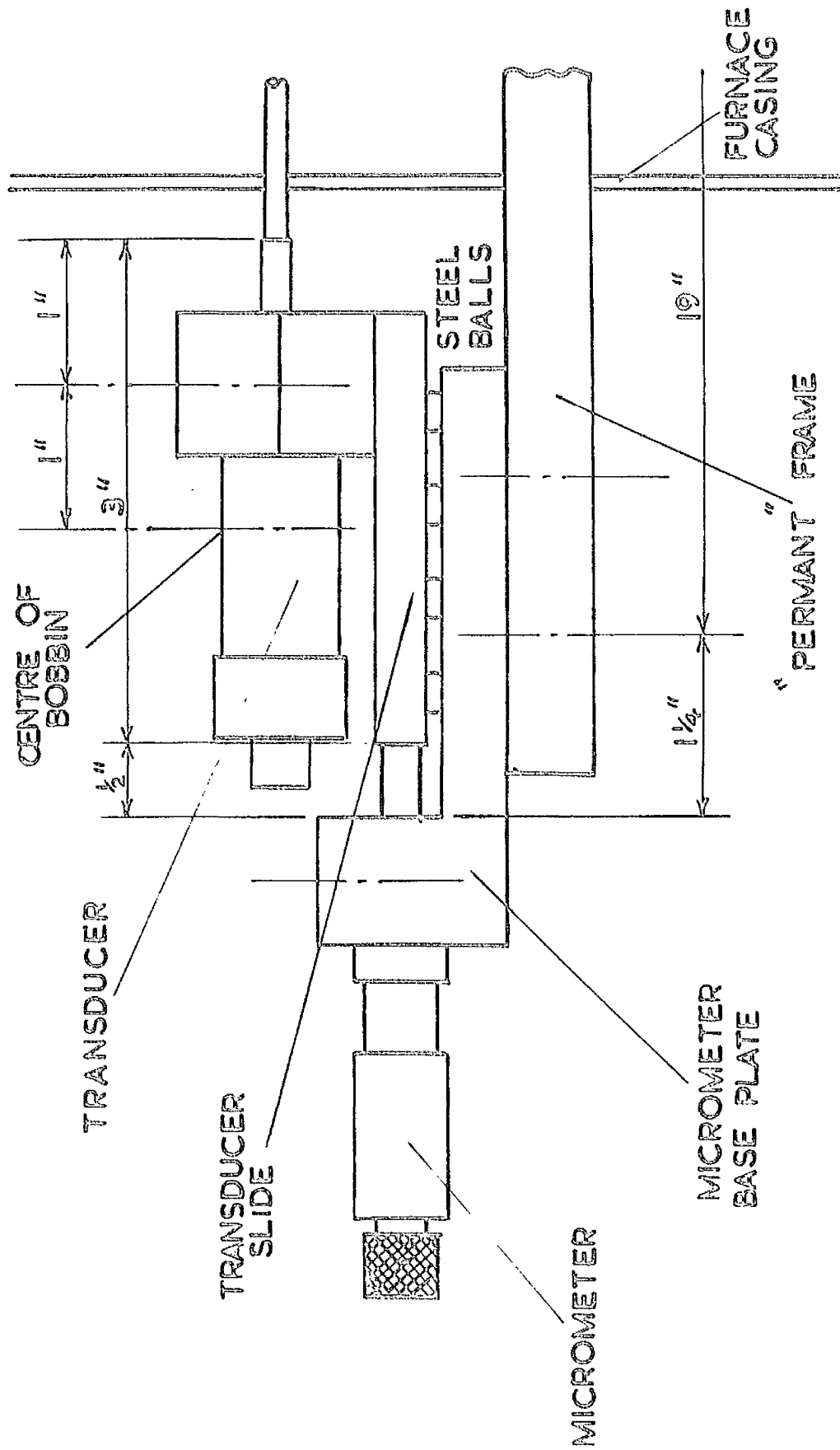


fig 53



DIAGRAMMATIC ARRANGEMENT  
OF ELECTRIC JACK



THERMAL COMPENSATION OF TRANSDUCER SYSTEM

fig 55

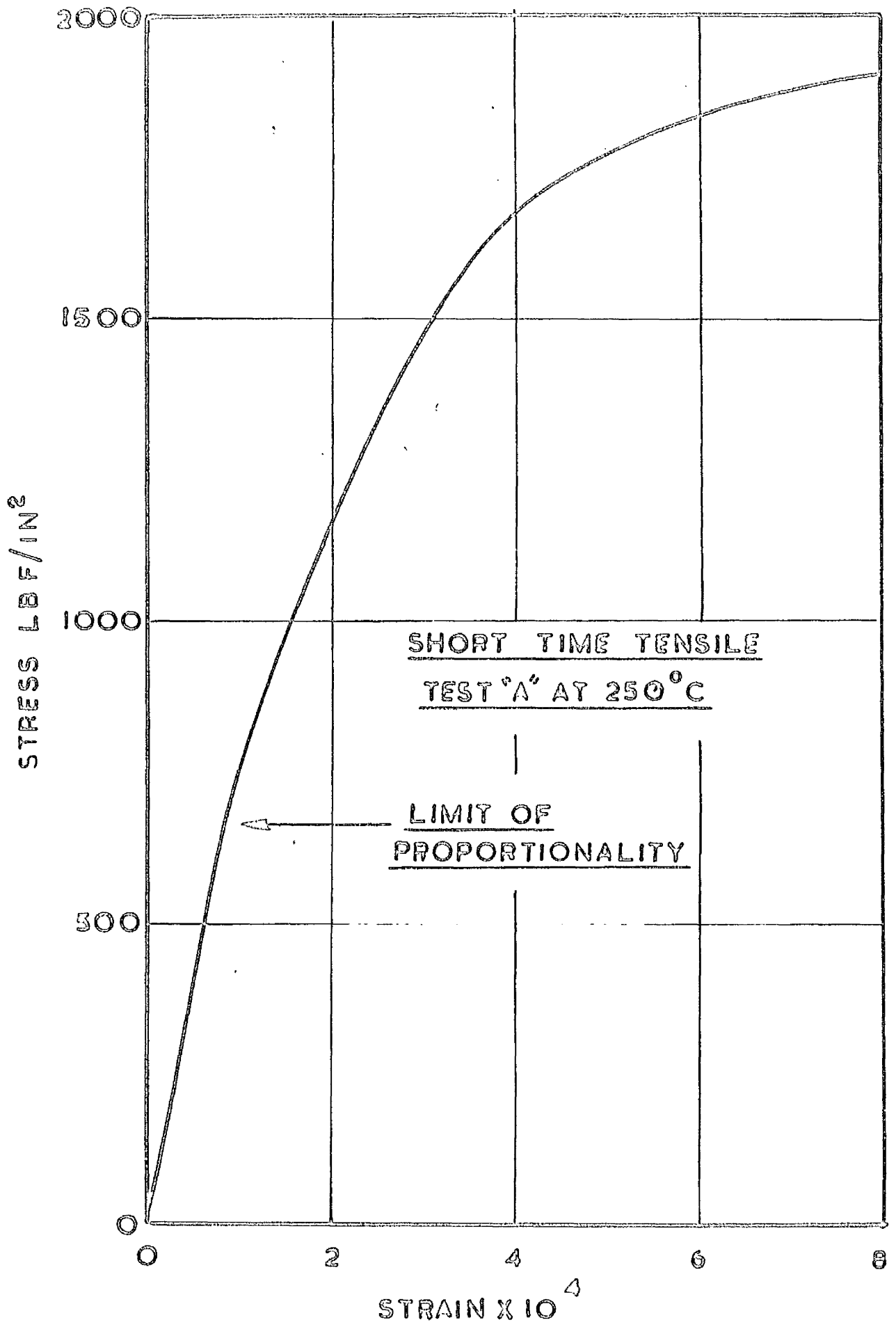


fig 56

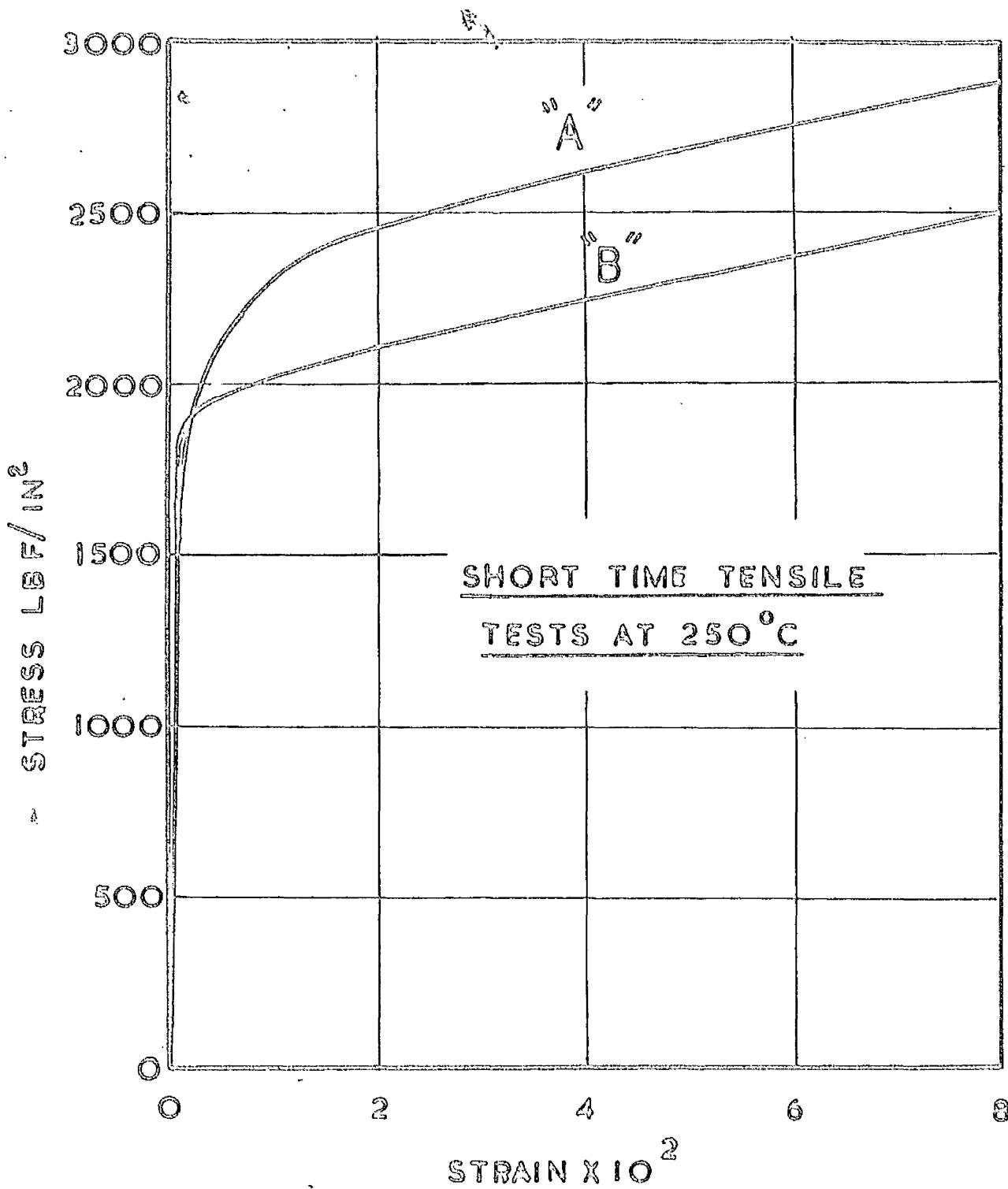


fig 57

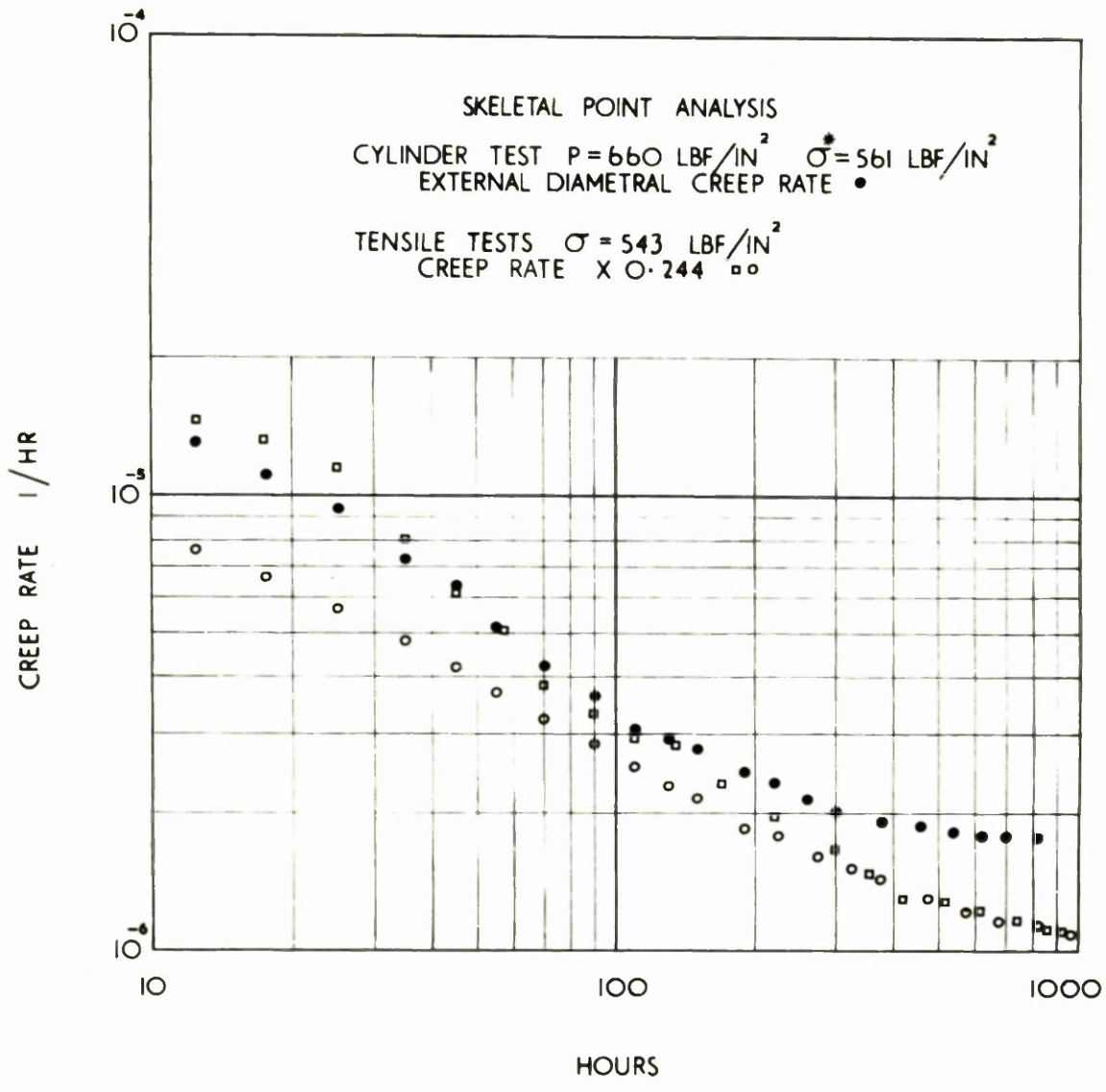


fig 58